ISSN 1007-9327 (print)
ISSN 2219-2840 (online)

World Journal of *Gastroenterology*

World J Gastroenterol 2020 September 21; 26(35): 5223-5386

Published by Baishideng Publishing Group Inc

World Journal of Gastroenterology

Contents

Weekly Volume 26 Number 35 September 21, 2020

REVIEW

MINIREVIEWS

ORIGINAL ARTICLE

Basic Study

Retrospective Cohort Study

Retrospective Study

Observational Study

SYSTEMATIC REVIEWS

CASE REPORT

ABOUT COVER

Editorial board of *World Journal of Gastroenterology*, Dr. Somashekar Krishna is an Associate Professor of Medicine in the Gastroenterology Division of the Ohio State University Wexner Medical Center in Columbus, OH, United States. He trained in advanced endoscopy at the University of Texas MD Anderson Cancer Center (Houston). Dr. Krishna has served on the American Society of Gastrointestinal Endoscopy Research Committee and the *Gastrointestinal Endoscopy* journal editorial board. He is a fellow of the ACG, AGA, and ASGE. Throughout his career, Dr. Krishna has published more than 125 peer-reviewed publications on his research, which encompass studies of advances in early and accurate detection of precancerous pancreatic lesions using novel endoscopic technologies, innovation in endoscopic ultrasound and novel imaging, endoscopy-guided ablation of pancreatic lesions, and large-database analyses and clinical outcomes with focus on acute pancreatitis. (L-Editor: Filipodia)

AIMS AND SCOPE

The primary aim of *World Journal of Gastroenterology* (*WJG*, *World J Gastroenterol*) is to provide scholars and readers from various fields of gastroenterology and hepatology with a platform to publish high-quality basic and clinical research articles and communicate their research findings online. *WJG* mainly publishes articles reporting research results and findings obtained in the field of gastroenterology and hepatology and covering a wide range of topics including gastroenterology, hepatology, gastrointestinal endoscopy, gastrointestinal surgery, gastrointestinal oncology, and pediatric gastroenterology.

INDEXING/ABSTRACTING

The *WJG* is now indexed in Current Contents®/Clinical Medicine, Science Citation Index Expanded (also known as SciSearch®), Journal Citation Reports®, Index Medicus, MEDLINE, PubMed, PubMed Central, and Scopus. The 2020 edition of Journal Citation Report® cites the 2019 impact factor (IF) for *WJG* as 3.665; IF without journal self cites: 3.534; 5-year IF: 4.048; Ranking: 35 among 88 journals in gastroenterology and hepatology; and Quartile category: Q2.

RESPONSIBLE EDITORS FOR THIS ISSUE

NAME OF JOURNAL
World Journal of Gastroenterology

ISSN
ISSN 1007-9327 (print) ISSN 2219-2840 (online)

LAUNCH DATE
October 1, 1995

FREQUENCY
Weekly

EDITORS-IN-CHIEF
Andrzej S Tarnawski, Subrata Ghosh

EDITORIAL BOARD MEMBERS
http://www.wjgnet.com/1007-9327/editorialboard.htm

PUBLICATION DATE
September 21, 2020

INSTRUCTIONS TO AUTHORS
https://www.wjgnet.com/bpg/gerinfo/204

GUIDELINES FOR ETHICS DOCUMENTS
https://www.wjgnet.com/bpg/GerInfo/287

GUIDELINES FOR NON-NATIVE SPEAKERS OF ENGLISH
https://www.wjgnet.com/bpg/gerinfo/240

PUBLICATION ETHICS
https://www.wjgnet.com/bpg/GerInfo/288

PUBLICATION MISCONDUCT
https://www.wjgnet.com/bpg/gerinfo/208

ARTICLE PROCESSING CHARGE
https://www.wjgnet.com/bpg/gerinfo/242

STEPS FOR SUBMITTING MANUSCRIPTS
https://www.wjgnet.com/bpg/GerInfo/239

ONLINE SUBMISSION
https://www.f6publishing.com

E-mail: bpgoffice@wjgnet.com https://www.wjgnet.com

World Journal of Gastroenterology

Submit a Manuscript: https://www.f6publishing.com

World J Gastroenterol 2020 September 21; 26(35): 5223-5247

DOI: 10.3748/wjg.v26.i35.5223

ISSN 1007-9327 (print) ISSN 2219-2840 (online)

REVIEW

Stress granules in colorectal cancer: Current knowledge and potential therapeutic applications

Noémie Legrand, Dan A Dixon, Cyril Sobolewski

ORCID number: Noémie Legrand 0000-0003-0516-0786; Dan A Dixon 0000-0001-5631-4365; Cyril Sobolewski 0000-0002-9404-6290.

Author contributions: Sobolewski C, Legrand N, Dixon DA contributed to the writing of the manuscript; Sobolewski C contributed to the supervision of the manuscript; Dixon DA performed the critical revision of the manuscript for important intellectual content; all authors critically revised the manuscript and approved the final version for publication.

Supported by Geneva Cancer League, No. 1711; National Institutes of Health, No. R01 CA243445; and National Cancer Institute Cancer Center Support Grant, No. P30 CA168524.

Conflict-of-interest statement: The authors declare no conflicts of interest.

Noémie Legrand, Department of Medicine, Faculty of Medicine, University of Geneva, Geneva CH-1211, Switzerland

Dan A Dixon, Department of Molecular Biosciences, University of Kansas, Lawrence, Kansas, and University of Kansas Cancer Center, Lawrence, KS 66045, United States

Cyril Sobolewski, Department of Cell Physiology and Metabolism, Faculty of Medicine, University of Geneva, Geneva CH-1211, Switzerland

Corresponding author: Cyril Sobolewski, PhD, Research Associate, Senior Scientist, Department of Cell Physiology and Metabolism, Faculty of Medicine, University of Geneva, CMU, 1 rue Michel-Servet, Geneva CH-1211, Switzerland. cyril.sobolewski@unige.ch

Abstract

Stress granules (SGs) represent important non-membrane cytoplasmic compartments, involved in cellular adaptation to various stressful conditions (*e.g.*, hypoxia, nutrient deprivation, oxidative stress). These granules contain several scaffold proteins and RNA-binding proteins, which bind to mRNAs and keep them translationally silent while protecting them from harmful conditions. Although the role of SGs in cancer development is still poorly known and vary between cancer types, increasing evidence indicate that the expression and/or the activity of several key SGs components are deregulated in colorectal tumors but also in pre-neoplastic conditions (*e.g.*, inflammatory bowel disease), thus suggesting a potential role in the onset of colorectal cancer (CRC). It is therefore believed that SGs formation importantly contributes to various steps of colorectal tumorigenesis but also in chemoresistance. As CRC is the third most frequent cancer and one of the leading causes of cancer mortality worldwide, development of new therapeutic targets is needed to offset the development of chemoresistance and formation of metastasis. Abolishing SGs assembly may therefore represent an appealing therapeutic strategy to re-sensitize colon cancer cells to anti-cancer chemotherapies. In this review, we summarize the current knowledge on SGs in colorectal cancer and the potential therapeutic strategies that could be employed to target them.

Key Words: Stress-Granules; Colorectal cancer; Adenylate-Uridylate-rich element-binding proteins; Post-transcriptional regulation; Oncogenes; Tumor suppressors

Manuscript source: Invited manuscript

Received: July 22, 2020
Peer-review started: July 22, 2020
First decision: August 8, 2020
Revised: August 12, 2020
Accepted: September 3, 2020
Article in press: September 3, 2020
Published online: September 21, 2020

P-Reviewer: Kaplan MA
S-Editor: Yan JP
L-Editor: A
P-Editor: Ma YJ

Core Tip: Colorectal cancer (CRC) represent the second cause of cancer mortality worldwide. Although changes in genetic landscape associated with CRC development have been identified, most frequent mutations are currently undruggable. The development of chemoresistance represent a major cause of CRC-associated mortality and identifying mechanisms allowing cancer cells to avoid these treatments may considerably improve clinical outcomes. Current findings indicate that cancers cells can preserve their expressed mRNAs in harmful conditions by storing them in small cytoplasmic granules, called Stress granules (SGs), where they are kept translationally silent. Targeting these SGs proteins may therefore represent a novel and efficient therapeutic approach.

Citation: Legrand N, Dixon DA, Sobolewski C. Stress granules in colorectal cancer: Current knowledge and potential therapeutic applications. *World J Gastroenterol* 2020; 26(35): 5223-5247
URL: https://www.wjgnet.com/1007-9327/full/v26/i35/5223.htm
DOI: https://dx.doi.org/10.3748/wjg.v26.i35.5223

INTRODUCTION

Colorectal cancer (CRC) represents the second cause of cancer mortality worldwide and the third most frequent cancer, with 1.8 million new cases and 881000 death in 2018[1]. CRC development results from a long term-deregulated process starting with the development of small adenomas, which evolve toward large adenomas and CRC. In most of the cases CRC develops sporadically (70%) and occurs in an aging population (> 50 years), whereas inherited genetic disorders such as Familial Adenomatous Polyposis or Lynch Syndrome are relatively rare and occurs at a younger age (before 50). Although the causes of sporadic CRC remain unclear, several risk factors have been identified, including inflammatory bowel disease (IBD) (*e.g.*, Crohn's disease and ulcerative colitis), obesity, diabetes, sedentary lifestyle, alcohol consumption, high fat-containing diet, and aging. Therefore, with the prevalence of obesity and diabetes worldwide, CRC incidence is expected to dramatically increase in the future, making this cancer a major public health concern and a growing economic burden. CRC is mostly treated by surgery, chemotherapy (*e.g.*, FOLFOX: Folinic acid, 5-fluorouracil, oxaliplatin) and targeted therapy. However, despite these therapeutic options, the average survival rate of colon cancer between 2009 and 2015 was 63% (all SEER stages combined) and only 14% for distant CRC (American Cancer Society: https://www.cancer.org/cancer/colon-rectal-cancer/detection-diagnosis staging/survival-rates.html). This high mortality rate is predominantly due to metastasis and the development of chemoresistance[2]. Therefore, greater efforts are needed in identifying and targeting the mechanisms involved in both these processes in order to improve patient outcomes.

The development of chemoresistance is a major feature of CRC-associated mortality. Several chemoresistance mechanisms have been identified, including the induction of pro-survival factors and downregulation of pro-apoptotic proteins, along with the induction of transporters or detoxifications enzymes (*e.g.*, P-glycoprotein), which reduce the efficiency of chemotherapy. More recently, it has been proposed that cancer cells can adapt to stress conditions (*e.g.*, oxidative stress, hypoxia, chemotherapy) by generating small cytoplasmic ribonucleoprotein (RNP) foci called stress granules (SGs), which protect expressed mRNAs from degradation. SGs represent membrane-less cytoplasmic compartments containing mRNAs stalled at translation initiation. The mechanism underlying their formation is complex and tightly regulated by several proteins, which interact with mRNAs. SGs formation is also reversible, but in cases of prolonged stress, mRNAs are degraded into other cytoplasmic foci called processing bodies (P-Bodies). In cancer cells, SGs importantly contribute to cancer cell survival but also to resistance to various anti-cancerous agents. Several SGs components are upregulated in cancer cells as compared to their normal cellular counterparts. Moreover, several anti-cancerous agents elicit SGs assembly in cancer cells. Recent efforts aiming at identifying the mRNA/protein content of SGs have uncovered key players in carcinogenesis (*e.g.*, oncogenes or tumor suppressors). Finally, impairment of SGs formation can re-sensitize several cancer types to chemotherapy or other anti-cancer agents (*e.g.*, sorafenib) and thus may represent an appealing approach in combination with current treatments (*e.g.*, FOLFOX, FOLFIRI)[3]. In this review, we

discuss the role of SGs in colon cancer but also in pre-cancerous conditions favoring its development (*e.g.*, inflammatory bowel disease). Because this cellular process has not been extensively studied in the context of CRC, we also discuss the current gaps in knowledge of SGs biology in CRC cells. Finally, we discuss potential therapeutic approaches that could be used to impact SGs assembly in cancer cells.

COMPLEXITY OF STRESS GRANULES FORMATION AND CARCINOGENESIS

Basics of SGs assembly

SGs are non-membrane cytoplasmic compartments, composed of untranslated RNPs formed in stressful conditions. SGs exhibit liquid-like behavior allowing rapid exchanges of components (*e.g.*, mRNAs and proteins) with the cytosol[4,5]. The formation of SGs is a dynamic and conserved process, triggered by various stress conditions (*e.g.*, nutrients deprivation, osmotic shock, hypoxia, heat shock, ultraviolet irradiation, oxidative stress), but also various molecules (*e.g.*, chemotherapy, endoplasmic reticulum stressors, translation/proteasome inhibitors). Proteomic-based approaches have identified many of proteins located within mammalian SGs (https://msgp.pt/; http://rnagranuledb.lunenfeld.ca/). To date, more than 400 proteins have been identified in stress granules, but their composition may vary between cell types and/or stimuli. Among them, about 50% are RNA-Binding Proteins, while the remaining proteins are presumably recruited through protein-protein interaction and are involved in various cellular processes (*e.g.*, cell cycle progression, apoptosis) or SGs assembly regulation.

The mechanisms involved in SGs formation are still unclear and several models have been proposed. SGs assembly is a multi-step process starting with the phosphorylation of eIF2α, which prevents the formation of the eIF2/GTP/tRNAi initiation complex[6] and leads to the dissociation of mRNAs from polysomes. However, this step is not mandatory for SGs assembly, as other non-canonical eIF2-independent models of SGs formation have been described (*e.g.*, change in the activity of the eIF4F complex, which is also involved in translation initiation)[7,8]. Currently two models of SGs formation have been proposed[9]. In the "*core first*" model, untranslated mRNAs are nucleated into oligomers through the binding of proteins (*e.g.*, T Cell-Restricted Intracellular Antigen-1, TIA1, G3BP1) having a Prion-Like Domain or Intrinsically Disordered Domains, which provide scaffolds necessary for the recruitment of other proteins (primary aggregation). These domains consist of polar residues, which favor liquid-liquid phase separation (LLPS) through electrostatic interactions. Due to these biophysical properties, SGs have been qualified as "*liquid droplets*"[10]. Then, the growth of these oligomers, through the addition of other untranslated RNPs give rise to the SGs "*cores*". This step is supported by the microtubule's cytoskeleton and motor proteins (*e.g.*, dyneins, kinesins), which bring additional RNPs to the SGs[11]. Finally, the heterotypic associations of SGs components (*e.g.*, G3BP1/TIA1; Polyadenylate-binding protein 1, PABP1) promote the growth and fusion of the granules (coalescence) and the recruitment of a dynamic shell, leading to the formation of large macroscopically visible SGs. However, this model has been challenged by the "*LLPS First*" model, where the nucleation of RNP generate phase separated droplets connected by weak interactions in which core granules are formed.

The formation of SGs is a tightly regulated process with participation of several signaling pathways and post-translational modifications (*e.g.*, phosphorylation, acetylation)[12] of SGs components that regulate SGs assembly. For instance, phosphorylation of G3BP1 on ser^{149} by casein kinase 2 (CK2)[13] impairs SGs assembly, while arginine methylation, or deacetylation of G3BP1 by PRMT1/5 (protein arginine methyltransferase) and HDAC6[12], respectively[14,15], promotes their formation. Several signaling pathways regulate SGs assembly, including the PI3K or the Stress-Activated Kinase (p38/MAPK) signaling, which enhance SGs formation by activating mTORC1 kinase in stress conditions[16]. These pathways are usually overactivated in many cancers, following mutations of their key regulators (*e.g.*, AKT, PTEN), thus providing a favorable landscape for SGs formation. However, it is still unclear the role of mTORC1 in SGs assembly, as other studies have suggested an opposite mechanism where AMPK inhibits mTORC1 and induces SGs assembly[17]. These differences may originate from the different models and stimuli used to trigger SGs. Finally, SGs formation is a reversible process and the clearance of SGs can be mediated by: (1) Translation re-initiation (after stress dissipates); (2) Chaperone proteins; (3) Autophagy (also referred as "*granulophagy*"); (4) mRNA degradation in processing

bodies (P-Bodies); and (5) Proteasome-dependent degradation of SGs proteins.

While SGs formation is an adaptive response to physiological conditions where transient mRNA storage can occur, the role of SGs in human diseases have been recently recognized[6,18]. Dysregulation of SGs in various pathologies including neurodegenerative, viral infections, vascular diseases, and cancers indicate that SGs to be linked to disease progression. The mechanisms underlying SGs dysregulation in disease are not fully understood, yet aberrant expression of SGs components and altered pathway activity regulating their assembly and clearance appear to be contributing factors to the development of disease-associated SGs formation.

SGs and carcinogenesis

Overexpression of SGs assembly-related proteins, along with impairment of proteins/processes involved in their clearance are the main causes of SGs formation in cancers cells. Overexpression of nucleating proteins (*e.g.*, G3BP1, TIA1, TIA-1-related, TIAR) is sufficient to trigger SGs formation in absence of stress[19]. Moreover, the stressful conditions present within the tumor microenvironment (*e.g.*, hypoxia, oxidative stress, nutrient deprivation, chronic inflammation)[20], as well as specific molecules present (prostaglandin J2 and A1), promote SGs assembly in cancer cells[19]. Other factors including oxidized-low density lipoprotein or high-fat diet are also contributing factors to SGs formation[21]. These data suggest that lifestyle and chronic inflammatory/metabolic diseases (*e.g.*, diabetes, fatty liver diseases, ulcerative colitis), which represent major risk factors for cancer development (*e.g.*, hepatocellular carcinoma, CRC), may considerably influence SGs formation. Several anti-cancer treatments such as sorafenib, bortezomib, 5-FU, Oxaliplatin[19], FCCP [Carbonyl cyanide p-(trifluoromethoxy) phenylhydrazone][22] and radiotherapy[19] increase SGs assembly in cancer cells, which in turn renders them more resistant to these treatments. SGs are also implicated in controlling cancer-related processes including apoptosis and migration/invasion of cancer cells. Although the precise mechanisms are still unclear, the sequestration and inhibition of pro-apoptotic factors (*e.g.*, TRAF2, RACK1) has been suggested[23]. Furthermore, several RNA-binding proteins (*e.g.*, tristetraprolin, HuR) located in SGs regulate the stability and translation of cancer-related mRNA transcripts involved in various cancerous hallmarks, including cell proliferation (*e.g.*, MYC)[24], angiogenesis (*e.g.*, VEGFA)[25], inflammation (*e.g.*, cyclooxygenase-2, COX-2)[26] and cell death (antiapoptotic protein: BCL2, MCL1)[27,28]. SGs also inhibits cellular senescence by sequestering plasminogen activator inhibitor-1 in fibroblasts[29]. As senescence represents an important barrier against carcinogenesis[30], these findings further support the oncogenic function of SGs. Finally, defective P-body formation is observed in several cancers (*e.g.*, CRC)[6], and this together with the increased SGs assembly may act in concert to promote tumor progression.

The current methodologies to study SGs functions are mostly based on gain and loss of function analyses of SGs components, microscopy, and cell fractionation methods to isolate SGs. This latest methodology, coupled with transcriptomic and proteomic-based approaches, have identified both proteins and mRNA transcripts associated with these granules. This information is publicly available in several databases (*e.g.*, https://msgp.pt/; http://rnagranuledb.lunenfeld.ca/) and interestingly several transcripts and proteins have been associated to various cancer-related processes, suggesting that the role of SGs in carcinogenesis is largely underestimated. While the majority of studies utilize cell-based *in vitro* approaches, *in vivo* mouse models with constitutive deletion of specific SGs factors (*e.g.*, TIA1KO or G3BP1KO mice) have been generated[31,32]. Further efforts utilizing tissue-specific and inducible knockout approaches will further aid in understanding the role of SGs play in development and progression of specific tumor types.

ROLE OF STRESS GRANULES IN COLORECTAL CANCER

Although the role of SGs has been studied in various cancers, their functions in the development of CRC and inflammatory bowel disease remain to be characterized. While more than 400 proteins have been identified in mammalian SGs (*e.g.*, https://msgp.pt/), only few of them have been involved in SGs assembly and disassembly are abundantly expressed in epithelial and goblet cells of the colon (single cell sequencing of large intestine: https://tabula-muris.ds.czbiohub.org/) and also in the other cell types (*e.g.*, enteroendocrine cells). In addition, several proteins (*e.g.*, RNA-binding proteins, pro-apoptotic factors, cell cycle-related proteins) involved in

cancer-related processes in CRC are localized in SGs.

SG nucleators and CRC

SGs nucleators refer to the proteins that are directly involved in the early aggregation phase of SGs formation and their sole overexpression is sufficient for spontaneous SGs assembly, even in absence of stress. Conversely, knockdown of these proteins severely impairs SGs assembly. Moreover, alteration of their expression occurs in preneoplasic conditions, such as ulcerative colitis, thus suggesting that defects in their expression are early alterations fostering CRC development.

UBAP2L: A component of the ubiquitin-proteasome pathway containing a ubiquitin-associated (UBA) domain which binds to ubiquitin and multi-ubiquitin chains[33]. UBAP2L plays a key role in stress granules assembly even in stress-null conditions[34,35]. The Arg-Gly-Gly (RGG) motif of UBAP2L plays a key role in SGs assembly[35] by mediating the recruitment of other components (*e.g.*, RNPs)[35]. Importantly, this domain can be methylated by the protein arginine methyltransferase PRMT1, which impairs SGs formation[35]. The Domain of Unknown Function motif of UBAP2L is also necessary to bind to G3BP1/2[35]. Recent findings have suggested thus that UBAP2L acts upstream of G3BP1/2 and can form SGs core independently of G3BP1/2[36]. The function of UBAP2L in cancers is poorly known but increasing evidence indicates that UBAP2L promotes progression of hepatocellular carcinoma[37], prostate cancer[38] and glioblastoma[39]. The expression of UBAP2L in CRC is currently unknown (Table 1) but its knockdown in colon cancer cells (*i.e.*, HCT116 and RKO cells)[40] hinders cell cycle progression[40] and induces apoptosis through activation of BAD, BAX, and the cleavage of Caspase-3 and Poly(ADP-ribose) Polymerase[40]. Although these results indicate an oncogenic function of UBAP2L in CRC, they are currently no studies documenting its function in SGs in CRC.

Ras GTPase-activating protein-binding protein (G3BP): A family of RNA-binding proteins composed of three different members, G3BP1, GBP2a and G3BP2b. Through their interaction with the SH3 domain of RasGAP (Ras GTPase activating protein), these proteins promote Ras signaling[41]. G3BP proteins contain a RNA recognition motif (RRM), which allows for interaction with the 40S subunit of ribosomes and RGG domains involved in mRNA binding[42]. Among them, G3BP1 is strongly overexpressed in a variety of cancers especially colon cancer[43] and exert oncogenic functions by promoting cancer cell proliferation, and inhibiting apoptosis[44]. Accordingly, downregulation of G3BP1 in colon cancer cells leads to a decrease of Ras signaling and cell growth arrest[43]. Despite the lack of a PLD, G3BP1 is an important SGs nucleator, as its sole overexpression is sufficient to trigger SGs assembly[45]. Although the mechanism involved is still unclear, recent studies have indicated that protein partners including CAPRIN1 or USP10, which promote and inhibit SGs assembly, respectively[46]. In CRC, the role of CAPRIN1 is currently unknown but a loss of USP10 expression was reported in 18.6% of CRC tumors[47]. Importantly, this loss was associated to distal metastasis and lymphovascular invasion.

The mechanism involved in G3BP1 overexpression is currently unknown but the RNA-binding protein Y-box binding protein (YB-1), which is overexpressed in CRC and ulcerative-associated lesions[48], may be involved in the increase of G3BP1 translation as suggested in other cancers[49]. G3BP1 is also regulated by post-translational modifications. G3BP1 phosphorylation on Ser^{149} by CK2 was reported to inhibits SGs formation[13]. However, the role of this phosphorylation is still controversial, as an *erratum* reporting that ser^{149} phosphorylation was unchanged during stress, has been published[50]. Arginine methylation in the RGG domain by protein arginine methyltransferase inhibits SGs formation[14]. Interestingly, this methylation is promoted by the Wnt/β-catenin pathway in mouse embryonic F9 cells[15], suggesting that overactivation of this oncogenic pathway in CRC may account for the increased SGs assembly in colon cancer cells. Finally, acetylation of Lysine-376 (K376) in the RRM domain, impairs the RNA binding function of G3BP1 as well as its interaction with PABP1, USP10 or Caprin1[12]. Accordingly, an increased acetylation of K376 was observed during SGs disassembly. HDAC6 and the CBP/p300 acetylase directly control the acetylation status of G3BP1[12] and thus HDAC6 inhibition impairs SGs formation[51]. While these findings indicate that the role of G3BP1 in SGs assembly, its role in CRC remains to be better characterized. Moreover, the other members of the G3BP family are potentially important for SGs assembly in colon cancer cells. For instance, G3BP2 overexpression can also trigger SGs formation in absence of stress[41,44]. The role of G3BP2 in CRC is currently unknown but *in silico* analysis of its mRNA level in CRC patients indicates an upregulation of G3BP2 in tumors as

Table 1 Expression and prognostic value of stress granule-associated proteins in colorectal cancer

Components	Role in SG	mRNA expression in tumors (GEPIA)	Expression in CRC patients (literature)	Overall survival (GEPIA)	Overall survival (Human Protein Atlas)
G3BP1	Promotes SG assembly	Up	Unknown	No significant difference	Better prognosis with high expression
G3BP2	Promotes SG assembly	Up	Unknown	No significant difference	Better prognosis with high expression
USP10	Promotes SG assembly	Up (trend)	Down in 18.6% of patients[47]	No significant difference	Better prognosis with high expression
CAPRIN1	Promotes SG assembly	Up	Unknown	No significant difference	Better prognosis with high expression
UBAP2L	Promotes SG assembly	No significant difference	Unknown	No significant difference	No significant difference
TIA1	Promotes SG assembly	Down (trend)	sTIA1 (spliced variant) is Up[171]	Poor prognosis with high expression	Better prognosis with high expression
TIAL1	Promotes SG assembly	Down (trend)	Unknown	Poor prognosis with high expression	No significant difference
DDX3	Promotes SG assembly	No significant difference	Poor prognosis with high expression[57]	No significant difference	Better prognosis with high expression
PABP1	Promotes SG assembly	Up	Unknown	NA	No significant difference
FMR1	Promotes SG assembly	No significant difference	Unknown	No significant difference	Better prognosis with high expression
PDCD4	Promotes SG assembly	Down (trend)	Down[172]	No significant difference	No significant difference
ATXN2	Promotes SG assembly	No significant difference	Unknown	No significant difference	No significant difference
ANG	Promotes SG assembly	No significant difference	Up	No significant difference	No significant difference
ZFP36	Promotes SG clearance and SG-P-Bodies fusion	Down	Down[26]	Poor prognosis with low expression (P = 0.16: trend)	No significant difference
ZFP36L1	Promotes SG-P-Bodies fusion	Down	Unknown	No significant difference	No significant difference
ELAVL1	mRNA stabilization	Up (trend)	Up[26]	No significant difference	Better prognosis with high expression
CUGBP2	mRNA stabilisation	No significant difference	Down[173]	No significant difference	Better prognosis with high expression
MSI-1	Promotes SG assembly	No significant difference	Up[54]	No significant difference	No significant difference
KHSRP	Unknown	No significant difference	Unknown	No significant difference	No significant difference
BAG3	Promotes SG clearance	No significant difference	Up[174]	No significant difference	Poor prognosis with high expression
PRMT1	Inhibition of SG formation	Up (trend)	(Poor prognosis with high expression[119]	Better prognosis with high expression (not significant: marked trend)	Better prognosis with high expression
PRMT5	Inhibition of SG formation	Up (trend)	Up[175]	Better prognosis with high expression (not significant: marked trend	Better prognosis with high expression
HDAC6	Promotes SG assembly	Down	Up[176]	Poor prognosis with high expression (not significant: marked trend	Poor prognosis with high expression
SIRT6	Promotes SG assembly	No significant difference	Down[113]	No significant difference	No significant difference
EP300	Inhibition of SG	No significant	Up[105]	No significant difference	No significant

	formation	difference			difference
JMJD6	Promotes SG assembly	No significant difference	Up[121]	No significant difference but marked trend for a poor prognosis with high expression	No significant difference
CK2	Inhibition of SG formation	Up (trend)	Up[177]	No significant difference	Poor prognosis with high expression
PRKAA1 (AMPK)	Promotes SG assembly	No significant difference	Up[126,127]	No significant difference	Better prognosis with high expression
MTOR	Unclear	No significant difference	mTORC1 Up[122]	No significant difference	No significant difference
TARDBP	Promotes SG assembly	No significant difference	Unknown	No significant difference	No significant difference
RBFOX2	Regulation of cell cycle	Down	Up[101]	No significant difference	No significant difference
RACK1	Regulation of apoptosis	Up		No significant difference	No significant difference
ULK1	Promotes SG disassembly	Down	Up[178] (Poor Prognosis)	No significant difference	Poor prognosis with high expression
ULK2	Promotes SG disassembly	Down	Down[179]	No significant difference	No significant difference
VCP	Promotes SG disassembly	No significant difference	Up (poor prognosis with high expression)[180]	No significant difference	No significant difference

The differential mRNA expression of stress granule proteins in colorectal cancer as compared to matched non-tumoral tissues were retrieved from the GEPIA database (http://gepia.cancer-pku.cn/detail; normal tissues: n = 349; tumors: n = 275) and compared with published studies. Survival analyses were retrieved from the GEPIA (cutoff-High: 80%; cutoff-Low: 20%) and the Human Protein Atlas Database (https://www.proteinatlas.org) using the best separation method between low and high expression of protein candidates. SG: Stress granule; NA: Not available.

compared to surrounding non-tumoral tissue (Table 1).

TIA1 and TIAR: TIA1 is an RNA-binding protein comprised of three RRMs necessary for the binding to AU-Rich Elements (AREs) within the 3'UTR of target mRNAs and a PLD in C-terminal, which promotes self-aggregation of the protein. In stress conditions (*i.e.*, hypoxia, oxidative stress), TIA1 interacts with co-factors (*e.g.*, TIAR) to promotes the sequestration of target transcripts into SGs and inhibits their translation. In CRC, TIA1 expression is reduced. The mechanisms involved in TIA1 silencing haven't been fully depicted but current findings indicate that the overexpression of miR-19a in CRC tissues and cell lines directly reduces TIA1 expression[52]. In CRC, TIA1 acts as a tumor suppressor by binding to the 3'UTR of COX-2 mRNA, thereby inhibiting its translation[53]. This tumor suppressive function is further supported with better prognosis observed in patients expressing a high level of TIA1 (Table 1). Intriguingly, TIA1 also contributes to chemoresistance to 5-FU in CRC cells[54]. These data suggest that although TIA1 exerts a tumor suppressive function in CRC, its role in SGs assembly may paradoxically favor cancer cell survival.

DEAD-Box RNA helicase 3 (DDX3 also called CAP-Rf): A ubiquitously expressed protein having an ATPase and helicase activity involved in RNA metabolism (*e.g.*, mRNA splicing, transcription). DDX3 inhibits translation by directly interacting with eIF4E and with the SGs component PABP1, as evidenced in HeLa cells[55], indicating that this protein is important for SGs assembly. The role of DDX3 in SGs assembly is independent of its ATPase and helicase activity and downregulation of DDX3 in HeLa cells leads to a reduction of SGs formation, a re-localization of PABP1 to the nucleus, and an increased susceptibility to death stimuli (*i.e.*, osmotic stress induced by sorbitol)[55]. However, the role of DDX3 in CRC is unclear with studies reporting both oncogenic[56,57] and tumor suppressive functions[58]. High tumor DDX3 expression correlates with a reduced survival in CRC patients[57]. Moreover, DDX3 expression is upregulated in colon biopsies from patients with inflammatory bowel disease[59], which may provide a favorable landscape for SGs formation. Interestingly, the DDX3 inhibitor RK-33 decreases expression of MMP-1, -2, -3 and -10 in HCEC1CT and HCEC2CT human colonic epithelial cells[59]. Interestingly, differentiation of HT-29 colon cancer cells is associated to decreased of DDX3 levels, suggesting that SGs

formation is also influenced by the differentiation status of cancer cells[59].

G-quadruplex DNA structures (G4DNA): Current models of SGs formation have primarily focused on protein components triggering SGs assembly (*e.g.*, G3BP, UBAP2L). However, recent studies have also highlighted the role of G-quadruplex DNA structures in liquid-liquid phase separation upon oxidative-stress-induced DNA damage. G4DNAs represent quartets of guanine linked by hydrogen bonds and organized as a planar ring[60]. Treatment of melanoma cells with hydrogen peroxide induces DNA damage and the production of ssDNA (single strand DNA), which forms G4DNA structures. Once exported into the cytosol, G4DNA interacts with various RNA-binding proteins involved in SG assembly, including YB-1, TIA1, TIAR, DHX36, and those involved in the control of the mRNA stability and translation (*e.g.*, HuR)[60]. Accordingly, transfection of G4DNA is sufficient to trigger SG assembly in melanoma cells even in absence of stress, establishing G4DNA structures as potent SG nucleators[60]. The role of G4DNA in SG assembly in CRC cells has not been studied yet. However, increasing evidence indicate that G4DNA promotes CRC development and their inhibition with specific ligands (*e.g.*, Emicoron) can promote antitumor activities[61].

tRNA-Derived stress-induced RNAs (tiRNA): Several non-coding RNAs, including microRNAs, long-non-coding RNAs and transfer RNAs have been involved in the adaptation of cells to stress stimuli[62]. Among them, tiRNA represent a novel class of non-coding RNAs generated in stress conditions by cleavage of mature tRNAs in the anticodon loop by angiogenin[62]. tiRNAs contribute to SGs formation by interacting with YB-1[62]. Moreover, tiRNAs can form G-quadruplex structures, which impair translation initiation by sequestering eIF4F complex[62]. Although the role of tiRNA in carcinogenesis is an emerging field, angiogenin is strongly upregulated in CRC as compared to non-tumoral tissues and promotes cancer progression by generating tiRNAs (*e.g.*, 5′-tiRNA-val)[63]. Therefore, the accumulation of tiRNA together with the overexpression of nucleating proteins (*e.g.*, G3BP) in colon cancer cells, provides a notable mechanism for SG assembly in absence of stress.

RNA-binding proteins controlling the expression of key oncogenes/tumor suppressors

During SGs formation, the binding of several RNA-binding proteins to their mRNA targets importantly regulate their stability and/or translation. Among them, Adenylate-Uridylate-rich elements binding proteins (AUBPs) represent critical post-transcriptional regulators of gene expression, through their ability to bind to AREs within the 3′UTR of mRNA transcripts and promote their recruitment toward P-bodies or SGs. Aberrant ARE-dependent post-transcriptional regulation has been associated to a variety of cancers, including CRC, by favoring the overexpression of oncogenes (*e.g.*, c-myc) and pro-inflammatory mediators (*e.g.*, COX-2), and the silencing of tumor suppressors (*e.g.*, p53).

Tristetraprolin (TTP): TTP (*ZFP36*) belongs to a family of Cys-Cys-Cys-His zinc finger proteins and is an immediate-early response gene, whose expression can be induced by diverse stimuli such as insulin[64,65], TGF-b[66,67], LPS[68] and TNFa[69]. TTP is the best-characterized AU-Rich Element binding protein (AUBP) involved in promoting ARE-mediated mRNA decay. This process occurs through TTP-dependent delivery of ARE-mRNAs to P-bodies and recruit mRNA decay enzymes involved in deadenylation, decapping, and exonucleolytic decay[66,70-72]. TTP is also localized in SGs under conditions of energy deprivation[22]. However, the presence of TTP in SGs appears to be context-dependent as in models of oxidative stress, TTP is excluded from SGs due to phosphorylation of TTP by MK2[22]. Current findings suggest that TTP is involved in the shuttling between SGs and P-bodies[22] and SG-P-bodies fusion[73], and thus can contribute to SG clearance. TTP is considered as a tumor suppressor due to its capacity to reduce the expression of key inflammatory cytokines and also control expression of several factors involved in CRC carcinogenesis (*e.g.*, COX-2, VEGFα)[74-76]. Accordingly, TTP expression is strongly reduced in colorectal tumors[26,77] as well as in early adenomas and adenocarcinomas, suggesting that early reduction of TTP may promote the establishment of a neoplasic phenotype. However, the link between TTP loss and SG dynamics in colon cancer cells remains unexplored.

Butyrate response factor 1 (TIS11b, ERF-1, cMGI, Berg36, ZFP36L1): An RNA-binding protein encoded by the *ZFP36L1* gene, which belongs to the ZFP36 family[78,79]. Similar to TTP, BRF1 contains a tandem zinc finger domain bearing a double zinc

finger motif (Cys-Cys-Cys-His) and promotes the decay of various cancer-promoting transcripts (*e.g.*, VEGFA, cIAP2) by targeting them to P-bodies[79]. BRF1 is also a SG component and its overexpression promotes SG and P-body fusion[73]. However, the role of BRF1 in CRC is limited with only one study showing that 17-beta-oestradiol induces BRF1 in COLO205 colon cancer cells[80]. Nevertheless, *in silico* analyses of its mRNA level in CRC patients (Table 1) indicate a significant reduction of its expression similar to TTP, which may account for the deregulated expression pattern of various oncogenic transcripts. This downregulation may also reduce SG-P-body fusion in cancer cells, warranting further investigation.

HuR: A ubiquitously expressed RNA-binding protein encoded by the *ELAVL1* gene, which belongs to the "*Embryonic-Lethal Abnormal Vision in Drosophila*" (ELAV) family[81]. HuR possess two tandem RRMs, followed by a hinge region and a third RRM. The HuR nucleocytoplasmic shuttling domain within the hinge region is subjected to phosphorylation by various kinases, which regulate the nucleo-cytoplasmic shuttling of the protein[82]. In the cytoplasm, HuR binds and stabilizes mRNA transcripts bearing an AU-rich sequences within their 3'UTR, by competing or displacing destabilizing factors (*e.g.*, microRNAs, TTP)[26]. Moreover, HuR can directly bind and sequester miRNAs (*e.g.*, miR-16, miR-21), thereby preventing the downregulation of their mRNA targets[83,84]. In stress conditions, HuR accumulates in SGs and promotes stabilization of various oncogenic transcripts[85]. However, other studies have suggested that the formation of SGs is dispensable for mRNA stabilization[86]. HuR is overexpressed in CRC as compared to normal tissues and exerts an oncogenic function by stabilizing the mRNAs of cancer and inflammatory-promoting factors involved in cancer cells proliferation, survival, and migration[26]. Moreover, HuR expression is also increased in colonic epithelial cells from patients with inflammatory bowel disease[87], thus adding another early event potentially fostering CRC development.

CUGBP2 (CUG-Binding Protein ELAV-like family member 2): CUGBP2 is a member of the CUGBP-ETR-3-like factors family that is ubiquitously expressed. This protein contains two N-terminal RRMs and one C-terminal RRM. CUGBP2 is a SG-associated RNA-binding protein involved in stabilizing and impairing the translation of bound target mRNAs[88]. Its expression is strongly reduced in various cancers and in CRC, CUGBP2 downregulation is mediated by Prostaglandin-E2 and its overexpression promotes apoptosis and mitotic catastrophe induced by radiation in colon cancer cells[89]. Furthermore, CUGBP2 overexpression in HCT-116 cells triggers cell cycle arrest in G2/M and an induction of apoptosis due to a direct binding to the 3'UTR of Mcl-1 mRNA and an impairment of its translation[90].

Musashi-1 (Msi-1): An RNA-binding protein, which promotes mRNA stability and translation inhibition[91]. Msi-1 is overexpressed in a variety of cancers and contributes to the overexpression of oncogenes (*e.g.*, oncotachykinin 1 in breast cancer)[92] or cancer-promoting factors[91]. Msi-1 is also overexpressed in CRC and its knockdown severely impairs tumor growth *in vitro* and *in vivo*[93,94]. Moreover, Msi-1 overexpression enhances the development of CD44 positive-colon cancer stem cells and promotes chemoresistance in cells treated with 5-FU, by enhancing SGs assembly[54].

K-homology splicing regulator protein (KSRP): An RNA-binding protein involved in mRNA stability, splicing, transcription, as well as microRNA biogenesis[95,96]. In CRC, KSRP acts as a tumor suppressor by promoting the mRNA decay of β-catenin and iNOS transcripts[97,98]. In stress conditions (*e.g.*, oxidative stress), KSRP localizes in SG[99,100]. However, it is unclear the role of KSRP in SGs and whether this event occurs in colorectal cancer cells.

Other proteins involved in CRC development

Proteome-based analysis has revealed more than 400 different proteins to be associated with SGs, and cross comparison with CRC-associated genes reveals 89 proteins (Figure 1A). Based on gene ontology analyses these proteins are involved in biological processes (negative regulation of apoptosis, cell adhesion, DNA repair) and pathways (*e.g.*, PI3K, cell cycle) promoting colon carcinogenesis (Figure 1B and C). Moreover, gene set enrichment analysis indicates a significant enrichment of SG-associated genes in tumors as compared to non-tumor tissues (Figure 1B), with several oncogenes (*e.g.*, CDK1, SND1, HSPD1) upregulated in CRC. Together, these data suggest that the SGs proteome represents an important "*reservoir*" of cancer-related

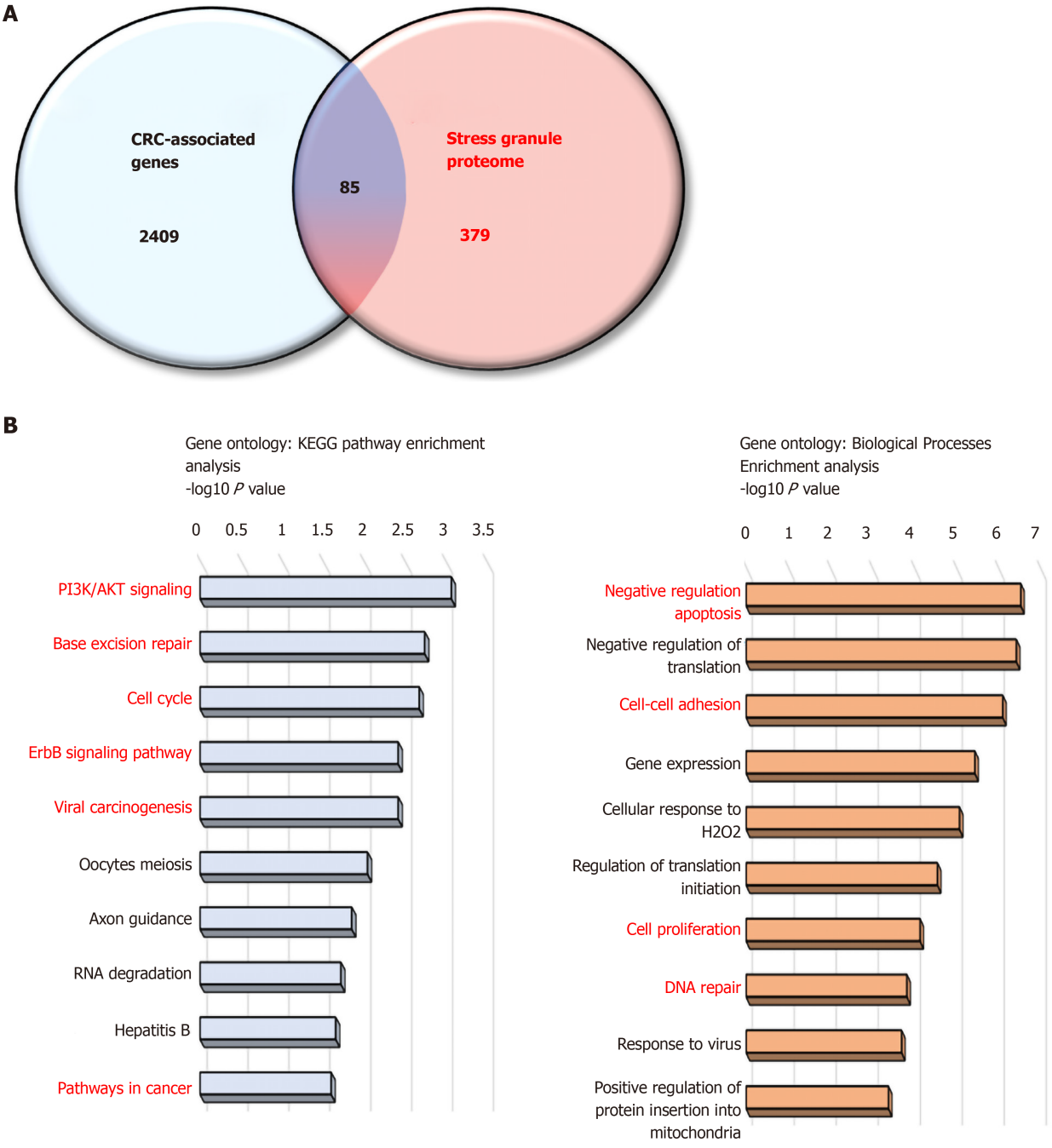
A
CRC-associated genes
2409
85
Stress granule proteome
379
B
Gene ontology: KEGG pathway enrichment analysis
-log10 P value
0 0.5 1 1.5 2 2.5 3 3.5
PI3K/AKT signaling
Base excision repair
Cell cycle
ErbB signaling pathway
Viral carcinogenesis
Oocytes meiosis
Axon guidance
RNA degradation
Hepatitis B
Pathways in cancer
Gene ontology: Biological Processes Enrichment analysis
-log10 P value
0 1 2 3 4 5 6 7
Negative regulation apoptosis
Negative regulation of translation
Cell-cell adhesion
Gene expression
Cellular response to H2O2
Regulation of translation initiation
Cell proliferation
DNA repair
Response to virus
Positive regulation of protein insertion into mitochondria

Figure 1 The stress granule proteome contains several colorectal cancer-associated proteins. A: Venn diagram merging a list of colorectal cancer (CRC) -associated genes (retrieved from Metacore software) and the mammalian stress granule (SG) proteome from https://msgp.pt; B: Gene ontology analysis of SG proteome using KEGG pathway and biological processes analysis. Enrichment is represented with a-log10 *P* value. Processes and pathways in red are those involved in cancer development; C: Gene-Set Enrichment Analysis (version 3.0, Broad Institute, Cambridge, MA, United States) of the SG proteome on CRC patients (GSE113513). The top 20 genes upregulated in CRC patients as compared to non-tumoral tissues are represented in a heatmap. The enrichment score was calculated using the number of genes ranking at the top or the bottom of the gene list (permutation type: Phenotype; with 1000 permutations). The Signal2Noise was used for ranking genes. A nominal *P* value < 0.05 and an FDR < 0.2 were considered significant.

factors, suggesting that the role of SGs in CRC is largely underestimated. Moreover, how various factors such as the genetic landscape (mutations), tumor etiology, lifestyle factors, and the gut microbiota influence the composition of the SGs proteome and tumor transcriptome is currently unknown. Therefore, it is likely that a different composition of SGs may differentially affect cancer-related processes based on intrinsic and external factors.

Several SG-associated proteins affect cancer hallmarks and pathways. For instance, under stress conditions the RBFOX2 (RBP fox-1 homolog 2) localizes in SGs and promotes cell cycle progression by decreasing RB1 protein expression in colon cancer cells[101]. Accordingly, RBFOX2 was found strongly upregulated in colon tumors, while RB1 was downregulated as compared to normal tissues. The pro-apoptotic factor RACK1 (Receptor for Activated C Kinase), which binds to and activates the stress responsive MTK1 MAPKKK[23], is sequestered into SGs in stress conditions and impairs its pro-apoptotic function. This effect has been also observed with chemotherapeutic agents such as 5-FU in HeLa cells, thus suggesting that RACK1 overexpression in CRC may also contribute to CRC chemoresistance[102]. In CRC, RACK1 is overexpressed and acts as a tumor promoter correlated with clinical outcomes[103]. Finally, PDCD4, another pro-apoptotic factor[104] is also localized in SGs[21] but it is currently unclear whether its sequestration in SGs impairs its pro-apoptotic function.

Post-translational modifications and SGs formation in CRC

Although several post-translational modifications of key proteins involved in SGs assembly have been identified, these alterations have yet to be studied in the CRC context. Nevertheless, it has been observed that the expression and activity of the proteins involved in modifying SGs factors can be altered in CRC.

Acetylation and deacetylation of SGs components: Acetylation of SG-associated proteins importantly regulate SGs assembly with several acetylases and deacetylases linked to this regulation. As previously discussed, acetylation of K376 of G3BP1 by the CBP/P300 acetylase is a key modification impeding SGs assembly by impairing its RNA binding function, as well as its interaction with PABP1, USP10 or Caprin1[12]. However, this link in CRC is unclear considering that the expression of CBP/P300 is

upregulated in CRC[105,106]. Conversely, the histone deacetylase HDAC6 directly interacts and deacetylates G3BP1 and promotes SGs formation[12]. In agreement with these findings, SG disassembly is associated with increased acetylation of K376[12] and inactivation of HDAC6 catalytic domain impairs SGs formation in 293T cells[51]. The interaction of HDAC6 with G3BP1 is prevented by G3BP1 phosphorylation on Ser^{149} [51]. Moreover, microtubules contribute to SG growth by supplying additional RNPs and other SG-associated proteins, are also subjected to acetylation modifications that markedly alter their dynamics. HDAC6 is also a microtubule-associated deacetylase[107] and its activity reduces tubulin-α acetylation on Lys40 in NIH3T3 cells and increases cell motility[107]. The activity of HDAC6 on microtubules and other motor proteins (*e.g.*, dyneins) promotes SGs formation[51]. Taken together, these findings indicate that HDAC6 displays pleiotropic functions to promotes SGs assembly. While the role of HDAC6 in SGs assembly in CRC is currently unknown, its overexpression is observed in colorectal tumors compared to adjacent normal tissue and this may considerably favor SGs assembly[51]. Moreover, HDAC6 inhibitors can sensitize CRC cells to oxaliplatin[108].

SIRT6 is a NAD+-dependent deacetylase, which directly interacts with G3BP1. SIRT6 deficiency promotes G3BP1 phosphorylation at Ser^{149} and reduces SGs assembly[109]. Similar to HDAC6, the link between SIRT6 and SGs in CRC has not been established and discrepant observations have been reported regarding SIRT6 level in human CRC with studies reporting downregulation[110,111] or overexpression[112]. Nevertheless, SIRT6 overexpression correlates with a better prognosis in CRC patients and inhibits tumor progression[113,111].

Casein Kinase-2 (CK2): Phosphorylation of G3BP1 on Ser^{149} by CK2 impairs SGs formation in U2OS osteosarcoma cells[13]. This link has not been explored in CRC and the role of CK2 in colon cancer is currently unclear, with studies reporting both oncogenic and tumor suppressive functions[114,115]. CK2 expression and activity is increased in animal models of ulcerative colitis[116], suggesting that its altered expression represents an early alteration, potentially involved in colorectal carcinogenesis. In colon cancer cells, CK2 overexpression sensitizes cells to 5-FU[117,118] and promotes the degradation of several cancer-promoting transcripts by enhancing TTP function[115]. In contrast, CK2 enhances colon cancer cell viability by promoting COX-2 expression and PGE2 production[114].

Methylation of SG components: Protein Arginine Methyltransferase 1/5 (PRMT1/5) methylates several SGs components including G3BP1, G3BP2, FUS/LTS and UBAP2L. This methylation impairs the interaction of these SGs components (*e.g.*, UBAP2L/G3BP1) and inhibits SGs assembly[35]. Paradoxically, various studies indicate an increase of SGs formation in colorectal cancer, PRMT1 and 5 are upregulated in tumors[119] (Table 1), suggesting that colon cancer cells adapt to circumvent this negative regulatory mechanism. A potential mechanism involves the histone arginine demethylase JMJD6 (Jumonji domain-containing 6), which promotes SGs formation by demethylating G3BP1[120]. In colon cancer JMJD6 is upregulated and exerts oncogenic functions (*e.g.*, negative regulation of p53 signaling)[121]. Therefore, SG formation in colon cancer may depend on a fine-tuned equilibrium between PRMTs and JMJD6 activities.

AMPK/mTORC1 signaling: The role of AMPK and mTORC1 signaling in SGs formation is intriguing because in many models, SGs formation has been associated to a reduction of mTORC1 activity and/or activation of AMPK. However, in CRC mTORC1 activity is increased[122] and the link between mTORC1 inhibition and SGs assembly is likely to be cell type and context dependent[123]. In agreement with this, increased activity of mTORC1 by PI3K or p38 MAPK kinases has been associated to SGs formation in breast cancer cells[16]. These pathways are commonly overactive in CRC[124,125], and the downstream activation of mTORC1 may represent an important event triggering SGs assembly in colon cancer cells. The complexity mTORC1 signaling is further enhanced by AMPKα, which is an negative upstream regulator of mTORC1 signaling, in promoting SGs assembly[17] and is frequently upregulated in CRC[126,127]. Besides its regulatory function on SGs assembly, mTORC1 is also localized to SGs in stress conditions, thus impairing protein synthesis[128]. Once the stress signals dissipate, DYRK3 (Dual Specificity Tyrosine Phosphorylation Regulated Kinase 3) promotes the re-localization of mTORC1 to the cytosol to facilitate protein synthesis[128]. However, this regulatory mechanism remains to be demonstrated in the context of CRC.

SGs clearance in CRC

In addition of overexpression of nucleating proteins, alteration of SGs clearance contribute also to increased SGs in cancer cells. In this section, we discuss the various mechanisms involved in SGs dissolution and deregulated in colon cancer cells.

HspB8-HSP70-Bag3 complex: Several chaperones proteins are required for SGs clearance. In particular, the HspB8-HSP70 complex and co-chaperone protein Bag3 is involved in the "*quality control*" of SGs composition by preventing accumulation of misfolded ubiquitinated proteins in SGs[129]. Through an interaction with p62, an autophagy receptor accumulating in SGs[130], the complex targets misfolded proteins for degradation by autophagy[131]. Although they are currently no studies pertaining to HSPB8 in CRC, HSP70 and Bag3 are frequently overexpressed in CRC and contribute to cancer progression[132,133]. Although the HspB8-HSP70-Bag3 complex favors the maintenance of a normal SGs proteome function[129], this complex can also promote SGs disassembly in cases where stress persists. While this function remains to be better defined, some studies suggest that SGs clearance is mediated by autophagy[129].

Autophagy-dependent SGs clearance: Autophagy plays an important role in SGs clearance (also called "*granulophagy*")[134]. Interestingly, autophagy and SGs are concomitantly increased in cancer cells[134] and have been recognized as important survival mechanisms in cancer cells, thus suggesting that these two processes act in concert to favor cancer cells survival. The role of autophagy in CRC development has been well characterized and like for many cancers, autophagic flux is strongly increased in CRC[135]. However, the link between autophagy and SGs clearance in CRC is currently unknown.

Valosin-containing protein (VCP/p97): An ATPase, which belongs to the AAA family (ATPases-associated with diverse cellular activities)[136]. Together with several cofactors, VCP interacts with ubiquitinated proteins and promotes their extraction from protein complexes for degradation[136]. This function is required during SGs disassembly[137]. In addition, VCP is essential for autophagosome maturation[138]. Accordingly, in several diseases (*e.g.*, Inclusion body myopathy, Paget Disease), *VCP* mutations leads to a reduction of autophagy and an accumulation of SGs. VCP is also subjected to post-translational modifications, in particular phosphorylation by Unc-51-like kinases 1 and 2 (ULK1 and 2), which activates Vcp/p97 and causes SGs disassembly[137]. In CRC, ULK1 is overexpressed, while ULK2 is downregulated in tumors and the respective impact of these alterations on SG dynamics is unknown.

P-Bodies: Similar to SGs, P-bodies are also non-membrane RNA-protein complexes and their assembly is triggered by various stimuli including stress or inflammation[73]. In contrast to SGs, P-Bodies are mostly involved in mRNA decay and do not contain any translation initiation and elongation factors, but contain enzymes required for deadenylation (CAF-1, CCR4), decapping (DCP1/2), 5′ to 3′ degradation (XRN1) of mRNA transcripts[139,140]. mRNA degradation by P-bodies importantly contributes to SGs dissolution and disruption of P-body formation is likely to foster SGs accumulation[77]. Our full current understanding of the crosstalk between SGs and P-bodies is limited but appears to be a determinant of the fate of cancer-related transcripts. Some proteins like tristetraprolin (TTP) or BRF1, are localized in both compartments and can mediate the shuttling of mRNAs and promotes SG-P-body fusion[73,141]. Thus, the loss of TTP and BRF1 expression and activity in colon cancer cells may considerably alter SGs clearance. Moreover, the loss of TTP expression has been associated with a reduction of P-bodies in CRC cells[66,77].

SGS AS POTENTIAL BIOMARKERS AND THERAPEUTIC TARGETS

SGs as potential biomarkers

SGs importantly contribute to cancer cell survival to harmful conditions and represent an important barrier to chemotherapy. Assessing the expression of SGs nucleators in CRC biopsies may therefore represent a predictive approach to evaluate patient response to chemotherapy. However, the expression levels of several SGs components as well as their links with the clinical outcome are limited or unclear. Only one study has suggested that the presence of TIA-1 in tumor infiltrating lymphocytes represents a favorable survival predictive marker in colorectal cancer patients[142]. The use of public available database combining transcriptomic and survival analyses of CRC patients (GEPIA database: http://gepia.cancer-pku.cn/) can be useful to correlate the

expression level of SGs components with clinical outcomes (Table 1). However, these correlations only consider respective mRNA levels in the analyses and these alterations do not necessarily translate at the protein level. As shown in Table 1, several discrepant findings between published observations and the transcriptomic data (*e.g.*, USP10, PRMT1) can be observed. These discrepancies may also originate from heterogeneity between the patients and clinical samples evaluated. Finally, assessing the expression of individual SGs components may be insufficient considering that these proteins act in concert to promote SGs assembly. While using bioinformatic approaches to identify potential novel SG-based correlations are a notable starting point, validation efforts are still required to conclude the relevance of SGs as potential biomarkers for CRC.

SGs as therapeutic target

Inhibiting SGs formation may re-sensitize cancers cells to physiological death stimuli and anti-cancer agents (chemotherapy), as evidenced in various pre-clinical models[143]. Several strategies impairing SG assembly or SG-oncogenic activities have been developed and tested in various cancer cell types, which are discussed in the following section (Table 2).

Reducing the expression of SGs nucleators: As previously discussed, the inhibition or silencing of several proteins can efficiently prevent SGs assembly in cancer cells (*e.g.*, G3BP1, UBAP2L). Therefore, developing therapeutic strategies to limit these SGs components specifically in cancer cells may represent a novel approach to reducing tumor growth and to re-sensitizing cells to chemotherapy. Although there are currently no studies assessing the therapeutic potential of inhibiting SGs in CRC, one approach using delivery of specific siRNAs (*e.g.*, Aptamers) as a means to reduce expression of specific oncogenic targets has shown anti-tumor efficacy in CRC[144]. Such approaches could be also applied for microRNA delivery as a means to control the expression of SGs nucleators. Moreover, various small molecules have been shown to reduce the expression of SGs components in CRC cells, such as resveratrol or EGCG (Epigallocatechin-Gallate) for G3BP1[145,146]. Similarly, the peptide GAP161 can efficiently reduce G3BP1 activity and may represent a valuable tool to prevent SGs formation. This peptide markedly inhibits colon cancer cell proliferation by inducing apoptosis and sensitizing cells to cisplatin-induced apoptosis[43]. Furthermore, GAP161 reduces tumor growth *in vivo*, as evidenced in xenograft models. However, these antitumoral properties have been associated to an impairment of its interaction with RasGAP, so it is unclear whether SGs assembly is prevented in this model.

Targeting G4DNA/RNA structures: The importance of G4DNA/RNA structures in SGs assembly suggest them as novel therapeutic targets in various cancers. In agreement, the G-quadruplex ligand RHPS4 (3,11-difluoro-6,8,13-trimethyl-8Hquino) displays anti-tumor properties. However, this molecule also induces side effects such as cardiovascular alterations, suggesting caution regarding its clinical use. EMICORON, another G-quadruplex ligand displays also anti-tumor properties[147]. In colon cancer, EMICORON markedly reduces cancer progression[147] and potentiates chemotherapy in colon cancer cell lines[147].

A number of angiogenin inhibitors have been also developed and may reduce tiRNA accumulation in cancer cells. Among them, chANG, an antiangiogenin peptide, has been studied in colon cancer and shows antiangiogenic activity[148]. Moreover, a neutralizing monoclonal antibody to angiogenin prevents HT-29 colon cancer tumor progression in a xenograft model[149].

Targeting the AMPK/mTORC1 axis: SGs assembly is frequently associated to mTORC1 inhibition. Therefore, restoring normal mTORC1 activity has the potential to inhibit SGs assembly. However, increased activity of mTORC1 by PI3K or p38/MAPK kinases has been associated with SGs formation in MCF-7 breast cancer cells[150] and use of mTORC1 inhibitors may represent a potential therapeutic approach. Targeting upstream regulators of mTORC1, such as AMPK, which is a potent inhibitor of mTORC1 may also potentially impair SGs formation in cancer cells. The AMPK inhibitor Compound-C, efficiently prevents SGs assembly induced by a cold shock in yeast[151] and displays anti-cancer properties in colon cancer cells[152].

Targeting microtubules: The integrity of microtubules and motor proteins is required for RNP transport during SGs formation. Accordingly, microtubule destabilizing agents such as vinblastine or nocodazole can prevent SGs assembly, while drugs stabilizing them (*e.g.*, paclitaxel) promote SGs formation[153]. However, vinblastine is currently not used clinically for CRC treatment due to its gastrointestinal toxicity[154].

Table 2 Potential therapeutic approaches to impair stress granule function in cancer cells

Strategies	Target	Models	Known impact on SGs	Anticancer effect on CRC	Clinical trials for CRC (ID)
Targeting proteins involved in SG assembly					
EGCG	G3BP1	Lung cancer[146]	Reduction of SG assembly	Yes[181]	NCT02891538; NCT02321969; NCT01239095
Resveratrol	G3BP1	CRC[145]	Unknown	Yes[145]	NCT00433576; NCT00920803
GAP161 peptide	G3BP1	CRC[43]	Unknown	Yes[43]	None
RK-33	DDX3	CRC[182]	Unknown	Yes[182]	None
Targeting G4DNA/RNA structures					
EMICORON	G4DNA	CRC[147]	Unknown	Yes[147]	None
chANG	angiogenin	CRC[148]	Unknown	Yes[148]	None
(mAb), 26-2F	angiogenin	CRC[149]	Unknown	Yes[149]	None
Targeting AMPK/mTORC1 axis					
Compound C	AMPK	Yeast[151]CRC[152]	Impairs SG assembly in yeast[151]	Yes[152]	None
Rapamycin	mTORC1	CRC[183]	Unknown	Yes[183]	NCT00409994; NCT03439462
Everolimus	mTORC1	Breast[16]	SG inhibition	Yes[184]	NCT01154335; NCT00419159; NCT01387880
Temsirolimus	mTORC1	CRC[185]	Unknown	Yes[185]	NCT00593060; NCT00827684; NCT01183663
Targeting HDACS/SIRTs					
OSS_128167	SIRT6	Pancreas cancer[161]	Unknown	Unknown	No
A-452	HDAC6	CRC[158]	Unknown	Yes[158]	None
C1A	HDAC6	CRC[157]	Unknown	Yes[157]	None
ACY-1215	HDAC6	CRC[108]	Unknown	Yes[108]	None
MPT0G612	HDAC6	CRC[159]	Unknown	Yes[159]	None
Targeting SGs-associated RNA-binding proteins controlling cancer-related factors					
MS-444	HuR	CRC[166]	Unknown	Yes[166]	None
DHTS	HuR	CRC[186]	Unknown	Yes[186]	None
Resveratrol	RBFOX2	CRC[101]	Unknown	Yes[101]	NCT00433576; NCT00920803
Targeting microtubules					
Paclitaxel	Microtubules	Green monkey kidney fibroblasts (CV-1 cells)[153]	Promotes SG formation	Yes[187]	NCT00598247; NCT00024401; NCT00667641
Vinblastine	Microtubules	Green monkey kidney fibroblasts (CV-1 cells)[153]	Prevents SG assembly	Yes[188]	None

Several approaches can be used to efficiently reduce stress granule assembly and their oncogenic activities. This table provides some examples for each strategy. Some of them have been tested in colorectal cancers models and others have reached clinical trials (https://clinicaltrials.gov/). SG: Stress granule; CRC: Colorectal cancer.

Identifying new microtubule destabilizing agents with less side effects may potentially provide beneficial outcome to CRC patients. Several microtubule destabilizing agents have been developed and are currently used for the treatment of other cancers, such as eribulin for breast cancer[155,156].

HDAC and SIRT inhibitors: HDAC6 and SIRT6 activity promote SGs formation in cancer cells[51,109]. Several HDAC6 inhibitors have been developed such as A452, C1A, ACY-1215, MPT0G612, and have been shown to reduce CRC tumor growth and sensitize to cells to chemotherapeutic agents[108,157-159]. Targeting SIRT6 with specific inhibitors may also represent a potential approach to impair SGs assembly. However,

only few SIRT6 inhibitors have been developed (*e.g.*, OSS_128167)[160-162] and their effects on SGs assembly and CRC is currently unknown.

Targeting autophagy: The clearance of SGs is mediated by autophagy[163] and increasing autophagic flux in cancer cells may potentially lower the amount of SGs and re-sensitize cancer cells to chemotherapy. Alternatively, autophagy has been considered as an important survival mechanism of CRC cells and several molecules impairing autophagy have been implicated as novel therapeutics[135]. However, it remains to determine whether autophagy impairment can lead to an impairment of SGs clearance, which may potentially favor cancer cell survival and tumor recurrence.

Targeting SGs-associated RNA-binding proteins controlling cancer-related factors: Several RBPs are localized in SGs and control the translation/stability of various cancer-related transcripts (*i.e.*, oncogenes, tumor suppressors). Targeting these proteins may represent an appealing approach to reduce the oncogenic properties of SGs in CRC. In that sense, several strategies aiming at inhibiting HuR expression and activity have been proposed[164]. Among them, the HuR inhibitor MS-444, a polyketides purified from microbial extracts, represents an interesting candidate due to its potent anti-cancerous properties in various cancers (*e.g.*, colorectal cancer, pancreatic cancer, malignant glioma)[165,166]. MS-444 prevents HuR cytoplasmic export by inhibiting its homodimerization, thereby reducing the stability of its mRNA targets. Moreover, the anti-tumor properties of MS-444 was further observed in a mouse model of Familial Adenomatous Polyposis (*i.e.*, APC^{Min} mice)[87], thus showing the effectiveness of this molecule *in vivo*.

Finally, molecules preventing the sequestration of pro-apoptotic factors within SGs may also represent a potential approach to reduce cancer cell survival. For instance, resveratrol can prevent RBFOX2 localization in stress granules, thus inhibiting cancer cell proliferation[101].

CONCLUSION

Due to the aging population and increased incidence of chronic bowel diseases, coupled with less than optimal lifestyle habits, an increased incidence in CRC cases is expected in the near future[167]. Further investigation into the molecular mechanisms associated with colon carcinogenesis is therefore needed in order to identify new targets for novel therapeutic approaches. Increasing evidence indicate that SGs are key players involved in CRC tumorigenesis and chemoresistance. Based on current findings, the assembly of SGs and their role in CRC development relies on multiple changes in the factors involved in SG nucleation and clearance (Figure 2). Early alterations of SGs components in preneoplastic conditions (*e.g.*, IBD) may also allow altered cells to survive and accumulate further defects contributing to tumorigenesis. Moreover, the link between other chronic diseases such as diabetes and obesity, which are important risk factors for CRC development, represent new areas where SGs assembly needs to be clarified. Other potential contributing factors, such as gut microbiota dysbiosis should also be considered as a potential driver of SGs formation in cancer cells. Beside the proteins discussed in this review, several other SG components have been identified and have been recognized as regulators of SGs assembly in other cancer types, such as FMRP, ATX-2, the RNA helicase DDX3X[168], TDP-43[169], DYRK3[128], PDCD4[21] or FUS[170], and continued work will determine the function of these proteins in CRC. Other proteins, which are associated with SGs are also important regulators of cancerous processes (*e.g.*, cell cycle progression, cancer cell migration and invasion). Although the role of these factors in SG biology is currently unclear, their storage in these granules may represent an important "*reservoir*", favoring cancer cell survival in stress-related conditions. As CRC remains one of the deadliest cancers worldwide, employing strategies aimed at impairing SG assembly may re-sensitize cancer cells to chemotherapy and improve clinical outcomes. Such approaches may provide beneficial effects to CRC patients, along with other cancers where clinical options are limited and only a few therapeutic options exist. In this review, we discussed several strategies that could be employed to reduce SG formation in cancer cells. However, the efficiency of such approaches in colorectal cancer and SG assembly needs to be firmly established. Moreover, the potential side effects that could be associated with these strategies (*e.g.*, the G-quadruplex ligand RHPS4 which induces cardiovascular side effects) need to be carefully evaluated using *in vivo* models. Moreover, the role of some regulators of SGs formation in CRC is still

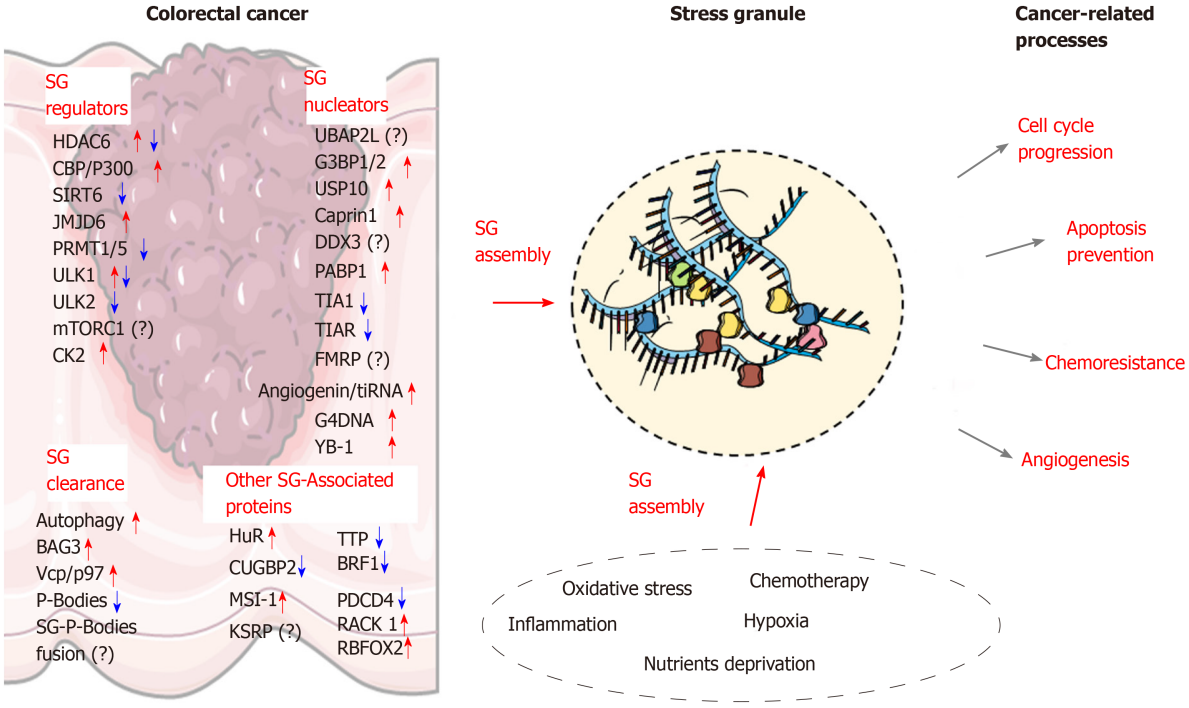

Figure 2 The molecular landscape underlying stress granules formation in colorectal cancer. Stress granules (SGs) assembly in colorectal cancer cells is associated with several alterations in the expression of proteins involved in SG nucleation or clearance. The stress-related conditions within the tumor microenvironment and various antitumor agents can further promote SGs assembly. Several SG-associated proteins (RNA-binding proteins or others) contribute to various cancer-related processes such as cell cycle progression, apoptosis inhibition, angiogenesis, and chemoresistance. Illustrations were retrieved from Servier Medical art (https://smart.servier.com/). SG: Stress granules.

unclear (*e.g.*, mTORC1, AMPK) and thus a better understanding of their function in SG formation in CRC is required prior to any therapeutic interventions.

REFERENCES

1 **Bray F**, Ferlay J, Soerjomataram I, Siegel RL, Torre LA, Jemal A. Global cancer statistics 2018: GLOBOCAN estimates of incidence and mortality worldwide for 36 cancers in 185 countries. *CA Cancer J Clin* 2018; **68**: 394-424 [PMID: 30207593 DOI: 10.3322/caac.21492]

2 **Marley AR**, Nan H. Epidemiology of colorectal cancer. *Int J Mol Epidemiol Genet* 2016; **7**: 105-114 [PMID: 27766137]

3 **De Rosa M**, Pace U, Rega D, Costabile V, Duraturo F, Izzo P, Delrio P. Genetics, diagnosis and management of colorectal cancer (Review). *Oncol Rep* 2015; **34**: 1087-1096 [PMID: 26151224 DOI: 10.3892/or.2015.4108]

4 **Anderson P**, Kedersha N. Stress granules: the Tao of RNA triage. *Trends Biochem Sci* 2008; **33**: 141-150 [PMID: 18291657 DOI: 10.1016/j.tibs.2007.12.003]

5 **Anderson P**, Kedersha N. RNA granules. *J Cell Biol* 2006; **172**: 803-808 [PMID: 16520386 DOI: 10.1083/jcb.200512082]

6 **Anderson P**, Kedersha N, Ivanov P. Stress granules, P-bodies and cancer. *Biochim Biophys Acta* 2015; **1849**: 861-870 [PMID: 25482014 DOI: 10.1016/j.bbagrm.2014.11.009]

7 **Panas MD**, Ivanov P, Anderson P. Mechanistic insights into mammalian stress granule dynamics. *J Cell Biol* 2016; **215**: 313-323 [PMID: 27821493 DOI: 10.1083/jcb.201609081]

8 **Kedersha N**, Ivanov P, Anderson P. Stress granules and cell signaling: more than just a passing phase? *Trends Biochem Sci* 2013; **38**: 494-506 [PMID: 24029419 DOI: 10.1016/j.tibs.2013.07.004]

9 **Protter DSW**, Parker R. Principles and Properties of Stress Granules. *Trends Cell Biol* 2016; **26**: 668-679 [PMID: 27289443 DOI: 10.1016/j.tcb.2016.05.004]

10 **Molliex A**, Temirov J, Lee J, Coughlin M, Kanagaraj AP, Kim HJ, Mittag T, Taylor JP. Phase separation by low complexity domains promotes stress granule assembly and drives pathological fibrillization. *Cell* 2015; **163**: 123-133 [PMID: 26406374 DOI: 10.1016/j.cell.2015.09.015]

11 **Chernov KG**, Barbet A, Hamon L, Ovchinnikov LP, Curmi PA, Pastré D. Role of microtubules in stress granule assembly: microtubule dynamical instability favors the formation of micrometric stress granules in cells. *J Biol Chem* 2009; **284**: 36569-36580 [PMID: 19843517 DOI: 10.1074/jbc.M109.042879]

12 **Gal J**, Chen J, Na DY, Tichacek L, Barnett KR, Zhu H. The Acetylation of Lysine-376 of G3BP1 Regulates RNA Binding and Stress Granule Dynamics. *Mol Cell Biol* 2019; **39**: e00052-19 [PMID: 31481451 DOI: 10.1128/MCB.00052-19]

13 **Reineke LC**, Tsai WC, Jain A, Kaelber JT, Jung SY, Lloyd RE. Casein Kinase 2 Is Linked to Stress

Granule Dynamics through Phosphorylation of the Stress Granule Nucleating Protein G3BP1. *Mol Cell Biol* 2017; **37**: e00596-16 [PMID: 27920254 DOI: 10.1128/MCB.00596-16]
14 **Tsai WC**, Gayatri S, Reineke LC, Sbardella G, Bedford MT, Lloyd RE. Arginine Demethylation of G3BP1 Promotes Stress Granule Assembly. *J Biol Chem* 2016; **291**: 22671-22685 [PMID: 27601476 DOI: 10.1074/jbc.M116.739573]
15 **Bikkavilli RK**, Malbon CC. Arginine methylation of G3BP1 in response to Wnt3a regulates β-catenin mRNA. *J Cell Sci* 2011; **124**: 2310-2320 [PMID: 21652632 DOI: 10.1242/jcs.084046]
16 **Heberle AM**, Razquin Navas P, Langelaar-Makkinje M, Kasack K, Sadik A, Faessler E, Hahn U, Marx-Stoelting P, Opitz CA, Sers C, Heiland I, Schäuble S, Thedieck K. The PI3K and MAPK/p38 pathways control stress granule assembly in a hierarchical manner. *Life Sci Alliance* 2019; **2**: e201800257 [PMID: 30923191 DOI: 10.26508/lsa.201800257]
17 **Mahboubi H**, Koromilas AE, Stochaj U. AMP Kinase Activation Alters Oxidant-Induced Stress Granule Assembly by Modulating Cell Signaling and Microtubule Organization. *Mol Pharmacol* 2016; **90**: 460-468 [PMID: 27430620 DOI: 10.1124/mol.116.105494]
18 **Chen L**, Liu B. Relationships between Stress Granules, Oxidative Stress, and Neurodegenerative Diseases. *Oxid Med Cell Longev* 2017; **2017**: 1809592 [PMID: 28194255 DOI: 10.1155/2017/1809592]
19 **Mahboubi H**, Stochaj U. Cytoplasmic stress granules: Dynamic modulators of cell signaling and disease. *Biochim Biophys Acta Mol Basis Dis* 2017; **1863**: 884-895 [PMID: 28095315 DOI: 10.1016/j.bbadis.2016.12.022]
20 **Herman AB**, Silva Afonso M, Kelemen SE, Ray M, Vrakas CN, Burke AC, Scalia RG, Moore K, Autieri MV. Regulation of Stress Granule Formation by Inflammation, Vascular Injury, and Atherosclerosis. *Arterioscler Thromb Vasc Biol* 2019; **39**: 2014-2027 [PMID: 31462091 DOI: 10.1161/ATVBAHA.119.313034]
21 **Bai Y**, Dong Z, Shang Q, Zhao H, Wang L, Guo C, Gao F, Zhang L, Wang Q. Pdcd4 Is Involved in the Formation of Stress Granule in Response to Oxidized Low-Density Lipoprotein or High-Fat Diet. *PLoS One* 2016; **11**: e0159568 [PMID: 27454120 DOI: 10.1371/journal.pone.0159568]
22 **Stoecklin G**, Stubbs T, Kedersha N, Wax S, Rigby WF, Blackwell TK, Anderson P. MK2-induced tristetraprolin:14-3-3 complexes prevent stress granule association and ARE-mRNA decay. *EMBO J* 2004; **23**: 1313-1324 [PMID: 15014438 DOI: 10.1038/sj.emboj.7600163]
23 **Arimoto K**, Fukuda H, Imajoh-Ohmi S, Saito H, Takekawa M. Formation of stress granules inhibits apoptosis by suppressing stress-responsive MAPK pathways. *Nat Cell Biol* 2008; **10**: 1324-1332 [PMID: 18836437 DOI: 10.1038/ncb1791]
24 **Rounbehler RJ**, Fallahi M, Yang C, Steeves MA, Li W, Doherty JR, Schaub FX, Sanduja S, Dixon DA, Blackshear PJ, Cleveland JL. Tristetraprolin impairs myc-induced lymphoma and abolishes the malignant state. *Cell* 2012; **150**: 563-574 [PMID: 22863009 DOI: 10.1016/j.cell.2012.06.033]
25 **Kurosu T**, Ohga N, Hida Y, Maishi N, Akiyama K, Kakuguchi W, Kuroshima T, Kondo M, Akino T, Totsuka Y, Shindoh M, Higashino F, Hida K. HuR keeps an angiogenic switch on by stabilising mRNA of VEGF and COX-2 in tumour endothelium. *Br J Cancer* 2011; **104**: 819-829 [PMID: 21285980 DOI: 10.1038/bjc.2011.20]
26 **Young LE**, Sanduja S, Bemis-Standoli K, Pena EA, Price RL, Dixon DA. The mRNA binding proteins HuR and tristetraprolin regulate cyclooxygenase 2 expression during colon carcinogenesis. *Gastroenterology* 2009; **136**: 1669-1679 [PMID: 19208339 DOI: 10.1053/j.gastro.2009.01.010]
27 **Ishimaru D**, Ramalingam S, Sengupta TK, Bandyopadhyay S, Dellis S, Tholanikunnel BG, Fernandes DJ, Spicer EK. Regulation of Bcl-2 expression by HuR in HL60 leukemia cells and A431 carcinoma cells. *Mol Cancer Res* 2009; **7**: 1354-1366 [PMID: 19671677 DOI: 10.1158/1541-7786.MCR-08-0476]
28 **Cui J**, Placzek WJ. Post-Transcriptional Regulation of Anti-Apoptotic BCL2 Family Members. *Int J Mol Sci* 2018; **19**: 308 [PMID: 29361709 DOI: 10.3390/ijms19010308]
29 **Omer A**, Patel D, Lian XJ, Sadek J, Di Marco S, Pause A, Gorospe M, Gallouzi IE. Stress granules counteract senescence by sequestration of PAI-1. *EMBO Rep* 2018; **19**: e44722 [PMID: 29592859 DOI: 10.15252/embr.201744722]
30 **Campisi J**. Cellular senescence as a tumor-suppressor mechanism. *Trends Cell Biol* 2001; **11**: S27-S31 [PMID: 11684439 DOI: 10.1016/s0962-8924(01)02151-1]
31 **Heck MV**, Azizov M, Stehning T, Walter M, Kedersha N, Auburger G. Dysregulated expression of lipid storage and membrane dynamics factors in Tia1 knockout mouse nervous tissue. *Neurogenetics* 2014; **15**: 135-144 [PMID: 24659297 DOI: 10.1007/s10048-014-0397-x]
32 **Martin S**, Zekri L, Metz A, Maurice T, Chebli K, Vignes M, Tazi J. Deficiency of G3BP1, the stress granules assembly factor, results in abnormal synaptic plasticity and calcium homeostasis in neurons. *J Neurochem* 2013; **125**: 175-184 [PMID: 23373770 DOI: 10.1111/jnc.12189]
33 **Madura K**. The ubiquitin-associated (UBA) domain: on the path from prudence to prurience. *Cell Cycle* 2002; **1**: 235-244 [PMID: 12429939 DOI: 10.4161/cc.1.4.130]
34 **Youn JY**, Dunham WH, Hong SJ, Knight JDR, Bashkurov M, Chen GI, Bagci H, Rathod B, MacLeod G, Eng SWM, Angers S, Morris Q, Fabian M, Côté JF, Gingras AC. High-Density Proximity Mapping Reveals the Subcellular Organization of mRNA-Associated Granules and Bodies. *Mol Cell* 2018; **69**: 517-532.e11 [PMID: 29395067 DOI: 10.1016/j.molcel.2017.12.020]
35 **Huang C**, Chen Y, Dai H, Zhang H, Xie M, Zhang H, Chen F, Kang X, Bai X, Chen Z. UBAP2L arginine methylation by PRMT1 modulates stress granule assembly. *Cell Death Differ* 2020; **27**: 227-241 [PMID: 31114027 DOI: 10.1038/s41418-019-0350-5]
36 **Cirillo L**, Cieren A, Barbieri S, Khong A, Schwager F, Parker R, Gotta M. UBAP2L Forms Distinct Cores that Act in Nucleating Stress Granules Upstream of G3BP1. *Curr Biol* 2020; **30**: 698-707.e6 [PMID: 31956030 DOI: 10.1016/j.cub.2019.12.020]
37 **Li Q**, Wang W, Hu YC, Yin TT, He J. Knockdown of Ubiquitin Associated Protein 2-Like (UBAP2L) Inhibits Growth and Metastasis of Hepatocellular Carcinoma. *Med Sci Monit* 2018; **24**: 7109-7118 [PMID: 30291221 DOI: 10.12659/MSM.912861]
38 **Li D**, Huang Y. Knockdown of ubiquitin associated protein 2-like inhibits the growth and migration of prostate cancer cells. *Oncol Rep* 2014; **32**: 1578-1584 [PMID: 25069639 DOI: 10.3892/or.2014.3360]

39 **Zhao B**, Zong G, Xie Y, Li J, Wang H, Bian E. Downregulation of ubiquitin-associated protein 2-like with a short hairpin RNA inhibits human glioma cell growth *in vitro*. *Int J Mol Med* 2015; **36**: 1012-1018 [PMID: 26310274 DOI: 10.3892/ijmm.2015.2323]

40 **Chai R**, Yu X, Tu S, Zheng B. Depletion of UBA protein 2-like protein inhibits growth and induces apoptosis of human colorectal carcinoma cells. *Tumour Biol* 2016; **37**: 13225-13235 [PMID: 27456362 DOI: 10.1007/s13277-016-5159-y]

41 **French J**, Stirling R, Walsh M, Kennedy HD. The expression of Ras-GTPase activating protein SH3 domain-binding proteins, G3BPs, in human breast cancers. *Histochem J* 2002; **34**: 223-231 [PMID: 12587999 DOI: 10.1023/a:1021737413055]

42 **Götte B**, Panas MD, Hellström K, Liu L, Samreen B, Larsson O, Ahola T, McInerney GM. Separate domains of G3BP promote efficient clustering of alphavirus replication complexes and recruitment of the translation initiation machinery. *PLoS Pathog* 2019; **15**: e1007842 [PMID: 31199850 DOI: 10.1371/journal.ppat.1007842]

43 **Zhang H**, Zhang S, He H, Zhao W, Chen J, Shao RG. GAP161 targets and downregulates G3BP to suppress cell growth and potentiate cisplaitin-mediated cytotoxicity to colon carcinoma HCT116 cells. *Cancer Sci* 2012; **103**: 1848-1856 [PMID: 22703643 DOI: 10.1111/j.1349-7006.2012.02361.x]

44 **Matsuki H**, Takahashi M, Higuchi M, Makokha GN, Oie M, Fujii M. Both G3BP1 and G3BP2 contribute to stress granule formation. *Genes Cells* 2013; **18**: 135-146 [PMID: 23279204 DOI: 10.1111/gtc.12023]

45 **Tourrière H**, Chebli K, Zekri L, Courselaud B, Blanchard JM, Bertrand E, Tazi J. The RasGAP-associated endoribonuclease G3BP assembles stress granules. *J Cell Biol* 2003; **160**: 823-831 [PMID: 12642610 DOI: 10.1083/jcb.200212128]

46 **Kedersha N**, Panas MD, Achorn CA, Lyons S, Tisdale S, Hickman T, Thomas M, Lieberman J, McInerney GM, Ivanov P, Anderson P. G3BP-Caprin1-USP10 complexes mediate stress granule condensation and associate with 40S subunits. *J Cell Biol* 2016; **212**: 845-860 [PMID: 27022092 DOI: 10.1083/jcb.201508028]

47 **Kim K**, Huh T, Park Y, Koo DH, Kim H, Hwang I, Choi CH, Yi JM, Chung JY. Prognostic significance of USP10 and p14ARF expression in patients with colorectal cancer. *Pathol Res Pract* 2020; **216**: 152988 [PMID: 32362421 DOI: 10.1016/j.prp.2020.152988]

48 **Fogt F**, Poremba C, Shibao K, Itoh H, Kohno K, Zimmerman RL, Görtz HG, Dockhorn-Dworniczak B, Urbanski SJ, Alsaigh N, Heinz D, Noffsinger AE, Shroyer KR. Expression of survivin, YB-1, and KI-67 in sporadic adenomas and dysplasia-associated lesions or masses in ulcerative colitis. *Appl Immunohistochem Mol Morphol* 2001; **9**: 143-149 [PMID: 11396632 DOI: 10.1097/00129039-200106000-00007]

49 **Somasekharan SP**, El-Naggar A, Leprivier G, Cheng H, Hajee S, Grunewald TG, Zhang F, Ng T, Delattre O, Evdokimova V, Wang Y, Gleave M, Sorensen PH. YB-1 regulates stress granule formation and tumor progression by translationally activating G3BP1. *J Cell Biol* 2015; **208**: 913-929 [PMID: 25800057 DOI: 10.1083/jcb.201411047]

50 **Panas MD**, Kedersha N, Schulte T, Branca RM, Ivanov P, Anderson P. Phosphorylation of G3BP1-S149 does not influence stress granule assembly. *J Cell Biol* 2019; **218**: 2425-2432 [PMID: 31171631 DOI: 10.1083/jcb.201801214]

51 **Kwon S**, Zhang Y, Matthias P. The deacetylase HDAC6 is a novel critical component of stress granules involved in the stress response. *Genes Dev* 2007; **21**: 3381-3394 [PMID: 18079183 DOI: 10.1101/gad.461107]

52 **Liu Y**, Liu R, Yang F, Cheng R, Chen X, Cui S, Gu Y, Sun W, You C, Liu Z, Sun F, Wang Y, Fu Z, Ye C, Zhang C, Li J, Chen X. miR-19a promotes colorectal cancer proliferation and migration by targeting TIA1. *Mol Cancer* 2017; **16**: 53 [PMID: 28257633 DOI: 10.1186/s12943-017-0625-8]

53 **Dixon DA**, Balch GC, Kedersha N, Anderson P, Zimmerman GA, Beauchamp RD, Prescott SM. Regulation of cyclooxygenase-2 expression by the translational silencer TIA-1. *J Exp Med* 2003; **198**: 475-481 [PMID: 12885872 DOI: 10.1084/jem.20030616]

54 **Chiou GY**, Yang TW, Huang CC, Tang CY, Yen JY, Tsai MC, Chen HY, Fadhilah N, Lin CC, Jong YJ. Musashi-1 promotes a cancer stem cell lineage and chemoresistance in colorectal cancer cells. *Sci Rep* 2017; **7**: 2172 [PMID: 28526879 DOI: 10.1038/s41598-017-02057-9]

55 **Shih JW**, Wang WT, Tsai TY, Kuo CY, Li HK, Wu Lee YH. Critical roles of RNA helicase DDX3 and its interactions with eIF4E/PABP1 in stress granule assembly and stress response. *Biochem J* 2012; **441**: 119-129 [PMID: 21883093 DOI: 10.1042/BJ20110739]

56 **Wu DW**, Lin PL, Cheng YW, Huang CC, Wang L, Lee H. DDX3 enhances oncogenic KRAS-induced tumor invasion in colorectal cancer *via* the β-catenin/ZEB1 axis. *Oncotarget* 2016; **7**: 22687-22699 [PMID: 27007150 DOI: 10.18632/oncotarget.8143]

57 **He TY**, Wu DW, Lin PL, Wang L, Huang CC, Chou MC, Lee H. DDX3 promotes tumor invasion in colorectal cancer *via* the CK1ε/Dvl2 axis. *Sci Rep* 2016; **6**: 21483 [PMID: 26892600 DOI: 10.1038/srep21483]

58 **Bol GM**, Xie M, Raman V. DDX3, a potential target for cancer treatment. *Mol Cancer* 2015; **14**: 188 [PMID: 26541825 DOI: 10.1186/s12943-015-0461-7]

59 **Tantravedi S**, Vesuna F, Winnard PT Jr, Van Voss MRH, Van Diest PJ, Raman V. Role of DDX3 in the pathogenesis of inflammatory bowel disease. *Oncotarget* 2017; **8**: 115280-115289 [PMID: 29383159 DOI: 10.18632/oncotarget.23323]

60 **Byrd AK**, Zybailov BL, Maddukuri L, Gao J, Marecki JC, Jaiswal M, Bell MR, Griffin WC, Reed MR, Chib S, Mackintosh SG, MacNicol AM, Baldini G, Eoff RL, Raney KD. Evidence That G-quadruplex DNA Accumulates in the Cytoplasm and Participates in Stress Granule Assembly in Response to Oxidative Stress. *J Biol Chem* 2016; **291**: 18041-18057 [PMID: 27369081 DOI: 10.1074/jbc.M116.718478]

61 **Porru M**, Artuso S, Salvati E, Bianco A, Franceschin M, Diodoro MG, Passeri D, Orlandi A, Savorani F, D'Incalci M, Biroccio A, Leonetti C. Targeting G-Quadruplex DNA Structures by EMICORON Has a Strong Antitumor Efficacy against Advanced Models of Human Colon Cancer. *Mol Cancer Ther* 2015; **14**: 2541-2551 [PMID: 26304235 DOI: 10.1158/1535-7163.MCT-15-0253]

62 **Tao EW**, Cheng WY, Li WL, Yu J, Gao QY. tiRNAs: A novel class of small noncoding RNAs that helps cells respond to stressors and plays roles in cancer progression. *J Cell Physiol* 2020; **235**: 683-690 [PMID:

31286522 DOI: 10.1002/jcp.29057]
63 **Li S**, Shi X, Chen M, Xu N, Sun D, Bai R, Chen H, Ding K, Sheng J, Xu Z. Angiogenin promotes colorectal cancer metastasis *via* tiRNA production. *Int J Cancer* 2019; **145**: 1395-1407 [PMID: 30828790 DOI: 10.1002/ijc.32245]
64 **Lai WS**, Stumpo DJ, Blackshear PJ. Rapid insulin-stimulated accumulation of an mRNA encoding a proline-rich protein. *J Biol Chem* 1990; **265**: 16556-16563 [PMID: 2204625]
65 **Cao H**, Urban JF Jr, Anderson RA. Insulin increases tristetraprolin and decreases VEGF gene expression in mouse 3T3-L1 adipocytes. *Obesity (Silver Spring)* 2008; **16**: 1208-1218 [PMID: 18388887 DOI: 10.1038/oby.2008.65]
66 **Blanco FF**, Sanduja S, Deane NG, Blackshear PJ, Dixon DA. Transforming growth factor β regulates P-body formation through induction of the mRNA decay factor tristetraprolin. *Mol Cell Biol* 2014; **34**: 180-195 [PMID: 24190969 DOI: 10.1128/MCB.01020-13]
67 **Ogawa K**, Chen F, Kim YJ, Chen Y. Transcriptional regulation of tristetraprolin by transforming growth factor-beta in human T cells. *J Biol Chem* 2003; **278**: 30373-30381 [PMID: 12754205 DOI: 10.1074/jbc.M304856200]
68 **Chen YL**, Jiang YW, Su YL, Lee SC, Chang MS, Chang CJ. Transcriptional regulation of tristetraprolin by NF-κB signaling in LPS-stimulated macrophages. *Mol Biol Rep* 2013; **40**: 2867-2877 [PMID: 23212617 DOI: 10.1007/s11033-012-2302-8]
69 **Carballo E**, Lai WS, Blackshear PJ. Feedback inhibition of macrophage tumor necrosis factor-alpha production by tristetraprolin. *Science* 1998; **281**: 1001-1005 [PMID: 9703499]
70 **Sandler H**, Kreth J, Timmers HT, Stoecklin G. Not1 mediates recruitment of the deadenylase Caf1 to mRNAs targeted for degradation by tristetraprolin. *Nucleic Acids Res* 2011; **39**: 4373-4386 [PMID: 21278420 DOI: 10.1093/nar/gkr011]
71 **Fenger-Grøn M**, Fillman C, Norrild B, Lykke-Andersen J. Multiple processing body factors and the ARE binding protein TTP activate mRNA decapping. *Mol Cell* 2005; **20**: 905-915 [PMID: 16364915 DOI: 10.1016/j.molcel.2005.10.031]
72 **Lykke-Andersen J**, Wagner E. Recruitment and activation of mRNA decay enzymes by two ARE-mediated decay activation domains in the proteins TTP and BRF-1. *Genes Dev* 2005; **19**: 351-361 [PMID: 15687258 DOI: 10.1101/gad.1282305]
73 **Kedersha N**, Stoecklin G, Ayodele M, Yacono P, Lykke-Andersen J, Fritzler MJ, Scheuner D, Kaufman RJ, Golan DE, Anderson P. Stress granules and processing bodies are dynamically linked sites of mRNP remodeling. *J Cell Biol* 2005; **169**: 871-884 [PMID: 15967811 DOI: 10.1083/jcb.200502088]
74 **Lee SR**, Jin H, Kim WT, Kim WJ, Kim SZ, Leem SH, Kim SM. Tristetraprolin activation by resveratrol inhibits the proliferation and metastasis of colorectal cancer cells. *Int J Oncol* 2018; **53**: 1269-1278 [PMID: 29956753 DOI: 10.3892/ijo.2018.4453]
75 **Cha HJ**, Lee HH, Chae SW, Cho WJ, Kim YM, Choi HJ, Choi DH, Jung SW, Min YJ, Lee BJ, Park SE, Park JW. Tristetraprolin downregulates the expression of both VEGF and COX-2 in human colon cancer. *Hepatogastroenterology* 2011; **58**: 790-795 [PMID: 21830391 DOI: 10.3928/1081597X-20110106-02]
76 **Lee HH**, Yang SS, Vo MT, Cho WJ, Lee BJ, Leem SH, Lee SH, Cha HJ, Park JW. Tristetraprolin down-regulates IL-23 expression in colon cancer cells. *Mol Cells* 2013; **36**: 571-576 [PMID: 24292977 DOI: 10.1007/s10059-013-0268-6]
77 **Sobolewski C**, Sanduja S, Blanco FF, Hu L, Dixon DA. Histone Deacetylase Inhibitors Activate Tristetraprolin Expression through Induction of Early Growth Response Protein 1 (EGR1) in Colorectal Cancer Cells. *Biomolecules* 2015; **5**: 2035-2055 [PMID: 26343742 DOI: 10.3390/biom5032035]
78 **Blackshear PJ**. Tristetraprolin and other CCCH tandem zinc-finger proteins in the regulation of mRNA turnover. *Biochem Soc Trans* 2002; **30**: 945-952 [PMID: 12440952 DOI: 10.1042/bst0300945]
79 **Sanduja S**, Blanco FF, Dixon DA. The roles of TTP and BRF proteins in regulated mRNA decay. *Wiley Interdiscip Rev RNA* 2011; **2**: 42-57 [PMID: 21278925 DOI: 10.1002/wrna.28]
80 **Qiu Y**, Langman MJ, Eggo MC. Targets of 17beta-oestradiol-induced apoptosis in colon cancer cells: a mechanism for the protective effects of hormone replacement therapy? *J Endocrinol* 2004; **181**: 327-337 [PMID: 15128281 DOI: 10.1677/joe.0.1810327]
81 **Brennan CM**, Steitz JA. HuR and mRNA stability. *Cell Mol Life Sci* 2001; **58**: 266-277 [PMID: 11289308 DOI: 10.1007/PL00000854]
82 **Grammatikakis I**, Abdelmohsen K, Gorospe M. Posttranslational control of HuR function. *Wiley Interdiscip Rev RNA* 2017; 8 [PMID: 27307117 DOI: 10.1002/wrna.1372]
83 **Poria DK**, Guha A, Nandi I, Ray PS. RNA-binding protein HuR sequesters microRNA-21 to prevent translation repression of proinflammatory tumor suppressor gene programmed cell death 4. *Oncogene* 2016; **35**: 1703-1715 [PMID: 26189797 DOI: 10.1038/onc.2015.235]
84 **Young LE**, Moore AE, Sokol L, Meisner-Kober N, Dixon DA. The mRNA stability factor HuR inhibits microRNA-16 targeting of COX-2. *Mol Cancer Res* 2012; **10**: 167-180 [PMID: 22049153 DOI: 10.1158/1541-7786.MCR-11-0337]
85 **Kedersha N**, Anderson P. Stress granules: sites of mRNA triage that regulate mRNA stability and translatability. *Biochem Soc Trans* 2002; **30**: 963-969 [PMID: 12440955 DOI: 10.1042/bst0300963]
86 **Bley N**, Lederer M, Pfalz B, Reinke C, Fuchs T, Glaß M, Möller B, Hüttelmaier S. Stress granules are dispensable for mRNA stabilization during cellular stress. *Nucleic Acids Res* 2015; **43**: e26 [PMID: 25488811 DOI: 10.1093/nar/gku1275]
87 **Lang M**, Berry D, Passecker K, Mesteri I, Bhuju S, Ebner F, Sedlyarov V, Evstatiev R, Dammann K, Loy A, Kuzyk O, Kovarik P, Khare V, Beibel M, Roma G, Meisner-Kober N, Gasche C. HuR Small-Molecule Inhibitor Elicits Differential Effects in Adenomatosis Polyposis and Colorectal Carcinogenesis. *Cancer Res* 2017; **77**: 2424-2438 [PMID: 28428272 DOI: 10.1158/0008-5472.CAN-15-1726]
88 **Markmiller S**, Soltanieh S, Server KL, Mak R, Jin W, Fang MY, Luo EC, Krach F, Yang D, Sen A, Fulzele A, Wozniak JM, Gonzalez DJ, Kankel MW, Gao FB, Bennett EJ, Lécuyer E, Yeo GW. Context-Dependent and Disease-Specific Diversity in Protein Interactions within Stress Granules. *Cell* 2018; **172**: 590-604.e13 [PMID: 29373831 DOI: 10.1016/j.cell.2017.12.032]
89 **Natarajan G**, Ramalingam S, Ramachandran I, May R, Queimado L, Houchen CW, Anant S. CUGBP2

downregulation by prostaglandin E2 protects colon cancer cells from radiation-induced mitotic catastrophe. *Am J Physiol Gastrointest Liver Physiol* 2008; **294**: G1235-G1244 [PMID: 18325984 DOI: 10.1152/ajpgi.00037.2008]

90 **Subramaniam D**, Natarajan G, Ramalingam S, Ramachandran I, May R, Queimado L, Houchen CW, Anant S. Translation inhibition during cell cycle arrest and apoptosis: Mcl-1 is a novel target for RNA binding protein CUGBP2. *Am J Physiol Gastrointest Liver Physiol* 2008; **294**: G1025-G1032 [PMID: 18292181 DOI: 10.1152/ajpgi.00602.2007]

91 **Kudinov AE**, Karanicolas J, Golemis EA, Boumber Y. Musashi RNA-Binding Proteins as Cancer Drivers and Novel Therapeutic Targets. *Clin Cancer Res* 2017; **23**: 2143-2153 [PMID: 28143872 DOI: 10.1158/1078-0432.CCR-16-2728]

92 **Nahas GR**, Murthy RG, Patel SA, Ganta T, Greco SJ, Rameshwar P. The RNA-binding protein Musashi 1 stabilizes the oncotachykinin 1 mRNA in breast cancer cells to promote cell growth. *FASEB J* 2016; **30**: 149-159 [PMID: 26373800 DOI: 10.1096/fj.15-278770]

93 **Sureban SM**, May R, George RJ, Dieckgraefe BK, McLeod HL, Ramalingam S, Bishnupuri KS, Natarajan G, Anant S, Houchen CW. Knockdown of RNA binding protein musashi-1 leads to tumor regression *in vivo* . *Gastroenterology* 2008; **134**: 1448-1458 [PMID: 18471519 DOI: 10.1053/j.gastro.2008.02.057]

94 **Wolfe AR**, Ernlund A, McGuinness W, Lehmann C, Carl K, Balmaceda N, Neufeld KL. Suppression of intestinal tumorigenesis in *Apc* mutant mice upon Musashi-1 deletion. *J Cell Sci* 2017; **130**: 805-813 [PMID: 28082422 DOI: 10.1242/jcs.197574]

95 **Baou M**, Norton JD, Murphy JJ. AU-rich RNA binding proteins in hematopoiesis and leukemogenesis. *Blood* 2011; **118**: 5732-5740 [PMID: 21917750 DOI: 10.1182/blood-2011-07-347237]

96 **Trabucchi M**, Briata P, Garcia-Mayoral M, Haase AD, Filipowicz W, Ramos A, Gherzi R, Rosenfeld MG. The RNA-binding protein KSRP promotes the biogenesis of a subset of microRNAs. *Nature* 2009; **459**: 1010-1014 [PMID: 19458619 DOI: 10.1038/nature08025]

97 **Bikkavilli RK**, Malbon CC. Dishevelled-KSRP complex regulates Wnt signaling through post-transcriptional stabilization of beta-catenin mRNA. *J Cell Sci* 2010; **123**: 1352-1362 [PMID: 20332102 DOI: 10.1242/jcs.056176]

98 **Linker K**, Pautz A, Fechir M, Hubrich T, Greeve J, Kleinert H. Involvement of KSRP in the post-transcriptional regulation of human iNOS expression-complex interplay of KSRP with TTP and HuR. *Nucleic Acids Res* 2005; **33**: 4813-4827 [PMID: 16126846 DOI: 10.1093/nar/gki797]

99 **David Gerecht PS**, Taylor MA, Port JD. Intracellular localization and interaction of mRNA binding proteins as detected by FRET. *BMC Cell Biol* 2010; **11**: 69 [PMID: 20843363 DOI: 10.1186/1471-2121-11-69]

100 **von Roretz C**, Di Marco S, Mazroui R, Gallouzi IE. Turnover of AU-rich-containing mRNAs during stress: a matter of survival. *Wiley Interdiscip Rev RNA* 2011; **2**: 336-347 [PMID: 21957021 DOI: 10.1002/wrna.55]

101 **Choi S**, Sa M, Cho N, Kim KK, Park SH. Rbfox2 dissociation from stress granules suppresses cancer progression. *Exp Mol Med* 2019; **51**: 1-12 [PMID: 31028247 DOI: 10.1038/s12276-019-0246-y]

102 **Kaehler C**, Isensee J, Hucho T, Lehrach H, Krobitsch S. 5-Fluorouracil affects assembly of stress granules based on RNA incorporation. *Nucleic Acids Res* 2014; **42**: 6436-6447 [PMID: 24728989 DOI: 10.1093/nar/gku264]

103 **Li XY**, Hu Y, Li NS, Wan JH, Zhu Y, Lu NH. RACK1 Acts as a Potential Tumor Promoter in Colorectal Cancer. *Gastroenterol Res Pract* 2019; **2019**: 5625026 [PMID: 30962803 DOI: 10.1155/2019/5625026]

104 **Long J**, Yin Y, Guo H, Li S, Sun Y, Zeng C, Zhu W. The mechanisms and clinical significance of PDCD4 in colorectal cancer. *Gene* 2019; **680**: 59-64 [PMID: 30243936 DOI: 10.1016/j.gene.2018.09.034]

105 **Ishihama K**, Yamakawa M, Semba S, Takeda H, Kawata S, Kimura S, Kimura W. Expression of HDAC1 and CBP/p300 in human colorectal carcinomas. *J Clin Pathol* 2007; **60**: 1205-1210 [PMID: 17720775 DOI: 10.1136/jcp.2005.029165]

106 **Lazarova DL**, Chiaro C, Wong T, Drago E, Rainey A, O'Malley S, Bordonaro M. CBP Activity Mediates Effects of the Histone Deacetylase Inhibitor Butyrate on WNT Activity and Apoptosis in Colon Cancer Cells. *J Cancer* 2013; **4**: 481-490 [PMID: 23901348 DOI: 10.7150/jca.6583]

107 **Hubbert C**, Guardiola A, Shao R, Kawaguchi Y, Ito A, Nixon A, Yoshida M, Wang XF, Yao TP. HDAC6 is a microtubule-associated deacetylase. *Nature* 2002; **417**: 455-458 [PMID: 12024216 DOI: 10.1038/417455a]

108 **Lee DH**, Won HR, Ryu HW, Han JM, Kwon SH. The HDAC6 inhibitor ACY-1215 enhances the anticancer activity of oxaliplatin in colorectal cancer cells. *Int J Oncol* 2018; **53**: 844-854 [PMID: 29749542 DOI: 10.3892/ijo.2018.4405]

109 **Jedrusik-Bode M**, Studencka M, Smolka C, Baumann T, Schmidt H, Kampf J, Paap F, Martin S, Tazi J, Müller KM, Krüger M, Braun T, Bober E. The sirtuin SIRT6 regulates stress granule formation in C. elegans and mammals. *J Cell Sci* 2013; **126**: 5166-5177 [PMID: 24013546 DOI: 10.1242/jcs.130708]

110 **Qi J**, Cui C, Deng Q, Wang L, Chen R, Zhai D, Xie L, Yu J. Downregulated SIRT6 and upregulated NMNAT2 are associated with the presence, depth and stage of colorectal cancer. *Oncol Lett* 2018; **16**: 5829-5837 [PMID: 30333863 DOI: 10.3892/ol.2018.9400]

111 **Tian J**, Yuan L. Sirtuin 6 inhibits colon cancer progression by modulating PTEN/AKT signaling. *Biomed Pharmacother* 2018; **106**: 109-116 [PMID: 29957460 DOI: 10.1016/j.biopha.2018.06.070]

112 **Geng CH**, Zhang CL, Zhang JY, Gao P, He M, Li YL. Overexpression of Sirt6 is a novel biomarker of malignant human colon carcinoma. *J Cell Biochem* 2018; **119**: 3957-3967 [PMID: 29227545 DOI: 10.1002/jcb.26539]

113 **Zhang Y**, Nie L, Xu K, Fu Y, Zhong J, Gu K, Zhang L. SIRT6, a novel direct transcriptional target of FoxO3a, mediates colon cancer therapy. *Theranostics* 2019; **9**: 2380-2394 [PMID: 31149050 DOI: 10.7150/thno.29724]

114 **Yefi R**, Ponce DP, Niechi I, Silva E, Cabello P, Rodriguez DA, Marcelain K, Armisen R, Quest AF, Tapia JC. Protein kinase CK2 promotes cancer cell viability *via* up-regulation of cyclooxygenase-2 expression and enhanced prostaglandin E2 production. *J Cell Biochem* 2011; **112**: 3167-3175 [PMID: 21732411 DOI: 10.1002/jcb.23247]

115 **Lee WH**, Lee HH, Vo MT, Kim HJ, Ko MS, Im YC, Min YJ, Lee BJ, Cho WJ, Park JW. Casein kinase 2 regulates the mRNA-destabilizing activity of tristetraprolin. *J Biol Chem* 2011; **286**: 21577-21587 [PMID: 21507959 DOI: 10.1074/jbc.M110.201137]

116 **Koch S**, Capaldo CT, Hilgarth RS, Fournier B, Parkos CA, Nusrat A. Protein kinase CK2 is a critical regulator of epithelial homeostasis in chronic intestinal inflammation. *Mucosal Immunol* 2013; **6**: 136-145 [PMID: 22763408 DOI: 10.1038/mi.2012.57]

117 **Tapia JC**, Torres VA, Rodriguez DA, Leyton L, Quest AF. Casein kinase 2 (CK2) increases survivin expression *via* enhanced beta-catenin-T cell factor/lymphoid enhancer binding factor-dependent transcription. *Proc Natl Acad Sci USA* 2006; **103**: 15079-15084 [PMID: 17005722 DOI: 10.1073/pnas.0606845103]

118 **Kim HJ**, Han YS, Lee JH, Lee SH. Casein Kinase 2α Enhances 5-Fluorouracil Resistance in Colorectal Cancer Cells by Inhibiting Endoplasmic Reticulum Stress. *Anticancer Res* 2020; **40**: 1419-1426 [PMID: 32132038 DOI: 10.21873/anticanres.14083]

119 **Mathioudaki K**, Papadokostopoulou A, Scorilas A, Xynopoulos D, Agnanti N, Talieri M. The PRMT1 gene expression pattern in colon cancer. *Br J Cancer* 2008; **99**: 2094-2099 [PMID: 19078953 DOI: 10.1038/sj.bjc.6604807]

120 **Tsai WC**, Reineke LC, Jain A, Jung SY, Lloyd RE. Histone arginine demethylase JMJD6 is linked to stress granule assembly through demethylation of the stress granule-nucleating protein G3BP1. *J Biol Chem* 2017; **292**: 18886-18896 [PMID: 28972166 DOI: 10.1074/jbc.M117.800706]

121 **Wang F**, He L, Huangyang P, Liang J, Si W, Yan R, Han X, Liu S, Gui B, Li W, Miao D, Jing C, Liu Z, Pei F, Sun L, Shang Y. JMJD6 promotes colon carcinogenesis through negative regulation of p53 by hydroxylation. *PLoS Biol* 2014; **12**: e1001819 [PMID: 24667498 DOI: 10.1371/journal.pbio.1001819]

122 **Francipane MG**, Lagasse E. mTOR pathway in colorectal cancer: an update. *Oncotarget* 2014; **5**: 49-66 [PMID: 24393708 DOI: 10.18632/oncotarget.1548]

123 **Heberle AM**, Prentzell MT, van Eunen K, Bakker BM, Grellscheid SN, Thedieck K. Molecular mechanisms of mTOR regulation by stress. *Mol Cell Oncol* 2015; **2**: e970489 [PMID: 27308421 DOI: 10.4161/23723548.2014.970489]

124 **Papadatos-Pastos D**, Rabbie R, Ross P, Sarker D. The role of the PI3K pathway in colorectal cancer. *Crit Rev Oncol Hematol* 2015; **94**: 18-30 [PMID: 25591826 DOI: 10.1016/j.critrevonc.2014.12.006]

125 **Pranteda A**, Piastra V, Stramucci L, Fratantonio D, Bossi G. The p38 MAPK Signaling Activation in Colorectal Cancer upon Therapeutic Treatments. *Int J Mol Sci* 2020; **21**: 2773 [PMID: 32316313 DOI: 10.3390/ijms21082773]

126 **Wang YN**, Lu YX, Liu J, Jin Y, Bi HC, Zhao Q, Liu ZX, Li YQ, Hu JJ, Sheng H, Jiang YM, Zhang C, Tian F, Chen Y, Pan ZZ, Chen G, Zeng ZL, Liu KY, Ogasawara M, Yun JP, Ju HQ, Feng JX, Xie D, Gao S, Jia WH, Kopetz S, Xu RH, Wang F. AMPKα1 confers survival advantage of colorectal cancer cells under metabolic stress by promoting redox balance through the regulation of glutathione reductase phosphorylation. *Oncogene* 2020; **39**: 637-650 [PMID: 31530934 DOI: 10.1038/s41388-019-1004-2]

127 **Guo B**, Han X, Tkach D, Huang SG, Zhang D. AMPK promotes the survival of colorectal cancer stem cells. *Animal Model Exp Med* 2018; **1**: 134-142 [PMID: 30891558 DOI: 10.1002/ame2.12016]

128 **Wippich F**, Bodenmiller B, Trajkovska MG, Wanka S, Aebersold R, Pelkmans L. Dual specificity kinase DYRK3 couples stress granule condensation/dissolution to mTORC1 signaling. *Cell* 2013; **152**: 791-805 [PMID: 23415227 DOI: 10.1016/j.cell.2013.01.033]

129 **Ganassi M**, Mateju D, Bigi I, Mediani L, Poser I, Lee HO, Seguin SJ, Morelli FF, Vinet J, Leo G, Pansarasa O, Cereda C, Poletti A, Alberti S, Carra S. A Surveillance Function of the HSPB8-BAG3-HSP70 Chaperone Complex Ensures Stress Granule Integrity and Dynamism. *Mol Cell* 2016; **63**: 796-810 [PMID: 27570075 DOI: 10.1016/j.molcel.2016.07.021]

130 **Matus S**, Bosco DA, Hetz C. Autophagy meets fused in sarcoma-positive stress granules. *Neurobiol Aging* 2014; **35**: 2832-2835 [PMID: 25444610 DOI: 10.1016/j.neurobiolaging.2014.08.019]

131 **Minoia M**, Boncoraglio A, Vinet J, Morelli FF, Brunsting JF, Poletti A, Krom S, Reits E, Kampinga HH, Carra S. BAG3 induces the sequestration of proteasomal clients into cytoplasmic puncta: implications for a proteasome-to-autophagy switch. *Autophagy* 2014; **10**: 1603-1621 [PMID: 25046115 DOI: 10.4161/auto.29409]

132 **Zhong MA**, Zhang H, Qi XY, Lu AG, You TG, Gao W, Guo XL, Zhou ZQ, Yang Y, Wang CJ. ShRNA-mediated gene silencing of heat shock protein 70 inhibits human colon cancer growth. *Mol Med Rep* 2011; **4**: 805-810 [PMID: 21725599 DOI: 10.3892/mmr.2011.528]

133 **Soleimani A**, Zahiri E, Ehtiati S, Norouzi M, Rahmani F, Fiuji H, Avan A, Ferns GA, Khazaei M, Hashemy SI, Hassanian SM. Therapeutic potency of heat-shock protein-70 in the pathogenesis of colorectal cancer: current status and perspectives. *Biochem Cell Biol* 2019; **97**: 85-90 [PMID: 30273495 DOI: 10.1139/bcb-2018-0177]

134 **Buchan JR**, Kolaitis RM, Taylor JP, Parker R. Eukaryotic stress granules are cleared by autophagy and Cdc48/VCP function. *Cell* 2013; **153**: 1461-1474 [PMID: 23791177 DOI: 10.1016/j.cell.2013.05.037]

135 **Burada F**, Nicoli ER, Ciurea ME, Uscatu DC, Ioana M, Gheonea DI. Autophagy in colorectal cancer: An important switch from physiology to pathology. *World J Gastrointest Oncol* 2015; **7**: 271-284 [PMID: 26600927 DOI: 10.4251/wjgo.v7.i11.271]

136 **Meyer H**, Weihl CC. The VCP/p97 system at a glance: connecting cellular function to disease pathogenesis. *J Cell Sci* 2014; **127**: 3877-3883 [PMID: 25146396 DOI: 10.1242/jcs.093831]

137 **Wang B**, Maxwell BA, Joo JH, Gwon Y, Messing J, Mishra A, Shaw TI, Ward AL, Quan H, Sakurada SM, Pruett-Miller SM, Bertorini T, Vogel P, Kim HJ, Peng J, Taylor JP, Kundu M. ULK1 and ULK2 Regulate Stress Granule Disassembly Through Phosphorylation and Activation of VCP/p97. *Mol Cell* 2019; **74**: 742-757.e8 [PMID: 30979586 DOI: 10.1016/j.molcel.2019.03.027]

138 **Tresse E**, Salomons FA, Vesa J, Bott LC, Kimonis V, Yao TP, Dantuma NP, Taylor JP. VCP/p97 is essential for maturation of ubiquitin-containing autophagosomes and this function is impaired by mutations that cause IBMPFD. *Autophagy* 2010; **6**: 217-227 [PMID: 20104022 DOI: 10.4161/auto.6.2.11014]

139 **Sheth U**, Parker R. Decapping and decay of messenger RNA occur in cytoplasmic processing bodies. *Science* 2003; **300**: 805-808 [PMID: 12730603 DOI: 10.1126/science.1082320]

140 **Sen GL**, Blau HM. Argonaute 2/RISC resides in sites of mammalian mRNA decay known as cytoplasmic bodies. *Nat Cell Biol* 2005; **7**: 633-636 [PMID: 15908945 DOI: 10.1038/ncb1265]

141 **Franks TM**, Lykke-Andersen J. TTP and BRF proteins nucleate processing body formation to silence mRNAs with AU-rich elements. *Genes Dev* 2007; **21**: 719-735 [PMID: 17369404 DOI: 10.1101/gad.1494707]

142 **Zlobec I**, Karamitopoulou E, Terracciano L, Piscuoglio S, Iezzi G, Muraro MG, Spagnoli G, Baker K, Tzankov A, Lugli A. TIA-1 cytotoxic granule-associated RNA binding protein improves the prognostic performance of CD8 in mismatch repair-proficient colorectal cancer. *PLoS One* 2010; **5**: e14282 [PMID: 21179245 DOI: 10.1371/journal.pone.0014282]

143 **Gao X**, Jiang L, Gong Y, Chen X, Ying M, Zhu H, He Q, Yang B, Cao J. Stress granule: A promising target for cancer treatment. *Br J Pharmacol* 2019; **176**: 4421-4433 [PMID: 31301065 DOI: 10.1111/bph.14790]

144 **Xu Y**, Pang L, Wang H, Xu C, Shah H, Guo P, Shu D, Qian SY. Specific delivery of delta-5-desaturase siRNA *via* RNA nanoparticles supplemented with dihomo-γ-linolenic acid for colon cancer suppression. *Redox Biol* 2019; **21**: 101085 [PMID: 30584980 DOI: 10.1016/j.redox.2018.101085]

145 **Oi N**, Yuan J, Malakhova M, Luo K, Li Y, Ryu J, Zhang L, Bode AM, Xu Z, Li Y, Lou Z, Dong Z. Resveratrol induces apoptosis by directly targeting Ras-GTPase-activating protein SH3 domain-binding protein 1. *Oncogene* 2015; **34**: 2660-2671 [PMID: 24998844 DOI: 10.1038/onc.2014.194]

146 **Shim JH**, Su ZY, Chae JI, Kim DJ, Zhu F, Ma WY, Bode AM, Yang CS, Dong Z. Epigallocatechin gallate suppresses lung cancer cell growth through Ras-GTPase-activating protein SH3 domain-binding protein 1. *Cancer Prev Res (Phila)* 2010; **3**: 670-679 [PMID: 20424128 DOI: 10.1158/1940-6207.CAPR-09-0185]

147 **Porru M**, Zizza P, Franceschin M, Leonetti C, Biroccio A. EMICORON: A multi-targeting G4 ligand with a promising preclinical profile. *Biochim Biophys Acta Gen Subj* 2017; **1861**: 1362-1370 [PMID: 27838395 DOI: 10.1016/j.bbagen.2016.11.010]

148 **Gho YS**, Yoon WH, Chae CB. Antiplasmin activity of a peptide that binds to the receptor-binding site of angiogenin. *J Biol Chem* 2002; **277**: 9690-9694 [PMID: 11782452 DOI: 10.1074/jbc.M105526200]

149 **Olson KA**, Fett JW, French TC, Key ME, Vallee BL. Angiogenin antagonists prevent tumor growth *in vivo*. *Proc Natl Acad Sci USA* 1995; **92**: 442-446 [PMID: 7831307 DOI: 10.1073/pnas.92.2.442]

150 **Sfakianos AP**, Mellor LE, Pang YF, Kritsiligkou P, Needs H, Abou-Hamdan H, Désaubry L, Poulin GB, Ashe MP, Whitmarsh AJ. The mTOR-S6 kinase pathway promotes stress granule assembly. *Cell Death Differ* 2018; **25**: 1766-1780 [PMID: 29523872 DOI: 10.1038/s41418-018-0076-9]

151 **Hofmann S**, Cherkasova V, Bankhead P, Bukau B, Stoecklin G. Translation suppression promotes stress granule formation and cell survival in response to cold shock. *Mol Biol Cell* 2012; **23**: 3786-3800 [PMID: 22875991 DOI: 10.1091/mbc.E12-04-0296]

152 **Yang WL**, Perillo W, Liou D, Marambaud P, Wang P. AMPK inhibitor compound C suppresses cell proliferation by induction of apoptosis and autophagy in human colorectal cancer cells. *J Surg Oncol* 2012; **106**: 680-688 [PMID: 22674626 DOI: 10.1002/jso.23184]

153 **Ivanov PA**, Chudinova EM, Nadezhdina ES. Disruption of microtubules inhibits cytoplasmic ribonucleoprotein stress granule formation. *Exp Cell Res* 2003; **290**: 227-233 [PMID: 14567982 DOI: 10.1016/s0014-4827(03)00290-8]

154 **Rtibi K**, Grami D, Selmi S, Amri M, Sebai H, Marzouki L. Vinblastine, an anticancer drug, causes constipation and oxidative stress as well as others disruptions in intestinal tract in rat. *Toxicol Rep* 2017; **4**: 221-225 [PMID: 28959642 DOI: 10.1016/j.toxrep.2017.04.006]

155 **Cortes J**, O'Shaughnessy J, Loesch D, Blum JL, Vahdat LT, Petrakova K, Chollet P, Manikas A, Diéras V, Delozier T, Vladimirov V, Cardoso F, Koh H, Bougnoux P, Dutcus CE, Seegobin S, Mir D, Meneses N, Wanders J, Twelves C; EMBRACE (Eisai Metastatic Breast Cancer Study Assessing Physician's Choice Versus E7389) investigators. Eribulin monotherapy versus treatment of physician's choice in patients with metastatic breast cancer (EMBRACE): a phase 3 open-label randomised study. *Lancet* 2011; **377**: 914-923 [PMID: 21376385 DOI: 10.1016/S0140-6736(11)60070-6]

156 **Perez-Garcia JM**, Cortes J. The safety of eribulin for the treatment of metastatic breast cancer. *Expert Opin Drug Saf* 2019; **18**: 347-355 [PMID: 31107111 DOI: 10.1080/14740338.2019.1608946]

157 **Kaliszczak M**, van Hechanova E, Li Y, Alsadah H, Parzych K, Auner HW, Aboagye EO. The HDAC6 inhibitor C1A modulates autophagy substrates in diverse cancer cells and induces cell death. *Br J Cancer* 2018; **119**: 1278-1287 [PMID: 30318510 DOI: 10.1038/s41416-018-0232-5]

158 **Won HR**, Ryu HW, Shin DH, Yeon SK, Lee DH, Kwon SH. A452, an HDAC6-selective inhibitor, synergistically enhances the anticancer activity of chemotherapeutic agents in colorectal cancer cells. *Mol Carcinog* 2018; **57**: 1383-1395 [PMID: 29917295 DOI: 10.1002/mc.22852]

159 **Chen MC**, Lin YC, Liao YH, Liou JP, Chen CH. MPT0G612, a Novel HDAC6 Inhibitor, Induces Apoptosis and Suppresses IFN-γ-Induced Programmed Death-Ligand 1 in Human Colorectal Carcinoma Cells. *Cancers (Basel)* 2019; **11**: 1617 [PMID: 31652644 DOI: 10.3390/cancers11101617]

160 **Jiang H**, Cheng ST, Ren JH, Ren F, Yu HB, Wang Q, Huang AL, Chen J. SIRT6 Inhibitor, OSS_128167 Restricts Hepatitis B Virus Transcription and Replication Through Targeting Transcription Factor Peroxisome Proliferator-Activated Receptors α. *Front Pharmacol* 2019; **10**: 1270 [PMID: 31708789 DOI: 10.3389/fphar.2019.01270]

161 **Damonte P**, Sociali G, Parenti MD, Soncini D, Bauer I, Boero S, Grozio A, Holtey MV, Piacente F, Becherini P, Sanguineti R, Salis A, Damonte G, Cea M, Murone M, Poggi A, Nencioni A, Del Rio A, Bruzzone S. SIRT6 inhibitors with salicylate-like structure show immunosuppressive and chemosensitizing effects. *Bioorg Med Chem* 2017; **25**: 5849-5858 [PMID: 28958848 DOI: 10.1016/j.bmc.2017.09.023]

162 **Khan RI**, Nirzhor SSR, Akter R. A Review of the Recent Advances Made with SIRT6 and its Implications on Aging Related Processes, Major Human Diseases, and Possible Therapeutic Targets. *Biomolecules* 2018; **8**: 44 [PMID: 29966233 DOI: 10.3390/biom8030044]

163 **Krisenko MO**, Higgins RL, Ghosh S, Zhou Q, Trybula JS, Wang WH, Geahlen RL. Syk Is Recruited to Stress Granules and Promotes Their Clearance through Autophagy. *J Biol Chem* 2015; **290**: 27803-27815 [PMID: 26429917 DOI: 10.1074/jbc.M115.642900]

164 **Schultz CW**, Preet R, Dhir T, Dixon DA, Brody JR. Understanding and targeting the disease-related RNA

binding protein human antigen R (HuR). *Wiley Interdiscip Rev RNA* 2020; **11**: e1581 [PMID: 31970930 DOI: 10.1002/wrna.1581]

165 **Wang J**, Hjelmeland AB, Nabors LB, King PH. Anti-cancer effects of the HuR inhibitor, MS-444, in malignant glioma cells. *Cancer Biol Ther* 2019; **20**: 979-988 [PMID: 30991885 DOI: 10.1080/15384047.2019.1591673]

166 **Blanco FF**, Preet R, Aguado A, Vishwakarma V, Stevens LE, Vyas A, Padhye S, Xu L, Weir SJ, Anant S, Meisner-Kober N, Brody JR, Dixon DA. Impact of HuR inhibition by the small molecule MS-444 on colorectal cancer cell tumorigenesis. *Oncotarget* 2016; **7**: 74043-74058 [PMID: 27677075 DOI: 10.18632/oncotarget.12189]

167 **Durko L**, Malecka-Panas E. Lifestyle Modifications and Colorectal Cancer. *Curr Colorectal Cancer Rep* 2014; **10**: 45-54 [PMID: 24659930 DOI: 10.1007/s11888-013-0203-4]

168 **Valentin-Vega YA**, Wang YD, Parker M, Patmore DM, Kanagaraj A, Moore J, Rusch M, Finkelstein D, Ellison DW, Gilbertson RJ, Zhang J, Kim HJ, Taylor JP. Cancer-associated DDX3X mutations drive stress granule assembly and impair global translation. *Sci Rep* 2016; **6**: 25996 [PMID: 27180681 DOI: 10.1038/srep25996]

169 **Colombrita C**, Zennaro E, Fallini C, Weber M, Sommacal A, Buratti E, Silani V, Ratti A. TDP-43 is recruited to stress granules in conditions of oxidative insult. *J Neurochem* 2009; **111**: 1051-1061 [PMID: 19765185 DOI: 10.1111/j.1471-4159.2009.06383.x]

170 **Sama RR**, Ward CL, Kaushansky LJ, Lemay N, Ishigaki S, Urano F, Bosco DA. FUS/TLS assembles into stress granules and is a prosurvival factor during hyperosmolar stress. *J Cell Physiol* 2013; **228**: 2222-2231 [PMID: 23625794 DOI: 10.1002/jcp.24395]

171 **Hamdollah Zadeh MA**, Amin EM, Hoareau-Aveilla C, Domingo E, Symonds KE, Ye X, Heesom KJ, Salmon A, D'Silva O, Betteridge KB, Williams AC, Kerr DJ, Salmon AH, Oltean S, Midgley RS, Ladomery MR, Harper SJ, Varey AH, Bates DO. Alternative splicing of TIA-1 in human colon cancer regulates VEGF isoform expression, angiogenesis, tumour growth and bevacizumab resistance. *Mol Oncol* 2015; **9**: 167-178 [PMID: 25224594 DOI: 10.1016/j.molonc.2014.07.017]

172 **Wang Q**, Zhu J, Wang YW, Dai Y, Wang YL, Wang C, Liu J, Baker A, Colburn NH, Yang HS. Tumor suppressor Pdcd4 attenuates Sin1 translation to inhibit invasion in colon carcinoma. *Oncogene* 2017; **36**: 6225-6234 [PMID: 28692058 DOI: 10.1038/onc.2017.228]

173 **Ramalingam S**, Ramamoorthy P, Subramaniam D, Anant S. Reduced Expression of RNA Binding Protein CELF2, a Putative Tumor Suppressor Gene in Colon Cancer. *Immunogastroenterology* 2012; **1**: 27-33 [PMID: 23795348 DOI: 10.7178/ig.1.1.7]

174 **Li N**, Chen M, Cao Y, Li H, Zhao J, Zhai Z, Ren F, Li K. Bcl-2-associated athanogene 3(BAG3) is associated with tumor cell proliferation, migration, invasion and chemoresistance in colorectal cancer. *BMC Cancer* 2018; **18**: 793 [PMID: 30081850 DOI: 10.1186/s12885-018-4657-2]

175 **Jeon JY**, Lee JS, Park ER, Shen YN, Kim MY, Shin HJ, Joo HY, Cho EH, Moon SM, Shin US, Park SH, Han CJ, Choi DW, Gu MB, Kim SB, Lee KH. Protein arginine methyltransferase 5 is implicated in the aggressiveness of human hepatocellular carcinoma and controls the invasive activity of cancer cells. *Oncol Rep* 2018; **40**: 536-544 [PMID: 29749478 DOI: 10.3892/or.2018.6402]

176 **Wang Q**, Tan R, Zhu X, Zhang Y, Tan Z, Su B, Li Y. Oncogenic K-ras confers SAHA resistance by up-regulating HDAC6 and c-myc expression. *Oncotarget* 2016; **7**: 10064-10072 [PMID: 26848526 DOI: 10.18632/oncotarget.7134]

177 **Lin KY**, Tai C, Hsu JC, Li CF, Fang CL, Lai HC, Hseu YC, Lin YF, Uen YH. Overexpression of nuclear protein kinase CK2 α catalytic subunit (CK2α) as a poor prognosticator in human colorectal cancer. *PLoS One* 2011; **6**: e17193 [PMID: 21359197 DOI: 10.1371/journal.pone.0017193]

178 **Zou Y**, Chen Z, He X, He X, Wu X, Chen Y, Wu X, Wang J, Lan P. High expression levels of unc-51-like kinase 1 as a predictor of poor prognosis in colorectal cancer. *Oncol Lett* 2015; **10**: 1583-1588 [PMID: 26622714 DOI: 10.3892/ol.2015.3417]

179 **Choi EJ**, Lee JH, Kim MS, Song SY, Yoo NJ, Lee SH. Intratumoral Heterogeneity of Somatic Mutations for NRIP1, DOK1, ULK1, ULK2, DLGAP3, PARD3 and PRKCI in Colon Cancers. *Pathol Oncol Res* 2018; **24**: 827-832 [PMID: 28844109 DOI: 10.1007/s12253-017-0297-0]

180 **Yamamoto S**, Tomita Y, Hoshida Y, Sakon M, Kameyama M, Imaoka S, Sekimoto M, Nakamori S, Monden M, Aozasa K. Expression of valosin-containing protein in colorectal carcinomas as a predictor for disease recurrence and prognosis. *Clin Cancer Res* 2004; **10**: 651-657 [PMID: 14760088 DOI: 10.1158/1078-0432.ccr-1576-03]

181 **Jin H**, Gong W, Zhang C, Wang S. Epigallocatechin gallate inhibits the proliferation of colorectal cancer cells by regulating Notch signaling. *Onco Targets Ther* 2013; **6**: 145-153 [PMID: 23525843 DOI: 10.2147/OTT.S40914]

182 **Heerma van Voss MR**, Vesuna F, Trumpi K, Brilliant J, Berlinicke C, de Leng W, Kranenburg O, Offerhaus GJ, Bürger H, van der Wall E, van Diest PJ, Raman V. Identification of the DEAD box RNA helicase DDX3 as a therapeutic target in colorectal cancer. *Oncotarget* 2015; **6**: 28312-28326 [PMID: 26311743 DOI: 10.18632/oncotarget.4873]

183 **Wang XW**, Zhang YJ. Targeting mTOR network in colorectal cancer therapy. *World J Gastroenterol* 2014; **20**: 4178-4188 [PMID: 24764656 DOI: 10.3748/wjg.v20.i15.4178]

184 **Ng K**, Tabernero J, Hwang J, Bajetta E, Sharma S, Del Prete SA, Arrowsmith ER, Ryan DP, Sedova M, Jin J, Malek K, Fuchs CS. Phase II study of everolimus in patients with metastatic colorectal adenocarcinoma previously treated with bevacizumab-, fluoropyrimidine-, oxaliplatin-, and irinotecan-based regimens. *Clin Cancer Res* 2013; **19**: 3987-3995 [PMID: 23743569 DOI: 10.1158/1078-0432.CCR-13-0027]

185 **Spindler KL**, Sorensen MM, Pallisgaard N, Andersen RF, Havelund BM, Ploen J, Lassen U, Jakobsen AK. Phase II trial of temsirolimus alone and in combination with irinotecan for KRAS mutant metastatic colorectal cancer: outcome and results of KRAS mutational analysis in plasma. *Acta Oncol* 2013; **52**: 963-970 [PMID: 23514584 DOI: 10.3109/0284186X.2013.776175]

186 **Wang L**, Hu T, Shen J, Zhang L, Chan RL, Lu L, Li M, Cho CH, Wu WK. Dihydrotanshinone I induced apoptosis and autophagy through caspase dependent pathway in colon cancer. *Phytomedicine* 2015; **22**: 1079-1087 [PMID: 26547530 DOI: 10.1016/j.phymed.2015.08.009]

187 **Einzig AI**, Neuberg D, Wiernik PH, Grochow LB, Ramirez G, O'Dwyer PJ, Petrelli NJ. Phase II Trial of Paclitaxel in Patients with Advanced Colon Cancer Previously Untreated with Cytotoxic Chemotherapy: An Eastern Cooperative Oncology Group Trial (PA286). *Am J Ther* 1996; **3**: 750-754 [PMID: 11862233 DOI: 10.1097/00045391-199611000-00003]

188 **Auyeung KK**, Law PC, Ko JK. Combined therapeutic effects of vinblastine and Astragalus saponins in human colon cancer cells and tumor xenograft *via* inhibition of tumor growth and proangiogenic factors. *Nutr Cancer* 2014; **66**: 662-674 [PMID: 24660995 DOI: 10.1080/01635581.2014.894093]

World Journal of Gastroenterology

Submit a Manuscript: https://www.f6publishing.com

World J Gastroenterol 2020 September 21; 26(35): 5248-5255

DOI: 10.3748/wjg.v26.i35.5248

ISSN 1007-9327 (print) ISSN 2219-2840 (online)

MINIREVIEWS

Is artificial intelligence the final answer to missed polyps in colonoscopy?

Thomas K L Lui, Wai K Leung

ORCID number: Thomas KL Lui 0000-0002-2986-3681; Wai K Leung 0000-0002-5993-1059.

Author contributions: Lui TKL contributed to drafting of manuscript; Leung WK contributed to critical review of manuscript.

Conflict-of-interest statement: There is no conflict of interest associated with any of the senior author or other coauthors contributed their efforts in this manuscript.

Manuscript source: Invited manuscript

Received: May 28, 2020
Peer-review started: May 28, 2020

Thomas K L Lui, Wai K Leung, Department of Medicine, Queen Mary Hospital, University of Hong Kong, Hong Kong, China

Corresponding author: Wai K Leung, MD, Professor, Department of Medicine, Queen Mary Hospital, University of Hong Kong, 102 Pokfulam Road, Hong Kong, China. waikleung@hku.hk

Abstract

Lesions missed by colonoscopy are one of the main reasons for post-colonoscopy colorectal cancer, which is usually associated with a worse prognosis. Because the adenoma miss rate could be as high as 26%, it has been noted that endoscopists with higher adenoma detection rates are usually associated with lower adenoma miss rates. Artificial intelligence (AI), particularly the deep learning model, is a promising innovation in colonoscopy. Recent studies have shown that AI is not only accurate in colorectal polyp detection but can also reduce the miss rate. Nevertheless, the application of AI in real-time detection has been hindered by heterogeneity of the AI models and study design as well as a lack of long-term outcomes. Herein, we discussed the principle of various AI models and systematically reviewed the current data on the use of AI on colorectal polyp detection and miss rates. The limitations and future prospects of AI on colorectal polyp detection are also discussed.

Key Words: Artificial intelligence; Adenoma; Colonoscopy; Colorectal cancer; Polyps

Core Tip: This review highlights the results of recent studies on the use of artificial intelligence for the detection of colorectal polyps and its role in reducing missed lesions during colonoscopy.

Citation: Lui TKL, Leung WK. Is artificial intelligence the final answer to missed polyps in colonoscopy? *World J Gastroenterol* 2020; 26(35): 5248-5255
URL: https://www.wjgnet.com/1007-9327/full/v26/i35/5248.htm
DOI: https://dx.doi.org/10.3748/wjg.v26.i35.5248

First decision: June 18, 2020
Revised: June 30, 2020
Accepted: August 26, 2020
Article in press: August 26, 2020
Published online: September 21, 2020

P-Reviewer: Coghlan E
S-Editor: Ma YJ
L-Editor: Filipodia
P-Editor: Ma YJ

INTRODUCTION

Colorectal cancer (CRC) is the third most common cancer worldwide. In 2015, there were 1.7 million new cases, resulting in more than 800000 deaths worldwide[1]. Screening colonoscopy and polypectomy have been shown to be effective in reducing the incidence of colorectal cancer as well as the associated cancer mortalities[2,3]. However, colonoscopy is not risk proof, and CRC can still develop within a short interval after a negative colonoscopy for cancer. In particular, post-colonoscopy colorectal cancer (PCCRC) is the preferred term used to define cancers appearing after a colonoscopy in which no cancer is diagnosed. Specifically, PCCRC can be further subdivided into "interval cancer," where cancer is identified before the next recommended screening or surveillance examination. PCCRC, or interval cancer, could account for up to 9% of all colorectal cancers and is usually associated with an adverse outcome[4]. Recent studies showed that missed polyps and adenoma by colonoscopy accounted for at least 50% of all PCCRCs[5-7]. Therefore, ways to minimize missed lesions during colonoscopy are of utmost importance to maintain the quality and effectiveness of colonoscopy in preventing CRC.

STRATEGY TO MINIMIZE MISSED POLYPS

It was shown in a recent meta-analysis that up to 26% of colonoscopies could have missed adenomas[8]. While many factors could affect the adenoma miss rate (AMR), the endoscopist factor was recognized to be one of the main determinants of AMR. High adenoma detection rate (ADR), high adenomas per index colonoscopy and high adenomas per positive index colonoscopy of the endoscopist were all shown to be negatively associated with AMR[8]. In particular, higher adenomas per positive index colonoscopy was independently associated with a lower advanced adenoma miss rate, which was an important predictor for PCCRC. Intuitively, ways to improve the ADR could also help to minimize AMR[9].

While "to err is human," the mitigation of human factors, such as distraction, fatigue, impaired level of alertness, visual perception and recognition errors, may be the key to improving adenoma detection and hence reducing miss rates[10-14]. Additionally, patient factors, mainly poor bowel preparation, were also associated with lower ADR[15] and higher AMR[8]. However, there was minimal difference between fair- and good-quality bowel preparation in ADR and AMR[8], implying that at least fair bowel preparation should be achieved. Adequate withdrawal time, a minimum of 6 min, is another important quality measure to optimize ADR and AMR[16-18]. Another factor that would improve the ADR and reduce the AMR was the use of auxiliary techniques. There are a large number of auxiliary techniques, including second-pass colonoscopy[19], retroflexion in right-sided colon[20], water-aided colonoscopy[21], team detection approach (endoscopist and experienced nurse)[13,22], wide-angle endoscopy[23], high-definition endoscopy with or without a special imaging technique[24-26] and add-on devices[27], that have been reported to increase the ADR.

ARTIFICIAL INTELLIGENCE SYSTEMS USED IN THE DETECTION OF COLORECTAL POLYPS

Artificial intelligence (AI) has been applied in the medical field since the early 1950s. AI is defined as any machine that has cognitive functions mimicking humans, *e.g.*, problem solving or learning[28]. The machine learning model, which is a subtype of AI, is characterized by a set of methods that can automatically detect patterns in data and then use the uncovered patterns to predict outcomes[29]. Conventional AI systems utilize a supervised type of machine learning model that extracts the covariates of training data to achieve pattern recognition or classification. It is important to note that each piece of information included in the representation of the patient is known as a covariate, and the traditional type of machine learning, *e.g.*, logistic regression, only examines the relationships of "predefined covariates" with the outcome[30]. Nevertheless, the machine learning model cannot change the way in which covariates are defined. The deep learning model actually solves this problem by defining covariates and builds up complex concepts from simple covariates, which is particularly useful in image classification and object location because features of a group of similar subjects can be complex and difficult to be defined by humans[30]

(Figure 1).

In recent years, the deep learning model was increasingly used in the detection and localization of colorectal polyps. Once training data were provided with proper labels, the deep learning model could automatically extract the important features in the training data for differentiation and classification. Without the need of human intervention or indication, the internal parameters of each "neuron" in a single layer would be tuned towards a model with the least degree of error[31]. The most common architecture used in the deep learning model of early colonoscopy studies was convolutional neural networks, which mimics the structure of the human brain and contains multiple layers with "artificial neurons" under each layer. The convoluted layers actually act as a filter for extraction of the important features from the original image or data. The pooling layers can downsize the parameters of the layers to streamline the underlying computation. Finally, with the fully connected layers, these features are combined together to create a model to classify different outputs[32,33].

ROLE OF AI IN THE DETECTION OF COLORECTAL POLYPS DURING COLONOSOCPY

Our meta-analysis of recently published AI studies on colorectal polyp detection suggested that a well-designed AI system could achieve more than 90% accuracy[34-36]. Compared to a traditional machine learning based algorithm, studies using the deep learning model were found to have high accuracy (up to 91%) with a pooled sensitivity of 94% and a specificity of 92% on the detection of colorectal polyps[36].

As yet, most of the previously published studies have been retrospective in nature, and there have been limited high-quality prospective real-time studies on the use of AI in actual patients until recently. The first randomized controlled trial was reported in 2019 by Wang *et al*[37]. They showed that the use of real-time automatic polyp detection system (CADe) based on a deep learning architecture can increase the ADR in patients with a low prevalence of adenoma (20%-30%). Among the 1130 patients randomized, the ADR of the CADe group was significantly higher than that of the conventional colonoscopy group (0.29 *vs* 0.20, $P < 0.001$). The mean numbers of polyp and adenoma detected in the CADe group also increased from 0.50 to 0.95 ($P < 0.001$) and from 0.31 to 0.53 ($P < 0.001$), respectively, when compared with conventional colonoscopy.

Five recently published randomized controlled trials (RCTs) in 2020 again confirmed that AI-assisted colonoscopy significantly increased the adenoma detection rate when compared to conventional colonoscopy. Wang *et al*[38] further reported another RCT to compare a CADe system with a sham system. Again, the CADe system had a significantly higher ADR than the sham system (34% *vs* 28%, $P = 0.03$). In the same trial, adenoma or sessile serrated adenoma missed by endoscopists were characterized by isochromatic color, flat shape and located at the edge of the visual field or even partly behind colonic folds. Another randomized controlled trial by Repici *et al*[39] involving three centers in Italy also found that the CADe system was associated with a higher ADR with an odds ratio (OR) of 1.30 (95%CI: 1.14-1.45). Subgroup analysis showed that the performance of the CADe system was not affected by the size, shape and location of the polyps.

In addition to polyp location systems, Gong *et al*[40] reported a CADe system that aimed to monitor real-time withdrawal speed and to minimize blind spots during withdrawal. Their study showed that the ADR also improved from 8% to 16% ($P = 0.001$) with the CADe system. Similarly, Su *et al*[41] reported an automatic quality control system on colorectal polyp and adenoma detection that would also remind the endoscopist of the withdrawal time and speed and the need to re-examine unclear colonic segments on top of a polyp localization system. The system was found to have a significantly higher ADR than conventional colonoscopy (28.9% *vs* 16.5%, $P < 0.001$).

In view of these newly available RCTs after the publication of our meta-analysis[36], we have summarized the results of the latest prospective RCTs here in a new meta-analysis. In this meta-analysis of six RCTs, the pooled OR for the improvement of ADR was 1.91 (95%CI: 1.51-2.41) under a random effects model with a heterogeneity of $I^2 = 63\%$ (Figure 2). Hence, there is convincing data from RCTs to show that the existing AI models could already help to boost the ADR by 90%.

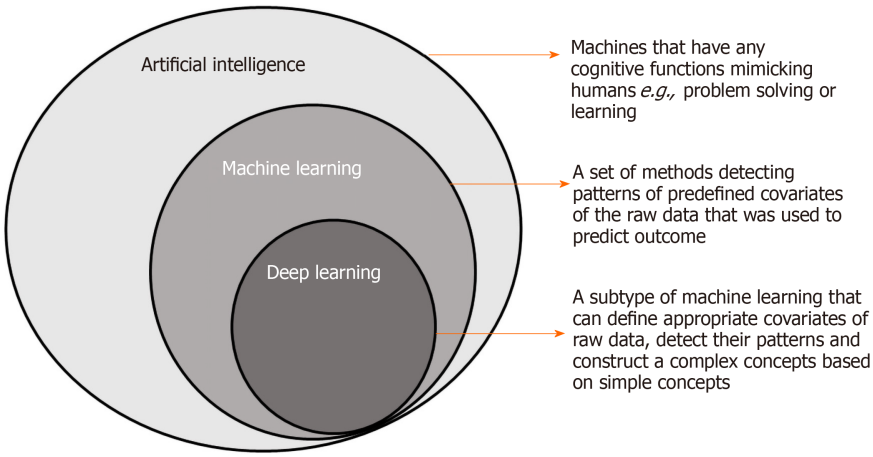

Figure 1 Diagrammatic presentation of artificial intelligence, machine learning and deep learning.

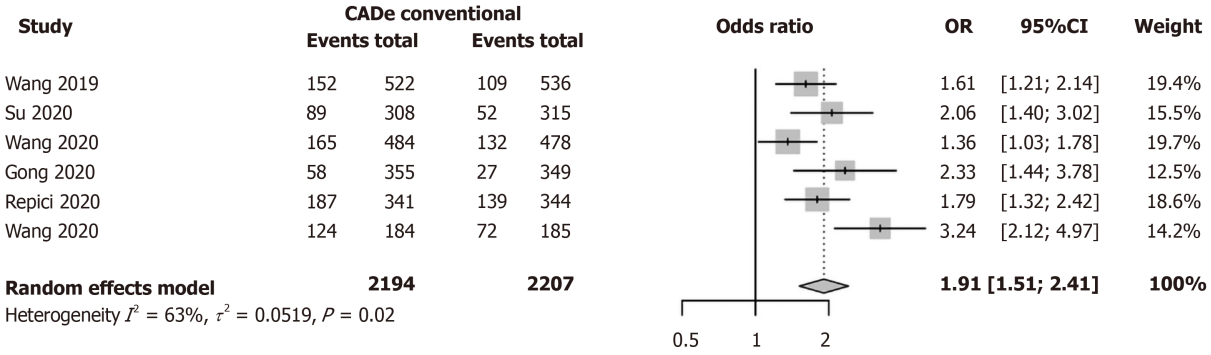

Figure 2 Pooled analysis for improvement of adenoma detection rate of all the randomized controlled trials. Events: number of patients with adenoma detected. CADe: Real-time automatic polyp detection system; CI: Confidence interval; OR: Odds ratio.

ROLE OF AI IN MISSED POLYPS

In addition to its role in enhanced colorectal polyp detection, there are emerging data to suggest that AI could also help to reduce missed lesions during colonoscopy. In our recent study[42], we showed that the validated real-time deep learning AI model could help endoscopists to prevent missed colorectal lesions. We first applied the validated AI system to review 65 videos of tandem examinations of the proximal colon (from cecum to splenic flexure) and found that the AI system could detect up to 79.1% of adenomas that were missed by the endoscopist during the first-pass examination. In the second part of the prospective study, the same deep learning AI model was able to detect missed adenomas in 26.9% of patients during real-time examination. In multivariable analysis, missed adenomas were associated with findings of multiple polyps during colonoscopy (adjusted OR, 1.05) or colonoscopy performed by less-experienced endoscopists (adjusted OR, 1.30).

A recent single-center RCT by Wang *et al*[43] also showed that the use of CADe-assisted colonoscopy can reduce AMR from 40.0% to 14.0%. In particular, there were significant improvements in the ascending, transverse and descending colon. However, the AMR in this RCT (up to 40%) was much higher than previously reported. Therefore, a multicenter trial would still be required to validate this finding.

STATE OF THE ART: ROLE OF AI IN MISSED COLORECTAL POLYPS

While supporting the role of AI in reducing missed lesions, these results suggested that the main reason for missed adenoma could still be due to human factors, as nearly 80% of these missed lesions were actually shown on screen and were not picked up by endoscopists for various reasons, such as inexperience, fatigue or distraction. Therefore, the AI could serve as an additional "eye" for the endoscopist with which

distraction and fatigue would never occur.

However, our study also showed that approximately 20% of missed adenomas were still not detected even by AI. These missed lesions were usually not shown "on screen." They were located behind a fold or at a difficult flexure position or hidden under the fecal contents in patients with poor bowel preparation. In a recent meta-analysis by Zhao *et al*[8] including 43 studies and 15000 tandem colonoscopies, the use of auxiliary techniques and good bowel preparation were associated with fewer missed adenomas. Intuitively, the combination of AI and auxiliary devices in the presence of satisfactory bowel preparation may be necessary to completely eliminate the risk of missed colonic lesions during colonoscopy.

USE OF AI IN THE CHARACTERIZATION OF POLYPS

In addition to detection of colorectal polyps, AI has also been shown to be accurate in histology prediction and polyp characterization in a number of studies[36]. Although there was a high degree of heterogeneity in the algorithms and design, along with potential selection biases, studies using a deep learning model as a backbone generally performed better than those using other types of algorithms. A study by Byrne *et al*[44] showed that the use of a deep learning model can achieve a 94% accuracy in the real-time classification of polyps. A similar result was reproduced by a study[45] using magnifying colonoscopy, and both studies used narrow-band imaging as the imaging technique. Our recent meta-analysis further showed that the pooled accuracy from studies using narrow-band imaging was generally better than that of non-narrow-band imaging studies in histology characterization[36].

LIMITATIONS AND FUTURE DIRECTIONS

Although there have been promising prospective trials supporting the use of AI in real-time polyp detection during colonoscopy, there are a number of issues to be addressed before AI can be implemented in routine clinical practice. Because the algorithms of AI and deep learning models are still evolving and there is substantial heterogeneity among different models and training data[36], an independent prospective validation would be required for each AI system. The latest guideline issued by the European Society of Gastrointestinal Endoscopy suggested that the possible incorporation of computer-aided diagnosis (detection and characterization of lesions) into colonoscopy should be supported by an acceptable and reproducible accuracy for colorectal neoplasia, as demonstrated in high-quality multicenter clinical studies[14]. Another important question regarding the use of AI in colonoscopy is the actual impact on long-term clinical outcomes. It is still unknown whether the use of AI-assisted colonoscopy can decrease the PCCRC rate or lengthen the current recommended surveillance interval after colonoscopy, which would require long-term prospective cohort studies to address.

The current role of AI in colonoscopy is possibly to act as a virtual assistant to the endoscopist during real-time colonoscopy, particularly in withdrawal time monitoring and polyp detection. The prospect of a fully automated independent colonoscopy system is still too premature at this stage. Moreover, the "black box" nature of the AI algorithm, especially the deep learning model, may require considerable effort to convince the regulatory authority to approve for its routine use. The liability and indemnity issues related to the manufacturers of the AI system also need to be resolved. Hence, there are still considerable obstacles to overcome before the application of AI-assisted colonoscopy becomes widespread in daily practice.

CONCLUSION

An externally validated AI system could be one of the promising solutions to increase adenoma detection and to minimize missed lesions during real-time colonoscopy. As of yet, means to ensure adequate mucosal exposure, such as add-on devices and optimal bowel preparation, are also critical in reducing the polyp miss rate in daily colonoscopy practice. Long-term data are also needed to determine the actual clinical benefits of this emerging technology in the reduction of PCCRC.

REFERENCES

1 **Global Burden of Disease Cancer Collaboration**, Fitzmaurice C, Allen C, Barber RM, Barregard L, Bhutta ZA, Brenner H, Dicker DJ, Chimed-Orchir O, Dandona R, Dandona L, Fleming T, Forouzanfar MH, Hancock J, Hay RJ, Hunter-Merrill R, Huynh C, Hosgood HD, Johnson CO, Jonas JB, Khubchandani J, Kumar GA, Kutz M, Lan Q, Larson HJ, Liang X, Lim SS, Lopez AD, MacIntyre MF, Marczak L, Marquez N, Mokdad AH, Pinho C, Pourmalek F, Salomon JA, Sanabria JR, Sandar L, Sartorius B, Schwartz SM, Shackelford KA, Shibuya K, Stanaway J, Steiner C, Sun J, Takahashi K, Vollset SE, Vos T, Wagner JA, Wang H, Westerman R, Zeeb H, Zoeckler L, Abd-Allah F, Ahmed MB, Alabed S, Alam NK, Aldhahri SF, Alem G, Alemayohu MA, Ali R, Al-Raddadi R, Amare A, Amoako Y, Artaman A, Asayesh H, Atnafu N, Awasthi A, Saleem HB, Barac A, Bedi N, Bensenor I, Berhane A, Bernabé E, Betsu B, Binagwaho A, Boneya D, Campos-Nonato I, Castañeda-Orjuela C, Catalá-López F, Chiang P, Chibueze C, Chitheer A, Choi JY, Cowie B, Damtew S, das Neves J, Dey S, Dharmaratne S, Dhillon P, Ding E, Driscoll T, Ekwueme D, Endries AY, Farvid M, Farzadfar F, Fernandes J, Fischer F, G/Hiwot TT, Gebru A, Gopalani S, Hailu A, Horino M, Horita N, Husseini A, Huybrechts I, Inoue M, Islami F, Jakovljevic M, James S, Javanbakht M, Jee SH, Kasaeian A, Kedir MS, Khader YS, Khang YH, Kim D, Leigh J, Linn S, Lunevicius R, El Razek HMA, Malekzadeh R, Malta DC, Marcenes W, Markos D, Melaku YA, Meles KG, Mendoza W, Mengiste DT, Meretoja TJ, Miller TR, Mohammad KA, Mohammadi A, Mohammed S, Moradi-Lakeh M, Nagel G, Nand D, Le Nguyen Q, Nolte S, Ogbo FA, Oladimeji KE, Oren E, Pa M, Park EK, Pereira DM, Plass D, Qorbani M, Radfar A, Rafay A, Rahman M, Rana SM, Søreide K, Satpathy M, Sawhney M, Sepanlou SG, Shaikh MA, She J, Shiue I, Shore HR, Shrime MG, So S, Soneji S, Stathopoulou V, Stroumpoulis K, Sufiyan MB, Sykes BL, Tabarés-Seisdedos R, Tadese F, Tedla BA, Tessema GA, Thakur JS, Tran BX, Ukwaja KN, Uzochukwu BSC, Vlassov VV, Weiderpass E, Wubshet Terefe M, Yebyo HG, Yimam HH, Yonemoto N, Younis MZ, Yu C, Zaidi Z, Zaki MES, Zenebe ZM, Murray CJL, Naghavi M. Global, Regional, and National Cancer Incidence, Mortality, Years of Life Lost, Years Lived With Disability, and Disability-Adjusted Life-years for 32 Cancer Groups, 1990 to 2015: A Systematic Analysis for the Global Burden of Disease Study. *JAMA Oncol* 2017; **3**: 524-548 [PMID: 27918777 DOI: 10.1001/jamaoncol.2016.5688]

2 **Zauber AG**, Winawer SJ, O'Brien MJ, Lansdorp-Vogelaar I, van Ballegooijen M, Hankey BF, Shi W, Bond JH, Schapiro M, Panish JF, Stewart ET, Waye JD. Colonoscopic polypectomy and long-term prevention of colorectal-cancer deaths. *N Engl J Med* 2012; **366**: 687-696 [PMID: 22356322 DOI: 10.1056/NEJMoa1100370]

3 **Nishihara R**, Wu K, Lochhead P, Morikawa T, Liao X, Qian ZR, Inamura K, Kim SA, Kuchiba A, Yamauchi M, Imamura Y, Willett WC, Rosner BA, Fuchs CS, Giovannucci E, Ogino S, Chan AT. Long-term colorectal-cancer incidence and mortality after lower endoscopy. *N Engl J Med* 2013; **369**: 1095-1105 [PMID: 24047059 DOI: 10.1056/NEJMoa1301969]

4 **Cheung KS**, Chen L, Seto WK, Leung WK. Epidemiology, characteristics, and survival of post-colonoscopy colorectal cancer in Asia: A population-based study. *J Gastroenterol Hepatol* 2019; **34**: 1545-1553 [PMID: 30932240 DOI: 10.1111/jgh.14674]

5 **Robertson DJ**, Lieberman DA, Winawer SJ, Ahnen DJ, Baron JA, Schatzkin A, Cross AJ, Zauber AG, Church TR, Lance P, Greenberg ER, Martínez ME. Colorectal cancers soon after colonoscopy: a pooled multicohort analysis. *Gut* 2014; **63**: 949-956 [PMID: 23793224 DOI: 10.1136/gutjnl-2012-303796]

6 **le Clercq CM**, Bouwens MW, Rondagh EJ, Bakker CM, Keulen ET, de Ridder RJ, Winkens B, Masclee AA, Sanduleanu S. Postcolonoscopy colorectal cancers are preventable: a population-based study. *Gut* 2014; **63**: 957-963 [PMID: 23744612 DOI: 10.1136/gutjnl-2013-304880]

7 **Sanduleanu S**, le Clercq CM, Dekker E, Meijer GA, Rabeneck L, Rutter MD, Valori R, Young GP, Schoen RE; Expert Working Group on 'Right-sided lesions and interval cancers', Colorectal Cancer Screening Committee, World Endoscopy Organization. Definition and taxonomy of interval colorectal cancers: a proposal for standardising nomenclature. *Gut* 2015; **64**: 1257-1267 [PMID: 25193802 DOI: 10.1136/gutjnl-2014-307992]

8 **Zhao S**, Wang S, Pan P, Xia T, Chang X, Yang X, Guo L, Meng Q, Yang F, Qian W, Xu Z, Wang Y, Wang Z, Gu L, Wang R, Jia F, Yao J, Li Z, Bai Y. Magnitude, Risk Factors, and Factors Associated With Adenoma Miss Rate of Tandem Colonoscopy: A Systematic Review and Meta-analysis. *Gastroenterology* 2019; **156**: 1661-1674.e11 [PMID: 30738046 DOI: 10.1053/j.gastro.2019.01.260]

9 **Gupta N**. How to Improve Your Adenoma Detection Rate During Colonoscopy. *Gastroenterology* 2016; **151**: 1054-1057 [PMID: 27765692 DOI: 10.1053/j.gastro.2016.10.008]

10 **Mahmud N**, Cohen J, Tsourides K, Berzin TM. Computer vision and augmented reality in gastrointestinal endoscopy. *Gastroenterol Rep (Oxf)* 2015; **3**: 179-184 [PMID: 26133175 DOI: 10.1093/gastro/gov027]

11 **Wang W**, Xu L, Bao Z, Sun L, Hu C, Zhou F, Xu L, Shi D. Differences with experienced nurse assistance during colonoscopy in detecting polyp and adenoma: a randomized clinical trial. *Int J Colorectal Dis* 2018; **33**: 561-566 [PMID: 29541895 DOI: 10.1007/s00384-018-3003-0]

12 **Buchner AM**, Shahid MW, Heckman MG, Diehl NN, McNeil RB, Cleveland P, Gill KR, Schore A, Ghabril M, Raimondo M, Gross SA, Wallace MB. Trainee participation is associated with increased small adenoma detection. *Gastrointest Endosc* 2011; **73**: 1223-1231 [PMID: 21481861 DOI: 10.1016/j.gie.2011.01.060]

13 **Aslanian HR**, Shieh FK, Chan FW, Ciarleglio MM, Deng Y, Rogart JN, Jamidar PA, Siddiqui UD. Nurse observation during colonoscopy increases polyp detection: a randomized prospective study. *Am J Gastroenterol* 2013; **108**: 166-172 [PMID: 23381064 DOI: 10.1038/ajg.2012.237]

14 **Bisschops R**, East JE, Hassan C, Hazewinkel Y, Kamiński MF, Neumann H, Pellisé M, Antonelli G, Bustamante Balen M, Coron E, Cortas G, Iacucci M, Yuichi M, Longcroft-Wheaton G, Mouzyka S, Pilonis N, Puig I, van Hooft JE, Dekker E. Advanced imaging for detection and differentiation of colorectal neoplasia: European Society of Gastrointestinal Endoscopy (ESGE) Guideline - Update 2019. *Endoscopy* 2019; **51**: 1155-1179 [PMID: 31711241 DOI: 10.1055/a-1031-7657]

15 **Clark BT**, Rustagi T, Laine L. What level of bowel prep quality requires early repeat colonoscopy: systematic review and meta-analysis of the impact of preparation quality on adenoma detection rate. *Am J Gastroenterol* 2014; **109**: 1714-23; quiz 1724 [PMID: 25135006 DOI: 10.1038/ajg.2014.232]

16 **Barclay RL**, Vicari JJ, Doughty AS, Johanson JF, Greenlaw RL. Colonoscopic withdrawal times and adenoma detection during screening colonoscopy. *N Engl J Med* 2006; **355**: 2533-2541 [PMID: 17167136 DOI: 10.1056/NEJMoa055498]

17 **Barclay RI**, Vicari JJ, Johanson JF, Greenlaw RI. Variation in adenoma detection rates and colonoscopic withdrawal times during screening colonoscopy. *Gastrointest Endosc* 2005; **61**: Ab107 [DOI: 10.1016/S0016-5107(05)00682-6]

18 **Barclay RL**, Vicari JJ, Greenlaw RL. Effect of a time-dependent colonoscopic withdrawal protocol on adenoma detection during screening colonoscopy. *Clin Gastroenterol Hepatol* 2008; **6**: 1091-1098 [PMID: 18639495 DOI: 10.1016/j.cgh.2008.04.018]

19 **Lee HS**, Jeon SW, Park HY, Yeo SJ. Improved detection of right colon adenomas with additional retroflexion following two forward-view examinations: a prospective study. *Endoscopy* 2017; **49**: 334-341 [PMID: 27931050 DOI: 10.1055/s-0042-119401]

20 **Cohen J**, Grunwald D, Grossberg LB, Sawhney MS. The Effect of Right Colon Retroflexion on Adenoma Detection: A Systematic Review and Meta-analysis. *J Clin Gastroenterol* 2017; **51**: 818-824 [PMID: 27683963 DOI: 10.1097/MCG.0000000000000695]

21 **Cadoni S**, Falt P, Rondonotti E, Radaelli F, Fojtik P, Gallittu P, Liggi M, Amato A, Paggi S, Smajstrla V, Urban O, Erriu M, Koo M, Leung FW. Water exchange for screening colonoscopy increases adenoma detection rate: a multicenter, double-blinded, randomized controlled trial. *Endoscopy* 2017; **49**: 456-467 [PMID: 28282689 DOI: 10.1055/s-0043-101229]

22 **Lee CK**, Park DI, Lee SH, Hwangbo Y, Eun CS, Han DS, Cha JM, Lee BI, Shin JE. Participation by experienced endoscopy nurses increases the detection rate of colon polyps during a screening colonoscopy: a multicenter, prospective, randomized study. *Gastrointest Endosc* 2011; **74**: 1094-1102 [PMID: 21889137 DOI: 10.1016/j.gie.2011.06.033]

23 **Kudo T**, Saito Y, Ikematsu H, Hotta K, Takeuchi Y, Shimatani M, Kawakami K, Tamai N, Mori Y, Maeda Y, Yamada M, Sakamoto T, Matsuda T, Imai K, Ito S, Hamada K, Fukata N, Inoue T, Tajiri H, Yoshimura K, Ishikawa H, Kudo SE. New-generation full-spectrum endoscopy versus standard forward-viewing colonoscopy: a multicenter, randomized, tandem colonoscopy trial (J-FUSE Study). *Gastrointest Endosc* 2018; **88**: 854-864 [PMID: 29908178 DOI: 10.1016/j.gie.2018.06.011]

24 **Atkinson NSS**, Ket S, Bassett P, Aponte D, De Aguiar S, Gupta N, Horimatsu T, Ikematsu H, Inoue T, Kaltenbach T, Leung WK, Matsuda T, Paggi S, Radaelli F, Rastogi A, Rex DK, Sabbagh LC, Saito Y, Sano Y, Saracco GM, Saunders BP, Senore C, Soetikno R, Vemulapalli KC, Jairath V, East JE. Narrow-Band Imaging for Detection of Neoplasia at Colonoscopy: A Meta-analysis of Data From Individual Patients in Randomized Controlled Trials. *Gastroenterology* 2019; **157**: 462-471 [PMID: 30998991 DOI: 10.1053/j.gastro.2019.04.014]

25 **Leung WK**, Lo OS, Liu KS, Tong T, But DY, Lam FY, Hsu AS, Wong SY, Seto WK, Hung IF, Law WL. Detection of colorectal adenoma by narrow band imaging (HQ190) vs. high-definition white light colonoscopy: a randomized controlled trial. *Am J Gastroenterol* 2014; **109**: 855-863 [PMID: 24751581 DOI: 10.1038/ajg.2014.83]

26 **Leung WK**, Guo CG, Ko MKL, To EWP, Mak LY, Tong TSM, Chen LJ, But DYK, Wong SY, Liu KSH, Tsui V, Lam FYF, Lui TKL, Cheung KS, Lo SH, Hung IFN. Linked color imaging versus narrow-band imaging for colorectal polyp detection: a prospective randomized tandem colonoscopy study. *Gastrointest Endosc* 2020; **91**: 104-112.e5 [PMID: 31276672 DOI: 10.1016/j.gie.2019.06.031]

27 **Rameshshanker R**, Tsiamoulos Z, Wilson A, Rajendran A, Bassett P, Tekkis P, Saunders BP. Endoscopic cuff-assisted colonoscopy versus cap-assisted colonoscopy in adenoma detection: randomized tandem study-DEtection in Tandem Endocuff Cap Trial (DETECT). *Gastrointest Endosc* 2020; **91**: 894-904.e1 [PMID: 31836474 DOI: 10.1016/j.gie.2019.11.046]

28 **Russell SJ**, Norvig P, Davis E. Artificial intelligence: a modern approach. 3rd ed. Upper Saddle River: Prentice Hall; 2010

29 **Murphy KP**. Machine learning: a probabilistic perspective. Cambridge, MA: MIT Press; 2012

30 **Goodfellow I**, Bengio Y, Courville A. *Deep learning*. Cambridge, Massachusetts: The MIT Press; 2016;

31 **Takiyama H**, Ozawa T, Ishihara S, Fujishiro M, Shichijo S, Nomura S, Miura M, Tada T. Automatic anatomical classification of esophagogastroduodenoscopy images using deep convolutional neural networks. *Sci Rep* 2018; **8**: 7497 [PMID: 29760397 DOI: 10.1038/s41598-018-25842-6]

32 **Krizhevsky A**, Sutskever I, Hinton GE. ImageNet Classification with Deep Convolutional Neural Networks. *Commun Acm* 2017; **60**: 84-90 [DOI: 10.1145/3065386]

33 **Shin HC**, Roth HR, Gao M, Lu L, Xu Z, Nogues I, Yao J, Mollura D, Summers RM. Deep Convolutional Neural Networks for Computer-Aided Detection: CNN Architectures, Dataset Characteristics and Transfer Learning. *IEEE Trans Med Imaging* 2016; **35**: 1285-1298 [PMID: 26886976 DOI: 10.1109/TMI.2016.2528162]

34 **Urban G**, Tripathi P, Alkayali T, Mittal M, Jalali F, Karnes W, Baldi P. Deep Learning Localizes and Identifies Polyps in Real Time With 96% Accuracy in Screening Colonoscopy. *Gastroenterology* 2018; **155**: 1069-1078.e8 [PMID: 29928897 DOI: 10.1053/j.gastro.2018.06.037]

35 **Figueiredo PN**, Figueiredo IN, Pinto L, Kumar S, Tsai YR, Mamonov AV. Polyp detection with computer-aided diagnosis in white light colonoscopy: comparison of three different methods. *Endosc Int Open* 2019; **7**: E209-E215 [PMID: 30705955 DOI: 10.1055/a-0808-4456]

36 **Lui TKL**, Guo CG, Leung WK. Accuracy of artificial intelligence on histology prediction and detection of colorectal polyps: a systematic review and meta-analysis. *Gastrointest Endosc* 2020; **92**: 11-22.e6 [PMID: 32119938 DOI: 10.1016/j.gie.2020.02.033]

37 **Wang P**, Berzin TM, Glissen Brown JR, Bharadwaj S, Becq A, Xiao X, Liu P, Li L, Song Y, Zhang D, Li Y, Xu G, Tu M, Liu X. Real-time automatic detection system increases colonoscopic polyp and adenoma detection rates: a prospective randomised controlled study. *Gut* 2019; **68**: 1813-1819 [PMID: 30814121 DOI: 10.1136/gutjnl-2018-317500]

38 **Wang P**, Liu X, Berzin TM, Glissen Brown JR, Liu P, Zhou C, Lei L, Li L, Guo Z, Lei S, Xiong F, Wang H, Song Y, Pan Y, Zhou G. Effect of a deep-learning computer-aided detection system on adenoma detection during colonoscopy (CADe-DB trial): a double-blind randomised study. *Lancet Gastroenterol Hepatol* 2020;

5: 343-351 [PMID: 31981517 DOI: 10.1016/S2468-1253(19)30411-X]
39 **Repici A**, Badalamenti M, Maselli R, Correale L, Radaelli F, Rondonotti E, Ferrara E, Spadaccini M, Alkandari A, Fugazza A, Anderloni A, Galtieri PA, Pellegatta G, Carrara S, Di Leo M, Craviotto V, Lamonaca L, Lorenzetti R, Andrealli A, Antonelli G, Wallace M, Sharma P, Rosch T, Hassan C. Efficacy of Real-Time Computer-Aided Detection of Colorectal Neoplasia in a Randomized Trial. *Gastroenterology* 2020 [PMID: 32371116 DOI: 10.1053/j.gastro.2020.04.062]
40 **Gong D**, Wu L, Zhang J, Mu G, Shen L, Liu J, Wang Z, Zhou W, An P, Huang X, Jiang X, Li Y, Wan X, Hu S, Chen Y, Hu X, Xu Y, Zhu X, Li S, Yao L, He X, Chen D, Huang L, Wei X, Wang X, Yu H. Detection of colorectal adenomas with a real-time computer-aided system (ENDOANGEL): a randomised controlled study. *Lancet Gastroenterol Hepatol* 2020; **5**: 352-361 [PMID: 31981518 DOI: 10.1016/S2468-1253(19)30413-3]
41 **Su JR**, Li Z, Shao XJ, Ji CR, Ji R, Zhou RC, Li GC, Liu GQ, He YS, Zuo XL, Li YQ. Impact of a real-time automatic quality control system on colorectal polyp and adenoma detection: a prospective randomized controlled study (with videos). *Gastrointest Endosc* 2020; **91**: 415-424.e4 [PMID: 31454493 DOI: 10.1016/j.gie.2019.08.026]
42 **Lui TK**, Hui CK, Tsui VW, Cheung KS, Ko MK, aCC Foo D, Mak LY, Yeung CK, Lui TH, Wong SY, Leung WK. New insights on missed colonic lesions during colonoscopy through artificial intelligence-assisted real-time detection (with video). *Gastrointest Endosc* 2020 [PMID: 32376335 DOI: 10.1016/j.gie.2020.04.066]
43 **Wang P**, Liu P, Glissen Brown JR, Berzin TM, Zhou G, Lei S, Liu X, Li L, Xiao X. Lower Adenoma Miss Rate of Computer-aided Detection-Assisted Colonoscopy vs Routine White-Light Colonoscopy in a Prospective Tandem Study. *Gastroenterology* 2020 [PMID: 32562721 DOI: 10.1053/j.gastro.2020.06.023]
44 **Byrne MF**, Chapados N, Soudan F, Oertel C, Linares Pérez M, Kelly R, Iqbal N, Chandelier F, Rex DK. Real-time differentiation of adenomatous and hyperplastic diminutive colorectal polyps during analysis of unaltered videos of standard colonoscopy using a deep learning model. *Gut* 2019; **68**: 94-100 [PMID: 29066576 DOI: 10.1136/gutjnl-2017-314547]
45 **Chen PJ**, Lin MC, Lai MJ, Lin JC, Lu HH, Tseng VS. Accurate Classification of Diminutive Colorectal Polyps Using Computer-Aided Analysis. *Gastroenterology* 2018; **154**: 568-575 [PMID: 29042219 DOI: 10.1053/j.gastro.2017.10.010]

World Journal of Gastroenterology

Submit a Manuscript: https://www.f6publishing.com

World J Gastroenterol 2020 September 21; 26(35): 5256-5271

DOI: 10.3748/wjg.v26.i35.5256

ISSN 1007-9327 (print) ISSN 2219-2840 (online)

MINIREVIEWS

Artificial intelligence-assisted esophageal cancer management: Now and future

Yu-Hang Zhang, Lin-Jie Guo, Xiang-Lei Yuan, Bing Hu

ORCID number: Yu-Hang Zhang 0000-0003-2268-6149; Lin-Jie Guo 0000-0002-0852-3186; Xiang-Lei Yuan 0000-0003-2281-5094; Bing Hu 0000-0002-9898-8656.

Author contributions: Zhang YH reviewed literatures and drafted the manuscript; Guo LJ provided critical comments and revision; Yuan XL did part of the literature review; Hu B provided critical comments regarding artificial intelligence and revision.

Supported by Sichuan Science and Technology Department Key R and D Projects, No. 2019YFS0257; and Chengdu Technological Innovation R and D Projects, No. 2018-YFYF-00033-GX.

Conflict-of-interest statement: All authors declare no conflict of interests.

Yu-Hang Zhang, Lin-Jie Guo, Xiang-Lei Yuan, Bing Hu, Department of Gastroenterology and Hepatology, West China Hospital, Sichuan University, Chengdu 610041, Sichuan Province, China

Corresponding author: Bing Hu, MD, Chief Doctor, Professor, Department of Gastroenterology and Hepatology, West China Hospital, Sichuan University, No. 37 Guoxue Alley, Wuhou District, Chengdu 610041, Sichuan Province, China. hubingnj@163.com

Abstract

Esophageal cancer poses diagnostic, therapeutic and economic burdens in high-risk regions. Artificial intelligence (AI) has been developed for diagnosis and outcome prediction using various features, including clinicopathologic, radiologic, and genetic variables, which can achieve inspiring results. One of the most recent tasks of AI is to use state-of-the-art deep learning technique to detect both early esophageal squamous cell carcinoma and esophageal adenocarcinoma in Barrett's esophagus. In this review, we aim to provide a comprehensive overview of the ways in which AI may help physicians diagnose advanced cancer and make clinical decisions based on predicted outcomes, and combine the endoscopic images to detect precancerous lesions or early cancer. Pertinent studies conducted in recent two years have surged in numbers, with large datasets and external validation from multi-centers, and have partly achieved intriguing results of expert's performance of AI in real time. Improved pre-trained computer-aided diagnosis algorithms in the future studies with larger training and external validation datasets, aiming at real-time video processing, are imperative to produce a diagnostic efficacy similar to or even superior to experienced endoscopists. Meanwhile, supervised randomized controlled trials in real clinical practice are highly essential for a solid conclusion, which meets patient-centered satisfaction. Notably, ethical and legal issues regarding the black-box nature of computer algorithms should be addressed, for both clinicians and regulators.

Key Words: Artificial intelligence; Computer-aided diagnosis; Deep learning; Esophageal squamous cell cancer; Barrett's esophagus; Endoscopy

Manuscript source: Invited manuscript

Received: May 25, 2020
Peer-review started: May 25, 2020
First decision: July 29, 2020
Revised: July 29, 2020
Accepted: August 12, 2020
Article in press: August 12, 2020
Published online: September 21, 2020

P-Reviewer: Jennane R, Kravtsov V, Yoshida H
S-Editor: Yan JP
L-Editor: MedE-Ma JY
P-Editor: Ma YJ

Core Tip: Deep-learning-based artificial intelligence (AI) is a breakthrough technology that has been widely explored in diagnosis, treatment and prediction of esophageal cancer. Recent studies have dealt with limitations of previous researches, including small sample size, selection bias, lack of external validation and algorithm efficiency. Favorable outcomes that are comparable to experienced endoscopists have been achieved with satisfactory robustness, indicating a real-time potential. Future randomized controlled trials are needed to further address these issues concerning AI to provide an ultimate patient-centered satisfaction, in an interpretable, ethical and legal manner.

Citation: Zhang YH, Guo LJ, Yuan XL, Hu B. Artificial intelligence-assisted esophageal cancer management: Now and future. *World J Gastroenterol* 2020; 26(35): 5256-5271
URL: https://www.wjgnet.com/1007-9327/full/v26/i35/5256.htm
DOI: https://dx.doi.org/10.3748/wjg.v26.i35.5256

INTRODUCTION

Esophageal cancer (EC) is one of the top ten leading prevalent malignancies worldwide, ranking the seventh in incidence and the sixth in mortality in 2018[1]. The major histological types are squamous cell carcinoma (SCC), which is predominant worldwide, and adenocarcinoma (AC) which is more prevalent in Caucasian people[2-4]. Data collected from 12 countries have indicated that AC will possibly experience a dramatic increase in incidence up to 2030, while the incidence of SCC will continuously decrease[5]. It is estimated that EC causes absolute years of life lost reduction of 7.8 (95%CI: 2.3-12.7)[6]. Although EC is not the most common cause of admission or readmission to hospital[7], it certainly imposes economic burdens. A cohort study conducted in the United Kingdom showed that the mean net costs of care per 30 patient-days of AC were $1016, $669, and $8678 for the initial phase, continuing care phase and terminal phase, respectively[8]. The cost grows with an increase of tumor node metastasis (TNM) staging at first diagnosis[8].

Apparently, EC is a serious health threat, imposing economic burden on both high-income and low-income countries. Therefore, early diagnosis and evidence-based expert opinions on selecting the optimal treatment modality are crucial for reducing such burden. Although various diagnostic methodologies [including endoscopic ultrasonography (EUS), chromoendoscopy, optical coherence tomography (OCT), high-resolution microendoscopy (HRM), confocal laser endomicroscopy (CLE), volumetric laser endomicroscopy (VLE), and positron emission tomography (PET)], serous and genetic predictors have been developed to improve diagnostic accuracy and predict outcomes, inter-observer variabilities in interpreting images and heavy workloads limit their clinical efficiency[9-11]. A practical tool that can improve accuracy and reduce workload is in urgent need for clinical practice.

Artificial intelligence (AI), which mimics human mind's cognitive behavior, has been an emerging hot spot globally in various disciplines. Numerous models have been attempted for machine learning (ML), and the terminologies can be referred in the previous studies[12,13]. ML models are trained by datasets to extract and transform features, thereby achieving the goal of classification and prediction by self-learning[13-15]. In gastroenterology, AI-based technologies, which are characterized by deep learning (DL) as state-of-the-art machine learning algorithms, have been mainly developed to identify dysplasia in Barrett's esophagus (BE), SCC, gastric cancers, and *Helicobacter pylori* in upper gastrointestinal (UGI) tract[16], and to diagnose polyps, inflammatory bowel diseases, celiac disease, and gastrointestinal (GI) bleeding in lower GI tract[17]. Various models have been developed and studied to detect anatomical structure, discriminate dysplasia, and predict therapeutic and survival outcomes of EC. The ultimate goal of AI is to assist physicians and patients to make a superior data-based diagnosis or decision. In the following sections, we will (1) provide an overview of AI applications in diagnosis and prediction of advanced cancer; (2) specify computer-aided diagnosis (CAD) for early detection of esophageal SCC (ESCC) and esophageal adenocarcinoma (EAC) based on optical imaging; and (3) outline limitations of the existing studies and future perspectives. We searched PubMed database using terms "esophageal cancer" and "artificial intelligence" for papers published up to March 1, 2020, and initially obtained 172 studies. After exclusion of 128 items, 44 research articles that provided detailed data were included

in the review and discussion (Figure 1).

IMPLICATIONS FOR DIAGNOSIS AND THERAPEUTIC DECISIONS

EC is highly malignant, and the 5-year survival rate of late-stage EC is less than 25%[18]. Radical therapies, including surgery, chemotherapy, radiotherapy or their combination are highly essential to improve survival outcome. Accurate diagnosis, precise staging, optimal modality selection, as well as responsiveness and survival outcome prediction are necessary in making true clinical decisions. However, these decisions are made mainly based on the current guidelines and expertise in clinical practice. AI technologies have been therefore developed to enhance the reliability of those decisions in an individualized manner.

Diagnosis

One of the important roles of AI is to detect malignant lesions. In 1996, Liu *et al*[19] proposed a tree-based algorithm called PREDICTOR, to classify patients with dyspeptic symptoms into EC, which achieved a discriminating accuracy of 61.3%, with sensitivity (SEN) and specificity (SPE) of 94.9% and 39.8%, respectively. In 2002, a probabilistic network-based decision-support system was developed, which could correctly predict the cancer stage of 85% of tested data in reasonable time[20]. In the same year, a robust classifier, artificial neural network (ANN), imitating neural network of the human brain, was adopted to distinguish BE from EC[21]. The ANN was trained using 160 genes selected by significance analysis of microarrays (SAM) from cDNA microarray data of esophageal lesions. This ANN outperformed cluster analysis by correctly diagnosing all the tested samples. Kan *et al*[22] also combined ANN with SAM-extracted 60 gene clones to accurately predict lymph node metastasis in 86% of all SCC cases, with SEN and SPE of 88% and 82%, respectively, better than clustering or predictive scoring. Kan *et al*[22] suggested that AI was a potential tool to detect lymph node metastasis when the SEN of coherence tomography (CT), EUS, and PET is insufficient[23,24]. Since tumor risk factors have complex nonlinear correlations, a fuzzy neural network, trained on hybridization of chaotic optimization algorithm and error back propagation (EBP), was able to correctly diagnose 87.36% of ESCC and 70.53% of dysplasia[25]. This fuzzy-logic based model outperformed traditional statistics, such as multivariate logistic regression model that was previously described by Etemadi *et al*[26].

While symptoms are not quite reliable and gene analysis or PET scans are expensive, a simpler noninvasive detection method may be more practical. Li *et al*[27] combined support vector machine (SVM), a traditional classifier, with surface-enhanced Raman spectroscopy in order to distinguish serum spectra of EC patients from healthy controls. Eventually, a combination of SVM with principle component analysis (PCA) on the basis of radial basis function (RBF), namely RBF PCA-SVM algorithm, exhibited the greatest efficacy among others with accuracy, SEN, and SPE of 85.2%, 83.3% and 86.7%, respectively.

Outcome prediction

Another significant role of AI is to predict prognosis of EC based on various demographic, clinicopathologic, hematologic, radiologic, and genetic variables. Surgery and neoadjuvant chemotherapy, radiotherapy or chemoradiotherapy are important definitive modalities for advanced EC. Selecting the optimal strategy with superior predictive outcome is of vital importance.

Traditionally, TNM staging system is used as a predictor. However, a previous study showed that it was not very accurate[28]. Hence, multiple computational algorithms were developed to assist more reliable predictions. In 2005, Sato *et al*[29] trained an ANN to predict survival outcome. They found that the best predictive accuracy was obtained, with 65 clinicopathologic, genetic and biologic variables for 1-year survival and 60 variables for 5-year survival. The area under ROC curve (AUC), SEN, and SPE were 0.883, 78.1%, 84.7% and 0.884, 80.7%, 86.5%, respectively. Similar results with higher SEN and SPE could be achieved in another ANN model to predict the 1- and 3-year post-operative survival of EC and esophagogastric junction cancer[30]. These two ANNs both outperformed TNM staging system[29,30].

In addition to ANN, other models were also proposed to solve certain problems. A prognostic scoring system, using serum C-reactive protein and albumin concentrations, was fused with expertise by fuzzy logic[31]. The proposed model could perform 1-year survival prediction with an AUC of 0.773. Another hierarchical

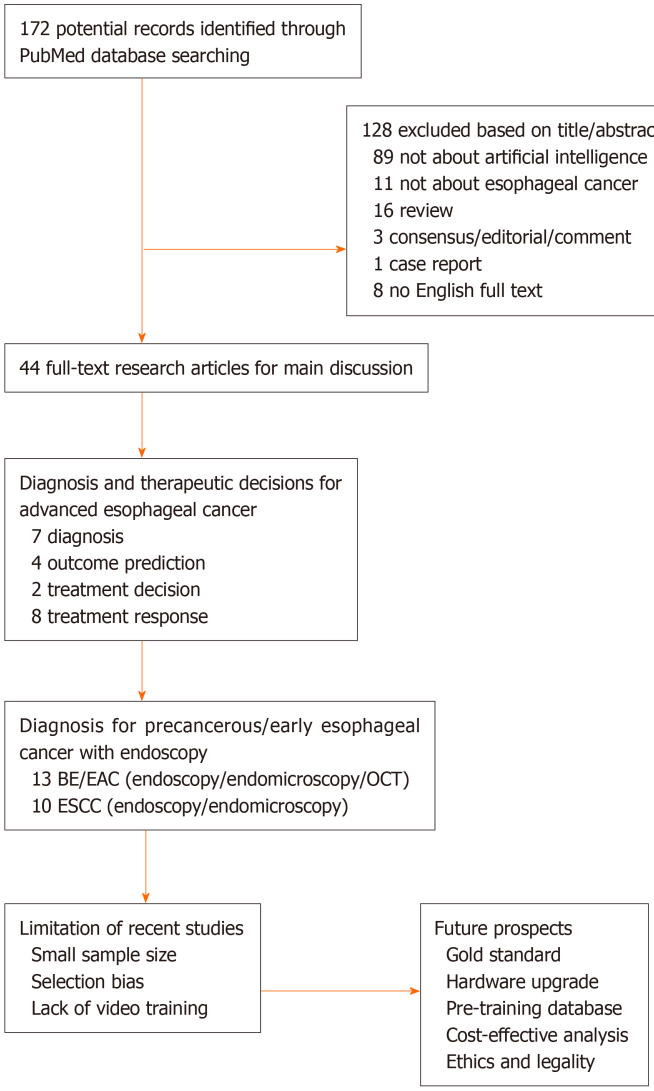

Figure 1 Flow chart of study selection and logic arrangement of review. BE: Barrett's esophagus; EAC: Esophageal adenocarcinoma; OCT: Optical coherence tomography; ESCC: Esophageal squamous cell carcinoma.

forward selection (HFS), a wrapper feature selection method, was developed to solve the problem of small sample size[32]. In this SVM-validated model, clinical and PET features were learned to predict disease-free survival. The results unveiled that HFS achieved the highest accuracy of 94%, with robustness of 96%. Robustness could be further increased to 98%, if HFS was incorporated prior knowledge (pHFS).

Treatment decision

Based on the condition and prognosis of patient, an individualized treatment strategy is needed. For instance, when chemotherapy is prescribed for a patient, what is the optimal medication with appropriate dosage and period? Generally, clinicians make decisions according to their own experience, guidelines or consensus. However, those recommendations are often fixed and human errors are sometimes inevitable. A group of Iranian experts attempted to train a multilayer neural network with particle swarm optimization and EBP algorithms, in order to determine the dosage of chemotherapy[33]. Encouraging results showed that accuracy of particle swarm optimization and EBP was both 77.3%. Zahedi *et al*[33] were positive about its future application as a supplementary decision-making system.

While the majority of decisions are made before treatment, is it possible to make real-time treatment decisions? The answer is YES. Maktabi *et al*[34] tested a relatively new hyperspectral imaging system. They found that SVM was able to detect cancerous tissue with 63% SEN and 69% SPE within 1s. It is promising that hyperspectral imaging may assist surgeons in identifying tumor borders intra-operatively in real

time.

Treatment response

A good treatment response is crucial for consequential therapeutic decision and predicting outcome[35]. Endeavors have been made to select candidate factors that correlate with responsiveness to treatment. However, it is often extremely laborious to testify these numerous variables in clinical trials. AI technologies are potential powerful tools for this selection.

One indicator is the genetic biomarker. In 2010, Warnecke-Eberz *et al*[36] reported their usage of ANN to predict histopathologic responsiveness of treatment-naïve patients to neoadjuvant chemoradiotherapy by analyzing 17 genes using the TaqMan low-density arrays. Their results were promising, with 85.4% accuracy, 80% SEN, and 90.5% SPE. Radiology is another important indicator to assess tumor regression after treatment. One rationale for this exploration is that tumor heterogeneity exists within radiologic images[37]. The standardized uptake values of ^{18}F-fluorodeoxyglucose in PET imaging were reported to have predictive potential[38]. However, this predictive power is limited[39] due to some confounding factors, such as intra-observer variations. Ypsilantis *et al*[40] adopted a three-slice convolutional neural network that could extract features from pre-treatment PET scans automatically to predict response to chemotherapy. It achieved a moderate accuracy of 73.4%, with SEN and SPE of 80.7% and 81.6%, respectively, which outperformed other ML algorithms trained on handcrafted PET scan features. Recently, CT radiomics three months after chemoradiotherapy were combined with dosimetric features of gross tumor volume and organs at risk to identify non-responders. Jin *et al*[41] found that these combinative features trained by the model of extreme gradient boosting plus PCA achieved an accuracy of 70.8%, with AUC of 0.541.

While tumor regression is an important indicator to assess responsiveness, post-treatment distant metastasis is also vital to evaluate responsiveness, which is correlated with survival outcome. In order to predict post-operative distant metastasis of ESCC, further SVM models incorporated with clinicopathological and immunohistological variables were established[42]. Finally, the SVM model with four clinicopathological features and nine immunomarkers had better performance, with accuracy, SEN, SPE, positive predictive value, and negative predictive value of 78.7%, 56.6%, 97.7%, 95.6%, and 72.3%, respectively. Another least squares SVM model was also proposed to predict post-operative lymph node metastasis in patients who received chemotherapy preoperatively, by exploiting preoperative CT radiomics[43]. Tumor length, thickness, CT value, long axis and short axis size of the largest regional lymph node were analyzed. The model reached an AUC of 0.887.

In addition to its diagnostic and predictive value, AI has learned to identify meaningful alterations in molecular and genetic level. In 2017, Lin *et al*[44] compared the serum chemical elements concentrations between ESCC patient and healthy controls, and found that nearly half of the elements were different between the two groups. They then trained several classifiers to perform the discrimination, with Random Forest being the best (98.38% accuracy) and SVM the second (96.56% accuracy). Later, Mourikis *et al*[45] developed a robust sysSVM algorithm to identify 952 genes that promoted EAC development, using 34 biological features of known cancer genes. They called these rare and highly individualized genes "helper" genes, which function alongside known drivers.

AI may be a feasible option to help determine an optimal treatment strategy. This was previously evidenced by a study of 13 365 EACs from 33 cancer centers worldwide, which incorporated random forest algorithm, and found that the predicted survival of AI-generated therapy was superior to actual human decisions[46]. However, most of the above-mentioned ML algorithms described were developed for the sake of advanced cancer. Diagnosing EC in an early stage contributes to a far better outcome when treatment is undertaken appropriately. This is highly dependent on the development of optical imaging technologies that can directly visualize the morphology of esophageal lesions.

MORPHOLOGY-BASED CAD

In recent decades, endoscopic optical imaging techniques have been rapidly advanced, which provide endoscopists a fine inspection of the morphology of esophageal mucosa, micro-vessels, and even cells. In lieu of white light imaging (WLI) and magnifying endoscopy (ME), emerging OCT, CLE, VLE, and HRM techniques have

been developed to diagnose BE[47-49]. Meanwhile, the diagnosis of SCC more relies on chromoendoscopy and intra-epithelial papillary capillary loop (IPCL) observed under narrow band imaging (NBI) plus ME[50]. Although these modalities have yielded preferable diagnostic value, the interpretation of these images need expert's experience (inter- and intra-observer variability[51]), and processing large dataset is laborious and time consuming. Researchers in medicine and information engineering have collaborated to develop different AI models for this purpose.

BE versus dysplasia or EAC

The current screening and surveillance recommendation for BE is endoscopic examination plus random biopsy[52] , which is limited by sampling error. AI models trained with various endoscopic modalities and pathologies aimed to overcome these shortcomings (Table 1).

Endoscopy: In 2009, German experts developed a content-based image retrieval framework[53]. In this frame, novel color-texture features were combined with an interactive feedback loop. The algorithm could correctly recognize 95% of normal mucosa and 70% of BE from 390 training images, with a moderate inter-rater reliability of 0.71. The authors thought that the CAD system might be incorporated to the endoscopic system to help lesser experienced clinicians. In 2013, van der Sommen *et al*[54] tried an SVM algorithm, which could automatically identify and locate irregularities of esophagus on high-definition endoscopy with an accuracy of 95.9% and AUC of 0.99, taking a first step towards CAD. Later, these authors used a CAD system to automatically recognize region of interest (ROI) in dysplastic BE[55]. The SVM-based classification yielded a SEN and SPE of 83% for per-image level, and 86% and 87%, for the patient level, respectively. However, the *f*-score of the system, which indicates the similarity with the gold standard, was lower than experts.

In order to improve the outcome, Horie *et al*[56] were the first who adopted a deep CNN (Single Shot MultiBox Detector, SSD) model to detect EC from WLI and NBI images in 2018. Only 8 EACs were used in that study. The diagnostic accuracy for EAC was 90%, and SEN for WLI and NBI at patient level was both equal to 88%. The system processed one image in only 0.02 s, which is promising for a real-time job. This ability of SSD to detect EAC was assessed in another study, which outperformed their proposed regional-based CNN (R-CNN), Fast R-CNN and Faster R-CNN in both precision and speed, which achieved F-measure, SEN, and SPE of 0.94, 96% and 92%, respectively[57]. The authors stated that SSD worked faster due to its single forward pass network nature. CNN was then validated in a more recent study to detect early dysplastic BE[58]. The system was pretrained on ImageNet, and was then trained with 1853 images and tested with 458 images. The CNN accurately detected 95.4% of the dysplasia, with 96.4% SEN and 94.2% SPE. One highlight for this study is that it studied WLI and NBI images, as well as images with standard focus and near focus. Another highlight is its ability to deal with real-time videos.

Except for the above-mentioned CNNs, another CNN built upon residual net (ResNet) was introduced. Ebigbo *et al*[59] tested this system in two databases, Augsburg and Medical Image Computing and Computer-Assisted Intervention, with SEN both being over 90%. Later, de Groof *et al*[60] used a custom-made hybrid ResNet/U-Net which was pretrained on GastroNet to distinguish non-dysplastic BE from dysplasia. The system was trained using state-of-the-art ML techniques (transfer learning and ensemble learning) and validated in a sequential five datasets, with accuracy of 89% and 88% for two external validation datasets, which were slightly superior to the model pre-trained with ImageNet in its supplementary ablation experiment.

Endomicroscopy: In 2017, Hong *et al*[61] reported their experience in adopting CNN as a classifier to distinguish intestinal metaplasia (IM), gastric metaplasia (GM) and neoplasia (NPL) of BE using endomicroscopic images. The total accuracy was 80.77%. It performed well for IM and NPL. However, it could not identify GM in the tested samples. VLE is an advanced imaging techinique that can provide a 3-mm deep scan of the esophagus in full circumference, which is commercially available (Nvision VLE™ Imaging System). In the same year, Swager *et al*[62] reported the first attempt of using CAD to detect NPL by adopting histology-correlated *ex-vivo* VLE. The authors used eight separate ML algorithms that were trained with clinically inspired features. They found that "layering and signal decay statistics" feature performed the best, with AUC, SEN, and SPE of 0.95, 90%, and 93%, respectively. Similar results were obtained by van der Sommen *et al*[63], with a maximum AUC of 0.93 in identifying early EAC in BE. Notably, the authors discovered that scanning depth of 0.5-1 mm was the most appropriate range for classifying tissue categories.

Table 1 Computer-aided endoscopic diagnosis for dysplastic Barrett's esophagus

Ref.	Year	Study design	Lesions	Diagnostic method	AI technology	Dataset capacity	Validation	Outcomes	Compared to expert	Processing speed
Münzenmayer *et al*[53]	2009	Retrospective	BE	WLI	Color-texture analysis in a CBIR framework	390 images with 482 ROIs	LOO (N-fold cross-validation)	Accuracy: BE/CC/EP 70%/74%/95%	NA	NA
van der Sommen *et al*[55]	2016	Retrospective	HGD, early EAC	WLI	SVM	100 images	LOO	Per-image SEN/SPE: 83%/83%; Per-patient SEN/SPE: 86%/87%	Inferior	NA
Horie *et al*[56]	2019	Retrospective	EAC	WLI; NBI	CNN-SSD	8 patients	Caffe DL framework	Accuracy: 90%; Per-image SEN: WLI/NBI: 69%/71%; Per-case SEN: WLI/NBI: 88%/88%	NA	0.02 s/image
Ghatwary *et al*[57]	2019	Retrospective	EAC	WLI	VGG'16-based; R-CNN; Fast R-CNN; Faster R-CNN; SSD	100 images (train 50, test 50)	5-fold cross-validation and LOO	F-measure: 0.94 (SSD); SEN/SPE: 96%/92% (SSD)	NA	0.1-0.2 s/image
Hashimoto *et al*[58]	2020	Retrospective	HGD, early EAC	WLI and NBI with both standard and near focus	CNN	1835 images	NA	Per-image accuracy: 95.4%; Per-image SEN/SPE: 96.4%/94.2%; 98.6%/88.8% (WLI); 92.4%/99.2% (NBI)	NA	GPU gtx 1070: 0.014 s/frame; YOLO v2: 0.022 s/frame
Ebigbo *et al*[59]	2019	Retrospective	Early EAC	WLI; NBI	CNN-ResNet	248 images	LOO	SEN/SPE of Augsburg database: 97%/88% (WLI); 94%/80% (NBI); SEN/SPE of MICCAI database: 92%/100%	Superior	NA
de Groof *et al*[60]	2019	Retrospective	Early dysplastic BE	WLI	ResNet-UNet hybrid	1704 images (train 1544, validation 160)	4-fold cross-validation (external validation)	Accuracy/SEN/SPE: 89%/90%/88% (dataset 4); 88%/93%/83% (dataset 5)	NA (superior to non-expert)	Classification: 0.111 s/image; Segmentation: 0.124 s/image
Swager *et al*[62]	2017	Retrospective	HGD, early EAC	VLE	SVM, DA, Adaboost, RF, kNN, NB, LR, LogReg	60 images	LOO	AUC: 0.95; SEN/SPE: 90%/93%	Superior	NA
van der Sommen *et al*[63]	2018	Retrospective	HGD, early EAC	VLE	SVM, RF; AdaBoost; CNN, kNN; DA, LogReg	60 frames	LOO	AUC: 0.90-0.93	Superior	24 ms/full dataset for clinically-inspired features
Struyvenberg *et al*[65]	2020	Prospective	HGD, early EAC	VLE	PCA-CAD	3060 frames	NA	AUC of Multi-frame: 0.91; AUC of Single-frame: 0.83	NA	0.001 s/frame; 1.5s/full VLE scan
van der Putten *et al*[66]	2020	Prospective	HGD, early EAC	VLE	Multi-step PDE-CNN on an A-line basis	In-vivo: 140 images (train 111, test 29)	4-fold cross-validation	AUC: 0.93; F1 score: 87.4%	NA	50000 A-lines/s
Shin *et al*[67]	2016	Retrospective	HGD, EAC	HRM	Two-class LDA-based automated sequential classification algorithm	230 sites (train 77, validation 153)	NA	Accuracy: 84.9%; SEN/SPE: 88%/85%	NA	52 s/image

Qi *et al*[68]	2006	Retrospective	Dysplastic BE	OCT	PCA	106 images	LOO	Accuracy: 83%; SEN/SPE: 82%/74%	NA	NA

AdaBoost: Adaptive boost; AUC: Area under ROC curve; BE: Barrett's esophagus; CAD: Computer-aided diagnosis; CBIR: Content-based image retrieval; CC: Mucosa of cardia; CNN: Convolutional neural network; DA: Discriminant analysis; EAC: Esophageal adenocarcinoma; EP: Epithelium; HGD: High-grade dysplasia; HRM: High-resolution microendoscopy; Knn: K-nearest neighbor; LDA: Linear discriminant analysis; LogReg: Logistic regression; LOO: Leave-one-out cross-validation; LR: Linear regression; NA: Not available; NB: Naïve bayes; NBI: Narrow band imaging; OCT: Optical coherence tomography; PCA: Principle component analysis; PDE: Principle dimension encoding; R-CNN: Regional-based CNN; RF: Random forest; SEN: Sensitivity; SPE: Specificity; SSD: Single shot multibox detector; SVM: Support vector machine; VLE: Volumetric laser endomicroscopy; WLI: White light imaging.

Since VLE produces an overwhelming number of images in a short time, a real-time CAD system is more helpful in actual clinical practice. In 2019, Trindade *et al*[64] reported a video case illustrating an intelligent real-time image segmentation system which employed three established features to dynamically enhance abnormal VLE images with color in endoscopic procedure. They are now undergoing a multicenter RCT (NCT03814824) to further validate this CAD system. While most studies use single frame to include ROI, a recent study tried to add neighboring VLE images to pathology-correlated ROI[65]. Hopefully, the so-called multi-frame analysis combing PCA improved the performance of single-frame analysis, from an AUC of 0.83 to 0.91. Meanwhile, the novel CAD system needs only 1.3 ms to automatically differentiate non-dysplastic BE from dysplasia in one image, and this is also a promising result for a real-time setting.

While previous studies employed *ex-vivo* scan images, the following study conducted by van der Putten *et al*[66] used *in-vivo* histology-correlated images. In addition, they used principle dimension encoding (PDE) to encode images into score vector. They combined this PDE with traditional ML algorithms, *e.g.*, random forest and SVM, to classify the degree of dysplasia (high-grade dysplasia *vs* early EAC). They obtained an AUC of 0.93 and F1 score of 87.4%, which outperformed some traditional DL classifiers, such as Squeezenet and Inception.

Another kind of endomicroscopic technique is HRM. Shin *et al*[67] designed an automated imaging processing algorithm extracting epithelium morphology and BE glandular architecture features, and a classification algorithm, which distinguished NPL from dysplasia in BE with an accuracy, SEN and SPE of 84.9%, 88%, and 85% in validation dataset, respectively. This quantitative CAD is cost-effective and may be applied in clinical settings after improvement of image acquisition quality and processing speed.

OCT: OCT is also a noninvasive imaging technique that can detect BE, dysplasia and early EAC, in compensation to routine endoscopy. In 2006, Qi *et al*[68] attempted to extract image features using center-symmetric auto-correlation method and a PCA-based CAD algorithm was used for classification. A total of 106 pathology-paired images were included for training, which ended up with an accuracy of 83%, SEN of 82% and SPE of 74% to distinguish non-dysplastic BE from dysplasia. In general, the accuracy of OCT in identifying dysplasia is not satisfactory, which limits its

application[69].

In addition to endoscopic images, pathologic morphology has also been studied. Sabo *et al*[70] employed an ANN-validated computerized nuclear morphometry (pseudostratification, pleomorphism, chromatin texture, symmetry and orientation) model to discriminate the degree of dysplasia in BE. The model was able to differentiate non-dysplastic BE from low-grade dysplasia with an accuracy of 89%, and low-grade dysplasia from high-grade dysplasia with an accuracy of 86%.

ESCC

ESCC is the dominant histological type of esophageal cancer worldwide. Diagnosing early cancer mainly depends on endoscopic screening, which also produces a large number of images that needs special training to interpret. AI technologies have also been explored globally to address this issue (Table 2).

Endoscopy: In 2016, Liu *et al*[71] designed an algorithm called joint diagonalization principle component analysis, which correctly detected 90.75% of EC with an AUC of 0.9471. To improve the performance of CAD system, Horie *et al*[56] did the first attempt to use DL to diagnose ESCC with a large number of endoscopic images. The CNN had a diagnostic accuracy of 99% for ESCC, 99% for superficial cancer, and 92% for advanced one. The SEN of CNN was 97% for per-patient level and 77% for per-image level. Later in 2019, Cai *et al*[72] proposed a novel CAD system called deep neural network (DNN). They used only standard WLI images to train the model. The DNN-CAD model could detect 91.4% of early ESCC, higher than senior endoscopists. By using this model, the average diagnostic performance of endoscopists improved satisfactorily, in terms of accuracy, SEN, and SPE. However, these studies excluded magnified images.

Later, Ohmori *et al*[73] evaluated both ME and non-ME images [including WLI and NBI/blue laser imaging (BLI)] using a CNN based on SSD to recognize SCC. The accuracy for ME, non-ME + WLI, and non-ME + NBI/BLI was 77%, 81%, and 77%, respectively, all with high SEN and moderate SPE. The result was similar to experienced endoscopists tested in this study. Zhao *et al*[74] conducted another study and evaluated ME + NBI images by employing a double-labeling fully convolutional network. This system used ROI-label and segmentation-label to delineate IPCLs based on the AB classification by the Japan Esophageal Society[75]. The study showed that senior observers had significant higher diagnostic accuracy than mid-level and junior ones. The model reached a diagnostic accuracy of 89.2% and 93% in lesion and pixel level, respectively, for distinguishing type A, B1 and B2 IPCLs, which was similar to that of senior group. Specifically, the model had a higher sensitivity for type A IPCL than clinicians (71.5% *vs* 28.2%-64.9%), which might avoid unnecessary radical treatment. Instead of identifying IPCL patterns, the study conducted by Nakagawa *et al*[76] aimed to predict invasion depths. The authors developed two separate SSD-based CNNs for ME and non-ME images. The ability of the system to correctly distinguish EP/submucosal (SM) 1 cancers from SM2/SM3 cancers was 91%, 92.9%, and 89.7% for the ME+ non-ME, non-ME and ME images, respectively. Regrading M and SM cancers, the differentiating accuracy was 89.7%, 90.3%, and 92.3% for the total, non-ME, and ME, respectively. The performance of this CAD model was also comparable to experts, but much faster.

A processing speed over 30 images/s is necessary for dynamic video analysis[56]. Although Horie *et al*[56], Ohmori *et al*[73] and Nakagawa *et al*[76] reported that their systems could process one image in 0.02, 0.027, and 0.033 s, respectively, they have not tested the systems in real-time videos. After Cai *et al*[72] had validated the efficacy of their DNN-CAD model, they split the video into images and then assembled them, enabling the model to delineate early cancer in real time. Everson *et al*[77] validated another CNN investigating IPCLs using sequential still images in real time of 0.026 to 0.037 s per image. The CNN could differentiate type A from type B IPCLs with a mean accuracy of 93.3%. Last year, Luo *et al*[78] reported a multicenter, comparative study, exploiting 1 036 496 endoscopic images to construct a gastrointestinal artificial intelligence diagnostic system (GRAIDS) based on the concept of DeepLab's V3+. The GRAIDS yielded a diagnostic accuracy of UGI cancer ranging from 91.5% to 97.7% for internal, external, and prospective validation datasets, with favorable sensitivities, which were similar to experts and superior to non-experts. They also incorporated the CAD model to endoscopic videos in real time, with the highest speed of 0.008 s per image and latency less than 0.04 s. However, they did not report their outcome in distinct histology. Recently, Guo *et al*[79] specially developed a CNN-CAD system built on SegNet architecture, aiming at real-time application in clinical settings. In this

Table 2 Computer-aided endoscopic diagnosis for early esophageal squamous cell cancer

Ref.	Year	Study design	Lesions	Diagnostic method	AI technology	Dataset capacity	Validation	Outcomes	Compared to expert	Processing speed
Liu *et al*[71]	2016	Retrospective	Early ESCC	WLI	JDPCA + CCV	400 images	10-fold cross-validation	Accuracy: 90.75%; AUC: 0.9471; SEN/SPE: 93.33%/89.2%	NA	NA
Horie *et al*[56]	2019	Retrospective	ESCC	WLI; NBI	CNN-SSD	41 pts (train 8428 images; test 1118 images without histology distinction)	Caffe DL framework	Accuracy: 99%; Per-image SEN: 72%/86% (WLI/NBI, respectively); Per-case SEN: 79%/89% (WLI/NBI, respectively)	NA	0.02 s/image
Cai *et al*[72]	2019	Retrospective	Early ESCC	WLI	DNN	2615 images (train 2428, test 187)	NA	Accuracy: 91.4%; SEN/SPE: 97.8%/85.4%	Superior	NA
Zhao *et al*[74]	2019	Retrospective	Early ESCC	ME + NBI	Double labeling FNN	1350 images with 1383 lesions	3-fold cross-validation	Accuracy/SEN/SPE at lesion level: 89.2%/87%/84.1%; Accuracy at pixel level: 93%	Comparable	NA
Ohmori *et al*[73]	2020	Retrospective	Superficial ESCC	ME + NBI/BLI; Non-ME + WLI/NBI/BLI	CNN	23289 images (train 22562, test 727)		Accuracy/SEN/SPE: 77%/100%/63% (Non-ME + NBI/BLI); 81%/90%76% (Non-ME + WLI); 77%/98%/56% (ME)	Comparable	0.028 s/image
Nakagawa *et al*[76]	2019	Retrospective	ESCC (EP-SM1/SM2+SM3)	ME; Non-ME	CNN-SSD	15252 images (train 14338, test 914)	Caffe DL framework	Accuracy/SEN/SPE: 91%/90.1%/95.8%	Comparable	0.033 s/image
Everson *et al*[77]	2019	Retrospective	ESCC IPCLs (type A/type B)	ME + NBI	CNN	7046 images	5-fold cross-validation+eCAM	Accuracy/SEN/SPE: 93.3%/89.3%/98%	NA	0.026-0.037 s/image
Guo *et al*[79]	2020	Retrospective	Early ESCC	NBI (ME + non-ME)	CNN-SegNet	13144 images (train 6473, validation 6671), 80 videos (47 lesions, 33 normal esophagus)	NA	Per-image SEN/SPE: 98.04%/95.03%; Per-frame SEN/SPE: 91.5%/99.9%	NA	< 0.04 s/frame; Latency <0.1 s
Shin *et al*[82]	2015	Retrospective	HGD, ESCC	HRM	Two-class LDA	375 sites of images (train 104, test 104, validation 167)	NA	AUC: 0.95; SEN/SPE: 84%/95%	NA	3.5 s/image
Quang *et al*[83]	2016	Retrospective	ESCC	HRM	A fully automated algorithm	375 biopsied sites from Shin *et al*[82] (train 104, test 104, validation 167)	NA	AUC: 0.937; SEN/SPE: 95%/91%	NA	Average 5 s for computing

BLI: Blue laser imaging; CCV: Color coherence vector; DL: Deep learning; CNN: Convolutional neural network; DNN: Deep neural network; eCAM: Explicit class activation map; EP: Epithelium; ESCC: Esophageal squamous cell cancer; FNN: Fuzzy neural network; HGD: High-grade dysplasia; HRM: High-resolution microendoscopy; IPCLs: Intra-papillary capillary loops; JDPCA: Joint diagonalisation principal component analysis; LDA: Linear discriminant analysis; ME: Magnifying endoscopy; NA: Not available; NBI: Narrow band imaging; SEN: Sensitivity; SM: Submucosa; SPE: Specificity; SSD: Single shot multibox detector; WLI: White light imaging.

study, 13144 NBI (ME + non-ME) images and 80 video clips were employed. In the image dataset, the SEN, SPE, and AUC were 98.04%, 95.03% and 0.989, respectively. For the video dataset, the SEN of per frame for non-ME and ME was 60.8% and 96.1%,

respectively; the SEN of per lesion for non-ME and ME was both 100%. When they analyzed 33 original videos of full-range normal esophagus, they acquired a SPE of 99.95% and 90.9% for per-frame and per-case analysis, respectively. The ability of this model to process each frame with a maximum time of 0.04 s and latency less than 0.1 s set a good example for future model optimization for real-time applications[80].

Endomicroscopy: In 2007, Kodashima *et al*[81] used ImageJ software to label the border of nuclei under endo-cytologic images from 10 ESCC patients. They found that the computer-labelled nuclei area of ESCC was significantly different from that of normal tissues, which demonstrated the diagnostic possibility of computer. HRM is another low-cost tool that can illustrate the esophageal epithelium in cellular level, which compensates the low specificity of iodine staining and is also more cost-effective compared with CLE. In 2015, Shin *et al*[82] developed a 2-class linear classification algorithm using nuclei-related features to identify neoplastic squamous mucosa (HGD + cancer). It resulted in an AUC, SEN, and SPE of 0.95, 87%, 97% and 0.93, 84%, 95% for the test and validation datasets, respectively. However, the application of this system for real-time practice needs acceleration of analyzing speed. To solve this problem and reduce the cost of equipment, a smaller, tablet-interfaced HRM with real-time algorithm was developed by Quang *et al*[83]. The algorithm was able to automatically identify SCC with an AUC, SEN, and SPE of 0.937, 95%, and 91%, respectively, which is comparable to the result achieved by the first generation bulky laptop-interfaced HRM[82] or the combination of Lugol chromoendoscopy and HRM[84].

STUDY LIMITATIONS AND FUTURE PERSPECTIVES

Limitations

The exciting and promising findings of various CAD models have been summarized in detail above. Researches are ongoing worldwide because none of the studies were perfect. The limitations and problems are driving forces for evolution and innovation. We hereby discuss several major drawbacks that limit the strength of the studies.

Firstly, the most mentioned drawback is insufficient training sample size. The number of endoscopic images that the majority of studies employed ranged from 248 to about 7000 (Tables 1 and 2). The limited number of training data, lack of imaging variability, and single-center nature are likely to cause overfitting[85], which attenuates the ability of AI models to perform well in unused datasets and leads to unstable results[12,55]. To overcome this problem, various regularization methods have been developed, such as segmenting the image or using cross validation with 5 folds or even 10 folds to augment the datasets. Recently, the size of datasets has been greatly enlarged in several studies[56,73,79], the largest of which included over one million UGI images from six centers[78]. Therefore, further multicenter studies including large dataset with different kinds of images (*i.e.*, WLI, NBI, ME and non-ME) harvested by different endoscopic systems for SCC and AC are likely to produce results with robustness and external generalizability. In addition, different AI algorithms tested in prospective external dataset need to be developed to increase the diversity of AI technology[13].

Secondly, selection bias is another contributor to limited generalizability. Most of the previous studies were retrospective and used only high-quality images. Suboptimal quality images with mucus, blur, or blood. were excluded. Additionally, unbalanced distribution of lesion types (SCC *vs* AC, type B1 *vs* B2 and B3 IPCLs), different numbers of images for each patient, and non-uniform processing method for different lesions all might cause bias in the result. Further prospective RCTs will be required in the future.

Thirdly, almost all of the studies employed still images to train AI model. Not until recently did the researchers validate the efficacy in dealing with endoscopic videos in a real-time manner. Future video-based researches are needed to narrow the gap between study and clinical practice.

Future perspectives

Gold standard: Consensus-based ground truth for lesions is preferred over a single expert's annotation. The committees of expert endoscopists and pathologists from different countries need to be formed to improve the precision of annotation. In addition, the AI should play a role in helping endoscopists recognize lesions and target biopsies for gold standard pathological examination, rather than replacing our "job".

Hardware upgrade: Computers equipped with powerful GPU are needed to perform more sophisticated algorithms and process large volume of graphical data, in order to achieve the goal of real-time recognition.

Pre-training database: ImageNet and GastroNet have been introduced, which store mass datasets of manually labeled images. These databases should be constantly enriched, since CAD models with prior knowledge are prone to have better discriminative ability[60].

Cost-effect analysis: When a novel diagnostic method is introduced to clinical practice, whether it is cost-effective is an important issue. A recent multi-center add-on analysis revealed that AI is able to reduce cost of colonoscopic management of polyps[86]. Since medical cost is one of the major concerns for both patients and government, it is necessary to assess whether AI can improve diagnostic performance of EC while reducing cost of unnecessary examinations and radical therapies. Future studies concerning medical cost and reimbursement should be conducted in different countries with different healthcare and insurance systems to address this issue.

Ethics and legality: Believe it or not to believe it, it is a real question. While we have taken a giant leap of AI technology in medicine which has the potential to improve the performance of clinicians with different experience and reduce error, the black-box[87] nature of the ML algorithms truly brings doubts[88]. Can we trust the results of AI, since they lack explainability? What should we do with these computer-generated results? Are they certified to be legal evidence? Challenges for legislation, regulation, insurance and clinical practice are inevitable. Supervised RCTs and AI participation in clinical workflow are needed to provide solid evidence that AI is acceptable within the range of legal and ethical concerns[89]. Nevertheless, trends of AI are irreversible. The ultimate role of AI in medicine might be a supervised task performer[90].

CONCLUSION

In this manuscript, we provided a comprehensive review of AI technology in diagnosis, treatment decision and outcome prediction for EC. We searched only PubMed database for clinical researches and applications. Issues regarding computer science and image processing are not our topics. The CAD systems have evolved from traditional ML algorithms to neural network-based DL, and from still image analysis to real-time video processing. AI can improve non-expert's performance while correct erroneous classification by experts[78]. Researches with larger datasets and more reliable CAD models are being conducted worldwide. It is promising that AI may facilitate early cancer screening, surveillance and treatment in high-risk regions. However, it is noteworthy that patient's consent and satisfaction are of first priority.

REFERENCES

1 **Bray F**, Ferlay J, Soerjomataram I, Siegel RL, Torre LA, Jemal A. Global cancer statistics 2018: GLOBOCAN estimates of incidence and mortality worldwide for 36 cancers in 185 countries. *CA Cancer J Clin* 2018; **68**: 394-424 [PMID: 30207593 DOI: 10.3322/caac.21492]

2 **Pennathur A**, Gibson MK, Jobe BA, Luketich JD. Oesophageal carcinoma. *Lancet* 2013; **381**: 400-412 [PMID: 23374478 DOI: 10.1016/S0140-6736(12)60643-6]

3 **Simard EP**, Ward EM, Siegel R, Jemal A. Cancers with increasing incidence trends in the United States: 1999 through 2008. *CA Cancer J Clin* 2012; **62**: 118-128 [PMID: 22281605 DOI: 10.3322/caac.20141]

4 **Arnold M**, Soerjomataram I, Ferlay J, Forman D. Global incidence of oesophageal cancer by histological subtype in 2012. *Gut* 2015; **64**: 381-387 [PMID: 25320104 DOI: 10.1136/gutjnl-2014-308124]

5 **Arnold M**, Laversanne M, Brown LM, Devesa SS, Bray F. Predicting the Future Burden of Esophageal Cancer by Histological Subtype: International Trends in Incidence up to 2030. *Am J Gastroenterol* 2017; **112**: 1247-1255 [PMID: 28585555 DOI: 10.1038/ajg.2017.155]

6 **Global Burden of Disease Cancer Collaboration, Fitzmaurice C**, Allen C, Barber RM, Barregard L, Bhutta ZA, Brenner H, Dicker DJ, Chimed-Orchir O, Dandona R, Dandona L, Fleming T, Forouzanfar MH, Hancock J, Hay RJ, Hunter-Merrill R, Huynh C, Hosgood HD, Johnson CO, Jonas JB, Khubchandani J, Kumar GA, Kutz M, Lan Q, Larson HJ, Liang X, Lim SS, Lopez AD, MacIntyre MF, Marczak L, Marquez N, Mokdad AH, Pinho C, Pourmalek F, Salomon JA, Sanabria JR, Sandar L, Sartorius B, Schwartz SM, Shackelford KA, Shibuya K, Stanaway J, Steiner C, Sun J, Takahashi K, Vollset SE, Vos T, Wagner JA, Wang H, Westerman R, Zeeb H, Zoeckler L, Abd-Allah F, Ahmed MB, Alabed S, Alam NK, Aldhahri SF, Alem G, Alemayohu MA, Ali R, Al-Raddadi R, Amare A, Amoako Y, Artaman A, Asayesh H, Atnafu N, Awasthi A, Saleem HB, Barac A, Bedi N, Bensenor I, Berhane A, Bernabé E, Betsu B, Binagwaho A,

Boneya D, Campos-Nonato I, Castañeda-Orjuela C, Catalá-López F, Chiang P, Chibueze C, Chitheer A, Choi JY, Cowie B, Damtew S, das Neves J, Dey S, Dharmaratne S, Dhillon P, Ding E, Driscoll T, Ekwueme D, Endries AY, Farvid M, Farzadfar F, Fernandes J, Fischer F, G/Hiwot TT, Gebru A, Gopalani S, Hailu A, Horino M, Horita N, Husseini A, Huybrechts I, Inoue M, Islami F, Jakovljevic M, James S, Javanbakht M, Jee SH, Kasaeian A, Kedir MS, Khader YS, Khang YH, Kim D, Leigh J, Linn S, Lunevicius R, El Razek HMA, Malekzadeh R, Malta DC, Marcenes W, Markos D, Melaku YA, Meles KG, Mendoza W, Mengiste DT, Meretoja TJ, Miller TR, Mohammad KA, Mohammadi A, Mohammed S, Moradi-Lakeh M, Nagel G, Nand D, Le Nguyen Q, Nolte S, Ogbo FA, Oladimeji KE, Oren E, Pa M, Park EK, Pereira DM, Plass D, Qorbani M, Radfar A, Rafay A, Rahman M, Rana SM, Søreide K, Satpathy M, Sawhney M, Sepanlou SG, Shaikh MA, She J, Shiue I, Shore HR, Shrime MG, So S, Soneji S, Stathopoulou V, Stroumpoulis K, Sufiyan MB, Sykes BL, Tabarés-Seisdedos R, Tadese F, Tedla BA, Tessema GA, Thakur JS, Tran BX, Ukwaja KN, Uzochukwu BSC, Vlassov VV, Weiderpass E, Wubshet Terefe M, Yebyo HG, Yimam HH, Yonemoto N, Younis MZ, Yu C, Zaidi Z, Zaki MES, Zenebe ZM, Murray CJL, Naghavi M. Global, Regional, and National Cancer Incidence, Mortality, Years of Life Lost, Years Lived With Disability, and Disability-Adjusted Life-years for 32 Cancer Groups, 1990 to 2015: A Systematic Analysis for the Global Burden of Disease Study. *JAMA Oncol* 2017; **3**: 524-548 [PMID: 27918777 DOI: 10.1001/jamaoncol.2016.5688]

7 **Peery AF**, Crockett SD, Murphy CC, Lund JL, Dellon ES, Williams JL, Jensen ET, Shaheen NJ, Barritt AS, Lieber SR, Kochar B, Barnes EL, Fan YC, Pate V, Galanko J, Baron TH, Sandler RS. Burden and Cost of Gastrointestinal, Liver, and Pancreatic Diseases in the United States: Update 2018. *Gastroenterology* 2019; **156**: 254-272.e11 [PMID: 30315778 DOI: 10.1053/j.gastro.2018.08.063]

8 **Thein HH**, Jembere N, Thavorn K, Chan KKW, Coyte PC, de Oliveira C, Hur C, Earle CC. Estimates and predictors of health care costs of esophageal adenocarcinoma: a population-based cohort study. *BMC Cancer* 2018; **18**: 694 [PMID: 29945563 DOI: 10.1186/s12885-018-4620-2]

9 **Schreurs LM**, Busz DM, Paardekooper GM, Beukema JC, Jager PL, Van der Jagt EJ, van Dam GM, Groen H, Plukker JT, Langendijk JA. Impact of 18-fluorodeoxyglucose positron emission tomography on computed tomography defined target volumes in radiation treatment planning of esophageal cancer: reduction in geographic misses with equal inter-observer variability: PET/CT improves esophageal target definition. *Dis Esophagus* 2010; **23**: 493-501 [PMID: 20113320 DOI: 10.1111/j.1442-2050.2009.01044.x]

10 **Liu J**, Li M, Li Z, Zuo XL, Li CQ, Dong YY, Zhou CJ, Li YQ. Learning curve and interobserver agreement of confocal laser endomicroscopy for detecting precancerous or early-stage esophageal squamous cancer. *PLoS One* 2014; **9**: e99089 [PMID: 24897112 DOI: 10.1371/journal.pone.0099089]

11 **Worrell SG**, Boys JA, Chandrasoma P, Vallone JG, Dunst CM, Johnson CS, Lada MJ, Louie BE, Watson TJ, DeMeester SR. Inter-Observer Variability in the Interpretation of Endoscopic Mucosal Resection Specimens of Esophageal Adenocarcinoma: Interpretation of ER specimens. *J Gastrointest Surg* 2016; **20**: 140-4; discussion 144-5 [PMID: 26503261 DOI: 10.1007/s11605-015-3009-7]

12 **Yang YJ**, Bang CS. Application of artificial intelligence in gastroenterology. *World J Gastroenterol* 2019; **25**: 1666-1683 [PMID: 31011253 DOI: 10.3748/wjg.v25.i14.1666]

13 **Ruffle JK**, Farmer AD, Aziz Q. Artificial Intelligence-Assisted Gastroenterology- Promises and Pitfalls. *Am J Gastroenterol* 2019; **114**: 422-428 [PMID: 30315284 DOI: 10.1038/s41395-018-0268-4]

14 **Min JK**, Kwak MS, Cha JM. Overview of Deep Learning in Gastrointestinal Endoscopy. *Gut Liver* 2019; **13**: 388-393 [PMID: 30630221 DOI: 10.5009/gnl18384]

15 **Deo RC**. Machine Learning in Medicine. *Circulation* 2015; **132**: 1920-1930 [PMID: 26572668 DOI: 10.1161/CIRCULATIONAHA.115.001593]

16 **Mori Y**, Kudo SE, Mohmed HEN, Misawa M, Ogata N, Itoh H, Oda M, Mori K. Artificial intelligence and upper gastrointestinal endoscopy: Current status and future perspective. *Dig Endosc* 2019; **31**: 378-388 [PMID: 30549317 DOI: 10.1111/den.13317]

17 **Le Berre C**, Sandborn WJ, Aridhi S, Devignes MD, Fournier L, Smaïl-Tabbone M, Danese S, Peyrin-Biroulet L. Application of Artificial Intelligence to Gastroenterology and Hepatology. *Gastroenterology* 2020; **158**: 76-94.e2 [PMID: 31593701 DOI: 10.1053/j.gastro.2019.08.058]

18 **Domper Arnal MJ**, Ferrández Arenas Á, Lanas Arbeloa Á. Esophageal cancer: Risk factors, screening and endoscopic treatment in Western and Eastern countries. *World J Gastroenterol* 2015; **21**: 7933-7943 [PMID: 26185366 DOI: 10.3748/wjg.v21.i26.7933]

19 **Liu WZ**, White AP, Hallissey MT, Fielding JW. Machine learning techniques in early screening for gastric and oesophageal cancer. *Artif Intell Med* 1996; **8**: 327-341 [PMID: 8870963 DOI: 10.1016/0933-3657(95)00039-9]

20 **van der Gaag LC**, Renooij S, Witteman CL, Aleman BM, Taal BG. Probabilities for a probabilistic network: a case study in oesophageal cancer. *Artif Intell Med* 2002; **25**: 123-148 [PMID: 12031603 DOI: 10.1016/s0933-3657(02)00012-x]

21 **Xu Y**, Selaru FM, Yin J, Zou TT, Shustova V, Mori Y, Sato F, Liu TC, Olaru A, Wang S, Kimos MC, Perry K, Desai K, Greenwald BD, Krasna MJ, Shibata D, Abraham JM, Meltzer SJ. Artificial neural networks and gene filtering distinguish between global gene expression profiles of Barrett's esophagus and esophageal cancer. *Cancer Res* 2002; **62**: 3493-3497 [PMID: 12067993]

22 **Kan T**, Shimada Y, Sato F, Ito T, Kondo K, Watanabe G, Maeda M, Yamasaki S, Meltzer SJ, Imamura M. Prediction of lymph node metastasis with use of artificial neural networks based on gene expression profiles in esophageal squamous cell carcinoma. *Ann Surg Oncol* 2004; **11**: 1070-1078 [PMID: 15545505 DOI: 10.1245/aso.2004.03.007]

23 **Fukuda M**, Hirata K, Natori H. Endoscopic ultrasonography of the esophagus. *World J Surg* 2000; **24**: 216-226 [PMID: 10633149 DOI: 10.1007/s002689910035]

24 **Himeno S**, Yasuda S, Shimada H, Tajima T, Makuuchi H. Evaluation of esophageal cancer by positron emission tomography. *Jpn J Clin Oncol* 2002; **32**: 340-346 [PMID: 12417599 DOI: 10.1093/jjco/hyf073]

25 **Moghtadaei M**, Hashemi Golpayegani MR, Malekzadeh R. A variable structure fuzzy neural network model of squamous dysplasia and esophageal squamous cell carcinoma based on a global chaotic optimization algorithm. *J Theor Biol* 2013; **318**: 164-172 [PMID: 23174279 DOI: 10.1016/j.jtbi.2012.11.013]

26 **Etemadi A**, Abnet CC, Golozar A, Malekzadeh R, Dawsey SM. Modeling the risk of esophageal squamous

cell carcinoma and squamous dysplasia in a high risk area in Iran. *Arch Iran Med* 2012; **15**: 18-21 [PMID: 22208438]

27 **Li SX**, Zeng QY, Li LF, Zhang YJ, Wan MM, Liu ZM, Xiong HL, Guo ZY, Liu SH. Study of support vector machine and serum surface-enhanced Raman spectroscopy for noninvasive esophageal cancer detection. *J Biomed Opt* 2013; **18**: 27008 [PMID: 23389685 DOI: 10.1117/1.JBO.18.2.027008]

28 **Rice TW**, Apperson-Hansen C, DiPaola LM, Semple ME, Lerut TE, Orringer MB, Chen LQ, Hofstetter WL, Smithers BM, Rusch VW, Wijnhoven BP, Chen KN, Davies AR, D'Journo XB, Kesler KA, Luketich JD, Ferguson MK, Räsänen JV, van Hillegersberg R, Fang W, Durand L, Allum WH, Cecconello I, Cerfolio RJ, Pera M, Griffin SM, Burger R, Liu JF, Allen MS, Law S, Watson TJ, Darling GE, Scott WJ, Duranceau A, Denlinger CE, Schipper PH, Ishwaran H, Blackstone EH. Worldwide Esophageal Cancer Collaboration: clinical staging data. *Dis Esophagus* 2016; **29**: 707-714 [PMID: 27731549 DOI: 10.1111/dote.12493]

29 **Sato F**, Shimada Y, Selaru FM, Shibata D, Maeda M, Watanabe G, Mori Y, Stass SA, Imamura M, Meltzer SJ. Prediction of survival in patients with esophageal carcinoma using artificial neural networks. *Cancer* 2005; **103**: 1596-1605 [PMID: 15751017 DOI: 10.1002/cncr.20938]

30 **Mofidi R**, Deans C, Duff MD, de Beaux AC, Paterson Brown S. Prediction of survival from carcinoma of oesophagus and oesophago-gastric junction following surgical resection using an artificial neural network. *Eur J Surg Oncol* 2006; **32**: 533-539 [PMID: 16618533 DOI: 10.1016/j.ejso.2006.02.020]

31 **Wang CY**, Lee TF, Fang CH, Chou JH. Fuzzy logic-based prognostic score for outcome prediction in esophageal cancer. *IEEE Trans Inf Technol Biomed* 2012; **16**: 1224-1230 [PMID: 22875252 DOI: 10.1109/TITB.2012.2211374]

32 **Mi H**, Petitjean C, Dubray B, Vera P, Ruan S. Robust feature selection to predict tumor treatment outcome. *Artif Intell Med* 2015; **64**: 195-204 [PMID: 26303106 DOI: 10.1016/j.artmed.2015.07.002]

33 **Zahedi H**, Mehrshad N, Anvari K. Intelligent modelling of oesophageal cancer treatment and its use to determine the dose of chemotherapy drug. *J Med Eng Technol* 2012; **36**: 261-266 [PMID: 22671958 DOI: 10.3109/03091902.2012.682112]

34 **Maktabi M**, Köhler H, Ivanova M, Jansen-Winkeln B, Takoh J, Niebisch S, Rabe SM, Neumuth T, Gockel I, Chalopin C. Tissue classification of oncologic esophageal resectates based on hyperspectral data. *Int J Comput Assist Radiol Surg* 2019; **14**: 1651-1661 [PMID: 31222672 DOI: 10.1007/s11548-019-02016-x]

35 **Huang FL**, Yu SJ. Esophageal cancer: Risk factors, genetic association, and treatment. *Asian J Surg* 2018; **41**: 210-215 [PMID: 27986415 DOI: 10.1016/j.asjsur.2016.10.005]

36 **Warnecke-Eberz U**, Metzger R, Bollschweiler E, Baldus SE, Mueller RP, Dienes HP, Hoelscher AH, Schneider PM. TaqMan low-density arrays and analysis by artificial neuronal networks predict response to neoadjuvant chemoradiation in esophageal cancer. *Pharmacogenomics* 2010; **11**: 55-64 [PMID: 20017672 DOI: 10.2217/pgs.09.137]

37 **Ganeshan B**, Skogen K, Pressney I, Coutroubis D, Miles K. Tumour heterogeneity in oesophageal cancer assessed by CT texture analysis: preliminary evidence of an association with tumour metabolism, stage, and survival. *Clin Radiol* 2012; **67**: 157-164 [PMID: 21943720 DOI: 10.1016/j.crad.2011.08.012]

38 **Javeri H**, Xiao L, Rohren E, Komaki R, Hofstetter W, Lee JH, Maru D, Bhutani MS, Swisher SG, Wang X, Ajani JA. Influence of the baseline 18F-fluoro-2-deoxy-D-glucose positron emission tomography results on survival and pathologic response in patients with gastroesophageal cancer undergoing chemoradiation. *Cancer* 2009; **115**: 624-630 [PMID: 19130466 DOI: 10.1002/cncr.24056]

39 **Schollaert P**, Crott R, Bertrand C, D'Hondt L, Borght TV, Krug B. A systematic review of the predictive value of (18)FDG-PET in esophageal and esophagogastric junction cancer after neoadjuvant chemoradiation on the survival outcome stratification. *J Gastrointest Surg* 2014; **18**: 894-905 [PMID: 24638928 DOI: 10.1007/s11605-014-2488-2]

40 **Ypsilantis PP**, Siddique M, Sohn HM, Davies A, Cook G, Goh V, Montana G. Predicting Response to Neoadjuvant Chemotherapy with PET Imaging Using Convolutional Neural Networks. *PLoS One* 2015; **10**: e0137036 [PMID: 26355298 DOI: 10.1371/journal.pone.0137036]

41 **Jin X**, Zheng X, Chen D, Jin J, Zhu G, Deng X, Han C, Gong C, Zhou Y, Liu C, Xie C. Prediction of response after chemoradiation for esophageal cancer using a combination of dosimetry and CT radiomics. *Eur Radiol* 2019; **29**: 6080-6088 [PMID: 31028447 DOI: 10.1007/s00330-019-06193-w]

42 **Yang HX**, Feng W, Wei JC, Zeng TS, Li ZD, Zhang LJ, Lin P, Luo RZ, He JH, Fu JH. Support vector machine-based nomogram predicts postoperative distant metastasis for patients with oesophageal squamous cell carcinoma. *Br J Cancer* 2013; **109**: 1109-1116 [PMID: 23942069 DOI: 10.1038/bjc.2013.379]

43 **Wang ZL**, Zhou ZG, Chen Y, Li XT, Sun YS. Support Vector Machines Model of Computed Tomography for Assessing Lymph Node Metastasis in Esophageal Cancer with Neoadjuvant Chemotherapy. *J Comput Assist Tomogr* 2017; **41**: 455-460 [PMID: 27879527 DOI: 10.1097/RCT.0000000000000555]

44 **Lin T**, Liu T, Lin Y, Zhang C, Yan L, Chen Z, He Z, Wang J. Serum levels of chemical elements in esophageal squamous cell carcinoma in Anyang, China: a case-control study based on machine learning methods. *BMJ Open* 2017; **7**: e015443 [PMID: 28947442 DOI: 10.1136/bmjopen-2016-015443]

45 **Mourikis TP**, Benedetti L, Foxall E, Temelkovski D, Nulsen J, Perner J, Cereda M, Lagergren J, Howell M, Yau C, Fitzgerald RC, Scaffidi P; Oesophageal Cancer Clinical and Molecular Stratification (OCCAMS) Consortium, Ciccarelli FD. Patient-specific cancer genes contribute to recurrently perturbed pathways and establish therapeutic vulnerabilities in esophageal adenocarcinoma. *Nat Commun* 2019; **10**: 3101 [PMID: 31308377 DOI: 10.1038/s41467-019-10898-3]

46 **Rice TW**, Lu M, Ishwaran H, Blackstone EH; Worldwide Esophageal Cancer Collaboration Investigators. Precision Surgical Therapy for Adenocarcinoma of the Esophagus and Esophagogastric Junction. *J Thorac Oncol* 2019; **14**: 2164-2175 [PMID: 31442498 DOI: 10.1016/j.jtho.2019.08.004]

47 **Goetz M**. Enhanced Imaging of the Esophagus: Confocal Laser Endomicroscopy. In: Pleskow DK, Erim T. Barrett's Esophagus. Boston: Academic Press, 2016: 123-132

48 **Gora MJ**, Tearney GJ. Enhanced Imaging of the Esophagus: Optical Coherence Tomography. In: Pleskow DK, Erim T. Barrett's Esophagus. Boston: Academic Press, 2016: 105-122

49 **Falk GW**, Wani S. Chandrasekhara V, Elmunzer BJ, Khashab MA, Muthusamy VR. Barrett's Esophagus: Diagnosis, Surveillance, and Medical Management. In: Chandrasekhara V, Elmunzer BJ, Khashab MA,

Muthusamy VR. Clinical Gastrointestinal Endoscopy (Third Edition). Philadelphia: Content Repository Only, 2019: 279-90.e5
50 **di Pietro M**, Canto MI, Fitzgerald RC. Endoscopic Management of Early Adenocarcinoma and Squamous Cell Carcinoma of the Esophagus: Screening, Diagnosis, and Therapy. *Gastroenterology* 2018; **154**: 421-436 [PMID: 28778650 DOI: 10.1053/j.gastro.2017.07.041]
51 **de Lange T**, Halvorsen P, Riegler M. Methodology to develop machine learning algorithms to improve performance in gastrointestinal endoscopy. *World J Gastroenterol* 2018; **24**: 5057-5062 [PMID: 30568383 DOI: 10.3748/wjg.v24.i45.5057]
52 **ASGE Standards of Practice Committee**, Qumseya B, Sultan S, Bain P, Jamil L, Jacobson B, Anandasabapathy S, Agrawal D, Buxbaum JL, Fishman DS, Gurudu SR, Jue TL, Kripalani S, Lee JK, Khashab MA, Naveed M, Thosani NC, Yang J, DeWitt J, Wani S; ASGE Standards of Practice Committee Chair. ASGE guideline on screening and surveillance of Barrett's esophagus. *Gastrointest Endosc* 2019; **90**: 335-359.e2 [PMID: 31439127 DOI: 10.1016/j.gie.2019.05.012]
53 **Münzenmayer C**, Kage A, Wittenberg T, Mühldorfer S. Computer-assisted diagnosis for precancerous lesions in the esophagus. *Methods Inf Med* 2009; **48**: 324-330 [PMID: 19562230 DOI: 10.3414/ME9230]
54 **van der Sommen F**, Aylward S, Zinger S, Schoon EJ, de With PHN. Proceedings of SPIE - The International Society for Optical Engineering; 2013 Feb 8; Proc SPIE Medical Imaging (SPIE 8670) [DOI: 10.1117/12.2001068]
55 **van der Sommen F**, Zinger S, Curvers WL, Bisschops R, Pech O, Weusten BL, Bergman JJ, de With PH, Schoon EJ. Computer-aided detection of early neoplastic lesions in Barrett's esophagus. *Endoscopy* 2016; **48**: 617-624 [PMID: 27100718 DOI: 10.1055/s-0042-105284]
56 **Horie Y**, Yoshio T, Aoyama K, Yoshimizu S, Horiuchi Y, Ishiyama A, Hirasawa T, Tsuchida T, Ozawa T, Ishihara S, Kumagai Y, Fujishiro M, Maetani I, Fujisaki J, Tada T. Diagnostic outcomes of esophageal cancer by artificial intelligence using convolutional neural networks. *Gastrointest Endosc* 2019; **89**: 25-32 [PMID: 30120958 DOI: 10.1016/j.gie.2018.07.037]
57 **Ghatwary N**, Zolgharni M, Ye X. Early esophageal adenocarcinoma detection using deep learning methods. *Int J Comput Assist Radiol Surg* 2019; **14**: 611-621 [PMID: 30666547 DOI: 10.1007/s11548-019-01914-4]
58 **Hashimoto R**, Requa J, Dao T, Ninh A, Tran E, Mai D, Lugo M, El-Hage Chehade N, Chang KJ, Karnes WE, Samarasena JB. Artificial intelligence using convolutional neural networks for real-time detection of early esophageal neoplasia in Barrett's esophagus (with video). *Gastrointest Endosc* 2020; **91**: 1264-1271.e1 [PMID: 31930967 DOI: 10.1016/j.gie.2019.12.049]
59 **Ebigbo A**, Mendel R, Probst A, Manzeneder J, Souza LA Jr, Papa JP, Palm C, Messmann H. Computer-aided diagnosis using deep learning in the evaluation of early oesophageal adenocarcinoma. *Gut* 2019; **68**: 1143-1145 [PMID: 30510110 DOI: 10.1136/gutjnl-2018-317573]
60 **de Groof AJ**, Struyvenberg MR, van der Putten J, van der Sommen F, Fockens KN, Curvers WL, Zinger S, Pouw RE, Coron E, Baldaque-Silva F, Pech O, Weusten B, Meining A, Neuhaus H, Bisschops R, Dent J, Schoon EJ, de With PH, Bergman JJ. Deep-Learning System Detects Neoplasia in Patients With Barrett's Esophagus With Higher Accuracy Than Endoscopists in a Multistep Training and Validation Study With Benchmarking. *Gastroenterology* 2020; **158**: 915-929.e4 [PMID: 31759929 DOI: 10.1053/j.gastro.2019.11.030]
61 **Hong J**, Park BY, Park H. Convolutional neural network classifier for distinguishing Barrett's esophagus and neoplasia endomicroscopy images. *Conf Proc IEEE Eng Med Biol Soc* 2017; **2017**: 2892-2895 [PMID: 29060502 DOI: 10.1109/EMBC.2017.8037461]
62 **Swager AF**, van der Sommen F, Klomp SR, Zinger S, Meijer SL, Schoon EJ, Bergman JJGHM, de With PH, Curvers WL. Computer-aided detection of early Barrett's neoplasia using volumetric laser endomicroscopy. *Gastrointest Endosc* 2017; **86**: 839-846 [PMID: 28322771 DOI: 10.1016/j.gie.2017.03.011]
63 **van der Sommen F**, Klomp SR, Swager AF, Zinger S, Curvers WL, Bergman JJGHM, Schoon EJ, de With PHN. Predictive features for early cancer detection in Barrett's esophagus using Volumetric Laser Endomicroscopy. *Comput Med Imaging Graph* 2018; **67**: 9-20 [PMID: 29684663 DOI: 10.1016/j.compmedimag.2018.02.007]
64 **Trindade AJ**, McKinley MJ, Fan C, Leggett CL, Kahn A, Pleskow DK. Endoscopic Surveillance of Barrett's Esophagus Using Volumetric Laser Endomicroscopy With Artificial Intelligence Image Enhancement. *Gastroenterology* 2019; **157**: 303-305 [PMID: 31078625 DOI: 10.1053/j.gastro.2019.04.048]
65 **Struyvenberg MR**, van der Sommen F, Swager AF, de Groof AJ, Rikos A, Schoon EJ, Bergman JJ, de With PHN, Curvers WL. Improved Barrett's neoplasia detection using computer-assisted multiframe analysis of volumetric laser endomicroscopy. *Dis Esophagus* 2020; **33** [PMID: 31364700 DOI: 10.1093/dote/doz065]
66 **van der Putten J**, Struyvenberg M, de Groof J, Scheeve T, Curvers W, Schoon E, Bergman JJGHM, de With PHN, van der Sommen F. Deep principal dimension encoding for the classification of early neoplasia in Barrett's Esophagus with volumetric laser endomicroscopy. *Comput Med Imaging Graph* 2020; **80**: 101701 [PMID: 32044547 DOI: 10.1016/j.compmedimag.2020.101701]
67 **Shin D**, Lee MH, Polydorides AD, Pierce MC, Vila PM, Parikh ND, Rosen DG, Anandasabapathy S, Richards-Kortum RR. Quantitative analysis of high-resolution microendoscopic images for diagnosis of neoplasia in patients with Barrett's esophagus. *Gastrointest Endosc* 2016; **83**: 107-114 [PMID: 26253018 DOI: 10.1016/j.gie.2015.06.045]
68 **Qi X**, Sivak MV, Isenberg G, Willis JE, Rollins AM. Computer-aided diagnosis of dysplasia in Barrett's esophagus using endoscopic optical coherence tomography. *J Biomed Opt* 2006; **11**: 044010 [PMID: 16965167 DOI: 10.1117/1.2337314]
69 **Kohli DR**, Schubert ML, Zfass AM, Shah TU. Performance characteristics of optical coherence tomography in assessment of Barrett's esophagus and esophageal cancer: systematic review. *Dis Esophagus* 2017; **30**: 1-8 [PMID: 28881898 DOI: 10.1093/dote/dox049]
70 **Sabo E**, Beck AH, Montgomery EA, Bhattacharya B, Meitner P, Wang JY, Resnick MB. Computerized morphometry as an aid in determining the grade of dysplasia and progression to adenocarcinoma in Barrett's esophagus. *Lab Invest* 2006; **86**: 1261-1271 [PMID: 17075582 DOI: 10.1038/labinvest.3700481]
71 **Liu DY**, Gan T, Rao NN, Xing YW, Zheng J, Li S, Luo CS, Zhou ZJ, Wan YL. Identification of lesion

images from gastrointestinal endoscope based on feature extraction of combinational methods with and without learning process. *Med Image Anal* 2016; **32**: 281-294 [PMID: 27236223 DOI: 10.1016/j.media.2016.04.007]

72 **Cai SL**, Li B, Tan WM, Niu XJ, Yu HH, Yao LQ, Zhou PH, Yan B, Zhong YS. Using a deep learning system in endoscopy for screening of early esophageal squamous cell carcinoma (with video). *Gastrointest Endosc* 2019; **90**: 745-753.e2 [PMID: 31302091 DOI: 10.1016/j.gie.2019.06.044]

73 **Ohmori M**, Ishihara R, Aoyama K, Nakagawa K, Iwagami H, Matsuura N, Shichijo S, Yamamoto K, Nagaike K, Nakahara M, Inoue T, Aoi K, Okada H, Tada T. Endoscopic detection and differentiation of esophageal lesions using a deep neural network. *Gastrointest Endosc* 2020; **91**: 301-309.e1 [PMID: 31585124 DOI: 10.1016/j.gie.2019.09.034]

74 **Zhao YY**, Xue DX, Wang YL, Zhang R, Sun B, Cai YP, Feng H, Cai Y, Xu JM. Computer-assisted diagnosis of early esophageal squamous cell carcinoma using narrow-band imaging magnifying endoscopy. *Endoscopy* 2019; **51**: 333-341 [PMID: 30469155 DOI: 10.1055/a-0756-8754]

75 **Oyama T**, Inoue H, Arima M, Momma K, Omori T, Ishihara R, Hirasawa D, Takeuchi M, Tomori A, Goda K. Prediction of the invasion depth of superficial squamous cell carcinoma based on microvessel morphology: magnifying endoscopic classification of the Japan Esophageal Society. *Esophagus* 2017; **14**: 105-112 [PMID: 28386209 DOI: 10.1007/s10388-016-0527-7]

76 **Nakagawa K**, Ishihara R, Aoyama K, Ohmori M, Nakahira H, Matsuura N, Shichijo S, Nishida T, Yamada T, Yamaguchi S, Ogiyama H, Egawa S, Kishida O, Tada T. Classification for invasion depth of esophageal squamous cell carcinoma using a deep neural network compared with experienced endoscopists. *Gastrointest Endosc* 2019; **90**: 407-414 [PMID: 31077698 DOI: 10.1016/j.gie.2019.04.245]

77 **Everson M**, Herrera L, Li W, Luengo IM, Ahmad O, Banks M, Magee C, Alzoubaidi D, Hsu HM, Graham D, Vercauteren T, Lovat L, Ourselin S, Kashin S, Wang HP, Wang WL, Haidry RJ. Artificial intelligence for the real-time classification of intrapapillary capillary loop patterns in the endoscopic diagnosis of early oesophageal squamous cell carcinoma: A proof-of-concept study. *United European Gastroenterol J* 2019; **7**: 297-306 [PMID: 31080614 DOI: 10.1177/2050640618821800]

78 **Luo H**, Xu G, Li C, He L, Luo L, Wang Z, Jing B, Deng Y, Jin Y, Li Y, Li B, Tan W, He C, Seeruttun SR, Wu Q, Huang J, Huang DW, Chen B, Lin SB, Chen QM, Yuan CM, Chen HX, Pu HY, Zhou F, He Y, Xu RH. Real-time artificial intelligence for detection of upper gastrointestinal cancer by endoscopy: a multicentre, case-control, diagnostic study. *Lancet Oncol* 2019; **20**: 1645-1654 [PMID: 31591062 DOI: 10.1016/S1470-2045(19)30637-0]

79 **Guo L**, Xiao X, Wu C, Zeng X, Zhang Y, Du J, Bai S, Xie J, Zhang Z, Li Y, Wang X, Cheung O, Sharma M, Liu J, Hu B. Real-time automated diagnosis of precancerous lesions and early esophageal squamous cell carcinoma using a deep learning model (with videos). *Gastrointest Endosc* 2020; **91**: 41-51 [PMID: 31445040 DOI: 10.1016/j.gie.2019.08.018]

80 **Thakkar SJ**, Kochhar GS. Artificial intelligence for real-time detection of early esophageal cancer: another set of eyes to better visualize. *Gastrointest Endosc* 2020; **91**: 52-54 [PMID: 31865996 DOI: 10.1016/j.gie.2019.09.036]

81 **Kodashima S**, Fujishiro M, Takubo K, Kammori M, Nomura S, Kakushima N, Muraki Y, Goto O, Ono S, Kaminishi M, Omata M. Ex vivo pilot study using computed analysis of endo-cytoscopic images to differentiate normal and malignant squamous cell epithelia in the oesophagus. *Dig Liver Dis* 2007; **39**: 762-766 [PMID: 17611178 DOI: 10.1016/j.dld.2007.03.004]

82 **Shin D**, Protano MA, Polydorides AD, Dawsey SM, Pierce MC, Kim MK, Schwarz RA, Quang T, Parikh N, Bhutani MS, Zhang F, Wang G, Xue L, Wang X, Xu H, Anandasabapathy S, Richards-Kortum RR. Quantitative analysis of high-resolution microendoscopic images for diagnosis of esophageal squamous cell carcinoma. *Clin Gastroenterol Hepatol* 2015; **13**: 272-279.e2 [PMID: 25066838 DOI: 10.1016/j.cgh.2014.07.030]

83 **Quang T**, Schwarz RA, Dawsey SM, Tan MC, Patel K, Yu X, Wang G, Zhang F, Xu H, Anandasabapathy S, Richards-Kortum R. A tablet-interfaced high-resolution microendoscope with automated image interpretation for real-time evaluation of esophageal squamous cell neoplasia. *Gastrointest Endosc* 2016; **84**: 834-841 [PMID: 27036635 DOI: 10.1016/j.gie.2016.03.1472]

84 **Protano MA**, Xu H, Wang G, Polydorides AD, Dawsey SM, Cui J, Xue L, Zhang F, Quang T, Pierce MC, Shin D, Schwarz RA, Bhutani MS, Lee M, Parikh N, Hur C, Xu W, Moshier E, Godbold J, Mitcham J, Hudson C, Richards-Kortum RR, Anandasabapathy S. Low-Cost High-Resolution Microendoscopy for the Detection of Esophageal Squamous Cell Neoplasia: An International Trial. *Gastroenterology* 2015; **149**: 321-329 [PMID: 25980753 DOI: 10.1053/j.gastro.2015.04.055]

85 **Mutasa S**, Sun S, Ha R. Understanding artificial intelligence based radiology studies: What is overfitting? *Clin Imaging* 2020; **65**: 96-99 [PMID: 32387803 DOI: 10.1016/j.clinimag.2020.04.025]

86 **Mori Y**, Kudo SE, East JE, Rastogi A, Bretthauer M, Misawa M, Sekiguchi M, Matsuda T, Saito Y, Ikematsu H, Hotta K, Ohtsuka K, Kudo T, Mori K. Cost savings in colonoscopy with artificial intelligence-aided polyp diagnosis: an add-on analysis of a clinical trial (with video). *Gastrointest Endosc* 2020 [PMID: 32240683 DOI: 10.1016/j.gie.2020.03.3759]

87 **London AJ**. Artificial Intelligence and Black-Box Medical Decisions: Accuracy versus Explainability. *Hastings Cent Rep* 2019; **49**: 15-21 [PMID: 30790315 DOI: 10.1002/hast.973]

88 **Lawrence DR**, Palacios-González C, Harris J. Artificial Intelligence. *Camb Q Healthc Ethics* 2016; **25**: 250-261 [PMID: 26957450 DOI: 10.1017/S0963180115000559]

89 **Yu KH**, Beam AL, Kohane IS. Artificial intelligence in healthcare. *Nat Biomed Eng* 2018; **2**: 719-731 [PMID: 31015651 DOI: 10.1038/s41551-018-0305-z]

90 **O'Sullivan S**, Nevejans N, Allen C, Blyth A, Leonard S, Pagallo U, Holzinger K, Holzinger A, Sajid MI, Ashrafian H. Legal, regulatory, and ethical frameworks for development of standards in artificial intelligence (AI) and autonomous robotic surgery. *Int J Med Robot* 2019; **15**: e1968 [PMID: 30397993 DOI: 10.1002/rcs.1968]

World Journal of Gastroenterology

Submit a Manuscript: https://www.f6publishing.com

World J Gastroenterol 2020 September 21; 26(35): 5272-5286

DOI: 10.3748/wjg.v26.i35.5272

ISSN 1007-9327 (print) ISSN 2219-2840 (online)

ORIGINAL ARTICLE

Basic Study

New approach of medicinal herbs and sulfasalazine mixture on ulcerative colitis induced by dextran sodium sulfate

Mi-Rae Shin, Hae-Jin Park, Bu-Il Seo, Seong-Soo Roh

ORCID number: Mi-Rae Shin 0000-0001-7630-384X; Hae-Jin Park 0000-0002-4283-0809; Bu-Il Seo 0000-0001-8349-8374; Seong-Soo Roh 0000-0002-4162-6849.

Author contributions: Shin MR performed the majority of experiments and wrote the paper; Park HJ and Seo BI analyzed the data; Roh SS designed and coordinated the research.

Supported by Traditional Korean Medicine R&D Program funded by the Ministry of Health & Welfare through the Korea Health Industry Development Institute (KHIDI), No. HI15C00255; and National Research Foundation of Korea (NRF) funded by the Korean government (MSIP), No. 2018R1A5A2025272.

Institutional animal care and use committee statement: All procedures involving animals were reviewed and approved by the Institutional Animal Care and Use Committee of the Daegu Haany University (No. DHU2017-043).

Conflict-of-interest statement: The authors declare no competing financial interests related to this study or its publication.

Data sharing statement: No additional data are available.

Mi-Rae Shin, Bu-Il Seo, Seong-Soo Roh, Department of Herbology, Korean Medicine College, Daegu Haany University, Suseong-gu, Deagu 42158, South Korea

Hae-Jin Park, DHU Bio Convergence Testing Center, Gyeongsan-si, Gyeongsangbuk-do 38610, South Korea

Corresponding author: Seong-Soo Roh, PhD, Director, Professor, Department of Herbology, Korean Medicine College, Daegu Haany University, 136 Shinchendong–ro, Suseong-gu, Deagu 42158, South Korea. ddede@dhu.ac.kr

Abstract

BACKGROUND

Sulfasalazine has been used as a standard-of-care in ulcerative colitis for decades, however, it results in severe adverse symptoms, such as hepatotoxicity, blood disorders, male infertility, and hypospermia. Accordingly, the new treatment strategy has to enhance pharmacological efficacy and stimultaneously minimize side effects.

AIM

To compare the anti-inflammatory action of sulfasalazine alone or in combination with herbal medicine for ulcerative colitis in a dextran sodium sulfate (DSS)-induced colitis mouse model.

METHODS

To induce ulcerative colitis, mice received 5% DSS in drinking water for 7 d. Animals were divided into five groups (n = 9 each) for use as normal (non-DSS), DSS controls, DSS + sulfasalazine (30 mg/kg)-treatment experimentals, DSS + sulfasalazine (60 mg/kg)-treatment experimentals, DSS + sulfasalazine (30 mg/kg) + *Citrus unshiu* peel and Bupleuri radix mixture (30 mg/kg) (SCPB)-treatment experimentals.

RESULTS

The SCPB treatment showed an outstanding effectiveness in counteracting the ulcerative colitis, as evidenced by reduction in body weight, improvement in crypt morphology, increase in antioxidant defenses, down-regulation of proinflammatory proteins and cytokines, and inhibition of proteins related to apoptosis.

ARRIVE guidelines statement: The authors have read the ARRIVE guidelines, and the manuscript was prepared and revised according to the ARRIVE guidelines.

Manuscript source: Unsolicited manuscript

Received: April 1, 2020
Peer-review started: April 1, 2020
First decision: April 25, 2020
Revised: April 29, 2020
Accepted: August 25, 2020
Article in press: August 25, 2020
Published online: September 21, 2020

P-Reviewer: Exbrayat JM
S-Editor: Gong ZM
L-Editor: A
P-Editor: Zhang YL

CONCLUSION
SCPB may represent a promising alternative therapeutic against ulcerative colitis, without inducing adverse effects.

Key Words: Dextran sulfate sodium; Ulcerative colitis; Anti-inflammatory; Sulfasalazine; *Citrus unshiu* peel and Bupleuri radix mixture; Apoptosis

Core Tip: Sulfasalazine has been used widely as a standard-of-care in ulcerative colitis; however, it is associated with a spectrum of side effects after long-term and high-dose intake. Since a single dose of sulfasalazine cannot provide satisfactory therapeutic results, we conducted a comparative evaluation of the pharmacological effect of sulfasalazine alone and when used in combination with *Citrus unshiu* peel and Bupleuri radix mixture in an experimentally-induced ulcerative colitis mouse model.

Citation: Shin MR, Park HJ, Seo BI, Roh SS. New approach of medicinal herbs and sulfasalazine mixture on ulcerative colitis induced by dextran sodium sulfate. *World J Gastroenterol* 2020; 26(35): 5272-5286
URL: https://www.wjgnet.com/1007-9327/full/v26/i35/5272.htm
DOI: https://dx.doi.org/10.3748/wjg.v26.i35.5272

INTRODUCTION

Inflammatory bowel diseases (IBDs), including ulcerative colitis (UC) and Crohn's disease, are chronic and uncontrolled intestinal disorders that have emerged collectively as an important public health problem worldwide[1]. The recommended drugs in clinical use for treatment of IBD patients currently include corticosteroids, sulfasalazine, immunosuppressants, antibiotics, and anti-tumor necrosis factor (TNF)-α antibodies. Conventional therapies also involve combinations of these agents[2,3]. Unfortunately, the incidence and prevalence of IBDs are continuing to increase[4] and the plethora of data from cases treated with the commonly used drugs have revealed a number of side effects and troubling issues, such as blood disorders, hepatotoxicity, hypospermia, male infertility, and economic burden[5]. Thus, alternatives for a safer, cheaper, and more efficacious approach to managing and/or treating IBDs is needed.

Diverse mixtures of herbal medicines have been screened as candidates for alleviating various inflammatory disorders[6,7]. Toki-shakuyaku-san, which is a traditional kampo medicine, was found to down-regulate the inflammatory and apoptotic signaling during colitis[8]. The rhizome mixture of *Anemarrhena asphodeloides* and *Coptidis chinensis* was found to exert an anti-colitic effect by inhibiting nuclear factor-kappa B (NF-κB) activation[9]. Moreover, Hange-shashin-to was found to suppress IBD in a rat model of experimental colitis[10]. Ultimately, the collective research findings support the potential benefit of anti-inflammatory herbal combinations in colitis.

Citrus unshiu peel has been used widely throughout East Asia for improving the common cold, dyspepsia, and blood circulation[11]. The *Citrus unshiu* peel — a seedless and easy-peeling citrus fruit — contains various flavonoids, such as hesperidin, naringin, and nobiletin[12-14]. These active compounds have been reported to exert potent anti-inflammatory, antioxidant, anti-adipogenic, anti-diabetic, anti-microbial, and anti-allergic activities[15,16]. On the other hand, Bupleuri radix has been mainly applied in clinical use for liver-related disease, and the recent pharmacological research has demonstrated its renoprotective and hepatoprotective effects[17,18]. Saikosaponins isolated from Bupleuri radix possess valuable pharmacological activities, including those of anti-inflammatory, antitumor, antiviral, and anti-allergic, working mainly through NF-κB or mitogen-activated protein kinase (MAPK) pathways[19-21]. On the basis of these reports, we estimated that *Citrus unshiu* peel according to its anti-inflammatory effect and Bupleuri radix according to its hepatoprotective and renoprotective effects may be able to exert therapeutic benefits in UC.

To date, there are no studies on the potential anti-inflammatory effect of a treatment

mixture of *Citrus unshiu* peel and Bupleuri radix nor on its underlying mechanisms. The present study was conducted to evaluate the pharmacological effect of sulfasalazine alone and in combination with *Citrus unshiu* peel and Bupleuri radix mixture in UC, using a well-established experimentally-induced UC mouse model system.

MATERIALS AND METHODS

Materials

Dextran sodium sulfate (DSS) (molecular weight: 36000-50000 Da) was purchased from MP Biologicals (Santa Ana, CA, United States). Sulfasalazine (purity ≥ 98%) and phenylmethylsulfonyl fluoride (commonly known as PMSF) were purchased from Sigma-Aldrich (St. Louis, MO, United States). Protease inhibitor mixture solution and ethylenediaminetetraacetic acid (commonly known as EDTA) were purchased from Wako Pure Chemical Industries, Ltd. (Osaka, Japan). 2',7'-dichlorofluorescein diacetate (referred to as DCF-DA) was obtained from Molecular Probes (Eugene, OR, United States). Pierce bicinchoninic acid protein assay kit was obtained from Thermo Fisher Scientific (Waltham, MA, United States). Enhanced chemiluminescence (commonly known as ECL) western blotting detection reagents and pure nitrocellulose membranes were supplied by GE Healthcare (Chicago, IL, United States). The following antibodies were obtained from Santa Cruz Biotechnology, Inc. (Santa Cruz, CA, United States): (mouse polyclonal) nuclear factor-kappa B p65 (NF-κBp65) (1:1000; SC-372), $p47^{phox}$ (1:1000; SC-14015), Rac 1 (1:1000; SC-217), superoxide dismutase (SOD) 1:1000; SC-11407), glutathione peroxidase-1/2 (GPx-1/2) 1:1000; SC-30147), Bax (1:1000; SC-7480), Bcl-2 (1:1000; SC-7382), monocyte chemoattractant peptide-1 (MCP-1) (1:1000; SC-28879), and intercellular adhesion molecule-1 (ICAM-1) (1:1000; SC-1511-R); (goat polyclonal) tumor necrosis factor-α (TNF-α) (1:1000; SC-1351) and interleukin-1β (IL-1β) (1:1000; SC-1252); (mouse monoclonal) phosphor-extracellular signal-regulated kinase 1/2 (p-ERK1/2) (1:1000; SC-7383), phosphor-p38 (p-p38) (1:1000; SC-7973), cyclooxygenase-2 (COX-2) (1:1000; SC-19999), inducible nitric oxide synthase (iNOS) (1:1000; SC-7271), histone (1:1000; SC-8030), and β-actin (1:1000; SC-4778); and rabbit anti-goat (1:3000; SC-2774), goat anti-rabbit (1:3000; SC-2004), and goat anti-mouse (1:3000; SC-2005) immunoglobulin G (IgG) horseradish peroxidase (HRP)-conjugated secondary antibodies. Mouse monoclonal anti-caspase-3 (1:1000; 3004-100) was purchased from BioVision Inc. (Mountain View, CA, United States). Rabbit polyclonal anti-reduced nicotinamide adenine dinucleotide phosphate oxidase 4 (NOX4) was purchased from LifeSpan BioSciences (Seattle, WA, United States). All other chemicals and reagents were purchased from Sigma-Aldrich (St. Louis, MO, United States).

Plant materials

Bupleuri radix was supplied by Bonchowon (Yeongcheon-si, Gyeongsangnam-do, South Korea) and two herbs were produced according to Korean Good Manufacturing Practice. Dried Bupleuri radix (100 g) was extracted with 10 volumes of water and boiled in distilled water (100°C for 2 h). After filtration, the water extracts were evaporated using a rotary evaporator at 45°C and the solvent was evaporated *in vacuo* to give an extract with a yield of 26%. In addition, a crude drug preparation of *Citrus unshiu* peel (*Citri unshiu* pericarpium) (1 kg; Wansan Medicinal Herbs Co. Ltd., Jeonju-si, South Korea) was extracted with ethanol: H_2O (1:1) under reflux (2 L × 3). After the solvent was evaporated under reduced pressure, the crude extract (220 g) was obtained. The two prepared herbs were kept at -80°C until use in animal experiments.

Experimental animals and induction of colitis

All procedures involving animals were reviewed and approved by the Institutional Animal Care and Use Committee of the Daegu Haany University (No. DHU2017-043). Eight-week-old male BALB/c mice, weighing 22-24 g, were purchased from Orient Bio Animal Center (Seongnam-si, South Korea). Mice were maintained under a 12h light/dark cycle, housed at a controlled temperature of 24 ± 2°C and humidity of approximately 60%). After adaptation (1 wk), acute colitis was induced by oral administration of 5% (*w*/*v*) DSS dissolved in drinking water, for 7 d[15]. The colitic mice were divided into four groups (n = 9 each) for use as DSS controls, DSS + sulfasalazine (30 mg/kg)-treatment experimentals, DSS + sulfasalazine (60 mg/kg)-treatment experimentals, DSS + sulfasalazine (30 mg/kg) + *Citrus unshiu* peel and Bupleuri radix mixture (30 mg/kg) (SCPB)-treatment experimentals. A group of 9 untreated (normal)

mice received drinking water without DSS throughout the entire experimental period. Sufasalazine was used as the positive reference agent and it was given at doses of 30 mg/kg/d or 60 mg/kg/d. The 30 mg/kg *Citrus unshiu* peel and Bupleuri radix mixture was comprised of 25 mg/kg *Citrus unshiu* peel and 5 mg/kg Bupleuri radix (for a 5:1 ratio) and mixed just before application as the drug treatment. At 18 h after the last dosage was given, 2.5% isoflurane (Troikaa Pharmaceuticals Ltd., India) was administered for blood sample collection (cardiac puncture), sacrifice, and removal of the entire colon. All collected specimens were snap-frozen in liquid nitrogen and stored at -80°C until analysis. Symptomatic index of colitis, such as body weight loss, rectal bleeding, and mucus or watery diarrhea, were observed during experimental periods (before sacrifice).

Measurement of serum reactive oxygen species

Serum reactive oxygen species (ROS) concentration was measured by employing the method of Ali *et al*[22]. Briefly, 25 mmol/L DCF-DA was added to the serum and allowed to incubate for 30 min, after which the changes in fluorescence values were determined at an excitation wavelength of 486 nm and emission wavelength of 530 nm.

Hematoxylin and eosin staining of colon tissue

For microscopic evaluation, intestine tissue was fixed in 10% neutral-buffered formalin and, after embedding in paraffin, cut into 2 mm sections and stained using hematoxylin and eosin (H&E), for microscopic evaluation. The stained slices were subsequently observed under an optical microscope and analyzed using the iSolution Lite software program (InnerView Co., Seongnam-si, Gyeonggi-do, South Korea).

Preparation of cytosol and nuclear fractions

Protein extraction was performed according to the method of Komatsu[23], with minor modifications. Briefly, colon tissues were processed to obtain the cytosol fraction by homogenization with ice-cold lysis buffer A (250 mL; containing 10 mmol/L HEPES (pH 7.8), 10 mmol/L KCl, 2 mmol/L $MgCl_2$, 1 mmol/L DTT, 0.1 mmol/L EDTA, 0.1 mmol/L PMSF, and 1250 μL protease inhibitor mixture solution). After incubation for 20 min at 4°C, the homogenate was mixed with 10% NP-40 and centrifuged (13400 × *g* for 2 min at 4°C; 5415R Centrifuge from Eppendorf, Hamburg, Germany). The supernatant liquid (cytosol fraction) was separated into a new e-tube and the pellets were washed twice with buffer A (wash supernatants were discarded). The washed pellets were resuspended with lysis buffer C (20 mL; containing 50 mmol/L HEPES (pH 7.8), 50 mmol/L KCl, 300 mmol/L NaCl, 1 mmol/L DTT, 0.1 mmol/L EDTA, 0.1 mmol/L PMSF, 1% (*v*/*v*) glycerol and 100 μL protease inhibitor mixture solution) and incubated for 30 min at 4°C. After centrifugation (13400 × *g* for 10 min at 4°C), the nuclear fraction was prepared to collect the supernatant. Both cytosol and nuclear fractions were stored at -80°C until analysis.

Immunoblotting analysis

For the estimation of NF-κBp65 and histone, 12 μg of protein from each nuclear fraction was electrophoresed through 10% sodium dodecylsulfate polyacrylamide gel (commonly known as SDS-PAGE). The electro-separated proteins were then transferred to a nitrocellulose membrane, blocked with 5% (w/v) skim milk solution for 1 h, and incubated with primary antibodies (NF-KBp65 and histone) overnight at 4 °C. After the blots were washed, they were incubated with anti-rabbit or anti-mouse IgG HRP-conjugated secondary antibody for 1 h at room temperature. In addition, 7.5 μg protein of each cytosol fraction was electrophoresed through 8%-12% SDS-PAGE for detection of NOX4, $p47^{phox}$, Rac1, Bax, Bcl-2, caspase-3, SOD, catalase, GPx-1/2, COX-2, iNOS, TNF-α IL-1β, MCP-1, ICAM-1, and β-actin. Each antigen-antibody complex was visualized using the ECL western blotting detection reagents and measured by chemiluminescence with Sensi-Q 2000 Chemidoc (Lugen Sci Co., Ltd., Gyeonggi-do, South Korea). Band densities were measured using ATTO Densitograph Software (ATTO Corp., Tokyo, Japan) and quantified as the ratio to histone or β-actin. The protein levels of the groups are expressed relative to those of the normal mice group (represented by the value of 1.0).

Statistical analysis

The data are expressed as the mean ± standard error of the mean. Statistical analysis was performed by one-way ANOVA followed by Least-significant differences (LSD) test using SPSS version 22.0 software (SPSS Inc., Chicago, IL, United States). *P* values

less than 0.05 were considered to indicate statistical significance.

RESULTS

SCPB attenuated the progression of DSS-induced colitis in mice

Compared with the normal (non-DSS) group, the DSS control group showed considerably greater body weight loss over the experimental period ($P < 0.001$). However, oral administration of SCPB and sulfasalazine mildly ameliorated the severity of body weight loss in the DSS control group (Figure 1A). As shown in Figure 1B, the DSS control group showed colon length reduction of 57.94% compared with that of the normal group ($P < 0.001$); however, the group treated with SCPB showed a 2.8% increase compared with that of the DSS control group but the difference did not reach the threshold for statistical significance.

Colonic inflammation involves the disruption of crypt morphology, resulting in the infiltration of inflammatory cells and thickening of the lamina propria[24]. As shown in Figure 1C, the colons of the DSS control group showed histologic alterations such as infiltration of numerous inflammatory cells, goblet cell degeneration, and crypt distortion consistent with UC. Treatment with sulfasalazine or SCPB appeared to preserve the broad crypt distortion and ameliorate the infiltration of inflammatory cells.

SCPB ameliorated biomarkers associated with oxidative stress in DSS-induced colitis in mice

As shown in Figure 2A, serum ROS levels in the DSS control group were markedly higher than that in the normal (non-DSS) group ($P < 0.001$); however, the administration of sulfasalazine or SCPB appeared to lead to a marked decrease in the DSS-induced elevated levels ($P < 0.001$). As shown in Figure 2B, the protein expressions of nicotinamide adenine dinucleotide phosphate (NADPH) oxidase enzymes in the DSS control group were significantly elevated compared with those in the normal (non-DSS) group (NOX4, $P < 0.05$; $p47^{phox}$, $P < 0.01$; Rac 1, $P < 0.001$). However, the SCPB administration appeared to decrease and ameliorate the levels of each, in a manner superior to that of sulfasalazine alone (NOX4, $P < 0.05$; $p47^{phox}$, $P < 0.05$; Rac 1, $P < 0.001$). The 60 mg/kg sulfasalazine dosage, especially, showed a remarkable tendency towards effecting this decrease, but the difference did not reach the threshold for statistical significance.

SCPB up-regulated antioxidant enzymes in DSS-induced colitis in mice

Oxidative stress plays a vital role in IBD[25]. The activities of SOD and catalase showed a significant decrease in the DSS control group compared to those in the normal (non-DSS) group (SOD, $P < 0.05$; catalase, $P < 0.001$). However, the SPCB treatment significantly elevated the activities of SOD and catalase, but not of GPx-1/2 and the differences did not reach the threshold for statistical significance. These results indicated that SCPB supplementation may decrease the extent of colonic injury *via* its antioxidant effect (SOD, $P < 0.05$; catalase, $P < 0.01$) and do so in a manner superior treatment with sulfasalazine alone (Figure 3).

SCPB suppressed MAPK-related protein expressions in DSS-induced colitis mice

The MAPK pathways can be activated by oxidative stress, leading to inflammation processes and apoptosis[26]. MAPK-related protein expressions showed augmentation in the colons of mice in the DSS control group compared to those of the normal (non-DSS) group (p-p38, $P < 0.05$; p-ERK1/2; $P < 0.01$); in contrast, the oral administration of SCPB significantly decreased the expression of both p-p38 and p-ERK1/2, which reached nearly normal levels ($P < 0.05$), as shown in Figure 4.

SCPB abrogated NF-κB activation and expressions of NF-κB–related inflammatory proteins in DSS-induced colitis mice

It has been confirmed that NF-κB is the central transcription factor in the regulation of proinflammatory mediators (*i.e.*, COX-2 and iNOS), proinflammatory cytokines (*i.e.*, TNF-α and IL-1β), and at least one chemokine (*i.e.*, MCP-1), and one adhesion molecule (*i.e.*, ICAM-1) during inflammation[27]. The DSS control group showed enhanced phosphorylation of NF-κB in colon ($P < 0.01$), whereas the elevation was significantly reversed upon SCPB ($P < 0.05$). As important downstream targets of NF-κB, the expressions of COX-2 and iNOS were increased in the DSS control group and

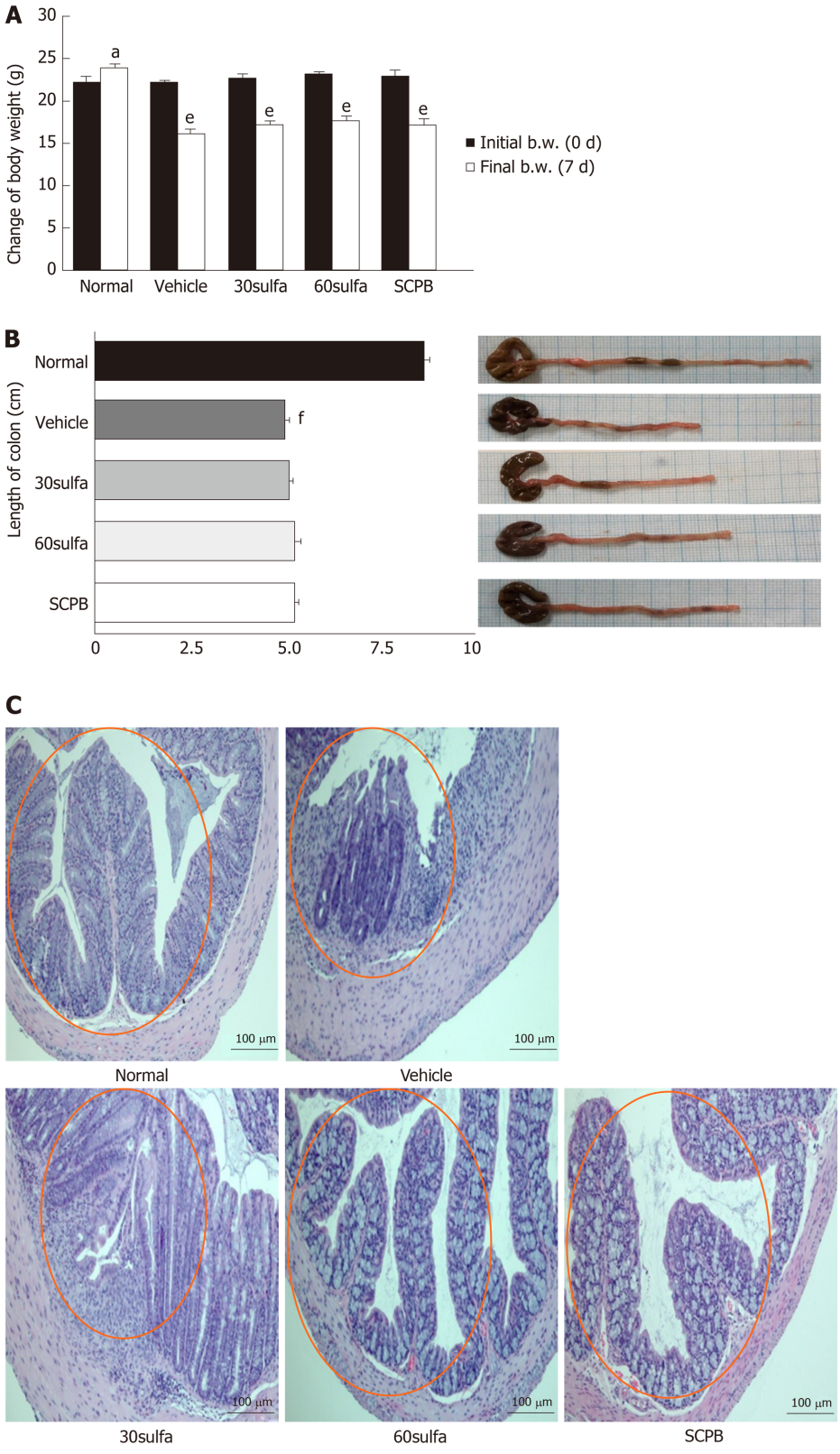

Figure 1 Sulfasalazine (30 mg/kg) + *Citrus unshiu* peel and Bupleuri radix mixture (30 mg/kg) alleviated Dextran Sodium Sulfate-induced experimental ulcerative colitis. A: Change of body weight after induction of colitis by DSS; B: Length of colon and macroscopic viewpoint; Normal (non-DSS), Vehicle (DSS control), 30sulfa (sulfasalazine 30 mg/kg-treated), 60sulfa (sulfasalazine 60 mg/kg-treated), and SCPB (30sulfa plus *Citrus unshiu* peel and Bupleuri radix mixture at 30 mg/kg-treated); C: Hematoxylin and eosin staining of colon (magnification × 200), orange line meaned crypt destruction and loss. Data are presented as mean ± standard error of the mean for $n = 7$. $^{a}P < 0.05$, $^{e}P < 0.001$ *vs* initial body weight (b.w.) per group; $^{f}P < 0.001$ *vs* normal (non-DSS) mice. SCPB: Sulfasalazine (30 mg/kg) + *Citrus unshiu* peel and Bupleuri radix mixture (30 mg/kg).

markedly blocked in mice given SCPB supplementation ($P < 0.05$). In contrast, treatment with sulfasalazine alone merely showed a tendency to decrease the

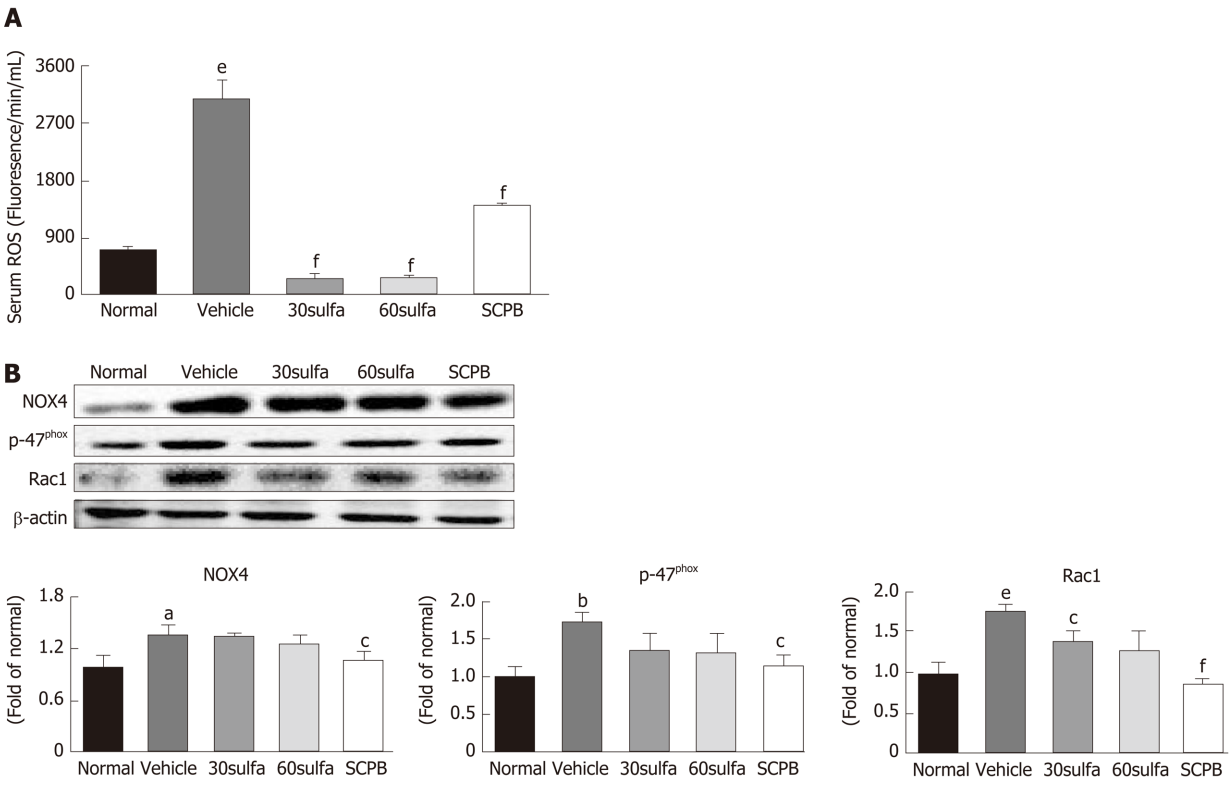

Figure 2 Sulfasalazine (30 mg/kg) + *Citrus unshiu* peel and Bupleuri radix mixture (30 mg/kg) reduced Serum reactive oxygen species and NADPH oxidase activity in colon. A: Serum reactive oxygen species (ROS); B: Western blot detection of NADPH oxidase proteins; NOX4, p47^{phox}, and Rac 1 protein expressions in mice from the groups of Normal (non-DSS), Vehicle (DSS control), 30sulfa (sulfasalazine 30 mg/kg-treated), 60sulfa (sulfasalazine 60 mg/kg-treated), and SCPB (30sulfa plus *Citrus unshiu* peel and Bupleuri radix mixture at 30 mg/kg-treated). Data are presented as mean ± standard error of the mean for $n = 7$. $^{a}P < 0.05$, $^{b}P < 0.01$, $^{e}P < 0.001$ *vs* normal (non-DSS and untreated) mice; $^{c}P < 0.05$, $^{f}P < 0.001$ *vs* DSS control mice. SCPB: Sulfasalazine (30 mg/kg) + *Citrus unshiu* peel and Bupleuri radix mixture (30 mg/kg); ROS: Reactive oxygen species.

expression of the two factors. Moreover, expressions of TNF-α and IL-1β as well as COX-2 and iNOS were noticeably amplified in the DSS control group but administration of both SCPB and sulfasalazine significantly inhibited this effect. These protein levels were down-regulated similarly or to an extent lower than normal levels (Figure 5). Furthermore, the level of MCP-1 and ICAM-1 protein expressions were decreased in the mice who received SCPB.

SCPB inhibited apoptosis in DSS-induced colitis mice

The excess exposure of ROS in the colonic mucosa is known to trigger apoptosis of colon epithelial cells, leading to progression of IBD[28]. The DSS control group showed the disease-characteristic apoptosis features of inflamed colon epithelial cells, supported by an observable increase in Bax and caspase-3 activities (Figure 6). In contrast, the SCPB treatment appeared to lead to marked down-regulation of the DSS-induced Bax and caspase-3 activities ($P < 0.001$ and $P < 0.05$, respectively). These findings suggest that SCPB may protect the colon mucosa from apoptosis in DSS-induced colitis. Meanwhile, Bcl-2 protein expression during UC didn't show a significant difference as only a mild increase.

DISCUSSION

UC is a type of IBD characterized by chronic inflammation of the intestinal mucosa, manifesting body weight loss, bloody diarrhea, tenesmus, abdominal pain, and fatigue. The incidence and prevalence of UC have been reported over many years and both continue to show a rapid increase worldwide[29]. Nowadays, sulfasalazine, a prodrug of 5-aminosalicylic acid, is currently used as the first-line therapy for mild-to-moderate UC[30]. Although its clinical prescription is executed routinely, the ratios of refractory and relapsed cases are comparatively high[31] and it remains at the limit of poor tolerability due to frequent gastrointestinal side effects[32]. DSS, used for the

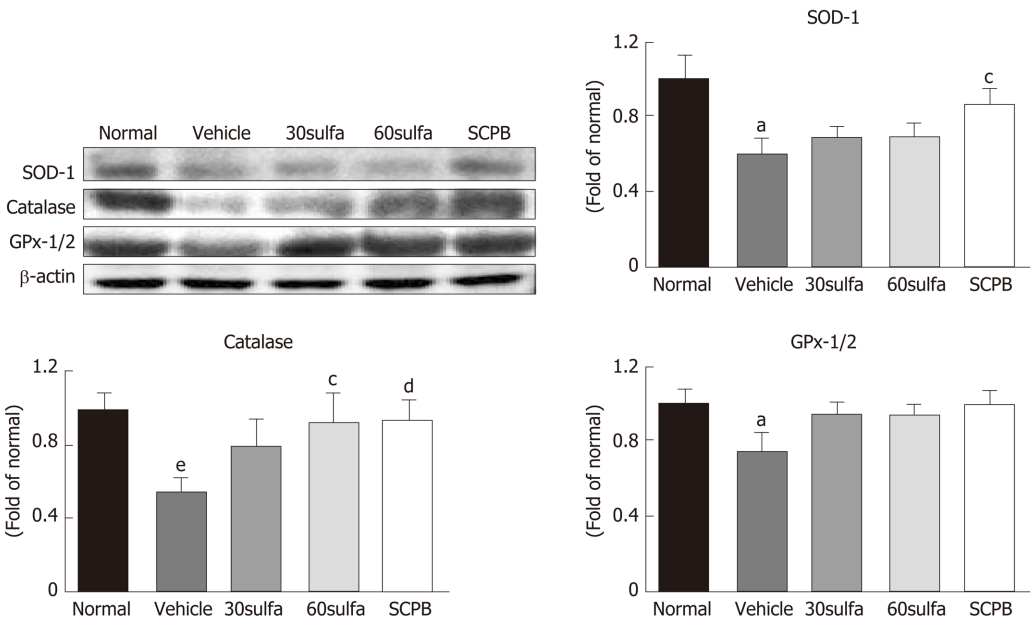

Figure 3 Effect of sulfasalazine (30 mg/kg) + *Citrus unshiu* peel and Bupleuri radix mixture (30 mg/kg) on antioxidant proteins in Dextran Sodium Sulfate-induced colitis mice. Western blot detection of the antioxidant proteins; SOD, Catalase, and GPx-1/2 protein expression levels in mice from the groups of Normal (non-DSS), Vehicle (DSS control), 30sulfa (sulfasalazine 30 mg/kg-treated), 60sulfa (sulfasalazine 60 mg/kg-treated), and SCPB (30sulfa plus *Citrus unshiu* peel and Bupleuri radix mixture at 30 mg/kg-treated). Data are presented as mean ± standard error of the mean for $n = 7$. $^{a}P < 0.05$, $^{e}P < 0.001$ *vs* normal (non-DSS and untreated) mice; $^{c}P < 0.05$, $^{d}P < 0.01$ *vs* DSS control mice. SCPB: Sulfasalazine (30 mg/kg) + *Citrus unshiu* peel and Bupleuri radix mixture (30 mg/kg).

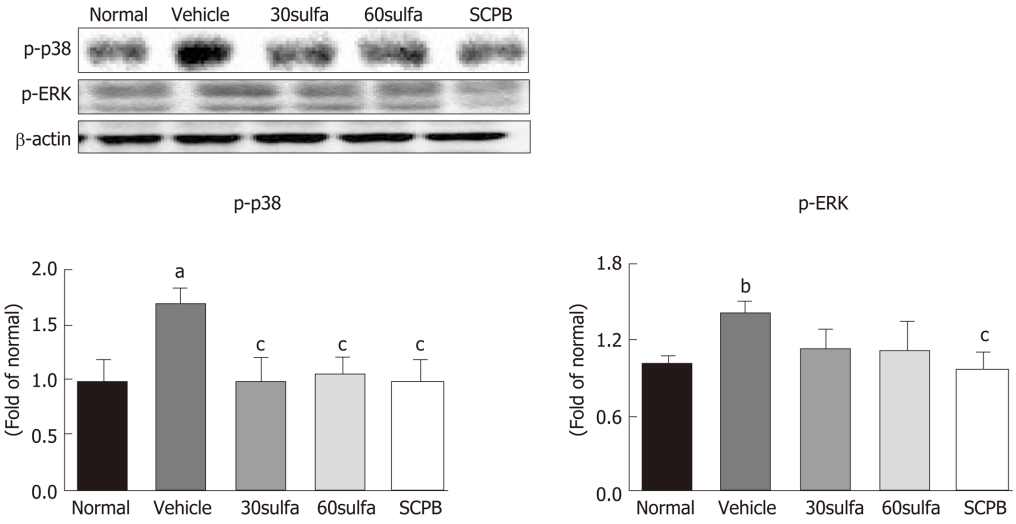

Figure 4 P-p38 and p-ERK protein expressions in Dextran Sodium Sulfate-induced colitis. Western blot detection of the mitogen-activated protein kinase-related proteins; p-p38 and p-ERK in mice from the groups of Normal (non-DSS), Vehicle (DSS control), 30sulfa (sulfasalazine 30 mg/kg-treated), 60sulfa (sulfasalazine 60 mg/kg-treated), and SCPB (30sulfa plus *Citrus unshiu* peel and Bupleuri radix mixture at 30 mg/kg-treated). Data are presented as mean ± standard error of the mean for $n = 7$. $^{a}P < 0.05$, $^{b}P < 0.01$ *vs* normal (non-DSS) mice; $^{c}P < 0.05$ *vs* DSS control mice. SCPB: sulfasalazine (30 mg/kg) + *Citrus unshiu* peel and Bupleuri radix mixture (30 mg/kg).

induction of UC in animal models, causes a marked inflammatory and immune response by affecting DNA replication, inhibiting the overgrowth of epithelial cells, inducing macrophage activation, increasing the release of cytokines, and breaking the balance of gut microflora. The gut microflora itself is a critical player in intestinal permeability with imbalance between beneficial and pathogenic bacteria being implicated in IBD pathogenesis[33]. Consequently, DSS supplementation results in acute UC, which is similar to human UC and making it is an ideal model that has been widely used to study the mechanism of UC and for screening of potential drugs[34,35].

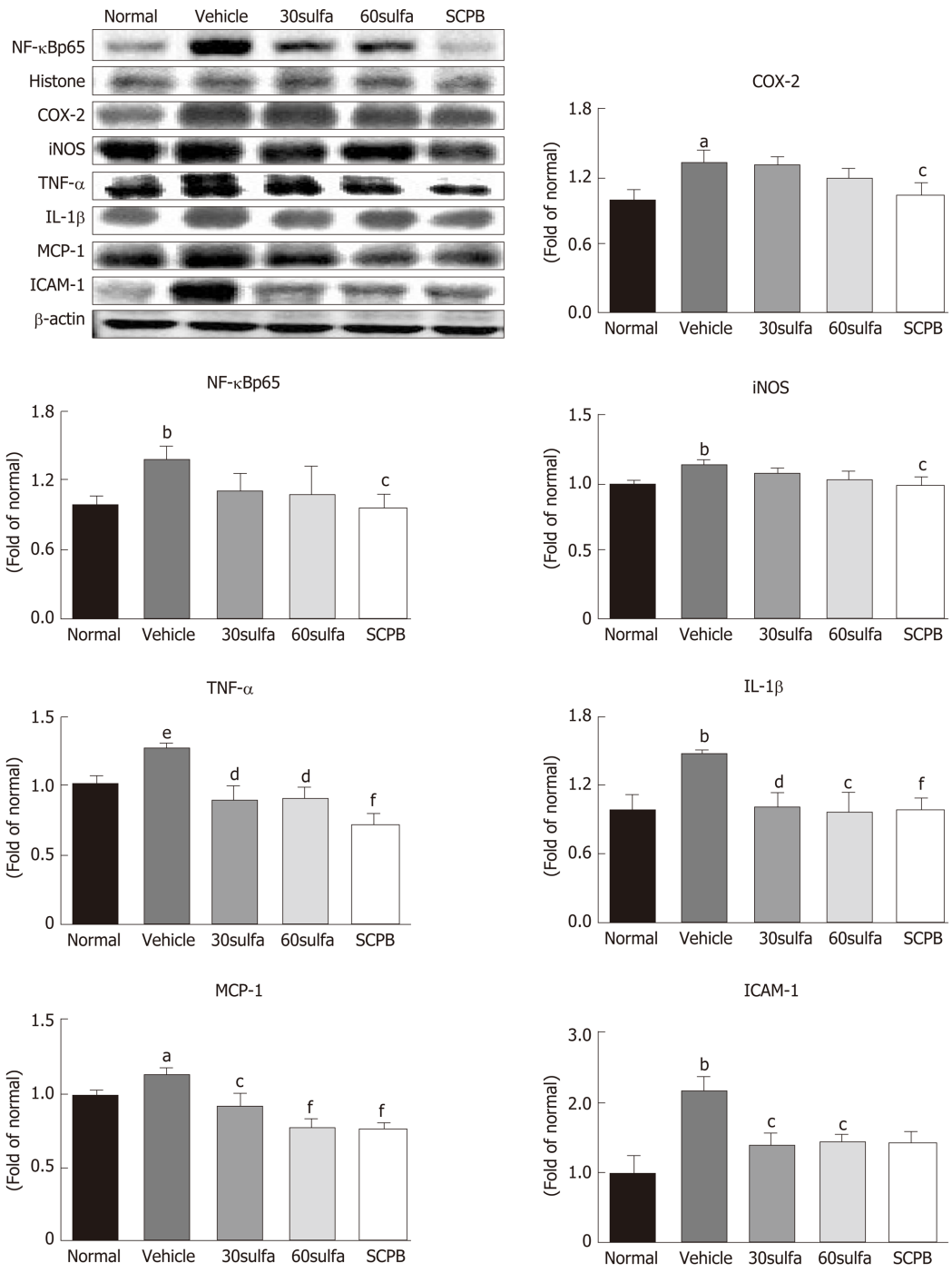

Figure 5 NF-κB p65, COX-2, iNOS, TNF-α, IL-1β MCP-1, and ICAM-1 protein expressions in Dextran Sodium Sulfate-induced colitis.

Western blot detection of the inflammatory proteins; NF-κBp65, COX-2, iNOS, TNF-α, IL-6, MCP-1, and ICAM-1 in mice from the groups of Normal (non-DSS), Vehicle (DSS control), 30sulfa (sulfasalazine 30 mg/kg-treated), 60sulfa (sulfasalazine 60 mg/kg-treated), and SCPB (30sulfa plus *Citrus unshiu* peel and Bupleuri radix mixture at 30 mg/kg-treated). Data are presented as mean ± standard error of the mean for $n = 7$. $^{a}P < 0.05$, $^{b}P < 0.01$, $^{e}P < 0.001$ *vs* normal (non-DSS) mice; $^{c}P < 0.05$, $^{d}P < 0.01$, $^{f}P < 0.001$ *vs* DSS control mice. SCPB: sulfasalazine (30 mg/kg) + *Citrus unshiu* peel and Bupleuri radix mixture (30 mg/kg).

The present study provided, for the first time, a comparative evaluation of the pharmacological efficacy of sulfasalazine combined with *Citrus unshiu* peel and Bupleuri radix mixture (the 'SCPB' treatment described herein), as compared with sulfasalazine alone, in a mouse model of UC. While our the DSS control mice had significantly increased body weight loss and decreased colon length, previous studies have showed length of colon to be inversely correlated with severity of the experimental colitis[36]. In our study, the DSS-induced mice showed significantly decreased final body weight and both the sulfasalazine and SCPB treatments curtailed the body weight loss and the shortening of the colon length. Herein, each groups showed the improvement effect like 30sulfa (1.96%), 60sulfa (5.36%), and SCPB (4.79%)

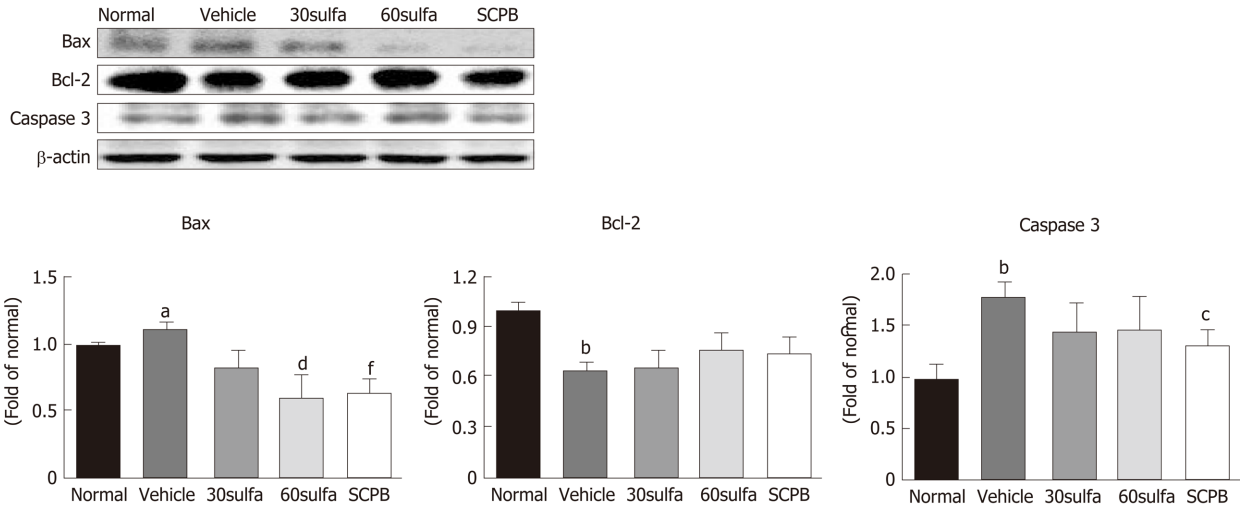

Figure 6 Bax, Bcl-2, and caspase-3 protein expressions in Dextran Sodium Sulfate-induced colitis. Western blot detection of the apoptotic and anti-apoptotic proteins; Bax, Bcl-2, and caspase-3 in mice from the groups of Normal (non-DSS), Vehicle (DSS control), 30sulfa (sulfasalazine 30 mg/kg-treated), 60sulfa (sulfasalazine 60 mg/kg-treated), and SCPB (30sulfa plus *Citrus unshiu* peel and Bupleuri radix mixture at 30 mg/kg-treated). Data are presented as mean ± standard error of the mean for $n = 7$. $^{a}P < 0.05$, $^{b}P < 0.01$ *vs* normal (non-DSS) mice; $^{c}P < 0.05$, $^{d}P < 0.01$, $^{f}P < 0.001$ *vs* DSS control mice. SCPB: sulfasalazine (30 mg/kg) + *Citrus unshiu* peel and Bupleuri radix mixture (30 mg/kg).

on the colon length compared to the DSS control mice although it was not significant. The DSS-induced colonic mucosal damage persisted till day 7, evidenced by epithelial necrosis, impaired mucosa integrity (with submucosa showing hyperemia and edema), and ulceration, accompanied by infiltration of numerous inflammatory cells, such as monocytes and macrophages[37]; importantly, these pathogenic features appeared to be alleviated by the SCPB treatment.

Excessive ROS, including superoxide radicals (O_2^-), hydroxyl radicals, hydrogen peroxide and singlet oxygen, may have detrimental effects on such basic cellular components as DNA, proteins, and lipids. The enzymatic process that can generate ROS is the reaction catalyzed by NADPH oxidase[38]. In resting cells, the subunits of NADPH oxidase are present in the cytosol and the membranes. Upon cell activation, the subunits are assembled on a membrane-bound vesicle, which then fuses with the plasma membrane, resulting in the release O_2^-[38,39]. Accumulation of O_2^- causes an elevation of the detectable ROS, leading to acceleration of an inflammatory cascade. The influence of ROS in the pathogenesis of gastrointestinal diseases, such as colon cancer and acute and chronic pancreatitis, has been demonstrated[40]. Above all, the previous studies have indicated the importance of ROS-induced oxidative stress in the development of UC[41,42] and overproduction of ROS *via* NADPH oxidases, including NOX4, $p47^{phox}$, and Rac 1, has been implicated in tissue damage observed in chronic inflammatory disorders[42]. In the current study, the DSS injury was accompanied by an elevated level of serum ROS, which was decreased upon treatment with either sulfasalazine or SCPB. The protein expressions of NOX4, $p47^{phox}$, and Rac 1 (the markers of NADPH oxidase activity) were augmented in the colons of the DSS control mice. While the 60 mg/kg sulfasalazine-alone treatment down-regulated the NADPH oxidase activity, the SCPB treatment did so to a much greater extent. Generally, ROS are neutralized by endogenous antioxidant enzymes[43]; namely, SOD converts O_2^- to hydrogen peroxide, which is subsequently neutralized to water by the actions of catalase and GPx-1/2. IBD patients present with serious impairment in antioxidant enzyme levels in their intestinal mucosa[44]. In our study, the SOD, catalase, and GPx-1/2 enzymic antioxidants were markedly decreased in the mice with DSS-induced colitis. SCPB administration significantly increased the activities of SOD and catalase but not of GPx-1/2. Overall, these results indicate that SCPB regulates antioxidant enzyme activity against oxidative stress in DSS-induced colitis mice; moreover, this effect was superior to that effected by sulfasalazine alone.

NF-κB participates in controlling the activation of various proinflammatory cytokine genes, such as IL-1β, IL-6, and TNF-α, underlying its critical role in the pathogenesis of UC. MAPKs are also implicated in the pathogenic mechanism, and their activity leads to the activation of various nuclear transcription factors. ROS overproduction activates MAPKs, including p38 and ERK1/2. Phosphorylation of p38 has been confirmed after induction of experimental colitis, wherein activation of p38

can greatly promote the activation of immune cells and aggravate inflammation[45]. In particular, p38 MAPK has numerous direct and indirect interactions with NF-κB. Namely, the phosphorylation of p38 MAPK is implicated by leading to the activation of NF-κB. Moreover, the phosphorylation of ERK1/2 MAPKs are also stimulated upon activation of NF-κB[46,47]. In the present study, the colons of DSS-induced colitis mice showed the expected increases in expressions of ERK1/2 and p38, which SCPB treatment was able to decrease significantly. The NF-κB transcription factor plays a critical role in inflammation, facilitating the expression and secretion of various proinflammatory cytokines, mediators, and chemokines to mediate a series of subsequent inflammatory cascades[48]. Blocking NF-κB activation is known to reduce the release of proinflammatory cytokines, thereby alleviating development of the inflammatory response and achieving a therapeutic effect. In this study, we evaluated the inhibitory effect of SCPB on NF-κB activation in DSS-induced colitis mice. The DSS-induced elevation in NF-κB levels was suppressed upon SCPB treatment but the inhibitory effect of SCPB was much lower than that of sulfasalazine alone. These results suggest that SCPB could ameliorate DSS-induced acute colitis by inhibiting NF-κB activation. NF-κB activation exerts a strong influence on the inflammatory response.

Our results also indicate that SCPB significantly inhibited the induction of COX-2 and iNOS expressions and the production of the proinflammatory cytokines TNF-α and IL-1β. Moreover, the SCPB treatment remarkably down-regulated the MCP-1 chemokine and attenuated the adhesion molecule ICAM-1. Excessive exposure of ROS under inflammatory conditions is known to increase epithelial cell apoptosis[49], which is likely to deteriorate epithelial barrier integrity and has an influence on intestinal damage. Thus, we postulated that DSS treatment is responsible for inducing apoptosis through activation of apoptosis proteins, specifically Bax and caspase-3, and suppression of anti-apoptotic protein, namely Bcl-2, as reported by other researchers[50,51]. Indeed, our DSS-induced colitis mice showed a considerable down-regulation of Bax and caspase-3 upon SCPB treatment. However, Bcl-2 just showed a tendency to increase without a significance. Maybe it judged that other anti-apoptotic protein such as survivin must have been is involved in apoptosis.

CONCLUSION

As a result, the administration of SCPB to mice treated with DSS ameliorated acute inflammation and apoptosis in the colon, as shown in Figure 7. Taken together, the present findings suggest that SCPB is an effective inhibitor of DSS-induced colitis in mice. The SCPB treatment showed enhanced therapeutic effect compared to that of the standard sulfasalazine treatment. Nevertheless, the underlying mechanism of SCPB is still ambiguous and further profound researches are needed.

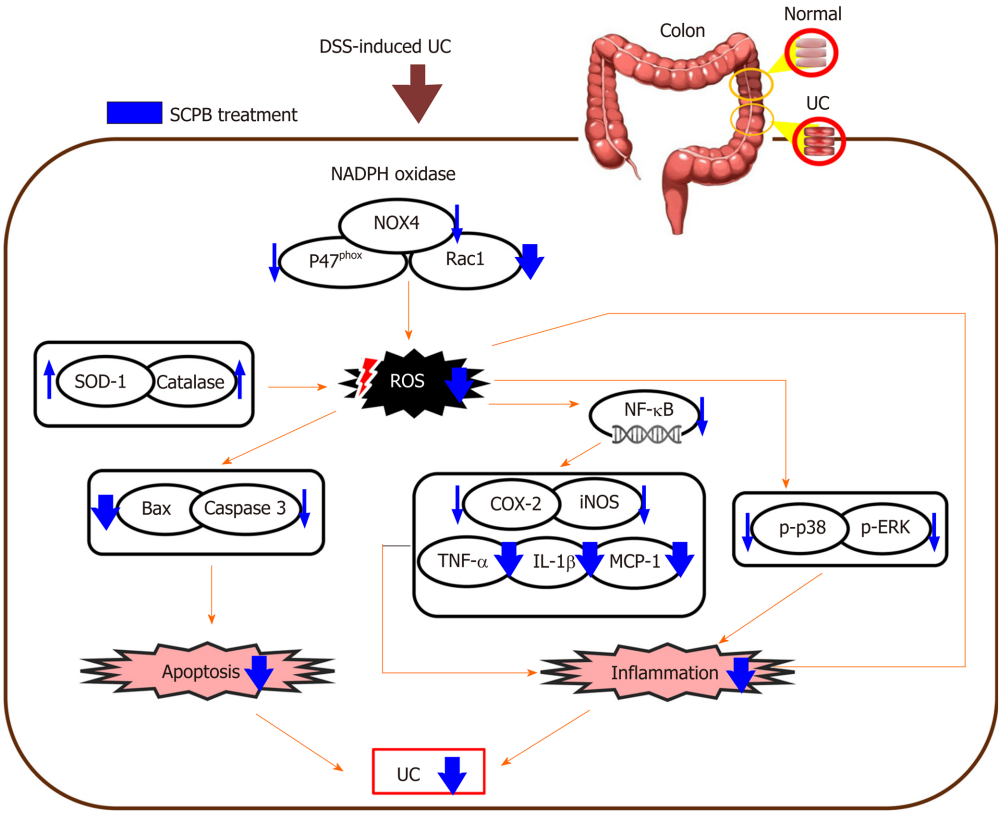

Figure 7 Possible mechanism of *Citrus unshiu* peel and Bupleuri radix mixture combined with sulfasalazine in Dextran Sodium Sulfate-induced ulcerative colitis. SCPB: 30sulfa plus *Citrus unshiu* peel and Bupleuri radix mixture 30 mg/kg-treated mice. DSS: Dextran Sodium Sulfate; SCPB: Sulfasalazine (30 mg/kg) + *Citrus unshiu* peel and Bupleuri radix mixture (30 mg/kg); ROS: Reactive oxygen species; UC: Ulcerative colitis.

ARTICLE HIGHLIGHTS

Research background

Ulcerative colitis (UC) has high incidence worldwide and is characterized by unintentional weight loss, abdominal pain, mucous and bloody diarrhea, and anemia. Generally, the recommended therapies for UC include anti-inflammatory drugs, antibiotics, immunosuppressants, and anti-tumor necrosis factor-alpha antibodies. Sulfasalazine, a drug composed of 5-aminosalicylic acid and sulfapyridine, has been prescribed as a standard-of-care in UC treatment. Otherwise, it can produce a variety of side effects upon long-term and high-dose intakes. Hence, an alternative approach for a safer, cheaper, and more efficacious management or treatment of UC is needed.

Research motivation

UC is chronic and complex autoimmune inflammatory disorder. The incidence of UC has grown worldwide over the recent decades and the quality of life for patients suffering from UC has been falling quickly, in tandem. The findings from our research will give essential help towards dealing with the problems of these patients, with sulfasalazine with *Citrus unshiu* peel and Bupleuri radix mixture (referred to as SCPB), one of more safe and effective herbal medicine mixtures, contributing to improving their quality of life.

Research objectives

The present study was conducted to evaluate the pharmacological effect of sulfasalazine alone and as the SCPB combination using an experimentally-induced UC mouse model.

Research methods

Ulcerative colitis was induced by 5% dextran sodium sulfate in drinking water for 7 d. The pharmacological effect of sulfasalazine alone and SCPB was evaluated using serum analysis, histological exam, and western blotting. The colon tissue was selected

as the region of interest for data analysis. One-way ANOVA followed by Least-significant differences (LSD) test were used for statistical inference.

Research results

The SCPB treatment significantly inhibited the induction of COX-2 and iNOS expressions and the production of the proinflammatory cytokines TNF-α and IL-1β. Moreover, the SCPB treatment remarkably down-regulated the MCP-1 chemokine and attenuated the adhesion molecule ICAM-1. The SCPB treatment exerted anti-apoptotic effect though a considerable down-regulation of Bax and caspase-3 upon SCPB treatment.

Research conclusions

The SCPB supplementation showed enhanced therapeutic effect compared to that of the standard sulfasalazine treatment. Accordingly, SCPB may represent a promising alternative therapeutic against ulcerative colitis without inducing adverse effects.

Research perspectives

A single dose of sulfasalazine cannot provide satisfactory therapeutic results because of a spectrum of side effects after long-term and high-dose intake. However, when we used in combination with *Citrus unshiu* peel and Bupleuri radix mixture in an experimentally-induced ulcerative colitis mouse model, its inflammation was alleviated significantly. SCPB therapy may be more efficious for symptom improvement of patients with ulcerative colitis in future.

REFERENCES

1 **Snider AJ**, Kawamori T, Bradshaw SG, Orr KA, Gilkeson GS, Hannun YA, Obeid LM. A role for sphingosine kinase 1 in dextran sulfate sodium-induced colitis. *FASEB J* 2009; **23**: 143-152 [PMID: 18815359 DOI: 10.1096/fj.08-118109]

2 **Larussa T**, Imeneo M, Luzza F. Potential role of nutraceutical compounds in inflammatory bowel disease. *World J Gastroenterol* 2017; **23**: 2483-2492 [PMID: 28465632 DOI: 10.3748/wjg.v23.i14.2483]

3 **Ross AS**, Cohen RD. Medical therapy for ulcerative colitis: the state of the art and beyond. *Curr Gastroenterol Rep* 2004; **6**: 488-495 [PMID: 15527679 DOI: 10.1007/s11894-004-0071-9]

4 **de Souza HS**, Fiocchi C. Immunopathogenesis of IBD: current state of the art. *Nat Rev Gastroenterol Hepatol* 2016; **13**: 13-27 [PMID: 26627550 DOI: 10.1038/nrgastro.2015.186]

5 **Linares V**, Alonso V, Domingo JL. Oxidative stress as a mechanism underlying sulfasalazine-induced toxicity. *Expert Opin Drug Saf* 2011; **10**: 253-263 [PMID: 21219240 DOI: 10.1517/14740338.2011.529898]

6 **Akinbo F**, Eze G. Combined Effects of Medicinal Plants on Induced Upper Gastrointestinal Tract Injury in Wistar Rats. *Ethiop J Health Sci* 2016; **26**: 573-580 [PMID: 28450774 DOI: 10.4314/ejhs.v26i6.11]

7 **Jeong SJ**, Kim OS, Yoo SR, Seo CS, Kim Y, Shin HK. Anti-inflammatory and antioxidant activity of the traditional herbal formula Gwakhyangjeonggi-san via enhancement of heme oxygenase-1 expression in RAW264.7 macrophages. *Mol Med Rep* 2016; **13**: 4365-4371 [PMID: 27052497 DOI: 10.3892/mmr.2016.5084]

8 **Sreedhar R**, Arumugam S, Thandavarayan RA, Giridharan VV, Karuppagounder V, Pitchaimani V, Afrin R, Harima M, Nakamura T, Ueno K, Nakamura M, Suzuki K, Watanabe K. Toki-shakuyaku-san, a Japanese kampo medicine, reduces colon inflammation in a mouse model of acute colitis. *Int Immunopharmacol* 2015; **29**: 869-875 [PMID: 26344429 DOI: 10.1016/j.intimp.2015.08.029]

9 **Jang SE**, Jeong JJ, Hyam SR, Han MJ, Kim DH. Anticolitic Effect of the Rhizome Mixture of Anemarrhena asphodeloides and Coptidis chinensis (AC-mix) in Mice. *Biomol Ther (Seoul)* 2013; **21**: 398-404 [PMID: 24244828 DOI: 10.4062/biomolther.2013.048]

10 **Kawashima K**, Nomura A, Makino T, Saito K, Kano Y. Pharmacological properties of traditional medicine (XXIX): effect of Hange-shashin-to and the combinations of its herbal constituents on rat experimental colitis. *Biol Pharm Bull* 2004; **27**: 1599-1603 [PMID: 15467203 DOI: 10.1248/bpb.27.1599]

11 **Oh YC**, Cho WK, Jeong YH, Im GY, Yang MC, Hwang YH, Ma JY. Anti-inflammatory effect of Citrus Unshiu peel in LPS-stimulated RAW 264.7 macrophage cells. *Am J Chin Med* 2012; **40**: 611-629 [PMID: 22745074 DOI: 10.1142/S0192415X12500462]

12 **Lim DW**, Lee Y, Kim YT. Preventive effects of Citrus unshiu peel extracts on bone and lipid metabolism in OVX rats. *Molecules* 2014; **19**: 783-794 [PMID: 24413833 DOI: 10.3390/molecules19010783]

13 **Lu Y**, Zhang C, Bucheli P, Wei D. Citrus flavonoids in fruit and traditional Chinese medicinal food ingredients in China. *Plant Foods Hum Nutr* 2006; **61**: 57-65 [PMID: 16816988 DOI: 10.1007/s11130-006-0014-8]

14 **Zhang C**, Lu Y, Tao L, Tao X, Su X, Wei D. Tyrosinase inhibitory effects and inhibition mechanisms of nobiletin and hesperidin from citrus peel crude extracts. *J Enzyme Inhib Med Chem* 2007; **22**: 91-98 [PMID: 17373553 DOI: 10.1080/14756360600988989]

15 **Kim A**, Im M, Gu MJ, Ma JY. Citrus unshiu peel extract alleviates cancer-induced weight loss in mice bearing CT-26 adenocarcinoma. *Sci Rep* 2016; **6**: 24214 [PMID: 27064118 DOI: 10.1038/srep24214]

16 **Lim H**, Yeo E, Song E, Chang YH, Han BK, Choi HJ, Hwang J. Bioconversion of Citrus unshiu peel extracts with cytolase suppresses adipogenic activity in 3T3-L1 cells. *Nutr Res Pract* 2015; **9**: 599-605 [PMID: 26634048 DOI: 10.4162/nrp.2015.9.6.599]

17 **Kang SJ**, Lee YJ, Kim BM, Kim YJ, Woo HD, Jeon HK, Chung HW. Effect of Bupleuri Radix extracts on the toxicity of 5-fluorouracil in HepG2 hepatoma cells and normal human lymphocytes. *Basic Clin Pharmacol Toxicol* 2008; **103**: 305-313 [PMID: 18834353 DOI: 10.1111/j.1742-7843.2008.00280.x]

18 **Ashour ML**, Wink M. Genus Bupleurum: a review of its phytochemistry, pharmacology and modes of action. *J Pharm Pharmacol* 2011; **63**: 305-321 [PMID: 21749378 DOI: 10.1111/j.2042-7158.2010.01170.x]

19 **Yuan B**, Yang R, Ma Y, Zhou S, Zhang X, Liu Y. A systematic review of the active saikosaponins and extracts isolated from Radix Bupleuri and their applications. *Pharm Biol* 2017; **55**: 620-635 [PMID: 27951737 DOI: 10.1080/13880209.2016.1262433]

20 **Xie JY**, Di HY, Li H, Cheng XQ, Zhang YY, Chen DF. Bupleurum chinense DC polysaccharides attenuates lipopolysaccharide-induced acute lung injury in mice. *Phytomedicine* 2012; **19**: 130-137 [PMID: 22112722 DOI: 10.1016/j.phymed.2011.08.057]

21 **Wang C**, Zhang T, Cui X, Li S, Zhao X, Zhong X. Hepatoprotective effects of a chinese herbal formula, longyin decoction, on carbon-tetrachloride-induced liver injury in chickens. *Evid Based Complement Alternat Med* 2013; **2013**: 392743 [PMID: 23533478 DOI: 10.1155/2013/392743]

22 **Ali SF**, LeBel CP, Bondy SC. Reactive oxygen species formation as a biomarker of methylmercury and trimethyltin neurotoxicity. *Neurotoxicology* 1992; **13**: 637-648 [PMID: 1475065]

23 **Komatsu S**. Extraction of nuclear proteins. *Methods Mol Biol* 2007; **355**: 73-77 [PMID: 17093304 DOI: 10.1385/1-59745-227-0:73]

24 **Jin BR**, Chung KS, Cheon SY, Lee M, Hwang S, Noh Hwang S, Rhee KJ, An HJ. Rosmarinic acid suppresses colonic inflammation in dextran sulphate sodium (DSS)-induced mice via dual inhibition of NF-κB and STAT3 activation. *Sci Rep* 2017; **7**: 46252 [PMID: 28383063 DOI: 10.1038/srep46252]

25 **Yan H**, Wang H, Zhang X, Li X, Yu J. Ascorbic acid ameliorates oxidative stress and inflammation in dextran sulfate sodium-induced ulcerative colitis in mice. *Int J Clin Exp Med* 2015; **8**: 20245-20253 [PMID: 26884937]

26 **Yan X**, Wu H, Wu Z, Hua F, Liang D, Sun H, Yang Y, Huang D, Bian JS. The New Synthetic H_2S-Releasing SDSS Protects MC3T3-E1 Osteoblasts against H_2O_2-Induced Apoptosis by Suppressing Oxidative Stress, Inhibiting MAPKs, and Activating the PI3K/Akt Pathway. *Front Pharmacol* 2017; **8**: 07 [PMID: 28163684 DOI: 10.3389/fphar.2017.00007]

27 **Schuliga M**. NF-kappaB Signaling in Chronic Inflammatory Airway Disease. *Biomolecules* 2015; **5**: 1266-1283 [PMID: 26131974 DOI: 10.3390/biom5031266]

28 **Kruidenier L**, Kuiper I, Lamers CB, Verspaget HW. Intestinal oxidative damage in inflammatory bowel disease: semi-quantification, localization, and association with mucosal antioxidants. *J Pathol* 2003; **201**: 28-36 [PMID: 12950014 DOI: 10.1002/path.1409]

29 **Lerebours E**, Savoye G, Guedon C. [Epidemiology and natural history of chronic inflammatory bowel disease]. *Gastroenterol Clin Biol* 2003; **27**: S76-S80 [PMID: 12704299]

30 **Tindall WN**, Boltri JM, Wilhelm SM. Mild-to-moderate ulcerative colitis: your role in patient compliance and health care costs. *J Manag Care Pharm* 2007; **13**: S2-12; quiz S13-4 [PMID: 17874873 DOI: 10.18553/jmcp.2007.13.s7-a.2]

31 **Watanabe Y**, Murata T, Amakawa M, Miyake Y, Handa T, Konishi K, Matsumura Y, Tanaka T, Takeuchi K. KAG-308, a newly-identified EP4-selective agonist shows efficacy for treating ulcerative colitis and can bring about lower risk of colorectal carcinogenesis by oral administration. *Eur J Pharmacol* 2015; **754**: 179-189 [PMID: 25704618 DOI: 10.1016/j.ejphar.2015.02.021]

32 **Tabit CE**, Holbrook M, Shenouda SM, Dohadwala MM, Widlansky ME, Frame AA, Kim BH, Duess MA, Kluge MA, Levit A, Keaney JF Jr, Vita JA, Hamburg NM. Effect of sulfasalazine on inflammation and endothelial function in patients with established coronary artery disease. *Vasc Med* 2012; **17**: 101-107 [PMID: 22496207 DOI: 10.1177/1358863X12440117]

33 **Mizoguchi A**. Animal models of inflammatory bowel disease. *Prog Mol Biol Transl Sci* 2012; **105**: 263-320 [PMID: 22137435 DOI: 10.1016/B978-0-12-394596-9.00009-3]

34 **Woo JK**, Choi S, Kang JH, Kim DE, Hurh BS, Jeon JE, Kim SY, Oh SH. Fermented barley and soybean (BS) mixture enhances intestinal barrier function in dextran sulfate sodium (DSS)-induced colitis mouse model. *BMC Complement Altern Med* 2016; **16**: 498 [PMID: 27912750 DOI: 10.1186/s12906-016-1479-0]

35 **Huang YF**, Zhou JT, Qu C, Dou YX, Huang QH, Lin ZX, Xian YF, Xie JH, Xie YL, Lai XP, Su ZR. Anti-inflammatory effects of Brucea javanica oil emulsion by suppressing NF-κB activation on dextran sulfate sodium-induced ulcerative colitis in mice. *J Ethnopharmacol* 2017; **198**: 389-398 [PMID: 28119098 DOI: 10.1016/j.jep.2017.01.042]

36 **Lyu W**, Jia H, Deng C, Saito K, Yamada S, Kato H. Zeolite-Containing Mixture Supplementation Ameliorated Dextran Sodium Sulfate-Induced Colitis in Mice by Suppressing the Inflammatory Bowel Disease Pathway and Improving Apoptosis in Colon Mucosa. *Nutrients* 2017; **9** [PMID: 28481231 DOI: 10.3390/nu9050467]

37 **Zhang ZL**, Fan HY, Yang MY, Zhang ZK, Liu K. Therapeutic effect of a hydroxynaphthoquinone fraction on dextran sulfate sodium-induced ulcerative colitis. *World J Gastroenterol* 2014; **20**: 15310-15318 [PMID: 25386079 DOI: 10.3748/wjg.v20.i41.15310]

38 **Ushio-Fukai M**, Nakamura Y. Reactive oxygen species and angiogenesis: NADPH oxidase as target for cancer therapy. *Cancer Lett* 2008; **266**: 37-52 [PMID: 18406051 DOI: 10.1016/j.canlet.2008.02.044]

39 **Yao J**, Cao X, Zhang R, Li YX, Xu ZL, Zhang DG, Wang LS, Wang JY. Protective Effect of Baicalin Against Experimental Colitis via Suppression of Oxidant Stress and Apoptosis. *Pharmacogn Mag* 2016; **12**: 225-234 [PMID: 27601854 DOI: 10.4103/0973-1296.186342]

40 **Kim YJ**, Kim EH, Hahm KB. Oxidative stress in inflammation-based gastrointestinal tract diseases: challenges and opportunities. *J Gastroenterol Hepatol* 2012; **27**: 1004-1010 [PMID: 22413852 DOI: 10.1111/j.1440-1746.2012.07108.x]

41 **Patlevič P**, Vašková J, Švorc P Jr, Vaško L, Švorc P. Reactive oxygen species and antioxidant defense in human gastrointestinal diseases. *Integr Med Res* 2016; **5**: 250-258 [PMID: 28462126 DOI: 10.1016/j.imr.2016.07.004]

42 **Mitani T**, Yoshioka Y, Furuyashiki T, Yamashita Y, Shirai Y, Ashida H. Enzymatically synthesized glycogen inhibits colitis through decreasing oxidative stress. *Free Radic Biol Med* 2017; **106**: 355-367

[PMID: 28257879 DOI: 10.1016/j.freeradbiomed.2017.02.048]
43 **da Costa Gonçalves F**, Grings M, Nunes NS, Pinto FO, Garcez TN, Visioli F, Leipnitz G, Paz AH. Antioxidant properties of mesenchymal stem cells against oxidative stress in a murine model of colitis. *Biotechnol Lett* 2017; **39**: 613-622 [PMID: 28032203 DOI: 10.1007/s10529-016-2272-3]
44 **Yeom Y**, Kim Y. The Sasa quelpaertensis Leaf Extract Inhibits the Dextran Sulfate Sodium-induced Mouse Colitis Through Modulation of Antioxidant Enzyme Expression. *J Cancer Prev* 2015; **20**: 136-146 [PMID: 26151047 DOI: 10.15430/JCP.2015.20.2.136]
45 **Seo JH**, Lim JW, Kim H. Differential Role of ERK and p38 on NF- κ B Activation in Helicobacter pylori-Infected Gastric Epithelial Cells. *J Cancer Prev* 2013; **18**: 346-350 [PMID: 25337564 DOI: 10.15430/jcp.2013.18.4.346]
46 **Feng YJ**, Li YY, Lin XH, Li K, Cao MH. Anti-inflammatory effect of cannabinoid agonist WIN55, 212 on mouse experimental colitis is related to inhibition of p38MAPK. *World J Gastroenterol* 2016; **22**: 9515-9524 [PMID: 27920472 DOI: 10.3748/wjg.v22.i43.9515]
47 **Tahir AA**, Sani NF, Murad NA, Makpol S, Ngah WZ, Yusof YA. Combined ginger extract & Gelam honey modulate Ras/ERK and PI3K/AKT pathway genes in colon cancer HT29 cells. *Nutr J* 2015; **14**: 31 [PMID: 25889965 DOI: 10.1186/s12937-015-0015-2]
48 **Feng J**, Guo C, Zhu Y, Pang L, Yang Z, Zou Y, Zheng X. Baicalin down regulates the expression of TLR4 and NFkB-p65 in colon tissue in mice with colitis induced by dextran sulfate sodium. *Int J Clin Exp Med* 2014; **7**: 4063-4072 [PMID: 25550915]
49 **Thompson WL**, Van Eldik LJ. Inflammatory cytokines stimulate the chemokines CCL2/MCP-1 and CCL7/MCP-3 through NFkB and MAPK dependent pathways in rat astrocytes [corrected]. *Brain Res* 2009; **1287**: 47-57 [PMID: 19577550 DOI: 10.1016/j.brainres.2009.06.081]
50 **Redza-Dutordoir M**, Averill-Bates DA. Activation of apoptosis signalling pathways by reactive oxygen species. *Biochim Biophys Acta* 2016; **1863**: 2977-2992 [PMID: 27646922 DOI: 10.1016/j.bbamcr.2016.09.012]
51 **Ju J**, Lee GY, Kim YS, Chang HK, Do MS, Park KY. Bamboo Salt Suppresses Colon Carcinogenesis in C57BL/6 Mice with Chemically Induced Colitis. *J Med Food* 2016; **19**: 1015-1022 [PMID: 27845862 DOI: 10.1089/jmf.2016.3798]

World Journal of Gastroenterology

Submit a Manuscript: https://www.f6publishing.com

World J Gastroenterol 2020 September 21; 26(35): 5287-5301

DOI: 10.3748/wjg.v26.i35.5287

ISSN 1007-9327 (print) ISSN 2219-2840 (online)

ORIGINAL ARTICLE

Basic Study

Immune infiltration-associated serum amyloid A1 predicts favorable prognosis for hepatocellular carcinoma

Wei Zhang, Hui-Fang Kong, Xu-Dong Gao, Zheng Dong, Ying Lu, Jia-Gan Huang, Hong Li, Yong-Ping Yang

ORCID number: Wei Zhang 0000-0002-2659-9627; Hui-Fang Kong 0000-0002-9288-635X; Xu-Dong Gao 0000-0002-6102-4722; Zheng Dong 0000-0002-4653-3991; Ying Lu 0000-0002-2333-7605; Jia-Gan Huang 0000-0002-0041-3097; Hong Li 0000-0002-4160-7779; Yong-Ping Yang 0000-0001-6232-9344.

Author contributions: Zhang W and Kong HF conducted data analysis, wrote the manuscript, and contributed equally to this study; Gao XD and Huang JG conducted the literature research and data collection; Dong Z, Lu Y and Li H discussed the results and statistical analysis; Yang YP designed the study and revised the manuscript.

Supported by Guizhou Provincial Natural Science Foundation, No. 2020-1Y299.

Institutional review board statement: This study was approved by the Ethical committee of the Fifth Medical Center of People's Liberation Army General Hospital.

Conflict-of-interest statement: All authors have nothing to declare.

Data sharing statement: No additional data are available.

Wei Zhang, Hui-Fang Kong, Xu-Dong Gao, Zheng Dong, Ying Lu, Jia-Gan Huang, Yong-Ping Yang, Center for Diagnosis and Research of Liver Tumor, Fifth Medical Center of People's Liberation Army General Hospital, Beijing 100191, China

Hong Li, Department of Infectious Diseases, the Affiliated Hospital of Guizhou Medical University, Guiyang 550001, Guizhou Province, China

Corresponding author: Yong-Ping Yang, MD, Chief Doctor, Center for Diagnosis and Research of Liver Tumor, Fifth Medical Center of People's Liberation Army General Hospital, No. 100 West Sihuan Road, Fengtai District, Beijing 100191, China. yyp1542@163.com

Abstract

BACKGROUND

Serum amyloid A1 (SAA1) is an acute-phase protein involved in acute or chronic hepatitis. Its function is still controversial. In addition, the effect of the expression of SAA1 and its molecular function on the progression in hepatocellular carcinoma (HCC) is still unclear.

AIM

To demonstrate the expression of SAA1 and its effect on the prognosis in HCC and explain further the correlation of SAA1 and immunity pathways.

METHODS

SAA1 expression in HCC was conducted with The Cancer Genome Atlas-Liver Hepatocellular Carcinoma (TCGA-LIHC) in GEPIA tool, and the survival analysis based on the SAA1 expression level was achieved in the Kaplan-Meier portal. The high or low expression group was then drawn based on the median level of SAA1 expression. The correlation of SAA1 and the clinical features were conducted in the UALCAN web-based portal with TCGA-LIHC, including tumor grade, patient disease stage, and the TP53 mutation. The correlation analysis between SAA1 expression and TP53 mutation was subjected to the TCGA portal. The tumor purity score and the immune score were analyzed with CIBERSORT. The correlation of SAA1 expression and tumor-infiltrating lymphocytes was achieved in TISIDB web-based integrated repository portal for tumor-immune system interactions. GSE125336 dataset was used to test the SAA1 expression in the responsive or resistant group with anti-PD1 therapy. Gene set enrichment analysis was applied to evaluate the gene enrichment signaling pathway in HCC. The similar genes of SAA1 in HCC were identified in GEPIA, and the protein-

Manuscript source: Unsolicited manuscript

Received: May 10, 2020
Peer-review started: May 10, 2020
First decision: July 29, 2020
Revised: August 3, 2020
Accepted: August 13, 2020
Article in press: August 13, 2020
Published online: September 21, 2020

P-Reviewer: Sitkin S
S-Editor: Ma YJ
L-Editor: Filipodia
P-Editor: Li JH

protein interaction of SAA1 was conducted in the Metascape tool. The expression of C-X-C motif chemokine ligand 2, C-C motif chemokine ligand 23, and complement C5a receptor 1 was studied and overall survival analysis in HCC was conducted in GEPIA and Kaplan-Meier portal, respectively.

RESULTS

SAA1 expression was decreased in HCC, and lower SAA1 expression predicted poorer overall survival, progression-free survival, and disease-specific survival. Furthermore, SAA1 expression was further decreased with increased tumor grade and patient disease stage. Also, SAA1 expression was further downregulated in patients with TP53 mutation compared with patients with wild type TP53. SAA1 expression was negatively correlated with the TP53 mutation. Lower SAA1 predicted poorer survival rate, especially in the patients with no hepatitis virus infection, other than those with hepatitis virus infection. Moreover, the SAA1 expression was negatively correlated with tumor purity. In contrast, SAA1 expression was positively correlated with the immune score in HCC, and the correlation analysis between SAA1 expression and tumor-infiltrating lymphocytes also showed a positive correlation in HCC. Decreased SAA1 was closely associated with the immune tolerance of HCC. C-X-C motif chemokine ligand 2 and C-C motif chemokine ligand 23 genes were identified as the hub genes associated with SAA1, which could also serve as favorable prognosis markers for HCC.

CONCLUSION

SAA1 is downregulated in the liver tumor, and it is closely involved in the progression of HCC. Lower SAA1 expression indicates lower survival rate, especially for those patients without hepatitis virus infection. Lower SAA1 expression also suggests lower immune infiltrating cells, especially for those with immune cells exerting anti-tumor immune function. SAA1 expression is closely associated with the anti-tumor immune pathways.

Key Words: Serum amyloid A1; Hepatocellular carcinoma; Low expression; Prognosis; Hepatitis; Immune pathways

Core Tip: In this study, we identified the downregulation of serum amyloid A1 (SAA1) in hepatocellular carcinoma (HCC). SAA1 expression could predict the favorable prognosis for HCC patients, especially for those patients without hepatitis virus infection. SAA1 expression was closely associated with anti-tumor immune signaling pathways. We also identified two signature genes associated with SAA1, suggesting a favorable prognosis function of SAA1 for HCC patients.

Citation: Zhang W, Kong HF, Gao XD, Dong Z, Lu Y, Huang JG, Li H, Yang YP. Immune infiltration-associated serum amyloid A1 predicts favorable prognosis for hepatocellular carcinoma. *World J Gastroenterol* 2020; 26(35): 5287-5301
URL: https://www.wjgnet.com/1007-9327/full/v26/i35/5287.htm
DOI: https://dx.doi.org/10.3748/wjg.v26.i35.5287

INTRODUCTION

Serum amyloid A1 (SAA1) is a kind of acute-phase protein that is also a member of the coding gene of serum amyloid A (SAA) protein, which consists of SAA2, SAA3, and SAA4[1,2]. SAA1, SAA2, and SAA3 contribute to the acute phase response, and SAA4 expression is constitutively expressed[3]. At present, SAA protein is regarded as the most important biomarker in acute inflammation and tissue injury, and it could serve as a marker for viral or bacterial infection. The sensitivity of SAA1 for inflammatory infection diagnosis is superior to C-reaction protein, which was confirmed in the diagnosis of several diseases, such as tuberculosis, lepriasis, Crohn's disease, and

rheumatoid arthritis[4-6]. In recent years, the importance of SAA in the malignant tumor has attracted much more attention. Some studies reported that serum SAA is a biomarker for some solid tumors, such as stomach, colon, pancreas, breast, and lung cancers, and that elevated SAA is also correlated with tumor stage[7-10]. SAA protein is mainly synthesized by the liver, and some literature has revealed its expression changes in liver diseases, such as liver injury and virus infection[11]. However, the expression and clinical correlation of SAA in hepatocellular carcinoma (HCC) are still unclear. SAA1, which is an important preproprotein of SAA, should also be examined. Thus, this study mainly focused on the significance of SAA1 in HCC.

HCC is a major malignant tumor of the digestive system with a high lethality rate, especially in Asians[12]. Clinical data have shown that hepatitis virus infection could be an important reason for the high frequency of HCC in Asians[13,14]. The clinical treatment for HCC includes chemotherapy, radiotherapy, immunotherapy, and interventional treatment[15]. The representative chemotherapy drug is sorafenib, from which some patients benefit in prolonging survival. However, clinical practice also revealed the true frequency of drug resistance, which contributed to the poor outcome of HCC patients[16]. The complex tumor microenvironment and side effects also interfered with the effect of radiotherapy or interventional therapy[17]. In recent years, immune-based treatments have attracted much attention. Immune checkpoint blockade therapy has been widely conducted in clinical trials (*e.g.*, the PD-1 blockade antibody[18]) with unsatisfactory outcomes. Considering the significance of the anti-PD1 antibody in other tumors, some researchers hypothesized that immune tolerance might contribute to the poor outcome. Researchers had been trying to explore solutions to overcome immune tolerance. Driving immune cytotoxic cells to kill tumor cells could be an encouraging strategy.

In this study, SAA1 expression was decreased in HCC, and its lower expression represented poorer prognosis, especially in those without hepatitis virus infection, suggesting that immune signaling pathways might be involved in SAA1-mediated HCC progression. The molecular mechanism exploration also confirmed the close association between SAA1 and immune tolerance. In summary, downregulation of SAA1 in HCC may be a candidate target for HCC therapy, especially in the practice of anti-tumor immunity.

MATERIALS AND METHODS

The cancer genome atlas analysis

The expression of SAA1, C-X-C motif chemokine ligand 2 (CXCL2), C-C motif chemokine ligand 23 (CCL23), and complement C5a receptor 1 (C5AR1) in the HCC tumor tissues and normal liver tissues was conducted in the GEPIA portal (http://gepia2.cancer-pku.cn/#index)[19]. Normal liver tissues were comprised of surrounding non-tumor and genotype-tissue expression liver tissues. The correlation of SAA1 with the clinical features (*e.g.*, tumor grade, patient disease stage, and TP53 mutation) was subjected to UALCAN (http://ualcan.path.uab.edu/index.html)[20]. The correlation of SAA1 expression with the frequency of TP53 mutation was conducted in Liver Hepatocellular Carcinoma (LIHC) of The Cancer Genome Atlas (TCGA) portal (www.tcgaportal.org).

Survival analysis

The overall survival (OS), progression-free survival (PFS), recurrence-free survival (RFS), and disease-specific survival (DSS) were subjected to Kaplan Meier plotter (http://kmplot.com/analysis/)[21]. The portal can assess the effect of SAA1 on the survival rate in HCC. The TCGA samples and gene expression omnibus (GEO) series samples were included in the liver tumor of the Kaplan Meier plotter portal. The standard level of high or low expression group was achieved by the best cutoff, which was between the lower and upper quartiles, and the best performing threshold was used as a cutoff.

Immune infiltration analysis

The correlation between SAA1 expression and the tumor purity of HCC was measured in TIMER (http://timer.cistrome.org/)[22], a comprehensive resource for systematic analysis of immune infiltrates. The interaction between SAA1 and the immune system was assessed in TISIDB[23], an integrated repository portal for tumor-immune system interactions. In this study, the transcriptomics data of SAA1 and clinical data of LIHC from TCGA were included to evaluate the correlation, elucidating the potential

interaction between SAA1 and the immune system.

Gene set enrichment analysis

The enrichment analysis of the Kyoto encyclopedia of genes and genomes pathways (KEGG) was conducted with gene set enrichment analysis (GSEA)[24]. The standard of sample clustering was based on the median level of SAA1 expression. The number of permutations was set as 1000, and the enrichment statistic was weighted. The Signal2Nosie was used as a metric for ranking genes. The minimum sets were above 15 genes. The normalized enrichment score (NES) was used to evaluate the enrichment intensity of SAA1 in indicated pathways. A P value < 0.05 and a false discovery rate < 0.05 for an enrichment gene sets were considered as the statistically significant.

GEO analysis

GSE125336 data set was from GEO, a public functional genomics data repository portal. The sequencing data were downloaded *via* the SangerBox tool (https://shengxin.ren/). This dataset was collected from the GPL21103 platform (Illumina Hiseq 4000).

Protein-protein interaction network construction

Similar genes that have a similar expression pattern with SAA1 in HCC were obtained from GEPIA. The top 300 similar genes were subjected to protein-protein interaction (PPI) analysis in Metascape[25].

Statistical analysis

The data were shown as mean ± standard deviation, and the difference between the two groups was determined by student's *t*-test. The correlation analysis was assessed by the Spearman method. The log-rank method was used to perform survival analysis. P value < 0.05 was considered a significant statistical difference.

RESULTS

SAA1 was downregulated in HCC and predicted the favorable prognosis for HCC patients

SAA1 as an acute-phase protein, which was reported to be involved in the regulation of pro-inflammation or anti-inflammation signaling, is controversial[4,26]. Furthermore, the expression of SAA1 in HCC was also unclear. Firstly, we evaluated the expression of SAA1 in HCC and found that SAA1 expression was decreased in liver tumor tissues compared with normal liver tissues (Figure 1A). Then, to determine the clinical significance of the downregulated SAA1 in HCC, we conducted survival analysis. As shown in Figure 1B-D, the patients with lower SAA1 showed poorer survival rates from OS, PFS, and RFS analysis. In detail, the median survival time of HCC patients with low SAA1 expression was significantly shorter than those with high SAA1 expression (OS: 33.5 mo *vs* 70.5 mo; PFS: 11.33 mo *vs* 29.3 mo; DSS: 81.87 mo *vs* 84.83 mo; RFS: 11.97 mo *vs* 34.4 mo). The Cox proportional hazards model also showed favorable prognosis of low SAA1 expression, and the hazard ratio value with 95% confidence interval (CI) of low SAA1 expression in OS, PFS, DSS, and RFS was 0.6 (0.43-0.85), 0.59 (0.43-0.81), 0.59 (0.37-0.91), 0.58 (0.41-0.83) respectively (Table 1). These results demonstrated that the decreased level of SAA1 in HCC could serve as a good prognostic biomarker for HCC patients.

SAA1 is closely involved in the development of HCC

SAA1 expression is downregulated in the liver tumor tissues, as above demonstrated, and the clinical significance of SAA1 in survival time was also confirmed, as shown in Figure 1. To understand further the expression of SAA1 in the development of HCC, we analyzed SAA1 expression in some clinical features, such as tumor grade, patient disease stage, and the TP53 mutation or not. As shown in Figure 2A, SAA expression was further decreased with the increase of tumor grade. Similarly, SAA1 expression was also decreased with increased patient disease stage (Figure 2B), suggesting that SAA1 was closely involved in the progression of HCC. Moreover, TP53 mutation is an important risk factor contributing to the poor prognosis in HCC[27]. Thus, this study included the TP53 mutation in the analysis of SAA1 in HCC, suggesting interestingly that SAA1 expression was further decreased in tumor tissues with TP53 mutation than those without TP53 mutation (Figure 2C). The correlation analysis between SAA1

Table 1 The survival analysis based on the serum amyloid A1 expression

Survival analysis	Median time in mo		HR (95%CI)	*P* value
	SAA1 high	SAA1 low		
OS	70.5	33.5	0.6 (0.43-0.85)	0.004
PFS	29.3	11.33	0.59 (0.43-0.81)	0.00091
DSS	84.73	81.87	0.59 (0.37-0.91	0.017
RFS	34.4	11.97	0.58 (0.41-0.83)	0.0021

SAA1: Serum amyloid A1; OS: Overall survival; PFS: Progression-free survival; DSS: Disease-specific survival; RFS: Recurrence-free survival.

expression and the frequency of TP53 mutation also showed that lower SAA1 expression was accompanied by the high incidence of TP53 mutation ($P < 0.05$, Figure 2D).

SAA1 is a specific prognostic marker for HCC patients without hepatitis virus infection

As shown in Figure 1, SAA1 could be a favorable prognostic biomarker for HCC. Considering the importance of SAA1 in the regulation of inflammation and the interaction between hepatitis virus infection and tumor in HCC, we evaluated the potential application of SAA1 as a prognostic biomarker in HCC patients with and without hepatitis virus infection. The patients with high SAA1 presented with a good possibility to survive in OS, PFS, and RFS analysis (Figure 3). On the contrary, there was no significant difference in the HCC patients with hepatitis virus infection (Figure 3D-F), suggesting that hepatitis virus infection could affect the value of SAA1 in the prediction of HCC prognosis.

SAA1 expression is closely associated with immune infiltration in HCC

SAA1 was downregulated in HCC, and the decreased SAA1 expression could predict the poor prognosis of HCC patients, especially in patients without hepatitis virus infection (Figure 3). However, there was no statistical significance in those patients with hepatitis virus infection. As an inflammation-responsive gene, some reports confirmed the expression difference of SAA1 in the physiological response, and the hepatitis virus infection was the most important driving factor in the development of HCC. Thus, it was easy to understand the difference of SAA1 as a prognosis factor in HCC patients with and without hepatitis virus infection.

As attention increases regarding immune regulation in the development of HCC, we further evaluated the importance of SAA1 in the tumor immunomodulation. Firstly, the correlation of SAA1 expression and tumor purity was analyzed, and the negative correlation between SAA1 and tumor purity was confirmed (Figure 4A), which was also consistent with the downregulated SAA1 expression in HCC (as mentioned in Figure 1). Moreover, the CIBERSORT method was applied to evaluate the correlation between SAA1 and immune score. The results showed a significant positive correlation ($P < 4.93 \times 10^{-11}$, Figure 4B), suggesting that the lower expression of SAA1 in HCC was followed with a low immune score. Next, this study analyzed the correlation between SAA1 and 27 kinds of tumor-infiltrating lymphocytes (TILs) across human pan-cancers. As shown in Figure 4C, SAA1 expression was widely positively correlated with TILs in many human cancer types, especially in bladder urothelial carcinoma, glioblastoma multiforme, kidney chromophobe, kidney renal papillary cell carcinoma, testicular germ cell tumor, and thyroid carcinoma. The positive correlation between SAA1 expression and TILs was also observed in LIHC. SAA1 was remarkably correlated with the abundance of activated CD8 T cells ($r = 0.292$, $P = 1.12 \times 10^{-8}$, Figure 5A), natural killer (NK) cells ($r = 0.289$, $P = 1.48 \times 10^{-8}$, Figure 5B), natural killer T (NKT) cells ($r = 0.324$, $P = 1.87 \times 10^{-10}$, Figure 5C), T helper (Th)1 cells ($r = 0.424$, $P = 2.2 \times 10^{-16}$, Figure 5D), and Th17 cells ($r = 0.251$, $P = 9.46 \times 10^{-7}$, Figure 5F), but there was no significant correlation between SAA1 and the abundance of Th2 cells ($P = 0.619$, Figure 5E).

Decreased SAA1 is closely associated with the immune tolerance of HCC

The decreased SAA1 expression was followed by lower immune score, especially with the lower cytotoxic T cell infiltration in the HCC, suggesting that SAA1 might

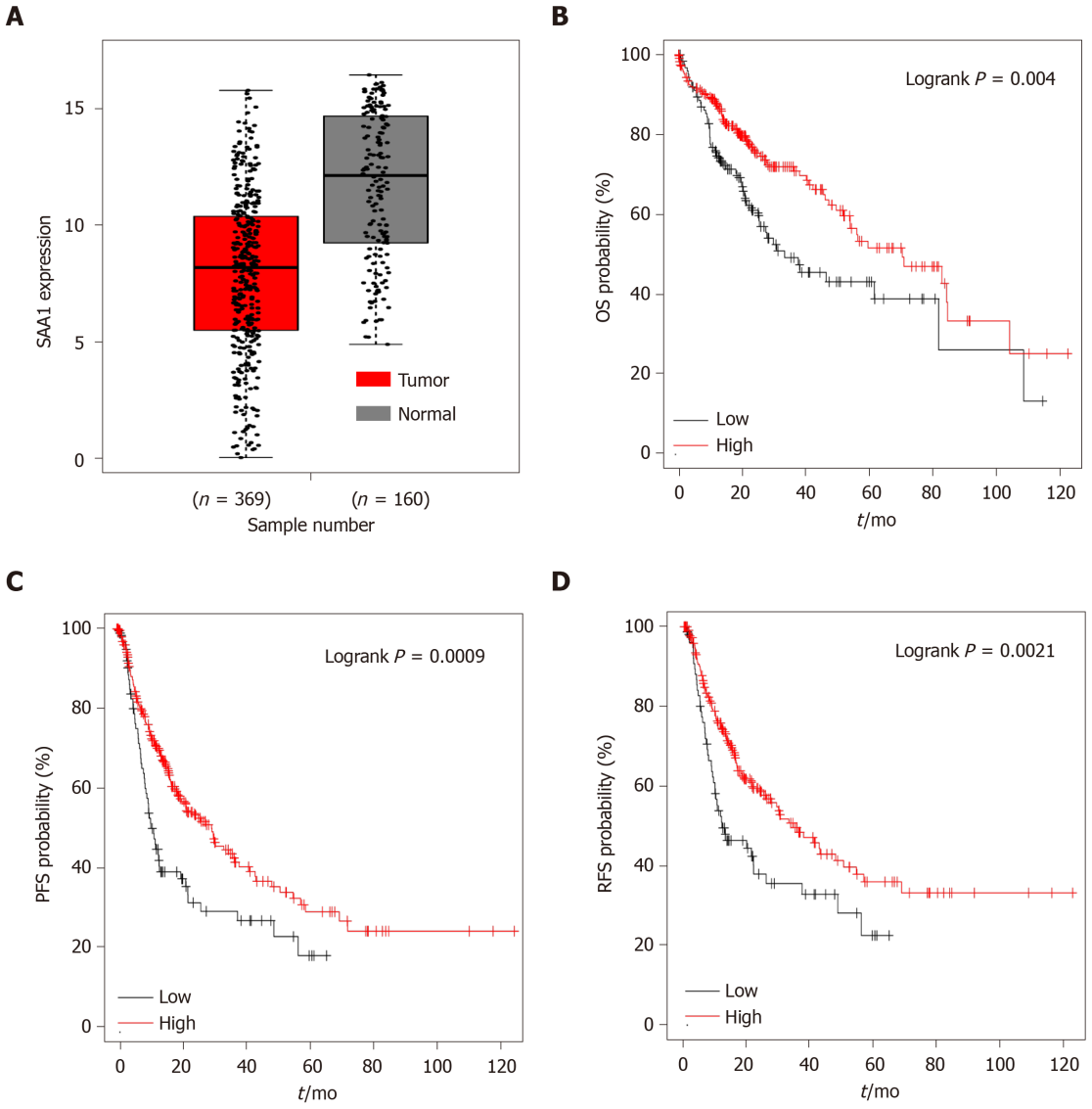

Figure 1 Serum amyloid A1 expression in hepatocellular carcinoma tumor and surrounding non-tumor or genotype-tissue expression liver tissues and its effect on the survival rate of hepatocellular carcinoma patients. A: A total of 160 hepatocellular carcinoma (HCC) tumor samples and 369 normal liver tissues were included to evaluate the serum amyloid A1 (SAA1) transcript expression level. Normal liver tissues are comprised of surrounding non-tumor and genotype-tissue expression liver tissues; B: HCC patients were divided into two groups based on the SAA1 expression level, and conducted the overall survival (OS); C: Progression-free survival (PFS); D: Recurrence-free survival analysis (RFS). The log-rank *P* value was subjected to evaluate the statistical difference.

contribute to the immune tolerance of HCC. To explain the hypothesis, the GSE125336 dataset was included, and the data showed that SAA1 expression was decreased in the patient group resistant to anti-PD1 therapy than those responsive to anti-PD1 therapy (Figure 6A). The GSEA was included to evaluate the significant pathways of SAA1 in LIHC. The results showed that the most enriched pathways related to decreased SAA1 included cytokine-cytokine receptor interaction (NES = -2.43, Figure 6B), NK cell-mediated cytotoxicity (NES = -2.15, Figure 6C), and antigen processing and presentation (NES = -2.08, Figure 6D).

Two signature genes associated with SAA1 were identified as favorable for prognosis of HCC

The gene enrichment analysis showed that higher SAA1 was enriched in the anti-tumor immunity pathways, including cytokine-cytokine receptor interaction, NK cell-mediated cytotoxicity, and antigen processing and presentation (Figure 6). High SAA1 predicted the favorable prognosis for HCC patients. To evaluate further the importance of SAA1 in the prognosis of HCC, we first conceived the similar genes of SAA1, which were analyzed with PPI analysis. As Figure 7A shows, SAA1 closely interacted with CXCL2, CCL23, and C5AR1. To determine the role of the three

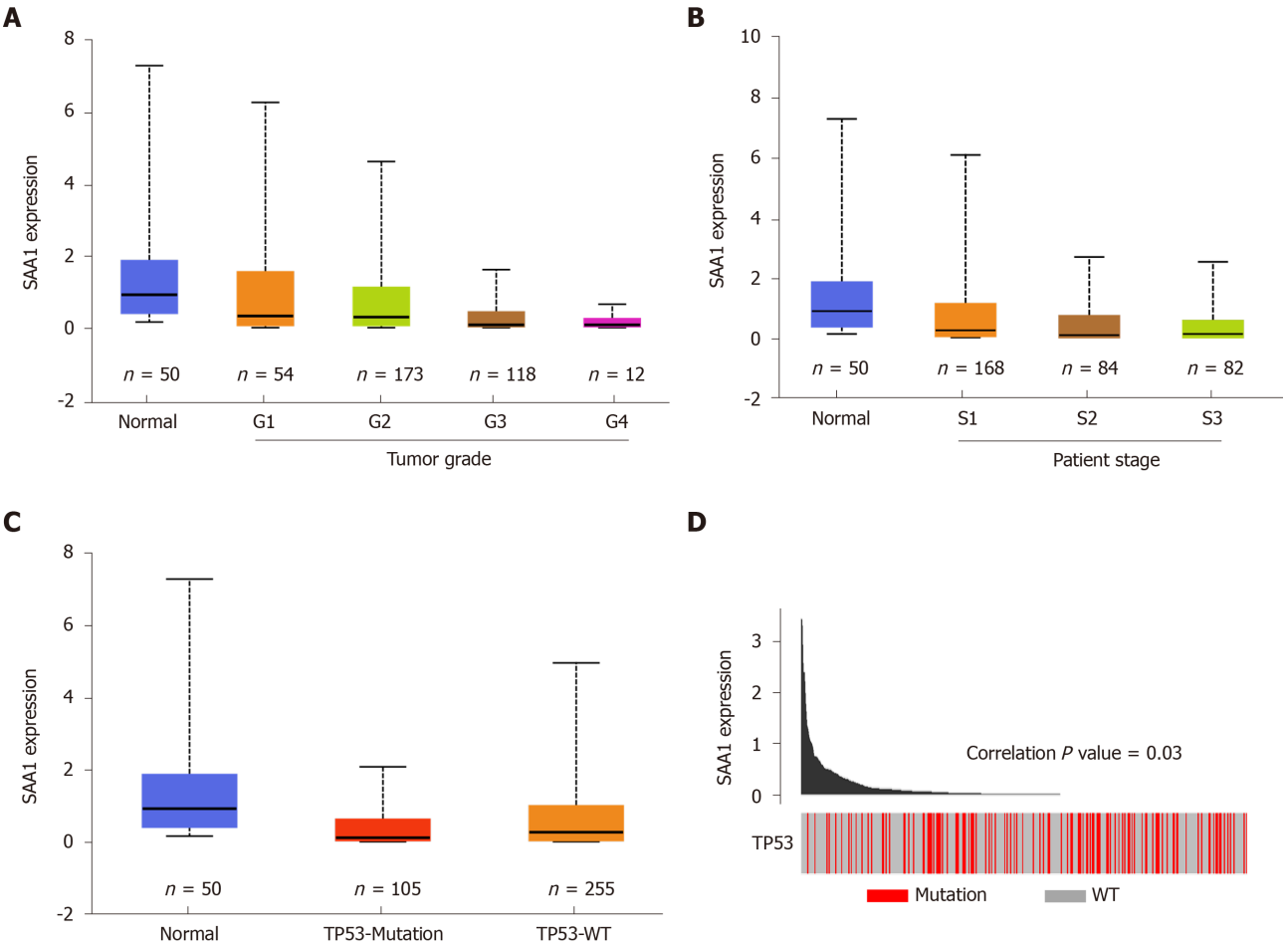

Figure 2 Serum amyloid A1 expression was correlated with hepatocellular carcinoma development. A: The tumor tissues with different grades and surrounding non-tumor tissues were included to analyze the serum amyloid A1 (SAA1) expression; B: The tumor tissues with different disease stage and non-tumor tissues were conducted with the SAA1 expression analysis; C: The SAA1 expression was analyzed in tumor tissues with TP53 mutation or wild type, the non-tumor tissues were used as control; D: The correlation of SAA1 expression and the TP53 mutation was analyzed in the cancer genome atlas portal. SAA1: Serum amyloid A1; WT: Wild type; G1: Tumor grade 1; G2: Tumor grade 2; G3: Tumor grade 3; G4: Tumor grade 4; S1: Patient disease stage 1; S2: Patient disease stage 2; S3: Patient disease stage 3.

associated genes in HCC, their expression levels were assessed (Figure 7B). CXCL2, CCL23, and C5AR1 were all decreased in HCC, which was similar to SAA1. Furthermore, the results of the overall survival analysis of the three genes are presented in Figure 7C and show that higher CXCL2 or CCL23 predicted better survival time. However, there was no clinical value of C5AR1 in the prediction of prognosis for HCC. Taken together, these results indicated that CXCL2 and CCL23, as an interacted protein of SAA1, could be complementary prognostic biomarkers for HCC patients.

DISCUSSION

SAA1, as the most important preproprotein of SAA, is an acute-phase protein involved in viral and bacterial infection, autoimmune disease, and some tumor pathogenesis[28]. To date, most SAA1 research focuses on its application as a disease marker. As an inflammation-related gene, SAA1 has been reported as a biomarker for the detection of stroke, ankylosing spondylitis, and acute aortic and acute hepatic injury[29-31]. However, whether SAA1 exerts * pro-inflammatory or anti-inflammatory role is still controversial. Lee *et al*[4] reported that SAA1 protein could promote inflammatory intestinal disease by inducing pro-inflammatory Th17 cell differentiation[4]. On the contrary, Cheng *et al*[26] identified that SAA1 could decrease lipopolysaccharide (LPS)-induced intestinal inflammation by directly binding to LPS to form a complex and induce LPS clearance by macrophage.

Similar to the inflammatory disease, the biological functions of SAA1 in tumors are

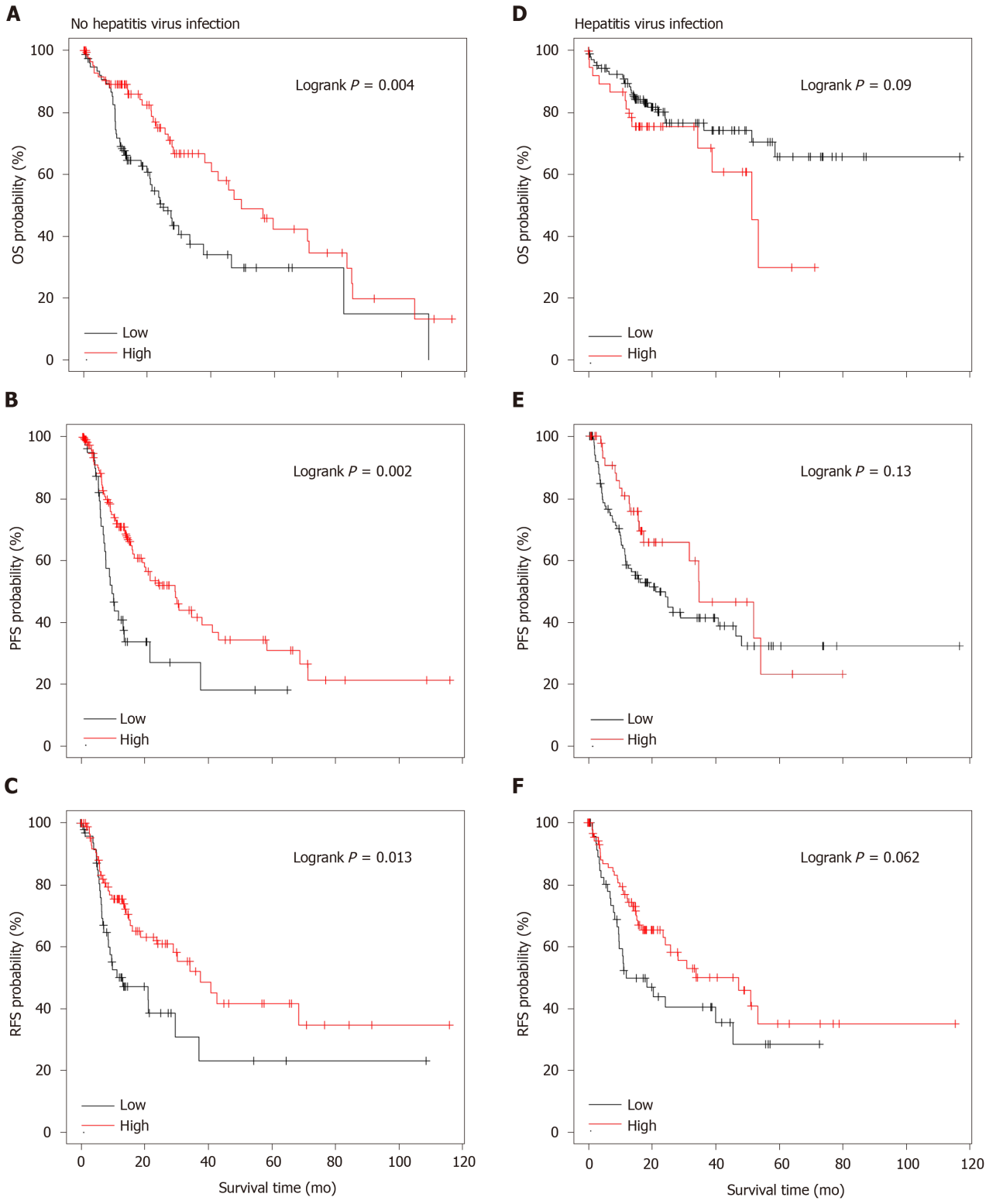

Figure 3 Serum amyloid A1 expression was a specific prognostic biomarker for hepatocellular carcinoma. A: The patients without hepatitis virus infection were subjected to overall survival (OS); B: Progression-free survival (PFS); C: Recurrence-free survival (RFS) analysis based on SAA1 expression level; D: The patients with hepatitis virus infection were subjected to OS; E: PFS; F: RFS analysis based on SAA1 expression level.

different. SAA1 was reported to be overexpressed in ovarian and renal cell carcinoma[32,33]; and serum SAA1 expression is positively correlated with the development of melanoma. Besides, SAA1 induced interleukin-10 production in neutrophils from melanoma patients, suggesting that SAA1 is a negative prognostic marker in melanoma[34]. In HCC, SAA1 was identified as the hub gene in the PPI analysis of differentially expressed genes[35], with unclear expression.

Hence, this study aimed to evaluate the expression of SAA1 and its clinical

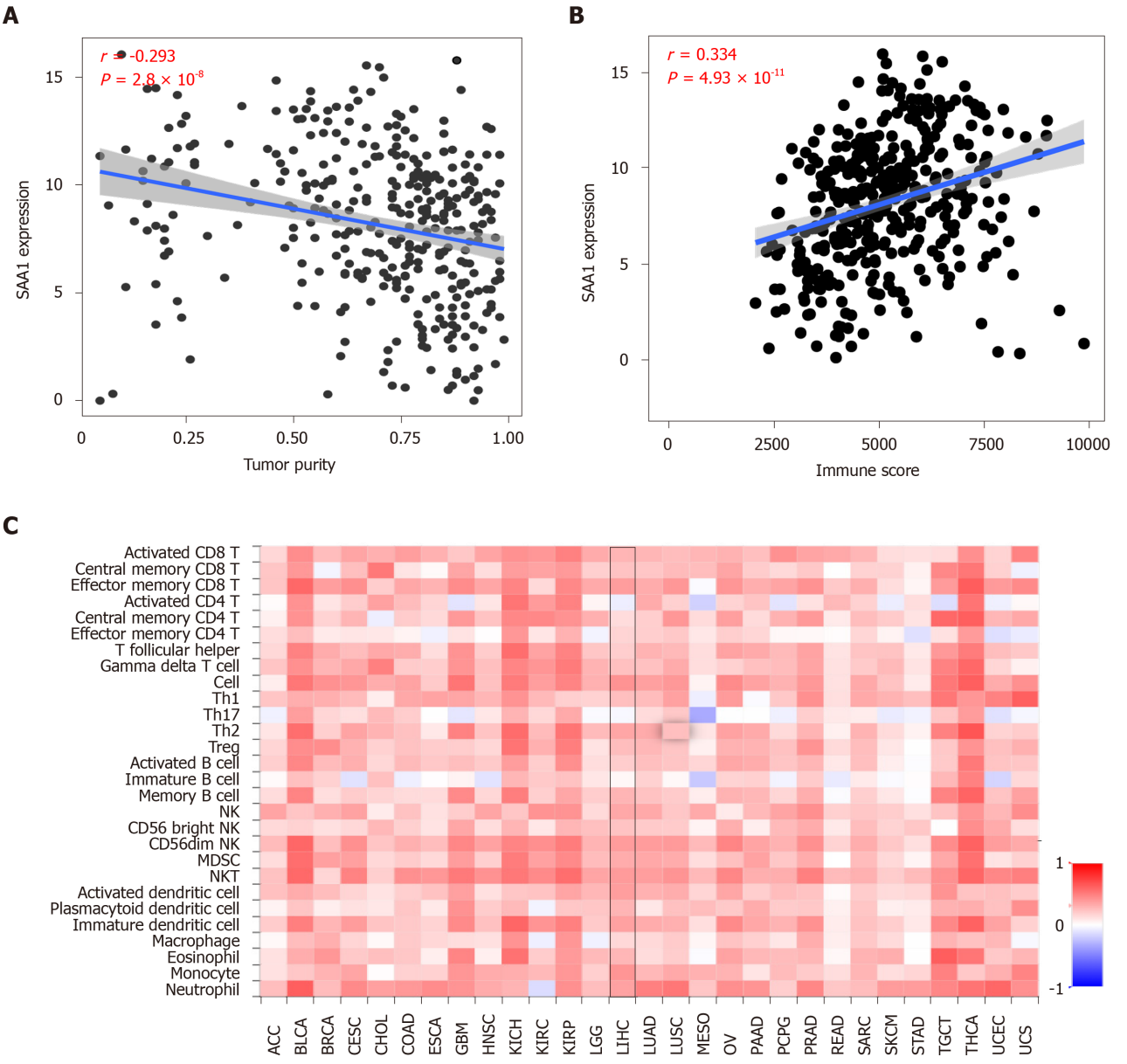

Figure 4 Serum amyloid A1 expression was correlated with immune infiltration in hepatocellular carcinoma. A: The correlation between serum amyloid A1 (SAA1) expression level and the tumor purity was analyzed with CIBERSORT; B: The correlation between SAA1 expression and the immune score was analyzed with CIBERSORT; C: The correlation between SAA1 expression and tumor-infiltrating lymphocytes across human cancer was conducted in TISIDB with Spearman method. SAA1: Serum amyloid A1; TILs: Tumor-infiltrating lymphocytes; NK: Natural killer cell; NKT: Natural killer T cell; ACC: Adrenocortical carcinoma; BLCA: Bladder Urothelial Carcinoma; BRCA: Breast invasive carcinoma; CESC: Cervical squamous cell carcinoma and endocervical adenocarcinoma; CHOL: Cholangiocarcinoma; COAD: Colon adenocarcinoma; ESCA: Esophageal carcinoma; GBM: Glioblastoma multiforme; HNSC: Head and Neck squamous cell carcinoma; KICH: Kidney chromophobe; KIRC: Kidney renal clear cell carcinoma; KIRP: Kidney renal papillary cell carcinoma; LGG: Brain lower-grade glioma; LIHC: Liver hepatocellular carcinoma; LUAD: Lung adenocarcinoma; LUSC: Lung squamous cell carcinoma; MESO: Mesothelioma; OV: Ovarian serous cystadenocarcinoma; PAAD: Pancreatic adenocarcinoma; PCPG: Pheochromocytoma and paraganglioma; PRAD: Prostate adenocarcinoma; READ: Rectum adenocarcinoma; SARC: Sarcoma; SKCM: Skin cutaneous melanoma; STAD: Stomach adenocarcinoma; TGCT: Testicular germ cell tumors; THCA: Thyroid carcinoma; UCEC: Uterine corpus endometrial carcinoma; UCS: Uterine carcinosarcoma.

significance in HCC. Firstly, we confirmed the downregulated expression of SAA1 in HCC tumor tissues (Figure 1A). The correlation analysis between SAA1 expression and tumor purity further confirmed its decreased expression in HCC tumor tissues (Figure 4A). Moreover, SAA1 expression decreased with increased tumor grade and disease stage (Figure 2A and B); and the lower SAA1 expression was accompanied with the higher frequency of TP53 mutation (Figure 2C and D), a marker of poor prognosis in HCC. The above results suggested that decreased SAA1 expression was closely involved in the progression of HCC. In the further study of clinical significance, the effect of SAA1 on the survival rate revealed that the lower SAA1 expression in HCC predicted worse survival time (Figure 1B-D), especially in HCC patients without hepatitis virus infection (Figure 3).

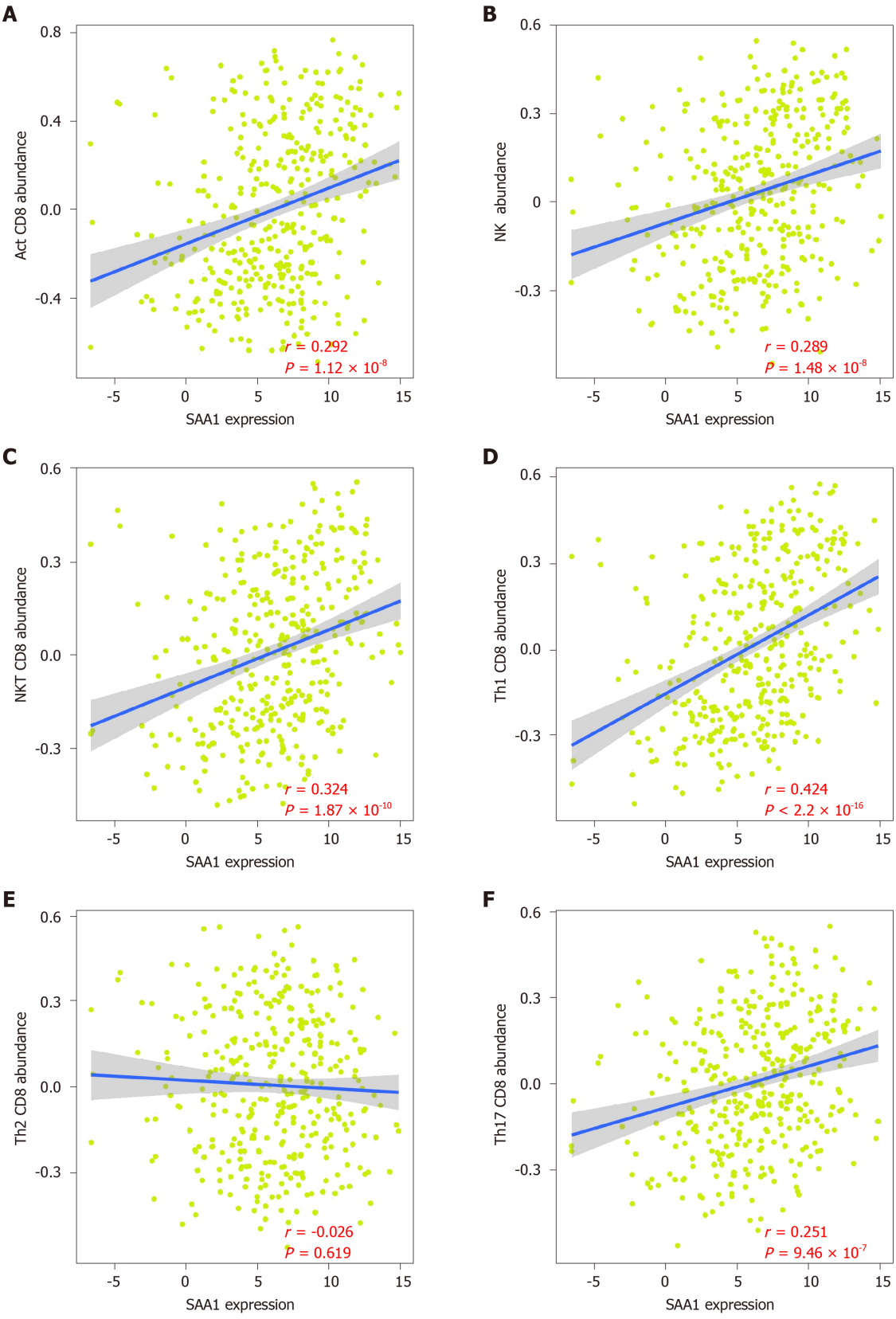

Figure 5 The association between serum amyloid A1 expression and immune cell abundance in hepatocellular carcinoma. A: A total of 373 hepatocellular carcinoma samples were included to analyze the correlation between SAA1 expression and activated CD8 T cell; B: Natural killer (NK) cell; C: Natural killer T (NKT) cell; D: Th1; E: Th2; F: Th17 cells abundance. SAA1: Serum amyloid A1.

Considering the induction of SAA1 in hepatitis by virus infection or tissue injury, the hepatitis virus infection-induced SAA1 expression could interfere with the prognostic value of SAA1 in HCC. This data also indicated that the immune signaling pathways might be closely associated with SAA1-mediated HCC progression.

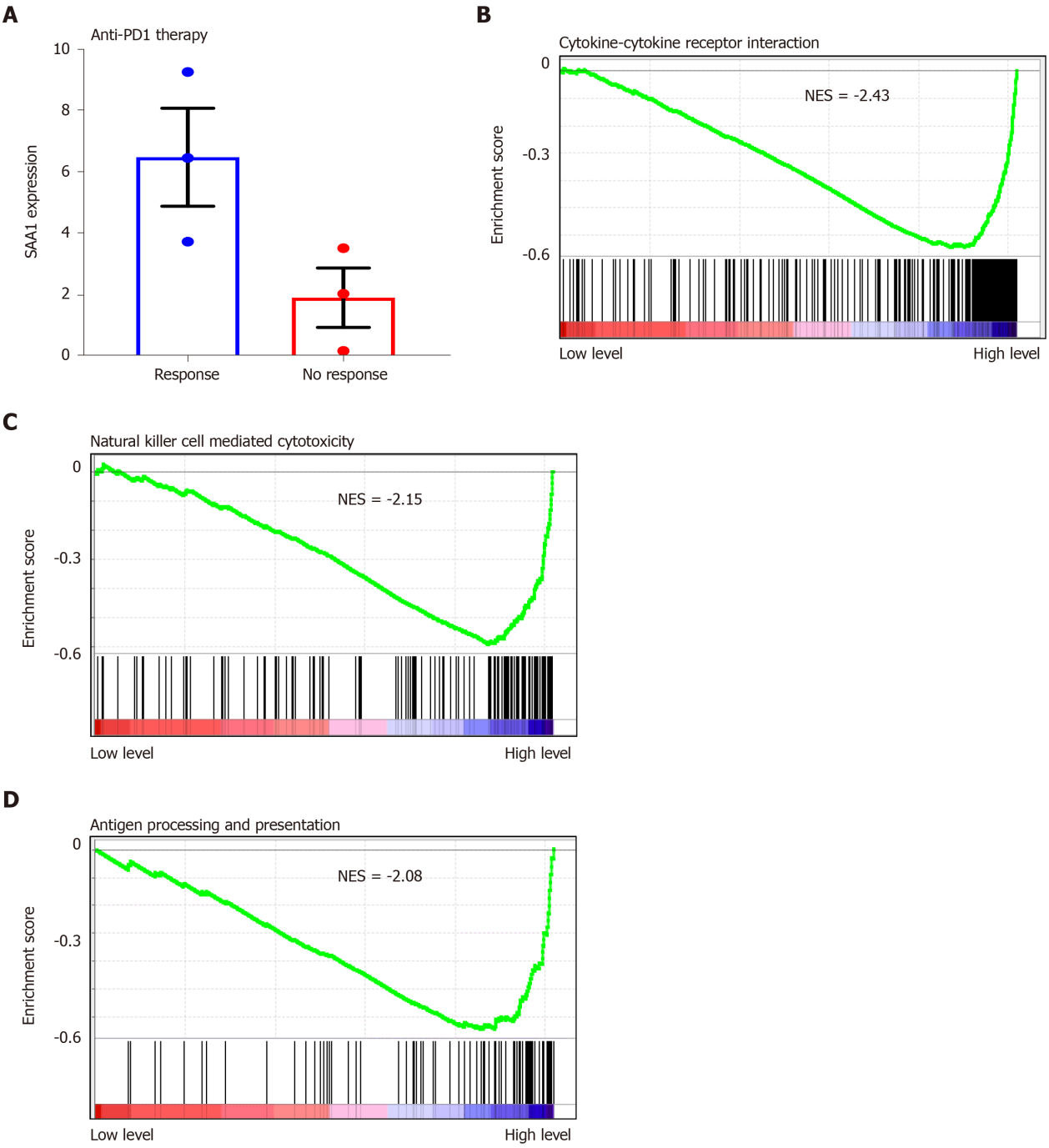

Figure 6 Low serum amyloid A1 expression was negatively correlated with the anti-immunity signaling. A: GSE125336 was used to evaluate the serum amyloid A1 expression in patients who were responsive and resistant to the anti-PD1 antibody; B-D: The gene set enrichment analysis in hepatocellular carcinoma revealed the top three pathways with KEGG. SAA1: Serum amyloid A1; NES: Normalized enrichment score; GSEA: Gene set enrichment analysis.

Interestingly, the immune infiltrating analysis showed that lower SAA1 expression represented lower immune score and immune cells infiltration (Figure 4B and C), especially in the cytotoxic T cells and anti-tumor associated immune cells, including activated CD8 T, NK, NKT, Th1, and Th17 cells (Figure 5). In the exploration of potential molecular mechanisms, the lower SAA1 might contribute to immune tolerance (Figure 6), which could be a potential therapeutic target for enhanced anti-tumor immunity. More significantly, this study also identified two signature genes that interacted with SAA1 as compensative prognostic biomarkers (Figure 7), which could enhance the prognostic value of SAA1 in HCC.

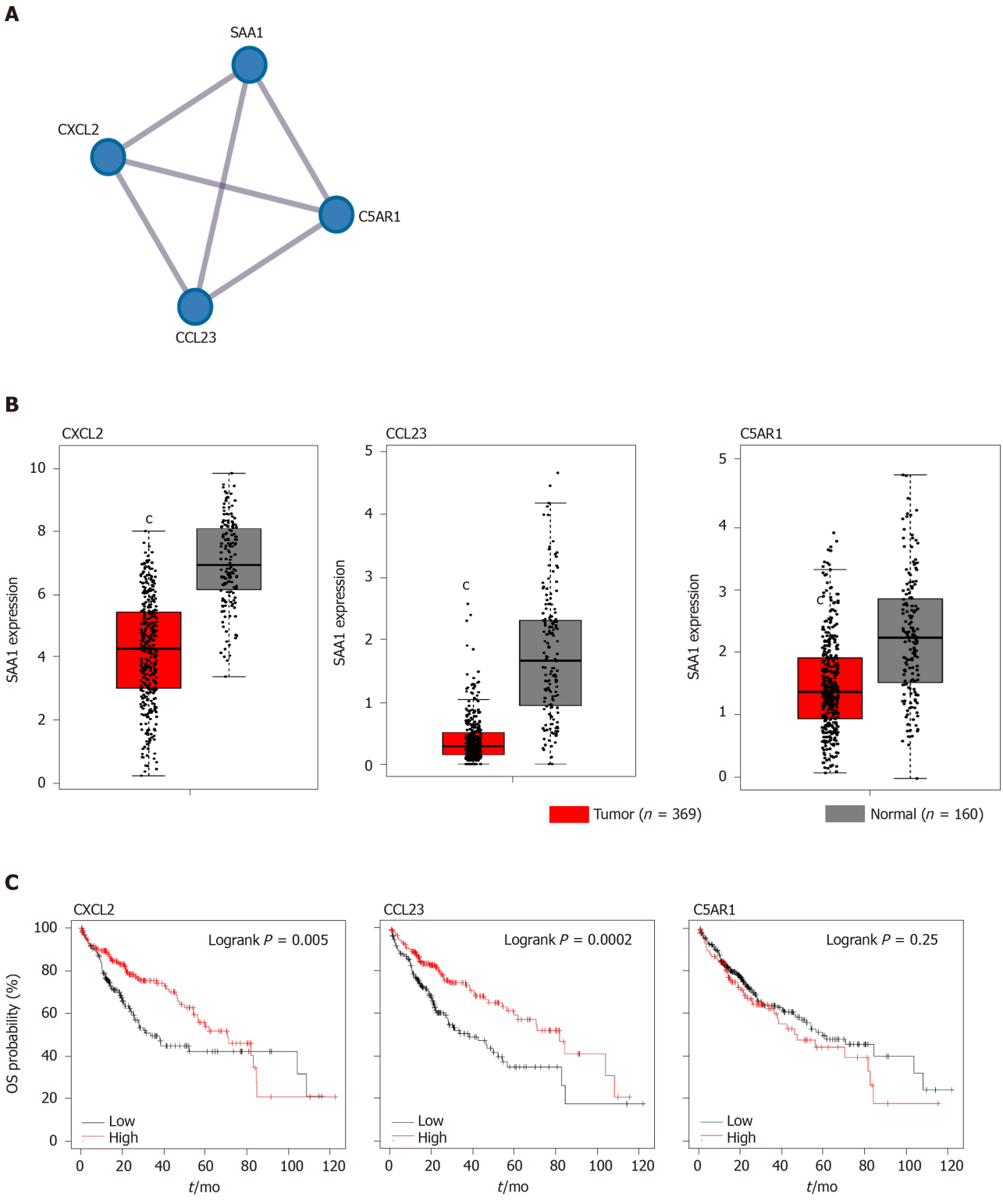

Figure 7 The two signature genes interacted with serum amyloid A1 and acted as a prognostic marker for hepatocellular carcinoma. A: The similar genes of serum amyloid A1 were achieved in GEPIA, and the similar genes were conducted in protein-protein interaction analysis; B: The expression of CXCL12, CCL23, and C5AR1 in hepatocellular carcinoma and non-tumor tissues were analyzed in GEPIA portal; C: The overall survival analysis was conducted based on the expression level of CXCL12, CCL23, and C5AR1. SAA1: Serum amyloid A1; OS: Overall survival; CXCL2: C-X-C motif chemokine ligand 2; CCL23: C-C motif chemokine ligand 23; C5AR1: Complement C5a receptor 1.

CONCLUSION

In summary, this study identified the downregulated expression of SAA1 as a potential prognostic biomarker for HCC, and decreased SAA1 was closely associated with immune tolerance signaling pathways. SAA1 could be an encouraging drug target for anti-tumor immunity. More experiments should be conceived to confirm the

significance of SAA1 in HCC immunotherapy.

ARTICLE HIGHLIGHTS

Research background

Serum amyloid A1 (SAA1) is regarded as an important regulator in the immune network. Recently, SAA1 was reported to regulate the development of some cancers, and it may function as a biomarker for some cancers.

Research motivation

SAA1 is a potential biomarker in some cancers, but its expression and function in hepatocellular carcinoma (HCC) are still unclear.

Research objectives

The project was designed to determine the expression level of SAA1 in HCC and to analyze the association between SAA1 expression and prognosis of HCC patient and its potential regulation on the immune network.

Research methods

GEPIA web-based analytical tool was subjected to evaluate the expression of SAA1 in HCC. The patients from The Cancer Genome Atlas-Liver Hepatocellular Carcinoma (TCGA-LIHC) were sub-grouped according to the median expression level of SAA1. Then, the Kaplan-Meier portal was used to analyze the survival curve of the high or low SAA1 expression groups. UALCAN tool was used to evaluate the expression of SAA1 in different tumor grades, stages, and TP53 mutation or not. The CIBERSORT method was subjected to test the correlation between SAA1 expression and immune infiltration score in HCC. TISIDB integrated portal was conducted to reveal the association between SAA1 level and the tumor-infiltrating lymphocytes. GSE125336 dataset was subjected to analyze the SAA1 level according to the anti-PD1 response. Gene set enrichment analysis method was subjected to analyze the enriched signaling pathways based on SAA1 in HCC. The co-expression genes of SAA1 was subjected to Metascape to evaluate the hub genes. These hub genes were subjected to GEPIA and Kaplan-Meier to analyze the expression and overall survival.

Research results

SAA1 level was downregulated in the liver tumor, and the lower expression could function as a prognostic biomarker in overall survival, progression-free survival, and disease-specific survival of HCC. Besides, the SAA1 expression level was closely associated with tumor grades and patient stages. More interestingly, the HCC patients with TP53 mutation showed a lower expression of SAA1. SAA1 could act as a good prognostic marker in HCC patients without hepatitis infection. SAA1 expression was positively correlated with the immune infiltration score and tumor-infiltrating lymphocytes. Low SAA1 expression was negatively correlated with anti-immune signaling, including cytokine-cytokine receptor interaction, natural killer cell-mediated cytotoxicity, and antigen processing and presentation. CXCL2 and CCL23 were identified as the hub genes that interacted with SAA1 and acted as prognostic markers for HCC.

Research conclusions

SAA1 expression is low in HCC, and its expression is closely associated with the progression of HCC. Besides, SAA1 can act as a poor prognostic biomarker for HCC patients. More interestingly, SAA1 is closely involved in the regulation of the immune infiltrating process.

Research perspectives

In this study, SAA1 was identified as a negative regulator for HCC, and its expression might be a poor prognostic biomarker for HCC patients. Interestingly, the SAA1 expression was closely related to the tumor-infiltrating immune cells network. However, these findings were based on the expression levels. SAA1 is a secreted protein from the liver, and the secreted levels could be much more practical clinically, especially in the prognosis analysis.

REFERENCES

1 **Kuret T**, Sodin-Šemrl S, Mrak-Poljšak K, Čučnik S, Lakota K, Erman A. Interleukin-1β Induces Intracellular Serum Amyloid A1 Expression in Human Coronary Artery Endothelial Cells and Promotes its Intercellular Exchange. *Inflammation* 2019; **42**: 1413-1425 [PMID: 31011929 DOI: 10.1007/s10753-019-01003-3]

2 **Sano T**, Huang W, Hall JA, Yang Y, Chen A, Gavzy SJ, Lee JY, Ziel JW, Miraldi ER, Domingos AI, Bonneau R, Littman DR. An IL-23R/IL-22 Circuit Regulates Epithelial Serum Amyloid A to Promote Local Effector Th17 Responses. *Cell* 2015; **163**: 381-393 [PMID: 26411290 DOI: 10.1016/j.cell.2015.08.061]

3 **Kovacevic A**, Hammer A, Stadelmeyer E, Windischhofer W, Sundl M, Ray A, Schweighofer N, Friedl G, Windhager R, Sattler W, Malle E. Expression of serum amyloid A transcripts in human bone tissues, differentiated osteoblast-like stem cells and human osteosarcoma cell lines. *J Cell Biochem* 2008; **103**: 994-1004 [PMID: 17849429 DOI: 10.1002/jcb.21472]

4 **Lee JY**, Hall JA, Kroehling L, Wu L, Najar T, Nguyen HH, Lin WY, Yeung ST, Silva HM, Li D, Hine A, Loke P, Hudesman D, Martin JC, Kenigsberg E, Merad M, Khanna KM, Littman DR. Serum Amyloid A Proteins Induce Pathogenic Th17 Cells and Promote Inflammatory Disease. *Cell* 2020; **180**: 79-91.e16 [PMID: 31866067 DOI: 10.1016/j.cell.2019.11.026]

5 **D'Haens G**, Kelly O, Battat R, Silverberg MS, Laharie D, Louis E, Savarino E, Bodini G, Yarur A, Boland BS, Afif W, Li XJ, Hale M, Ho J, Kondragunta V, Huang B, Kuy C, Okada L, Hester KD, Bray KR, Mimms L, Jain A, Singh S, Collins A, Valasek MA, Sandborn WJ, Vermeire S, Dulai PS. Development and Validation of a Test to Monitor Endoscopic Activity in Patients With Crohn's Disease Based on Serum Levels of Proteins. *Gastroenterology* 2020; **158**: 515-526.e10 [PMID: 31711925 DOI: 10.1053/j.gastro.2019.10.034]

6 **Yamada T**, Okuda Y, Takasugi K, Itoh K, Igari J. Relative serum amyloid A (SAA) values: the influence of SAA1 genotypes and corticosteroid treatment in Japanese patients with rheumatoid arthritis. *Ann Rheum Dis* 2001; **60**: 124-127 [PMID: 11156544 DOI: 10.1136/ard.60.2.124]

7 **Wu DC**, Wang KY, Wang SSW, Huang CM, Lee YW, Chen MI, Chuang SA, Chen SH, Lu YW, Lin CC, Lee KW, Hsu WH, Wu KP, Chen YJ. Exploring the expression bar code of SAA variants for gastric cancer detection. *Proteomics* 2017; **17** [PMID: 28493537 DOI: 10.1002/pmic.201600356]

8 **Liang B**, Li C, Zhao J. Identification of key pathways and genes in colorectal cancer using bioinformatics analysis. *Med Oncol* 2016; **33**: 111 [PMID: 27581154 DOI: 10.1007/s12032-016-0829-6]

9 **Djurec M**, Graña O, Lee A, Troulé K, Espinet E, Cabras L, Navas C, Blasco MT, Martín-Díaz L, Burdiel M, Li J, Liu Z, Vallespinós M, Sanchez-Bueno F, Sprick MR, Trumpp A, Sainz B Jr, Al-Shahrour F, Rabadan R, Guerra C, Barbacid M. Saa3 is a key mediator of the protumorigenic properties of cancer-associated fibroblasts in pancreatic tumors. *Proc Natl Acad Sci USA* 2018; **115**: E1147-E1156 [PMID: 29351990 DOI: 10.1073/pnas.1717802115]

10 **Ignacio RMC**, Gibbs CR, Kim S, Lee ES, Adunyah SE, Son DS. Serum amyloid A predisposes inflammatory tumor microenvironment in triple negative breast cancer. *Oncotarget* 2019; **10**: 511-526 [PMID: 30728901 DOI: 10.18632/oncotarget.26566]

11 **Kluve-Beckerman B**, Dwulet FE, Benson MD. Human serum amyloid A. Three hepatic mRNAs and the corresponding proteins in one person. *J Clin Invest* 1988; **82**: 1670-1675 [PMID: 3183061 DOI: 10.1172/jci113779]

12 **Gu J**, Zhang X, Miao R, Ma X, Xiang X, Fu Y, Liu C, Niu W, Qu K. A three-long non-coding RNA-expression-based risk score system can better predict both overall and recurrence-free survival in patients with small hepatocellular carcinoma. *Aging (Albany NY)* 2018; **10**: 1627-1639 [PMID: 30018179 DOI: 10.18632/aging.101497]

13 **Nahon P**, Layese R, Bourcier V, Cagnot C, Marcellin P, Guyader D, Pol S, Larrey D, De Lédinghen V, Ouzan D, Zoulim F, Roulot D, Tran A, Bronowicki JP, Zarski JP, Riachi G, Calès P, Péron JM, Alric L, Bourlière M, Mathurin P, Blanc JF, Abergel A, Serfaty L, Mallat A, Grangé JD, Attali P, Bacq Y, Wartelle C, Dao T, Thabut D, Pilette C, Silvain C, Christidis C, Nguyen-Khac E, Bernard-Chabert B, Zucman D, Di Martino V, Sutton A, Roudot-Thoraval F, Audureau E; ANRS CO12 CirVir Group. Incidence of Hepatocellular Carcinoma After Direct Antiviral Therapy for HCV in Patients With Cirrhosis Included in Surveillance Programs. *Gastroenterology* 2018; **155**: 1436-1450.e6 [PMID: 30031138 DOI: 10.1053/j.gastro.2018.07.015]

14 **Gil-García AI**, Madejón A, Francisco-Recuero I, López-López A, Villafranca E, Romero M, García A, Olveira A, Mena R, Larrubia JR, García-Samaniego J. Prevalence of hepatocarcinoma-related hepatitis B virus mutants in patients in grey zone of treatment. *World J Gastroenterol* 2019; **25**: 5883-5896 [PMID: 31636479 DOI: 10.3748/wjg.v25.i38.5883]

15 **Baldan Ferrari G**, Coelho França Quintanilha J, Berlofa Visacri M, Oliveira Vaz C, Cursino MA, Sampaio Amaral L, Brito Bastos, Pereira TT, de Oliveira Guarnieri JP, de Godoy Torso N, Passos Lima CS, Moriel P. Outcomes in hepatocellular carcinoma patients undergoing sorafenib treatment: toxicities, cellular oxidative stress, treatment adherence, and quality of life. *Anticancer Drugs* 2020; **31**: 523-527 [PMID: 32107349 DOI: 10.1097/CAD.0000000000000902]

16 **De Mattia E**, Cecchin E, Guardascione M, Foltran L, Di Raimo T, Angelini F, D'Andrea M, Toffoli G. Pharmacogenetics of the systemic treatment in advanced hepatocellular carcinoma. *World J Gastroenterol* 2019; **25**: 3870-3896 [PMID: 31413525 DOI: 10.3748/wjg.v25.i29.3870]

17 **Wang ZX**, Li J, Wang EX, Xia DD, Bai W, Wang QH, Yuan J, Li XM, Niu J, Yin ZX, Xia JL, Fan DM, Han GH. Validation of the six-and-twelve criteria among patients with hepatocellular carcinoma and performance score 1 receiving transarterial chemoembolization. *World J Gastroenterol* 2020; **26**: 1805-1819 [PMID: 32351295 DOI: 10.3748/wjg.v26.i15.1805]

18 **Voutsadakis IA**. PD-1 inhibitors monotherapy in hepatocellular carcinoma: Meta-analysis and systematic review. *Hepatobiliary Pancreat Dis Int* 2019; **18**: 505-510 [PMID: 31551142 DOI: 10.1016/j.hbpd.2019.09.007]

19 **Tang Z**, Li C, Kang B, Gao G, Li C, Zhang Z. GEPIA: a web server for cancer and normal gene expression profiling and interactive analyses. *Nucleic Acids Res* 2017; **45**: W98-W102 [PMID: 28407145 DOI:

10.1093/nar/gkx247]
20 **Chandrashekar DS**, Bashel B, Balasubramanya SAH, Creighton CJ, Ponce-Rodriguez I, Chakravarthi BVSK, Varambally S. UALCAN: A Portal for Facilitating Tumor Subgroup Gene Expression and Survival Analyses. *Neoplasia* 2017; **19**: 649-658 [PMID: 28732212 DOI: 10.1016/j.neo.2017.05.002]
21 **Menyhárt O**, Nagy Á, Győrffy B. Determining consistent prognostic biomarkers of overall survival and vascular invasion in hepatocellular carcinoma. *R Soc Open Sci* 2018; **5**: 181006 [PMID: 30662724 DOI: 10.1098/rsos.181006]
22 **Li T**, Fan J, Wang B, Traugh N, Chen Q, Liu JS, Li B, Liu XS. TIMER: A Web Server for Comprehensive Analysis of Tumor-Infiltrating Immune Cells. *Cancer Res* 2017; **77**: e108-e110 [PMID: 29092952 DOI: 10.1158/0008-5472.CAN-17-0307]
23 **Ru B**, Wong CN, Tong Y, Zhong JY, Zhong SSW, Wu WC, Chu KC, Wong CY, Lau CY, Chen I, Chan NW, Zhang J. TISIDB: an integrated repository portal for tumor-immune system interactions. *Bioinformatics* 2019; **35**: 4200-4202 [PMID: 30903160 DOI: 10.1093/bioinformatics/btz210]
24 **Reimand J**, Isserlin R, Voisin V, Kucera M, Tannus-Lopes C, Rostamianfar A, Wadi L, Meyer M, Wong J, Xu C, Merico D, Bader GD. Pathway enrichment analysis and visualization of omics data using g:Profiler, GSEA, Cytoscape and EnrichmentMap. *Nat Protoc* 2019; **14**: 482-517 [PMID: 30664679 DOI: 10.1038/s41596-018-0103-9]
25 **Zhou Y**, Zhou B, Pache L, Chang M, Khodabakhshi AH, Tanaseichuk O, Benner C, Chanda SK. Metascape provides a biologist-oriented resource for the analysis of systems-level datasets. *Nat Commun* 2019; **10**: 1523 [PMID: 30944313 DOI: 10.1038/s41467-019-09234-6]
26 **Cheng N**, Liang Y, Du X, Ye RD. Serum amyloid A promotes LPS clearance and suppresses LPS-induced inflammation and tissue injury. *EMBO Rep* 2018; **19** [PMID: 30126923 DOI: 10.15252/embr.201745517]
27 **Ge PL**, Li SF, Wang WW, Li CB, Fu YB, Feng ZK, Li L, Zhang G, Gao ZQ, Dang XW, Wu Y. Prognostic values of immune scores and immune microenvironment-related genes for hepatocellular carcinoma. *Aging (Albany NY)* 2020; **12**: 5479-5499 [PMID: 32213661 DOI: 10.18632/aging.102971]
28 **Kramer HB**, Lavender KJ, Qin L, Stacey AR, Liu MK, di Gleria K, Simmons A, Gasper-Smith N, Haynes BF, McMichael AJ, Borrow P, Kessler BM. Elevation of intact and proteolytic fragments of acute phase proteins constitutes the earliest systemic antiviral response in HIV-1 infection. *PLoS Pathog* 2010; **6**: e1000893 [PMID: 20463814 DOI: 10.1371/journal.ppat.1000893]
29 **Shridas P**, De Beer MC, Webb NR. High-density lipoprotein inhibits serum amyloid A-mediated reactive oxygen species generation and NLRP3 inflammasome activation. *J Biol Chem* 2018; **293**: 13257-13269 [PMID: 29976759 DOI: 10.1074/jbc.RA118.002428]
30 **Zapata-Arriaza E**, Mancha F, Bustamante A, Moniche F, Pardo-Galiana B, Serrano-Gotarredona P, Navarro-Herrero S, Pallisa E, Faura J, Vega-Salvatierra Á, Penalba A, Escudero-Martínez I, Ramos-Herrero VD, Azurmendi L, Charles Sanchez J, Montaner J. Biomarkers predictive value for early diagnosis of Stroke-Associated Pneumonia. *Ann Clin Transl Neurol* 2019; **6**: 1882-1887 [PMID: 31365180 DOI: 10.1002/acn3.50849]
31 **Yuan ZY**, Zhang XX, Wu YJ, Zeng ZP, She WM, Chen SY, Zhang YQ, Guo JS. Serum amyloid A levels in patients with liver diseases. *World J Gastroenterol* 2019; **25**: 6440-6450 [PMID: 31798280 DOI: 10.3748/wjg.v25.i43.6440]
32 **Urieli-Shoval S**, Finci-Yeheskel Z, Dishon S, Galinsky D, Linke RP, Ariel I, Levin M, Ben-Shachar I, Prus D. Expression of serum amyloid a in human ovarian epithelial tumors: implication for a role in ovarian tumorigenesis. *J Histochem Cytochem* 2010; **58**: 1015-1023 [PMID: 20713982 DOI: 10.1369/jhc.2010.956821]
33 **Wood SL**, Rogers M, Cairns DA, Paul A, Thompson D, Vasudev NS, Selby PJ, Banks RE. Association of serum amyloid A protein and peptide fragments with prognosis in renal cancer. *Br J Cancer* 2010; **103**: 101-111 [PMID: 20531413 DOI: 10.1038/sj.bjc.6605720]
34 **De Santo C**, Arscott R, Booth S, Karydis I, Jones M, Asher R, Salio M, Middleton M, Cerundolo V. Invariant NKT cells modulate the suppressive activity of IL-10-secreting neutrophils differentiated with serum amyloid A. *Nat Immunol* 2010; **11**: 1039-1046 [PMID: 20890286 DOI: 10.1038/ni.1942]
35 **Zhang Y**, Wang S, Xiao J, Zhou H. Bioinformatics analysis to identify the key genes affecting the progression and prognosis of hepatocellular carcinoma. *Biosci Rep* 2019; **39** [PMID: 30705088 DOI: 10.1042/bsr20181845]

World Journal of Gastroenterology

Submit a Manuscript: https://www.f6publishing.com

World J Gastroenterol 2020 September 21; 26(35): 5302-5313

DOI: 10.3748/wjg.v26.i35.5302

ISSN 1007-9327 (print) ISSN 2219-2840 (online)

ORIGINAL ARTICLE

Retrospective Cohort Study

Epidemiology of perforating peptic ulcer: A population-based retrospective study over 40 years

Aydin Dadfar, Tom-Harald Edna

ORCID number: Aydin Dadfar 0000-0002-3869-9975; Tom-Harald Edna 0000-0002-9948-0627.

Author contributions: Dadfar A made substantial contributions to the conception and design of the study, acquisition, analysis, and interpretation of data, and drafting the article; Edna TH made substantial contributions to the conception and design of the study, acquisition, analysis, and interpretation of data, and drafting the article; all authors read and approved the final manuscript.

Institutional review board statement: This study was reviewed and approved by the Levanger Hospital Institutional Review Board Committee on Human Rights Related to Research Involving Human Subjects (2018/2760 – 33974/2018).

Informed consent statement: Not necessary according to the Regional Committee for Medical and Health Research Ethics (REC), Helse Midt (2018/1510).

Conflict-of-interest statement: The authors declare the absence of conflicts of interest.

Data sharing statement: No additional data are available.

Aydin Dadfar, Tom-Harald Edna, Department of Surgery, Levanger Hospital, Nord-Trøndelag Hospital Trust, Levanger 7600, Norway

Tom-Harald Edna, Institute of Clinical and Molecular Medicine, Norwegian University of Science and Technology, Trondheim 7491, Norway

Corresponding author: Aydin Dadfar, MD, Surgeon, Department of Surgery, Levanger Hospital, Nord-Trøndelag Hospital Trust, Kirkegata 2, Levanger 7600, Norway. aydindadfar@gmail.com

Abstract

BACKGROUND

The incidence of peptic ulcer disease has decreased during the last few decades, but the incidence of reported peptic ulcer complications has not decreased. Perforating peptic ulcer (PPU) is a severe form of the disease.

AIM

To assess trends in the incidence, presentation, and outcome of PPU over a period of 40 years.

METHODS

This was a single-centre, retrospective, cohort study of all patients admitted to Levanger Hospital, Norway, with PPU from 1978 to 2017. The patients were identified in the Patient Administrative System of the hospital using International Classification of Diseases (ICD), revision 8, ICD-9, and ICD-10 codes for perforated gastric and duodenal ulcers. We reviewed the medical records of the patients to retrieve data. Vital statistics were available for all patients. The incidence of PPU was analysed using Poisson regression with perforated ulcer as the dependent variable, and sex, age, and calendar year from 1978 to 2017 as covariates. Relative survival analysis was performed to compare long-term survival over the four decades.

RESULTS

Two hundred and nine patients were evaluated, including 113 (54%) men. Forty-six (22%) patients were older than 80 years. Median age increased from the first to the last decade (from 63 to 72 years). The incidence rate increased with increasing age, but we measured a decline in recent decades for both sexes. A significant increase in the use of acetylsalicylic acid, from 5% (2/38) to 18% (8/45), was

STROBE statement: The authors have read the STROBE Statement – checklist of items, and the manuscript was prepared and revised according to the STROBE Statement.

Manuscript source: Unsolicited manuscript

Received: March 24, 2020
Peer-review started: March 24, 2020
First decision: April 25, 2020
Revised: June 23, 2020
Accepted: August 29, 2020
Article in press: August 29, 2020
Published online: September 21, 2020

P-Reviewer: Zhu Y
S-Editor: Liu M
L-Editor: A
P-Editor: Ma YJ

observed during the study period. Comorbidity increased significantly over the 40 years of the study, with 22% (10/45) of the patients having an American Society of Anaesthesiologists (ASA) score 4-5 in the last decade, compared to 5% (2/38) in the first decade. Thirty-nine percent (81/209) of the patients had one or more postoperative complications. Both 100-day mortality and long-term survival were associated with ASA score, without significant variations between the decades.

CONCLUSION
Declining incidence rates occurred in recent years, but the patients were older and had more comorbidity. The ASA score was associated with both short-term mortality and long-term survival.

Key Words: Perforated peptic ulcer; American Society of Anaesthesiologists classification; Charlson Comorbidity Index; Gastric ulcer; Duodenal ulcer; Epidemiology; Incidence; Clavien-Dindo classification of complications; Mortality

Core Tip: We sought to review the epidemiology of perforated peptic ulcer in a stable population at a primary hospital over a period of 40 years. The incidence rate has declined in recent decades for both sexes, though median age and comorbidity have both increased. Complications occurred more frequently and were more serious in recent decades, in older patients, in patients with comorbidities, and in patients with higher American Society of Anaesthesiologists (ASA) scores. Both short- and long-term survival were associated with ASA score, without significant variation between the decades.

Citation: Dadfar A, Edna TH. Epidemiology of perforating peptic ulcer: A population-based retrospective study over 40 years. *World J Gastroenterol* 2020; 26(35): 5302-5313
URL: https://www.wjgnet.com/1007-9327/full/v26/i35/5302.htm
DOI: https://dx.doi.org/10.3748/wjg.v26.i35.5302

INTRODUCTION

The incidence of peptic ulcer disease (PUD), either gastric or duodenal, has decreased during the last few decades with the discovery of the role of *Helicobacter pylori (H. pylori)*[1-5]. However, the incidence of peptic ulcer complications has not decreased in the same manner[6,7]. Bleeding and perforation are the most severe complications of PUD[8]. Due to progress in endoscopic and interventional radiological techniques, bleeding is mostly considered a medical emergency and outcomes have improved[9]. Although bleeding is far more common than perforated peptic ulcer (PPU), perforation accounts for most deaths associated with PUD[6,10,11] and PPU remains a surgical emergency, with high short-term mortality of 10%-30%[12-14].

Surgical repair with closure of the perforation, with or without an omental pedicle, is the preferred treatment for PPU[11,15,16]. This repair can be achieved through either open repair or laparoscopy[15,17]. Previous studies have shown a change in the demography of PPU over the last few decades, with an increasing age at diagnosis in recent years[15,18]. Less is known about the implications of increased age in patients with PPU in regards to treatment, complications, and mortality[12,13,15,19].

Thus, the aim of this study was to investigate changes in demography and the effect on treatment, complications, and short- and long-term mortality in patients admitted to our hospital with PPU over four decades.

MATERIALS AND METHODS

Study population

Levanger Hospital is located in Middle Norway, with a catchment area of 85000 at the start of the study period and 100000 in recent years. This retrospective study included all patients diagnosed with benign PPU between January 1978 and December 2017.

The patients were identified in the Patient Administrative System using International Classification of Diseases (ICD), ICD-8 codes (531.00-531.09, 532.00, 533.00, 534.00), ICD-9 codes (531.1-531.2, 531.5-531.6, 532- 533 with same decimals as for 531), and ICD-10 codes (K25.1-K25.2, K25.5-K25.6, K26-K28 with same decimals as for K25). Additional searches were done for the surgical codes for gastroraphy and duodenoraphy. Demographic and clinical data were collected from the hospital records.

The American Society of Anaesthesiologists (ASA) score was used to compare preoperative comorbidity[20], which was further classified using the Charlson Comorbidity Index[21]. Complications were classified according to the Clavien-Dindo classification[22,23]: Grade I, any small deviation from the normal postoperative course treated at bedside or with certain drugs (*e.g.*, antiemetics); grade II, complications treated with transfusion or medicines other than allowed for grade 1 (*e.g.*, antibiotics); grade III, complications requiring endoscopic, radiological, or surgical intervention; grade IV, life-threatening complications; grade V, complications leading to death of the patient.

Definitions

The incidence of PPU was defined as the number of new cases of PPU in the defined population within 1 year. The incidence rate (IR) was defined as the incidence divided by the total person-time at risk during the same year. The incidence rate ratio (IRR) was defined as the ratio between two incidence rates.

Ulcer localisation was considered gastric when present anywhere in the stomach, including pyloric ulcers. Localisation distal to the pylorus was categorised as duodenal.

Study ethics

The study was approved by the Regional Ethics Committee (REK Midt # 2018/1510). We also performed a data protection impact assessment in accordance with the European General Data Protection Regulation before collecting data[24].

Statistical analysis

The medians of two samples, such as age in men compared to women, were compared by the Wilcoxon rank sum test. The Cochran-Armitage test was used to test for trends in proportions. The Joncheere-Terpstra test was used to test for the distribution of age as a dependent variable across decade groups as an independent variable. Ordinal logistic regression was used to test associations in doubly ordered r × c tables, such as for the Charlson Comorbidity Index and ASA score by decades. Logistic regression analysis was used to test for an association between 100-day mortality as a dependent variable and sex, age, year of admittance, Charlson Comorbidity Index, and ASA score as independent variables.

The incidence of PPU was analysed using Poisson regression with perforated ulcer as the dependent variable and sex, age in 5-year intervals (20-24, 25-29, up to 90-94, 95-99), and calendar year from 1978 to 2017 as covariates. Non-linear relationships were explored using fractional polynomials[25]. Fractional polynomials are a method for checking if the effect of an explanatory variable is linear, as in the basic Poisson regression model.

The age and sex distribution for the 10 municipalities around Levanger Hospital for every year from 1980 to 2016 was obtained from Statistics Norway. To study long-term survival in this patient population over 40 years, we performed the relative survival analysis using the Ederer II method[26,27]. Multivariable analyses were performed using the full likelihood approach. Survival probabilities by sex and age for the Norwegian population for every year from 1978 were downloaded from the Human Mortality Database[28].

Two-sided P values < 0.05 were considered significant. Medians were reported with the range (minimum to maximum) and standard deviation (SD), as well as 95% confidence intervals (CIs), as appropriate. Analyses were carried out in Stata 16 (Stata Corp LP, College Station, Texas, United States), IBM SPSS Statistics 25 (SPSS Inc., Chicago, IL, United States), and StatXact 9 (1050 Winter St, Waltham, MA, United States).

RESULTS

Patient characteristics

Over 40 years, 209 patients with PPU were treated, including 113 (54%) men and 46 (22%) patients older than 80 years. In the first two decades of the observation period, PPU occurred more frequently among men than women (ratio 3:2). In the last two decades, this has evened out to nearly 1:1. Eighty-five percent of the patients presented within 24 h after the onset of pain. Only 7 patients (3.3%) were admitted with a systolic blood pressure < 90 mmHg.

Trends in patient characteristics according to decade of treatment are shown in Table 1. The median age increased from 63 to 72 years from the first 10 years to the last 10 years of study (P = 0.018). The mean time from debut of symptoms until hospital admission increased from 7 (SD 9) h in the first 10 years to 13 (SD 14) h in the last 10 years (P = 0.019).

Incidence rates

The IR varied between 3.3-5.3 and 4.2-8.7 per 100000/year for women and men, respectively, throughout the observation period. The IR increased with increasing age, without an upper limit (see Figure 1), until the second decade of the study period in men and to the third decade of the study period in women. Recent years have shown a declining tendency in both sexes (see Figure 1). Adjusted IRRs obtained from Poisson regression with calendar year and age as covariates are shown in Table 2. The IR increased significantly with age for both gastric and duodenal PPUs.

Figure 2 shows that the incidence of gastric ulcer perforations peaked around 1984, whereas duodenal ulcer perforations peaked approximately 15 years later.

Predisposing factors

The use of acetylsalicylic acid increased significantly over 40 years, from 5% (2/38) the first 10 years, to 18% (8/45) the last 10 years (Table 1). The proportion of patients with PPU who used non-steroidal anti-inflammatory drugs (NSAIDs) or smoked did not change significantly throughout the course of the study.

Comorbidity

The Charlson Comorbidity Index and ASA score increased significantly in patients with PPU over 40 years (Table 1). In 1978-1987, 5% (2/38) of the patients had an ASA score 4-5, increasing to 22% (10/45) during 2008-2017.

Treatment

Two hundred and six patients had open surgery; 201 with suture and omental patch, 5 with resections. Three patients were not operated on; one was 90 years old and about to die at admission. Another 90-year-old was deemed too sick to tolerate narcosis and operation. The third patient was 70 years old, multimorbid, and had previously undergone difficult operations involving the upper abdomen. He had localised peritonitis and was treated conservatively with nasogastric suction, intravenous drip, antibiotics, and close clinical supervision. He survived. All three were admitted in the last decade.

The median time from debut of symptoms to operation increased significantly (P = 0.004), from 8 h in the first decade to 17 h in the last decade. The median time from admittance to hospital to operation and the duration of the operation and hospital stay were stable through all four decades (see Table 3).

Complications

One or more complications occurred in 39% of patients (81/209). The two most common complications were pneumonia (n = 18, 8.6%) and wound infections (n = 12, 5.7%). Reoperation was performed in 14 (6.8%) patients for wound dehiscence (n = 7, 3.4%), postoperative leak (n = 4, 1.9%), intestinal obstruction (n = 1), severe bleeding from duodenal ulcer (n = 1), and drainage of subphrenic and pelvic abscesses (n = 1). The Clavien-Dindo classification of complications is shown in Table 3. Complications occurred more frequently and were more serious in recent decades, in older patients, and in patients with comorbidities and higher ASA scores.

Mortality and long-term survival

The 100-day mortality was 20.6% (43/209) without significant variations between decades. Based on ASA score, the 100-day mortality was 6% in patients with ASA

Table 1 Trends in patient characteristics according to decade of treatment, *n* (%)

n = 209	1978–1987 (*n* = 38)	1988–1997 (*n* = 64)	1998–2007 (*n* = 62)	2008-2017 (*n* = 45)	*P* value
Sex					
Women	14 (36.8)	26 (40.6)	31 (50.0)	25 (55.6)	0.049[a]
Men	24 (63.2)	38 (59.4)	31 (50.0)	20 (44.4)	
Incidence (No./100000)					
Women	3.3 (1.8 to 5.5)	6.0 (3.9 to 8.8)	7.0 (4.8 to 9.9)	5.3 (3.4 to 7.8)	0.14[b]
Men	5.5 (3.6 to 8.3)	8.7 (6.2 to 12.0)	7.0 (4.8 to 10.0)	4.2 (2.6 to 6.5)	0.32[b]
Age, mean ± SD, years	62 ± 17	64 ± 16	67 ± 16	69 ± 17	0.018[c]
Hours from symptom debut until admission, mean ± SD)	7 ± 9	8 ± 12	16 ± 29	13 ± 14	0.019[c]
ASA class					
II	30 (78.9)	46 (71.9)	33 (53.2)	24 (53.3)	0.001[d]
III	6 (15.8)	13 (20.3)	19 (30.6)	11 (24.2)	
IV	2 (5.3)	5 (7.8)	10 (16.1)	9 (20.0)	
V	0	0	0	1 (2.2)	
Ulcer localisation					
Gastric	25 (65.8)	27 (42.2)	26 (41.9)	19 (42.2)	0.059[a]
Duodenal	13 (34.2)	37 (57.8)	36 (58.1)	26 (57.8)	
Past ulcer history	5 (13.2)	25 (39.1)	16 (26.2)	0	0.022[a]
Smoker at present	19 (57.6)	40 (64.5)	27 (49.1)	26 (59.1)	0.89[a]
NSAID use	4 (10.5)	11 (17.2)	19 (31.1)	8 (17.8)	0.18[a]
Steroid use	2 (5.3)	2 (3.1)	7 (11.5)	3 (6.7)	0.42[a]
Salicylate use	2 (5.3)	4 (6.3)	10 (16.4)	8 (17.8)	0.025[a]
Charlson Comorbidity index					
0	26 (68.4)	37 (57.8)	29 (46.8)	18 (40.0)	0.003[d]
1	5 (13.2)	22 (34.4)	24 (38.7)	13 (28.9)	
2+	7 (18.4)	5 (7.8)	9 (14.5)	14 (31.1)	

[a]Cochran-Armitage exact trend test.
[b]Poisson regression with calendar year as covariate.
[c]Jonckheere-Terpstra exact test.
[d]Ordered logistic regression analysis. SD: Standard deviation; ASA: American Society of Anesthesiologists; NSAID: Non-steroidal anti-inflammatory drugs.

score 2, 39% with ASA score 3, and 59% with ASA score 4-5. We performed a multivariable, logistic regression analysis of 100-day mortality as a dependent variable and sex, age, year of admittance, Charlson Comorbidity Index, and ASA score as independent variables. Only ASA score was significantly associated with 100-day mortality [odds ratio (OR) = 12.5; 95%CI: 3.5-41.8 for ASA score 3 and OR = 31.2 (7.4-132) for ASA score 4-5].

The overall estimated 5-year relative survival was 95% (95%CI: 86-101) with ASA score 2, 56% (95%CI: 37-74) with ASA score 3, and 12% (95%CI: 2-35) with ASA score 4-5.

In those who survived the first 100 days, the estimated 5-year relative survival was 98% (95%CI: 89-104) for ASA score 2, 84% (95%CI: 58-102) for ASA score 3, and 26% (95%CI: 3-63) for ASA score 4 (see Figure 3).

Table 2 Factors associated with peptic ulcer perforation incidence rate ratios from 1978 to 2017. Data are presented as adjusted incidence rate ratios from Poisson regression with calendar year and age as covariates

	Male	*P* value	Female	*P* value
	IRR (CI)		IRR (CI)	
Total peptic ulcer perforation				
Calendar year	0.986 (0.970 to 1.001)	0.074	1.005 (0.988 to 1.023)	0.55
Age (per 5 yr)	1.040 (1.029 to 1.051)	< 0.001	1.060 (1.047 to 1.073)	< 0.001
Gastric ulcer perforation				
Calendar year	0.979 (0.956 to 1.001)	0.063	0.998 (0.973 to 1.024)	0.90
Age (per 5 yr)	1.037 (1.022 to 1.053)	< 0.001	1.056 (1.038 to 1.075)	< 0.001
Duodenal ulcer perforation				
Calendar year	0.992 (0.971 to 1.014)	0.49	1.011 (0.988 to 1.035)	0.36
Age (per 5 yr)	1.043 (1.028 to 1.058)	< 0.001	1.063 (1.045 to 1.080)	< 0.001

IRR: Incidence rate ratio; CI: Confidence interval.

Table 3 Trends in treatment and outcome according to decade of treatment, *n* (%)

n = 209	1978–1987 (*n* = 38)	1988–1997 (*n* = 64)	1998–2007 (*n* = 62)	2008-2017 (*n* = 45)	*P* value
Treatment					
Simple closure with orwithout omentopexy	37 (97)	64 (100)	62 (100)	38 (84)	
Gastric resection	1 (3)	0	0	4 (9)	
No operation	0	0	0	3 (7)	
Hours from admission to operation, mean ± SD	7 ± 9	8 ± 12	16 ± 29	13 ± 14	0.019[a]
Duration of operation, mean ± SD, min	72 ± 29	78 ± 35	61 ± 24	78 ± 40	0.15[a]
Re-operation	1 (3)	4 (6)	6 (10)	4 (9)	0.18[b]
Clavien-Dindo classification of complications					
0	28 (74)	45 (70)	38 (61)	17 (38)	0.001[c]
1-2	6 (16)	8 (13)	9 (15)	13 (29)	
3	1 (3)	1 (29)	4 (7)	4 (9)	
4	0	4 (6)	3 (5)	3 (7)	
5	3 (8)	6 (9)	8 (13)	8 (18)	
100-day mortality	7 (18)	11 (17)	16 (26)	9 (20)	0.56[b]
Estimated 10-yr relative survival in patients surviving 100 d, (95%CI)	97 (70-114)	71 (52-87)	86 (64-103)	86 (51-108)	0.44[d]

[a]Jonckheere-Terpstra exact test.
[b]Cochran-Armitage exact trend test.
[c]Ordered logistic regression analysis.
[d]Relative survival analysis with calendar period as covariate. SD: Standard deviation; CI: Confidence interval.

DISCUSSION

This study demonstrated a trend of increasing age and comorbidity in patients admitted for PPU over 40 years. Complications were more common in recent decades. However, we found no significant variations between short-term mortality between the decennia. Comorbidity measured bythrough ASA score was a good prognostic factor regarding short-term mortality and long-term survival.

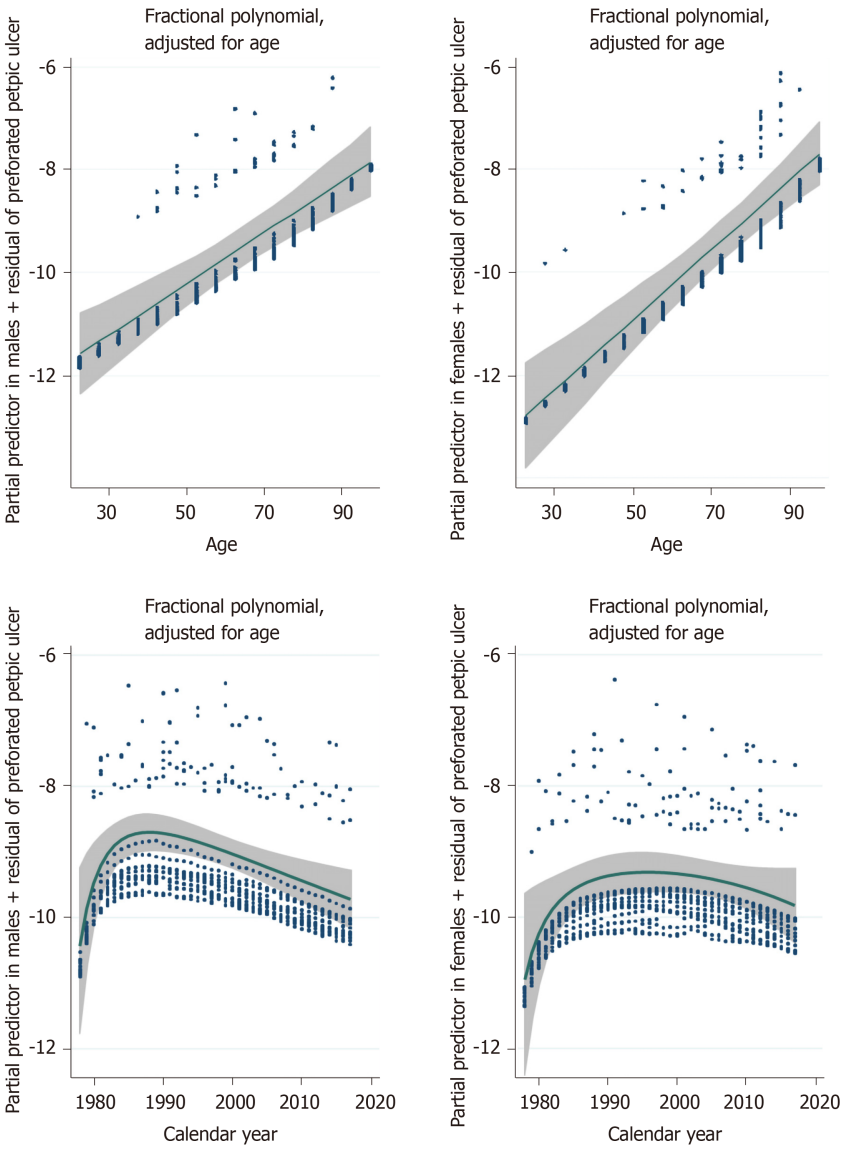

Figure 1 Effects of age and calendar year on the number of patients presenting with perforated peptic ulcer. Data are Poisson regression with fractional polynomials. 95% confidence intervals are shaded grey, and the y-axis is a logarithmic scale. Left, males. The effect of age was linear in both males and females, without an upper limit. Incidence increased, peaking 10 yr earlier in males than in females.

The median age of patients with PPU increased with each decade. In the last decade, more than half of the patients with PPU were > 70 years old. Women constituted a greater share of the patients with PPU with time, surpassing men in the last decade.

The incidence rates for PPU in our population were similar to previous studies, which reported an incidence of 4-15 per 100000/year[4,7,12]. The IR tended to decline during the last half of the observation period, and this tendency occurred almost one decade earlier for men than women. Over the same period, the IR was similar between the sexes. The Poisson regression with fractional polynomials indicated an increase in IR with increasing age for both sexes.

These epidemiological findings are in agreement with existing data showing a declining trend in PPU, equal gender distribution, and more frequent occurrence among the elderly[4,15,29,30]. These changes in the epidemiology of PPU may have numerous explanations. The identification and treatment of *H. pylori* as a cause of PUD is considered the main cause of reduced PPU incidence, especially in younger age groups[1,15]. The introduction of proton pump inhibitors is also postulated to be related to a reduced IR for PPU[4]. A shift in the occurrence of predisposing factors may also have contributed to these changes.

In addition to *H. pylori* infection, use of NSAIDs, corticosteroids, smoking, and previous history of PUD are known risk factors for PPU[31,32]. In our study, we found no significant change in trends regarding the use of NSAIDs, corticosteroids, or smoking habits.

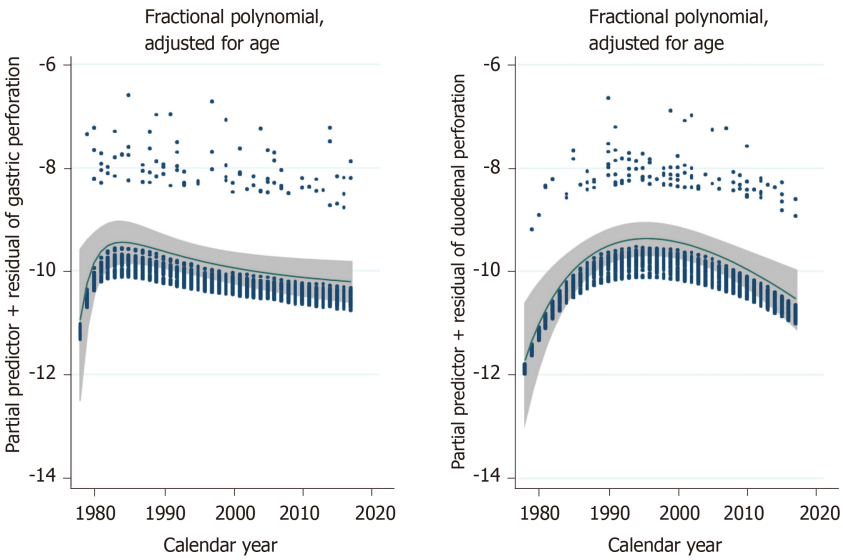

Figure 2 Effect of calendar year on the number of patients presenting with perforated gastric ulcer (left) and duodenal ulcer (right). Data were Poisson regression with fractional polynomials. 95% confidence intervals are shaded grey, and the y-axis is a logarithmic scale. The incidence of gastric ulcer perforations peaked around 1984, whereas the peak of duodenal ulcer perforations was approximately 15 yr later.

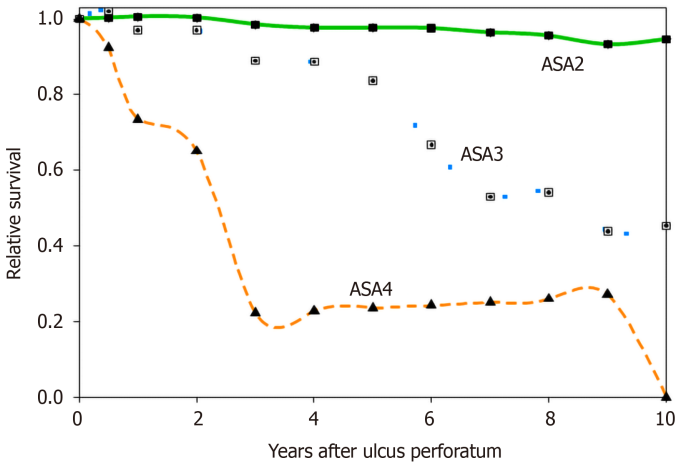

Yr	0	1	2	3	4	5	6	7	8	9	10
ASA2	125	124	123	118	112	107	101	96	88	88	75
ASA3	29	29	26	25	22	20	17	13	10	10	7
ASA4	11	9	7	5	1	1	1	1	1	1	0

Figure 3 Relative survival in each American Society of Anesthesiologists group of patients who survived the first 100 postoperative days. ASA: American Society of Anesthesiologists.

Acetylsalicylic acid is also technically considered an NSAID due to similar mechanisms of action[32,33]. It also has a similar profile regarding adverse events and is associated with an increased risk of PPU[32]. However, acetylsalicylic acid has a completely different area of use than other NSAIDs, mostly in secondary prevention of thrombotic cardiovascular events[33]. The significant increase in the use of acetylsalicylic acid through the study period may contribute to the increased IR with increasing age and the elderly being more prone to adverse effects[15,34].

The patients admitted with PPU had increasing comorbidity in recent decades according to the Charlson Comorbidity Index and ASA class. Increased comorbidity is associated with increased age[35]. Previous studies have also shown an association between comorbidity, complications, and mortality after PPU[14]. This is thought to be

related to delayed admittance, diagnosis, and treatment[15].

The surgical treatment for PPU in our cohort barely changed over four decades, with simple closure with or without omentopexy being the procedure of choice in 98% (201/206) of patients. Only one of the patients were treated with a laparoscopic technique. The length of the operation was stable over all decades, and this could be explained with little variation in surgical access and method.

Three patients in the cohort were treated without an operation, all in the last decade, two of whom died within a short timeframe. This could reflect more frequent "failure-to-rescue" in recent years, especially in elderly patients with severe comorbidity[29,36].

The increase in time from the debut of symptoms to hospital admission in recent decades may be related to the previously described epidemiological shift in the age of patients with PPU[4,14,30]. Elderly patients with comorbidity are less likely to present with peritonitis[29].

Post-operative complications occurred more frequently in recent decades. Increasing age and greater comorbidity in the patients treated for PPU could explain the increase in serious complications (Clavien-Dindo grade 4 and 5)[37]. We found no significant change in the frequency of reoperation. We also found a substantial increase in the frequency of grade 1-2 complications. This does not necessarily reflect an actual increase in low-grade complications, but may be related to a change in doctors' habits towards more frequent and detailed descriptions in documentation[38]. The accuracy of the collected data is limited to the amount of detail in the patient's journal. This represents a limitation of the retrospective study design.

Short-term mortality measured 100 d post-operatively was stable through all four decades and in concordance with existing data. The short-term mortality was associated with ASA score, supporting the understanding that patient comorbidity affects mortality. A similar association with degree of comorbidity expressed through ASA score was seen regarding long-term survival, measured as 5-year relative survival. This supports previous data suggesting that ASA score can be used as a prognostic factor regarding both short- and long-term survival[39-41].

The study had some limitations. The retrospective design has weaknesses. The quality of the database was dependent on the quality of the different patient records. Grade 1 Clavien-Dindo complications were often not documented in the patient records. More severe complications were regularly documented, and we expect very few missing grade II to V complications in the database.

CONCLUSION

In conclusion, this study confirmed that the IRR of PPU increased with increasing age, without an upper limit. The IRR increased until the second decade of the study period in men and the third decade in women. Recent years indicate a declining tendency in both sexes. In recent decades, patients were older and had more comorbidity. Post-operative complications increased over the 40 years of the study. ASA score was associated with both short-term mortality and long-term survival.

The results of this study would have external validity for populations similar to the Norwegian population.

ARTICLE HIGHLIGHTS

Research background

The incidence of peptic ulcer disease (PUD) has decreased during the last few decades. However, complicated PUD has not decreased likewise. Perforation is the complication that accounts for most deaths associated with PUD, and it remains a surgical emergency. Perforated peptic ulcer (PPU) has a high short-term mortality.

Research motivation

With the discovery of the role of Helicobacter pylori in PUD, it is important to investigate trends and changes in demography in patients with PPU. This will provide more precise characteristics regarding these patients, which in turn might contribute towards more rapid diagnostics and treatment.

Research objectives

The aim of this study was to investigate changes in demography and the effect on treatment, complications, and short- and long-term mortality in patients admitted to our hospital with PPU over four decades.

Research methods

All patients who were admitted to our hospital with PPU from 1978-2017 were retrospectively identified and included. We retrieved their medical records and reviewed them to obtain data concerning patient characteristics, treatment and complications.

Research results

The median age increased from 63 to 72 years from the first to the last decade. The incidence rate increased with increasing age, although we observed a decline in incidence rate in recent decades. Comorbidity increased significantly over the 40 years of the study. The median time from debut of symptoms to operation increased from 8 to 17 h from the first to the last decade. One or more complications occurred in 39 %. Both short- and long-term mortality were associated with American Society of Anaesthesiologists (ASA) score.

Research conclusions

Declining incidence rates occurred in recent years, but the patients were older and had more comorbidity. The ASA score was associated with both short-term mortality and long-term survival.

Research perspectives

This study has shown a demographic shift among patients with PPU. Future research should assess a better understanding of the association of increasing age, comorbidity and other risk factors with PPU. Clinical trials might serve to reduce the high number of complications in these patients.

ACKNOWLEDGEMENTS

We thank Stian Lydersen, Professor of Medical Statistics at NTNU, for advice on statistical methods and comments on the manuscript. We want to thank the clinicians and other employees at Nord-Trøndelag Hospital Trust for their support and for contributing to the data collection in this research project.

REFERENCES

1 **Oderda G**, Forni M, Dell'Olio D, Ansaldi N. Cure of peptic ulcer associated with eradication of Helicobacter pylori. *Lancet* 1990; **335**: 1599 [PMID: 1972523 DOI: 10.1016/0140-6736(90)91434-c]
2 **Eisner F**, Hermann D, Bajaeifer K, Glatzle J, Königsrainer A, Küper MA. Gastric Ulcer Complications after the Introduction of Proton Pump Inhibitors into Clinical Routine: 20-Year Experience. *Visc Med* 2017; **33**: 221-226 [PMID: 28785572 DOI: 10.1159/000475450]
3 **Dutta AK**, Chacko A, Balekuduru A, Sahu MK, Gangadharan SK. Time trends in epidemiology of peptic ulcer disease in India over two decades. *Indian J Gastroenterol* 2012; **31**: 111-115 [PMID: 22766645 DOI: 10.1007/s12664-012-0201-5]
4 **Hermansson M**, Ekedahl A, Ranstam J, Zilling T. Decreasing incidence of peptic ulcer complications after the introduction of the proton pump inhibitors, a study of the Swedish population from 1974-2002. *BMC Gastroenterol* 2009; **9**: 25 [PMID: 19379513 DOI: 10.1186/1471-230X-9-25]
5 **Lassen A**, Hallas J, Schaffalitzky de Muckadell OB. Complicated and uncomplicated peptic ulcers in a Danish county 1993-2002: a population-based cohort study. *Am J Gastroenterol* 2006; **101**: 945-953 [PMID: 16573778 DOI: 10.1111/j.1572-0241.2006.00518.x]
6 **Lau JY**, Sung J, Hill C, Henderson C, Howden CW, Metz DC. Systematic review of the epidemiology of complicated peptic ulcer disease: incidence, recurrence, risk factors and mortality. *Digestion* 2011; **84**: 102-113 [PMID: 21494041 DOI: 10.1159/000323958]
7 **Thorsen K**, Søreide JA, Kvaløy JT, Glomsaker T, Søreide K. Epidemiology of perforated peptic ulcer: age- and gender-adjusted analysis of incidence and mortality. *World J Gastroenterol* 2013; **19**: 347-354 [PMID: 23372356 DOI: 10.3748/wjg.v19.i3.347]
8 **Malfertheiner P**, Chan FK, McColl KE. Peptic ulcer disease. *Lancet* 2009; **374**: 1449-1461 [PMID: 19683340 DOI: 10.1016/S0140-6736(09)60938-7]
9 **Lu Y**, Loffroy R, Lau JY, Barkun A. Multidisciplinary management strategies for acute non-variceal upper gastrointestinal bleeding. *Br J Surg* 2014; **101**: e34-e50 [PMID: 24277160 DOI: 10.1002/bjs.9351]
10 **Søreide K**, Thorsen K, Søreide JA. Strategies to improve the outcome of emergency surgery for perforated

peptic ulcer. *Br J Surg* 2014; **101**: e51-e64 [PMID: 24338777 DOI: 10.1002/bjs.9368]
11 **Tarasconi A**, Coccolini F, Biffl WL, Tomasoni M, Ansaloni L, Picetti E, Molfino S, Shelat V, Cimbanassi S, Weber DG, Abu-Zidan FM, Campanile FC, Di Saverio S, Baiocchi GL, Casella C, Kelly MD, Kirkpatrick AW, Leppaniemi A, Moore EE, Peitzman A, Fraga GP, Ceresoli M, Maier RV, Wani I, Pattonieri V, Perrone G, Velmahos G, Sugrue M, Sartelli M, Kluger Y, Catena F. Perforated and bleeding peptic ulcer: WSES guidelines. *World J Emerg Surg* 2020; **15**: 3 [PMID: 31921329 DOI: 10.1186/s13017-019-0283-9]
12 **Svanes C**. Trends in perforated peptic ulcer: incidence, etiology, treatment, and prognosis. *World J Surg* 2000; **24**: 277-283 [PMID: 10658061 DOI: 10.1007/s002689910045]
13 **Møller MH**, Vester-Andersen M, Thomsen RW. Long-term mortality following peptic ulcer perforation in the PULP trial. A nationwide follow-up study. *Scand J Gastroenterol* 2013; **48**: 168-175 [PMID: 23215900 DOI: 10.3109/00365521.2012.746393]
14 **Thorsen K**, Glomsaker TB, von Meer A, Søreide K, Søreide JA. Trends in diagnosis and surgical management of patients with perforated peptic ulcer. *J Gastrointest Surg* 2011; **15**: 1329-1335 [PMID: 21567292 DOI: 10.1007/s11605-011-1482-1]
15 **Søreide K**, Thorsen K, Harrison EM, Bingener J, Møller MH, Ohene-Yeboah M, Søreide JA. Perforated peptic ulcer. *Lancet* 2015; **386**: 1288-1298 [PMID: 26460663 DOI: 10.1016/S0140-6736(15)00276-7]
16 **Byrne BE**, Bassett M, Rogers CA, Anderson ID, Beckingham I, Blazeby JM; Association of Upper Gastrointestinal Surgeons for the National Emergency Laparotomy Project Team. Short-term outcomes after emergency surgery for complicated peptic ulcer disease from the UK National Emergency Laparotomy Audit: a cohort study. *BMJ Open* 2018; **8**: e023721 [PMID: 30127054 DOI: 10.1136/bmjopen-2018-023721]
17 **Tan S**, Wu G, Zhuang Q, Xi Q, Meng Q, Jiang Y, Han Y, Yu C, Yu Z, Li N. Laparoscopic versus open repair for perforated peptic ulcer: A meta analysis of randomized controlled trials. *Int J Surg* 2016; **33** Pt A: 124-132 [PMID: 27504848 DOI: 10.1016/j.ijsu.2016.07.077]
18 **Sarosi GA Jr**, Jaiswal KR, Nwariaku FE, Asolati M, Fleming JB, Anthony T. Surgical therapy of peptic ulcers in the 21st century: more common than you think. *Am J Surg* 2005; **190**: 775-779 [PMID: 16226957 DOI: 10.1016/j.amjsurg.2005.07.019]
19 **Thorsen K**, Søreide JA, Søreide K. Long-Term Mortality in Patients Operated for Perforated Peptic Ulcer: Factors Limiting Longevity are Dominated by Older Age, Comorbidity Burden and Severe Postoperative Complications. *World J Surg* 2017; **41**: 410-418 [PMID: 27734076 DOI: 10.1007/s00268-016-3747-z]
20 **ASA House of Delegates/Executive Committee**. ASA Physical Status Classification System. 2019. [accessed 2020, June 22]. Available from: https://www.asahq.org/standards-and-guidelines/asa-physical-status-classification-system
21 **Charlson ME**, Pompei P, Ales KL, MacKenzie CR. A new method of classifying prognostic comorbidity in longitudinal studies: development and validation. *J Chronic Dis* 1987; **40**: 373-383 [PMID: 3558716 DOI: 10.1016/0021-9681(87)90171-8]
22 **Clavien PA**, Barkun J, de Oliveira ML, Vauthey JN, Dindo D, Schulick RD, de Santibañes E, Pekolj J, Slankamenac K, Bassi C, Graf R, Vonlanthen R, Padbury R, Cameron JL, Makuuchi M. The Clavien-Dindo classification of surgical complications: five-year experience. *Ann Surg* 2009; **250**: 187-196 [PMID: 19638912 DOI: 10.1097/SLA.0b013e3181b13ca2]
23 **Dindo D**, Demartines N, Clavien PA. Classification of surgical complications: a new proposal with evaluation in a cohort of 6336 patients and results of a survey. *Ann Surg* 2004; **240**: 205-213 [PMID: 15273542 DOI: 10.1097/01.sla.0000133083.54934.ae]
24 **The European Parliament and the Council of the European Union**. Regulation (EU) 2016/679 of the European Parliament and the Council of 27 April 2016 on the protection of natural persons with regard to the processing of personal data and on the free movement of such data, and repealing Directive 95/46/EC (General Data Protection Regulation). European Union: The Official Journal of the European Union, 2016. [accessed 2020, June 22]. Available from: https://eur-lex.europa.eu/legal-content/EN/TXT/HTML/?uri=CELEX:32016R0679&from=EN
25 **Royston PA**, Altman DG. Regression Using Fractional Polynomials of Continuous Covariates: Parsimonious Parametric Modelling. *Appl Statist* 1994; **43**: 429-453 [DOI: 10.2307/2986270]
26 **Dickman PW**, Sloggett A, Hills M, Hakulinen T. Regression models for relative survival. *Stat Med* 2004; **23**: 51-64 [PMID: 14695639 DOI: 10.1002/sim.1597]
27 **Dickman PW**, Coviello E. Estimating and modeling relative survival. *Stata Journal* 2015; 186-215 [DOI: 10.1177/1536867X1501500112]
28 **Database HM**. Human Mortality Database; 2018. [accessed 2020, March 20]. Available from: http://www.mortality.org
29 **Søreide K**, Thorsen K, Søreide JA. Clinical patterns of presentation and attenuated inflammatory response in octo- and nonagenarians with perforated gastroduodenal ulcers. *Surgery* 2016; **160**: 341-349 [PMID: 27067159 DOI: 10.1016/j.surg.2016.02.027]
30 **Bashinskaya B**, Nahed BV, Redjal N, Kahle KT, Walcott BP. Trends in Peptic Ulcer Disease and the Identification of Helicobacter Pylori as a Causative Organism: Population-based Estimates from the US Nationwide Inpatient Sample. *J Glob Infect Dis* 2011; **3**: 366-370 [PMID: 22224001 DOI: 10.4103/0974-777X.91061]
31 **Chung KT**, Shelat VG. Perforated peptic ulcer - an update. *World J Gastrointest Surg* 2017; **9**: 1-12 [PMID: 28138363 DOI: 10.4240/wjgs.v9.i1.1]
32 **Lanas A**, Chan FKL. Peptic ulcer disease. *Lancet* 2017; **390**: 613-624 [PMID: 28242110 DOI: 10.1016/S0140-6736(16)32404-7]
33 **Meek IL**, Van de Laar MA, E Vonkeman H. Non-Steroidal Anti-Inflammatory Drugs: An Overview of Cardiovascular Risks. *Pharmaceuticals (Basel)* 2010; **3**: 2146-2162 [PMID: 27713346 DOI: 10.3390/ph3072146]
34 **Lanas A**, Serrano P, Bajador E, Esteva F, Benito R, Sáinz R. Evidence of aspirin use in both upper and lower gastrointestinal perforation. *Gastroenterology* 1997; **112**: 683-689 [PMID: 9041228 DOI: 10.1053/gast.1997.v112.pm9041228]
35 **Divo MJ**, Martinez CH, Mannino DM. Ageing and the epidemiology of multimorbidity. *Eur Respir J* 2014; **44**: 1055-1068 [PMID: 25142482 DOI: 10.1183/09031936.00059814]

36 **Sheetz KH**, Waits SA, Krell RW, Campbell DA Jr, Englesbe MJ, Ghaferi AA. Improving mortality following emergent surgery in older patients requires focus on complication rescue. *Ann Surg* 2013; **258**: 614-7; discussion 617-8 [PMID: 23979275 DOI: 10.1097/SLA.0b013e3182a5021d]

37 **Møller MH**, Adamsen S, Thomsen RW, Møller AM. Preoperative prognostic factors for mortality in peptic ulcer perforation: a systematic review. *Scand J Gastroenterol* 2010; **45**: 785-805 [PMID: 20384526 DOI: 10.3109/00365521003783320]

38 **Kuhn T**, Basch P, Barr M, Yackel T; Medical Informatics Committee of the American College of Physicians. Clinical documentation in the 21st century: executive summary of a policy position paper from the American College of Physicians. *Ann Intern Med* 2015; **162**: 301-303 [PMID: 25581028 DOI: 10.7326/M14-2128]

39 **Thorsen K**, Søreide JA, Søreide K. What is the best predictor of mortality in perforated peptic ulcer disease? A population-based, multivariable regression analysis including three clinical scoring systems. *J Gastrointest Surg* 2014; **18**: 1261-1268 [PMID: 24610235 DOI: 10.1007/s11605-014-2485-5]

40 **Thorsen K**, Søreide JA, Søreide K. Scoring systems for outcome prediction in patients with perforated peptic ulcer. *Scand J Trauma Resusc Emerg Med* 2013; **21**: 25 [PMID: 23574922 DOI: 10.1186/1757-7241-21-25]

41 **Søreide K**, Thorsen K, Søreide JA. Predicting outcomes in patients with perforated gastroduodenal ulcers: artificial neural network modelling indicates a highly complex disease. *Eur J Trauma Emerg Surg* 2015; **41**: 91-98 [PMID: 25621078 DOI: 10.1007/s00068-014-0417-4]

World Journal of Gastroenterology

Submit a Manuscript: https://www.f6publishing.com

World J Gastroenterol 2020 September 21; 26(35): 5314-5327

DOI: 10.3748/wjg.v26.i35.5314

ISSN 1007-9327 (print) ISSN 2219-2840 (online)

ORIGINAL ARTICLE

Retrospective Study

Investigation of immune escape-associated mutations of hepatitis B virus in patients harboring hepatitis B virus drug-resistance mutations

Bi-Xia Huang, Yan Liu, Zhen-Ping Fan, Lan-Lan Si, Rong-Juan Chen, Jun Wang, Dan Luo, Fu-Sheng Wang, Dong-Ping Xu, Xin-Guang Liu

ORCID number: Bi-Xia Huang 0000-0002-4469-0467; Yan Liu 0000-0003-1498-4314; Zhen-Ping Fan 0000-0001-9761-3337; Lan-Lan Si 0000-0003-0222-5169; Rong-Juan Chen 0000-0001-8090-1682; Jun Wang 0000-0002-6261-8995; Dan Luo 0000-0002-1889-2882; Fu-Sheng Wang 0000-0002-8043-6685; Dong-Ping Xu 0000-0002-0754-4620; Xin-Guang Liu 0000-0001-6963-1386.

Author contributions: Huang BX was involved in the experiments, procedures, statistical analysis, writing of the original draft, and critical revision of manuscript; Liu Y performed the experiments and procedures; Fan ZP took part in the statistical analysis; Si LL was involved in the experiments and procedures; Chen RJ performed the experiments and procedures; Wang J took part in the statistical analysis; Luo D was involved in the study statistical analysis; Wang FS performed the study statistical analysis; Xu DP took part in the study conception, design, writing of the original draft, and critical revision of manuscript; Liu XG was involved in the study conception, design, writing of the original draft, and critical revision of manuscript; all authors have read

Bi-Xia Huang, Xin-Guang Liu, Guangdong Provincial Key Laboratory of Medical Molecular Diagnostics/Institute of Biochemistry & Molecular Biology, Guangdong Medical University, Dongguan 523808, Guangdong Province, China

Yan Liu, Zhen-Ping Fan, Lan-Lan Si, Rong-Juan Chen, Jun Wang, Fu-Sheng Wang, Dong-Ping Xu, Institute of Infectious Diseases, the Fifth Medical Center of Chinese PLA General Hospital, Beijing 100039, China

Dan Luo, Department of Infectious Diseases, the First Affiliated Hospital of Xi'an Jiaotong University, Xi'an 710061, Shaanxi Province, China

Corresponding author: Dong-Ping Xu, MD, PhD, Professor, Institute of Infectious Diseases, the Fifth Medical Center of Chinese PLA General Hospital, No. 100 Xisihuan Middle Road, Beijing 100039, China. xudongping302@sina.com

Abstract

BACKGROUND

It is unclear whether immune escape-associated mutations in the major hydrophilic region of hepatitis B virus surface antigen (HBsAg) are associated with nucleoside/nucleotide analog resistance.

AIM

To evaluate the association between immune escape-associated mutations and nucleoside/nucleotide analog resistance mutations.

METHODS

In total, 19440 patients with chronic hepatitis B virus infection, who underwent resistance testing at the Fifth Medical Center of Chinese PLA General Hospital between July 2007 and December 2017, were enrolled. As determined by sequence analysis, 6982 patients harbored a virus with resistance mutations and 12458 harbored a virus lacking resistance mutations. Phenotypic analyses were performed to evaluate HBsAg production, replication capacity, and drug-induced viral inhibition of patient-derived drug-resistant mutants with or without the coexistence of sA159V.

and approved the final manuscript.

Supported by the National Natural Science Foundation of China, No. 81572010, No. 81671399, No. 81721002 and No. 81971329; the Capital Health Research and Development of Special Fund Program, No. 2016-2-5032; and the Beijing Natural Science Foundation No. 7172206.

Institutional review board statement: The study was reviewed and approved by the Ethics Committee Approval Document of 302 Hospital, Institutional Review Board Approval No. 2012020D; The study was reviewed and approved by the Ethics Committee Approval Document of 302 Hospital, Institutional Review Board Approval No. 2013052D.

Informed consent statement: All study participants, or their legal guardian, provided informed written consent prior to study enrollment.

Conflict-of-interest statement: We do not have any patents, whether planned, pending or issued, broadly relevant to the work.

Data sharing statement: No additional data are available.

Manuscript source: Unsolicited manuscript

Received: April 23, 2020
Peer-review started: April 23, 2020
First decision: May 1, 2020

RESULTS

The rate of immune escape-associated mutation was significantly higher in 9 of the 39 analyzed mutation sites in patients with resistance mutations than in patients without resistance mutations. In particular, these mutations were sQ101H/K/R, sS114A/L/T, sT118A/K/M/R/S/V, sP120A/L/Q/S/T, sT/I126A/N/P/S, sM133I/L/T, sC137W/Y, sG145A/R, and sA159G/V. Among these, sA159V was detected in 1.95% (136/6982) of patients with resistance mutations and 1.08% (134/12,458) of patients lacking resistance mutations ($P < 0.05$). The coexistence of sA159V with lamivudine (LAM) and entecavir (ETV)-resistance mutations in the same viral genome was identified during follow-up in some patients with drug resistance. HBsAg production was significantly lower and the replication capacity was significantly higher, without a significant difference in LAM/ETV susceptibility, in sA159V-containing LAM/ETV-resistant mutants than in their sA159V-lacking counterparts.

CONCLUSION

In summary, we observed a close link between the increase in certain immune escape-associated mutations and the development of resistance mutations. sA159V might increase the fitness of LAM/ETV-resistant mutants under environmental pressure in some cases.

Key Words: Hepatitis B virus; Immune escape-associated mutation; Drug-resistance mutation; Nucleoside/nucleotide analogs; Hepatitis B surface antigen; Major hydrophilic region

Core Tip: A large number of patients were surveyed for immune escape-associated mutations, and the link between immune escape-associated and resistant mutations was identified. Contribution of sA159V to resistance was found in multiple followed up patients, in particular sA159V reduced hepatitis B surface antigen but raised the replication capacity of lamivudine/entecavir-resistant mutants.

Citation: Huang BX, Liu Y, Fan ZP, Si LL, Chen RJ, Wang J, Luo D, Wang FS, Xu DP, Liu XG. Investigation of immune escape-associated mutations of hepatitis B virus in patients harboring hepatitis B virus drug-resistance mutations. *World J Gastroenterol* 2020; 26(35): 5314-5327
URL: https://www.wjgnet.com/1007-9327/full/v26/i35/5314.htm
DOI: https://dx.doi.org/10.3748/wjg.v26.i35.5314

INTRODUCTION

It is estimated that 292 million people worldwide are chronically infected with hepatitis B virus (HBV), including 86 million residing in China[1]. The treatment of chronic HBV infection is aimed towards the long-term suppression of viral replication to prevent disease progression[2]. Currently, nucleoside/nucleotide analogs (NAs) including lamivudine (LAM), adefovir dipivoxil (ADV), entecavir (ETV), telbivudine (LdT), tenofovir disoproxil fumarate (TDF), and tenofovir alafenamide (TAF) are approved for the treatment of HBV infection. However, a concern is the drug resistance caused by mutations in the reverse transcriptase (RT) region of the HBV genome. Drug-resistance mutations tend to arise in patients treated with LAM, LdT, and ADV as well as in LAM-refractory patients subsequently treated with ETV[3,4]. Classical primary resistance mutations include rtM204I/V (LAM-r) for LAM (rtM204I also confers resistance to LdT), rtA181V/rtN236T for ADV as well as LAM-r along with at least one substitution at rt184 (A/C/F/G/I/L/M/S), rt202 (C/G/I), and rtM250 (I/L/V) for ETV[3,5,6]. In addition, rtS106C+rtH126Y+rtD134E+rtL269I quadruple mutations have recently been reported to confer TDF resistance[7]. TAF, also known as TDF II, has a higher intrahepatic drug concentration and lower plasma drug concentration than TDF as well as a lower probability of kidney and bone

Revised: July 27, 2020
Accepted: August 12, 2020
Article in press: August 12, 2020
Published online: September 21, 2020

P-Reviewer: Hossain MG, Yang R
S-Editor: Wang DM
L-Editor: Filipodia
P-Editor: Li JH

abnormalities during therapy[8].

The rapid selection of drug-resistant HBV mutants may depend on viral fitness, which could be influenced by the host immune response in addition to drug pressure[9,10,11]. A few drug-resistance mutations, such as rtS78T and rtA181T, introduce a stop codon in the overlapping S region and affect the immune response, thereby influencing the clinical presentation of NA-treated patients[12-15]. Hepatitis B surface antigen (HBsAg) is diagnostic marker of HBV infection and an important index for predicting the effects of antiviral treatment[16,17]. HBV immune escape-associated mutations, located mainly in the major hydrophilic region (MHR, amino acids 99−169), have the potential to weaken the immune response. Currently, it is unclear whether these mutations influence drug resistance. Only a few studies on a limited number of patients reference this issue, showing that the frequency of some immune escape-associated mutations is higher in LAM-treated patients than in NA-naive patients, suggesting that selection of drug-resistance mutations is associated with immune escape-associated mutation enrichment[18,19].

We recently identified several novel immune escape-associated mutations in patients with occult HBV infection; a summary of previously documented immune escape-associated mutations is provided in Table 1[20,21]. Notably, for many previously documented mutations, phenotypic information is lacking. In this study, we evaluated a large number of patients to determine whether immune escape-associated mutations are associated with drug-resistance mutations, with a focus on the sA159V mutation.

The rapidity of selection of drug-resistant HBV mutants may depend on viral fitness, which could be influenced by the host immune response in addition to drug pressure[9,10,11]. A few drug-resistance mutations, such as rtS78T and rtA181T, introduce a stop codon in the overlapping S region and affect the immune response, thereby influencing the clinical presentation of NA-treated patients[12-15]. HBsAg is diagnostic marker of HBV infection and an important index for predicting the effects of antiviral treatment[16,17]. HBV immune escape-associated mutations, located mainly in the MHR (amino acids 99−169), have the potential to weaken the immune response. Currently, it is unclear whether these mutations influence drug resistance. Only a few studies on a limited number of patients reference this issue, showing that the frequency of some immune escape-associated mutations is higher in LAM-treated patients than in NA-naïve patients, suggesting that selection of drug-resistance mutations is associated with immune escape-associated mutation enrichment[18,19].

We recently identified several novel immune escape-associated mutations in patients with occult HBV infection; a summary of previously documented immune escape-associated mutations is provided in Table 1[20,21]. Notably, for many previously documented mutations, phenotypic information is lacking. In this study, we evaluated a large number of patients to determine whether immune escape-associated mutations are associated with drug-resistance mutations, with a focus on the sA159V mutation.

MATERIALS AND METHODS

Patient samples

From July 2007 to December 2017, 19440 patients with chronic HBV infection who underwent resistance testing (by direct sequencing) at the Fifth Medical Center of Chinese PLA General Hospital (originally named Beijing 302 Hospital) were enrolled in the study, and their serum samples were collected. All patients were previously treated with NAs. Illness categories included chronic hepatitis B, HBV-related liver cirrhosis, and hepatocellular carcinoma. The diagnostic criteria were based on the guidelines for the prevention and treatment of chronic hepatitis B in China (2005)[22], and the updated guidelines were used according to the time of patient enrollment. Patients who were co-infected with other hepatitis viruses or human immunodeficiency virus were excluded from the study. All patients were from the Database of Beijing 302 Hospital and provided informed consent for the use of their samples for research before enrollment. The study was approved by the Ethics Committee of Beijing 302 Hospital.

Detection of serological markers and HBV deoxyribonucleic acid

Biochemical and serological markers as well as HBV deoxyribonucleic acid (DNA) levels in the serum samples were routinely detected at the Central Clinical Laboratory of the Fifth Medical Center of the Chinese PLA General Hospital. Roche Elecsys reagents (Basel, Switzerland) were used to measure the serum HBsAg levels, and the threshold for negativity was < 0.05 IU/mL in the quantitative assay or a cut-off index

Table 1 Summary of immune escape-associated mutations in the major hydrophilic region of hepatitis B surface antigen

Region in major hydrophilic region (aa 99–169)	Mutation pattern
Upstream "a" determinant (aa 99-123)	sY100S, sQ101H/K/R, sM103I/T, sL109I/P/R, sP111L/Q/S, sG112K/R, sS114A/L/T, sT115A/N, sT116N, sS117G/N/R, sT118A/K/M/R/S/V, sG119E/R/T, sP120A/L/Q/S/T, sC121R/S, sK122R, sT123A/I/N/S/V
Within "a" determinant (aa 124-147)	sC124R/Y, sT125A/M, sI/T126A/N/P/S, sP127H/L/S/T, sA128T/V, sQ129N/H/P/R, sG130A/K/N/R/S, sT131A/I/K/N, sS132F/P, sM133I/L/T, sF/Y134H/L/R/S/V, sS136F/P/Y, sC137W/Y, sC139R/S/Y, sT140I, sK141E/R, sP142L, sD144A/E, sG145A/R, sC147R/Y
Downstream "a" determinant (aa 148-169)	sS154P, sA159G/V, sV168A

aa: Amino acid.

of < 1.00 in the chemiluminescent immunoassay assay.

Sequence analysis of HBV reverse transcriptase/S genes and phylogenetic tree analysis

Sequence and phylogenetic analyses were performed as previously described[23,24]. In brief, a 1225-bp fragment [nucleotides (nt) 54-1278] spanning the full-length RT region (nt 130-1161) and S region (nt 155-835) of the viral genome was analyzed. Drug-resistance and immune escape-associated mutations were analyzed by direct sequencing using an in-house nested PCR method with a lower detection limit of 10 IU/mL. Clonal sequencing of the samples of interest was performed (20 clones per sample). Phylogenetic trees were constructed using MEGA 7 software.

Construction of 1.1-mer HBV reverse genome vectors and site-directed mutagenesis

Replication-competent vectors containing various mutant or wild-type (WT) RT/S genes were constructed for a phenotypic analysis based on the pTriEx-mod-1.1 vector, which was used for antigenicity analyses as previously described[21,24]. Eight recombinant vectors harboring RT/S genes from eight viral strains of a representative patient (patient A) were constructed. The eight strains were: WT, sA159V (M1), rtM204I (M2), sA159V+rtM204I (M3), rtL180M+rtM204V (M4), sA159V+rtL180M+rtM204V (M5), rtL180M+rtT184L+rtM204V (M6), and sA159V+rtL180M+rtT184L+rtM204V (M7). M6 was modified from M7 by the elimination of the sA159V mutation using the QuikChange Lightning Site-Directed Mutagenesis Kit (Stratagene, La Jolla, CA, United States). The primer (sense) was 5′-CCTGGGCTTTCGCAAAATTCCTATG-3′.

Phenotypic analysis of HBsAg, replication capacity, and drug-induced viral inhibition

Experiments were performed as described previously, with minor modifications[21,24]. Briefly, recombinant vectors were individually transfected into HepG2 cells. At 3 d after cultivation, the supernatant was harvested for the measurement of HBsAg by two assays, *i.e.* a chemiluminescence immunoassay (Roche) and an enzyme-linked immunosorbent assay (ELISA; Wantai Bio Pharm., Beijing, China).

To assess drug-induced viral inhibition, transfected HepG2 cells were cultured in the presence or absence of NAs for 4 d. Cells were lysed, and viral core particles were immunoprecipitated using anti-HBc/protein A+G. HBV replicative intermediates in the core particles were released and quantified by real-time PCR. The relative replication capacity of a mutant *vs* WT strain was determined in the absence of NAs. Approximately 90% effective concentrations of the four NAs were used, as previously determined[25,26]. These were 0.05 μmol/L for LAM, 0.05 μmol/L for ETV, 3.0 μmol/L for ADV, and 5.0 μmol/L for TDF. Viral inhibition was determined as the relative value of the NA-treated samples *vs* the NA-untreated samples. Experiments were performed at least three times independently.

Statistical analysis

Data are presented as the means (standard deviation) or medians (interquartile range). Differences between groups were examined by the Student's *t*-test (two-tailed) or chi-squared tests. Multivariate regression was used to determine independent risk factors.

Statistical analyses were performed using SPSS 23.0 for Windows (SPSS Inc., Chicago, IL, United States). A value of $P < 0.05$ was considered statistically significant.

RESULTS

Clinical profile of immune escape-associated mutations in patients with and without resistance mutations

Drug-resistance mutations were detected in 35.92% (6,982/19,440) of all patients included in the study. Moreover, patients harboring resistance mutations had higher HBV DNA levels than patients lacking resistance mutations. The rate of immune escape-associated mutation was significantly higher at 9 of 39 analyzed mutation sites in patients with resistance mutations than in patients without resistance mutations. These mutations were sQ101H/K/R, sS114A/L/T, sT118A/K/M/R/S/V, sP120A/L/Q/S/T, sT/I126A/N/P/S, sM133I/L/T, sC137W/Y, sG145A/R, and sA159G/V. The percentage of patients with MHR mutations was significantly higher in the resistance mutation-positive group than in the resistance mutation-negative group (23.32% *vs* 18.51%, $P < 0.05$) (Table 2). In particular, mutations were detected in 67/63/168 of 298 sQ101H/K/R-positive patients, 39/2/76 of 117 sS114A/L/T-positive patients, 5/5/15/3/1/2 of 31 sT118A/K/M/R/S/V-positive patients, 3/0/0/23/81 of 107 sP120A/L/Q/S/T-positive patients, 94/58/0/214 of 366 sT/I126A/N/P/S-positive patients, 14/46/136 of 196 sM133I/L/T-positive patients, 1/8 of 9 sC137W/Y-positive patients, 77/46 of 123 sG145A/R-positive patients, and 87/136 of 223 sA159G/V-positive patients.

Clinical incidence and features of the sA159V mutation

Restricted by the scale of the study, sA159V was selected as a representative immune escape-associated mutation for further analyses. The detection rate of sA159V was significantly higher in patients with resistance mutations than in patients lacking resistance mutations [1.95% (136/6982) *vs* 1.08% (134/12458), $P < 0.05$]. In contrast, the detection rate of sA159G did not differ significantly between the two patient groups (1.25% (87/6982) *vs* 1.48% (185/12458), $P > 0.05$). The clinical features of the sA159V-positive and sA159V-negative patients are summarized in Table 3. A multivariate analysis showed that age and the coexistence of ADV-r/LAM-r mutations were independently associated with the sA159V mutation. The sA159V-positive patients had higher rates of coexisting drug-resistance mutations than the sA159V-negative patients.

Longitudinal analysis of the clinical course of patients with HBV mutations during nucleotide analog therapy

Five representative sA159V-positive patients with available serial serum samples were subjected to clonal analysis of HBV RT/S genes. The five patients were infected with genotype C HBV and diagnosed with chronic hepatitis B or HBV-related liver cirrhosis.

Patient A, a 52-year-old male, was first admitted in October 2007 with chronic hepatitis B. The patient received LAM (from May 2008 to October 2009) and ETV+ADV (from October 2009 to June 2011). In tested clones of sample A-S1, WT, sA159V, sQ129R, and rtM204I detection rates were 80%, 10%, 5%, and 5%, respectively. In sample A-S2, six mutants were detected, *i.e.* sA159V+rtL180M+rtM204V (35%), rtL180M+rtM204V (35%), sA159V+rtM204I (15%), sA159V+rtL180M+rtM204I (5%), sA159V+rtM204V (5%), and rtM204I (5%). In sample A-S3, sA159V+rtL180M+rtM204V+rtT184L was the most abundant (Figure 1A). Clonal sequencing of sample A-S4 failed due to an extremely low viral load. The 10 viral clonal sequences from the patient were deposited in GenBank (MN642606-MN642615) and used to construct a phylogenetic tree (Figure 2).

Four patients received various NAs: LAM, ADV, or ETV, as monotherapy or in combination. Patient B had seven sA159V-containing mutants in samples B-S1 and B-S2 during ETV therapy. Resistant mutants were subsequently suppressed by ETV+ADV, whereas the sA159V mutation was observed in sample B-S3 (Figure 1B). Patient C and Patient D initially received ADV and failed to exhibit virological breakthrough. In both patients, the sA159V mutant existed before virological breakthrough (samples C-S1 and D-S1), and sA159V-containing ADV-resistant mutants were dominant in samples C-S2 and D-S2 at virological breakthrough (Figure 1C and D). Samples from Patient E included three sA159V-containing

Table 2 Analysis of immune escape-associated mutations in the major hydrophilic region in patients with and without resistance mutations

Clinical features	Resistance mutation (+), *n* = 6982	Resistance mutation (-), *n* = 12458	*P* value	The MHR Mutation occurrence [(+) *vs* (-)]
Age in year	44.01 ± 11.73	39.01 ± 13.08	< 0.05	
Gender, male	5709 (81.77%)	9982 (80.13%)	< 0.05	
HBV genotype, C%/B%	86.79/12.52	83.00/16.05	< 0.05	
HBV DNA as $\log_{10}$ IU/mL	4.62 (3.17, 6.47)	4.24 (2.83, 6.16)	< 0.05	
sY100S	20 (0.29%)	29 (0.23%)	NS	
sQ101H/K/R	298 (4.27%)	229 (1.84%)	< 0.05	↑
sM103I/T	8 (0.11%)	14 (0.11%)	NS	
sL109I/P/R	12 (0.17%)	24 (0.19%)	NS	
sP111L/Q/S	10 (0.14%)	21 (0.17%)	NS	
sG112K/R	4 (0.06%)	9 (0.07%)	NS	
sS114A/L/T	117 (1.68%)	137 (1.10%)	< 0.05	↑
sT115A/N	2 (0.03%)	8 (0.06%)	NS	
sT116N	6 (0.09%)	32 (0.26%)	< 0.05	↑
sS117G/N/R	5 (0.07%)	19 (0.15%)	NS	
sT118A/K/M/R/S/V	31 (0.44%)	32 (0.26%)	< 0.05	↑
sG119E/R/T	6 (0.09%)	10 (0.08%)	NS	
sP120A/L/Q/S/T	107 (1.53%)	35 (0.28%)	< 0.05	↑
sC121R/S	1 (0.01%)	1 (0.01%)	NS	
sK122R	154 (2.21%)	315 (2.53%)	NS	
sT123A/I/N/S/V	56 (0.80%)	91 (0.73%)	NS	
sC124R/Y	4 (0.06%)	9 (0.07%)	NS	
sT125A/M	8 (0.11%)	21 (0.17%)	NS	
sT/I126A/N/P/S	366 (5.24%)	534 (4.29%)	< 0.05	↑
sP127H/L/S/T	91 (1.30%)	165 (1.32%)	NS	
sA128T/V	7 (0.10%)	15 (0.12%)	NS	
sQ129N/H/P/R	90 (1.29%)	129 (1.04%)	NS	
sG130A/K/N/R/S	65 (0.93%)	85 (0.68%)	NS	
sT131A/I/K/N	133 (1.90%)	219 (1.76%)	NS	
sS132F/P	2 (0.03%)	9 (0.07%)	NS	
sM133I/L/T	196 (2.81%)	277 (2.22%)	< 0.05	↑
sF/Y134H/L/R/S/V	65 (0.93%)	51 (0.41%)	NS	
sS136F/P/Y	6 (0.09%)	4 (0.03%)	NS	
sC137W/Y	9 (0.13%)	5 (0.04%)	< 0.05	↑
sC139R/S/Y	3 (0.04%)	9 (0.07%)	NS	
sT140I	39 (0.56%)	61 (0.49%)	NS	
sK141E/R	3 (0.04%)	4 (0.03%)	NS	
sP142L	11 (0.16%)	9 (0.07%)	NS	
sD144A/E	17 (0.24%)	26 (0.21%)	NS	
sG145A/R	123 (1.76%)	163 (1.31%)	< 0.05	↑

sC147R/Y	0	0	NS
sS154P	1 (0.01%)	2 (0.02%)	NS
sA159G/V	223 (3.19%)	319 (2.56%)	< 0.05 ↑
sV168A	143 (2.05%)	234 (1.88%)	NS
Average number/patient	0.35	0.27	< 0.05 ↑
Patient percentage with the MHR mutation(s)	23.32% (1628/ 6982)	18.51% (2306/12458)	< 0.05 ↑

(+): Positive; (-): Negative; DNA: Deoxyribonucleic acid; HBV: Hepatitis B virus; MHR: Major hydrophilic region; NS: Not significant.

Table 3 Analysis of clinical features of sA159V-positive and sA159V-negative patients

Clinical features	sA159V-positive, *n* = 270	sA159V-negative, *n* = 19170	Univariate, *P* value	Univariate, *P*	Multivariate, *P* value	Multivariate , *P*
Age in year	46.67 ± 12.19	40.72 ± 12.83	0.00	< 0.05	0.00	< 0.05
Gender, male	214 (79.26%)	15477 (80.74%)	0.54	> 0.05	0.97	> 0.05
Genotype, C%/B%	90.00/10.00	84.31/14.82	0.03	< 0.05	0.40	> 0.05
HBV DNA as $\log_{10}$ IU/mL	4.54 (3.18, 6.55)	4.37(2.95, 6.27)	0.09	> 0.05	0.40	> 0.05
ALT in U/L	42 (25, 87)	42 (26, 82)	0.67	> 0.05	0.32	> 0.05
AST in U/L	41 (28, 83)	38 (26,71)	0.33	> 0.05	0.61	> 0.05
TBIL in μmol/L	16.10 (10.95, 25.45)	14.30 (10.40, 22.10)	0.13	> 0.05	0.58	> 0.05
CHE in U/L	5940 (3114, 8091)	6764 (4276, 8469)	0.11	> 0.05	0.87	> 0.05
HBsAg, COI	4987.83 ± 3128.43	5064.50 ± 2931.79	0.05	> 0.05	0.15	> 0.05
Coexistent with ADV-r mutation	41 (15.19%)	1663 (8.68%)	0.00	< 0.05	0.00	< 0.05
Coexistent with LAM-r mutation	97 (35.93%)	5316 (27.73%)	0.00	< 0.05	0.01	< 0.05
Coexistent with ETV-r mutation	20 (7.41%)	868 (4.53%)	0.04	< 0.05	0.40	> 0.05

ADV-r: Adefovir resistance; ALT: Alanine aminotransferase; AST: Aspartate aminotransferase; CHE: Cholinesterase; COI: Cut-off index; DNA: Deoxyribonucleic acid; ETV-r: Entecavir resistance; HBsAg: Hepatitis B surface antigen; HBV: Hepatitis B virus; LAM-r: Lamivudine resistance; TBIL: Total bilirubin.

ETV/LAM-resistant mutants (sample E-S2) when the virological response was inadequate upon ETV+TDF therapy (Figure 1E).

Quantitative HBsAg levels

As determined by the Roche quantitative assay, the HBsAg levels in the supernatant of the seven mutants decreased significantly to 46.2% (M1), 40.8% (M2), 14.0% (M3), 44.9% (M4), 20.6% (M5), 35.1% (M6), and 16.6% (M7) of the WT level. Three sA159V-containing resistant mutants had significantly lower HBsAg levels than their sA159V-lacking counterparts (M2 *vs* M3, M4 *vs* M5, M6 *vs* M7, all $P < 0.05$) (Figure 3). Consistent results were obtained by ELISA (data not shown).

Assessment of viral replication capacity

The replication capacities of the seven mutants (M1–M7) decreased significantly to 49.0% (M1), 16.4% (M2), 37.8% (M3), 22.0% (M4), 46.0% (M5), 15.4% (M6), and 33.0% (M7) of the WT level. Three sA159V-containing resistant mutants had significantly higher replication capacities than their sA159V-lacking counterparts (M2 *vs* M3, M4 *vs* M5, M6 *vs* M7, all $P < 0.05$) (Figure 4).

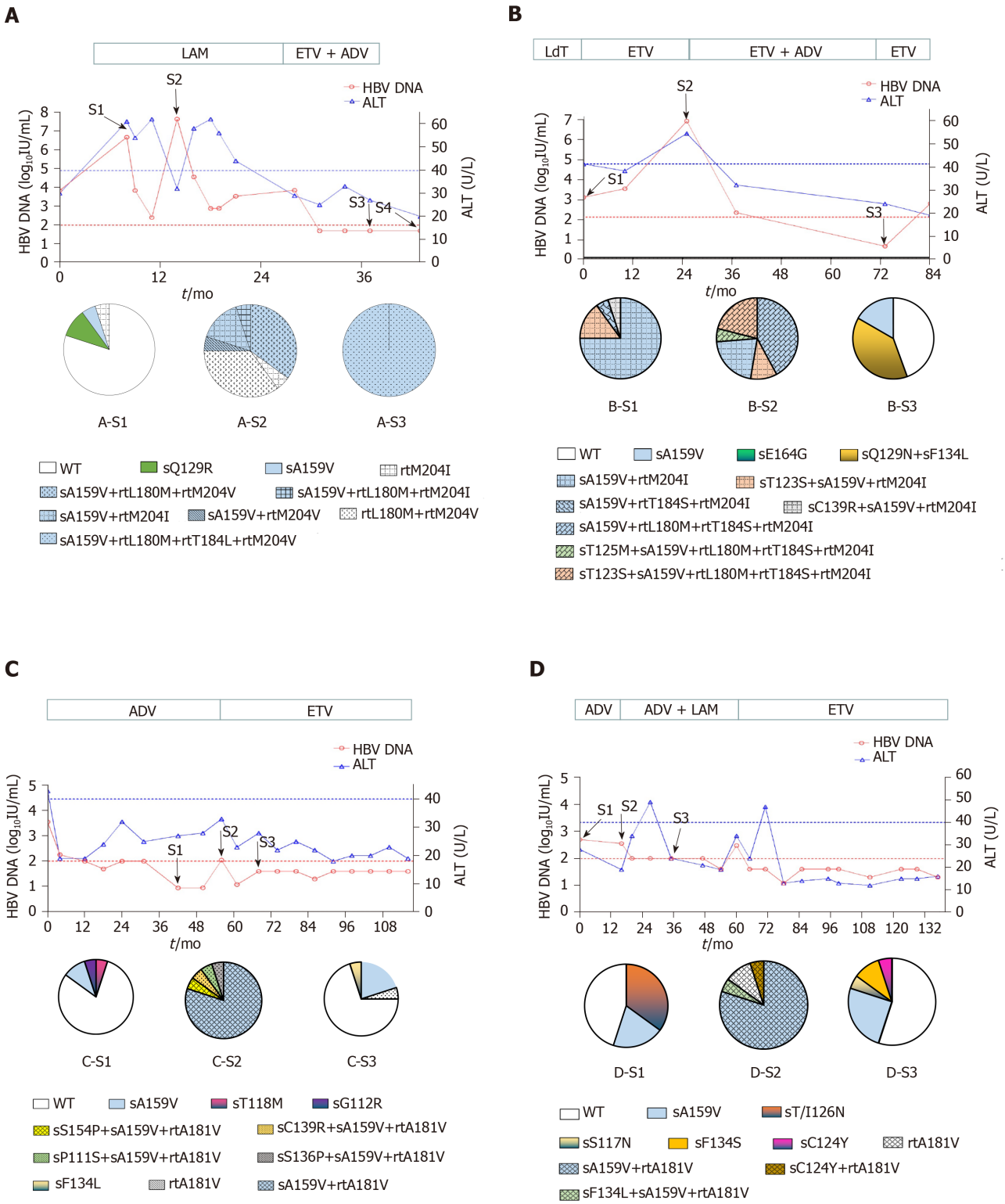
A
LAM
ETV + ADV
HBV DNA
ALT
S1
S2
S3
S4
HBV DNA (log10IU/mL)
ALT (U/L)
t/mo
A-S1
A-S2
A-S3
WT
sQ129R
sA159V
rtM204I
sA159V+rtL180M+rtM204V
sA159V+rtL180M+rtM204I
sA159V+rtM204I
sA159V+rtM204V
rtL180M+rtM204V
sA159V+rtL180M+rtT184L+rtM204V
B
LdT
ETV
ETV + ADV
ETV
HBV DNA
ALT
S1
S2
S3
HBV DNA (log10IU/mL)
ALT (U/L)
t/mo
B-S1
B-S2
B-S3
WT
sA159V
sE164G
sQ129N+sF134L
sA159V+rtM204I
sT123S+sA159V+rtM204I
sA159V+rtT184S+rtM204I
sC139R+sA159V+rtM204I
sA159V+rtL180M+rtT184S+rtM204I
sT125M+sA159V+rtL180M+rtT184S+rtM204I
sT123S+sA159V+rtL180M+rtT184S+rtM204I
C
ADV
ETV
HBV DNA
ALT
S1
S2
S3
HBV DNA (log10IU/mL)
ALT (U/L)
t/mo
C-S1
C-S2
C-S3
WT
sA159V
sT118M
sG112R
sS154P+sA159V+rtA181V
sC139R+sA159V+rtA181V
sP111S+sA159V+rtA181V
sS136P+sA159V+rtA181V
sF134L
rtA181V
sA159V+rtA181V
D
ADV
ADV + LAM
ETV
HBV DNA
ALT
S1
S2
S3
HBV DNA (log10IU/mL)
ALT (U/L)
t/mo
D-S1
D-S2
D-S3
WT
sA159V
sT/I126N
sS117N
sF134S
sC124Y
rtA181V
sA159V+rtA181V
sC124Y+rtA181V
sF134L+sA159V+rtA181V

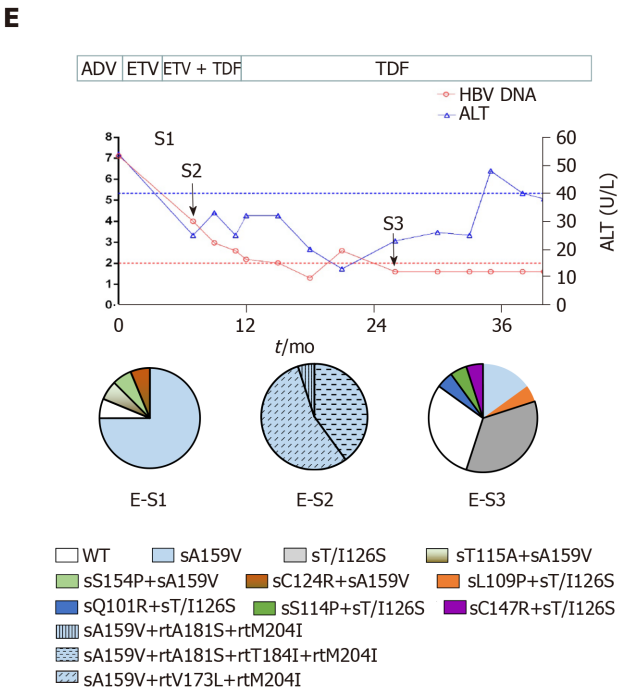

Figure 1 Evolution of drug-resistant hepatitis B virus strains and clinical responses during antiviral therapy in five representative patients. Dynamic changes in serum hepatitis B virus deoxyribonucleic acid (HBV DNA) and alanine aminotransferase (ALT) levels are shown along with antiviral therapies. The duration (months) of antiviral therapy is represented by bars above the graph, and the serum samples from the patient for cloning are indicated by arrows. Two dashed lines show the lower detection limit of HBV DNA (100 IU/mL) and normal ALT levels (40 U/L). Proportions of wild-type and mutant HBV reverse transcriptase from each sample are depicted by a series of pie charts. A: Evolution of drug-resistant hepatitis B virus strains and clinical responses during antiviral therapy in patient A; B:Evolution of drug-resistant hepatitis B virus strains and clinical responses during antiviral therapy in patient B; C:Evolution of drug-resistant hepatitis B virus strains and clinical responses during antiviral therapy in patient C; D:Evolution of drug-resistant hepatitis B virus strains and clinical responses during antiviral therapy in patient D; E:Evolution of drug-resistant hepatitis B virus strains and clinical responses during antiviral therapy in patient E.

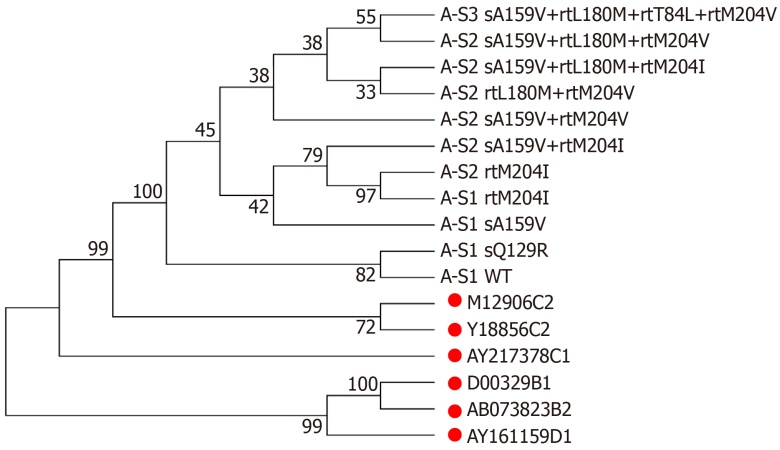

Figure 2 Phylogenetic tree analysis of hepatitis B virus reverse transcriptase sequences from a patient with sA159V + resistance mutations. Reference sequences are marked with solid red circles.

Assessment of drug-induced viral inhibition

A viral inhibition test was performed using the WT and seven mutant strains. Inhibition was evaluated by the levels of HBV replicative intermediates in the samples treated with NAs relative to those in the untreated samples. LAM strongly inhibited WT and M1, with rates of inhibition of 90.5% and 87.5%, respectively. In contrast, LAM-resistant mutants (M2–M5) and ETV-resistant mutants (M6-M7) were highly resistant to LAM, regardless of the presence or absence of the sA159V mutation in the viral genome (Figure 5A). ETV also strongly inhibited WT and M1 with rates of inhibition of 92.5% and 95.6%, respectively. M2–M5 were partially resistant to ETV,

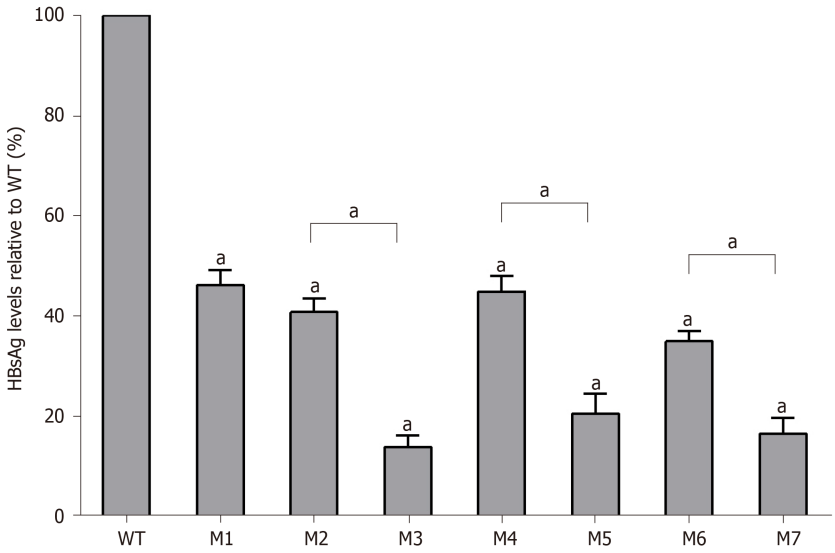

Figure 3 Quantitative analysis of hepatitis B surface antigen levels in individual viral vector-transfected human hepatocellular carcinoma cells. Relative values (%) of mutant hepatitis B surface antigen levels *vs* wild-type levels are shown. Data are expressed as means ± standard deviations. M1, sA159V; M2, rtM204I; M3, sA159V+rtM204I; M4, rtL180M+rtM204V; M5, sA159V+rtL180M+rtM204V; M6, rtL180M+rtT184L+rtM204V; M7,sA159V+rtL180M+rtT184L+rtM204V. $^{a}P < 0.05$ (mutant *vs* wild-type or other indicated mutant).

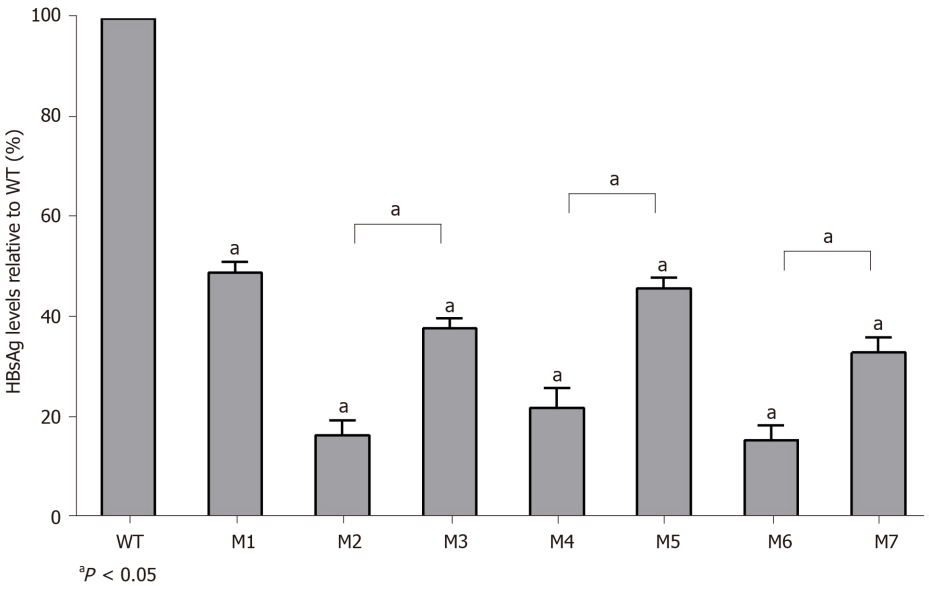

Figure 4 Quantitative analysis of hepatitis B virus deoxyribonucleic acid production levels in individual viral vector-transfected human hepatocellular carcinoma cells. Relative values (%) of mutant hepatitis B virus deoxyribonucleic acid levels *vs* wild-type levels are shown. Data are expressed as the means ± standard deviations. M1, sA159V; M2, rtM204I; M3, sA159V+rtM204I; M4, rtL180M+rtM204V; M5, sA159V+rtL180M+rtM204V; M6,sA159V+rtL180M+rtT184L+rtM204V; M7, rtL180M+rtT184L+rtM204V. $^{a}P < 0.05$ (mutant *vs* wild-type or other indicated mutants).

with 54.9%-64.7% inhibition. M6–M7 were highly resistant to ETV (Figure 5B). All the tested viral strains were highly sensitive to ADV and TDF, with rates of inhibition of 87.29%-95.04% (Figure 5C and D).

DISCUSSION

The clinical implications of immune escape-associated mutations arise from their relationship with occult HBV infections, HBV reactivation, and HB vaccination failure[27-30]. There is a paucity of data from population-based clinical investigations about the link between immune escape-associated mutations and drug-resistance

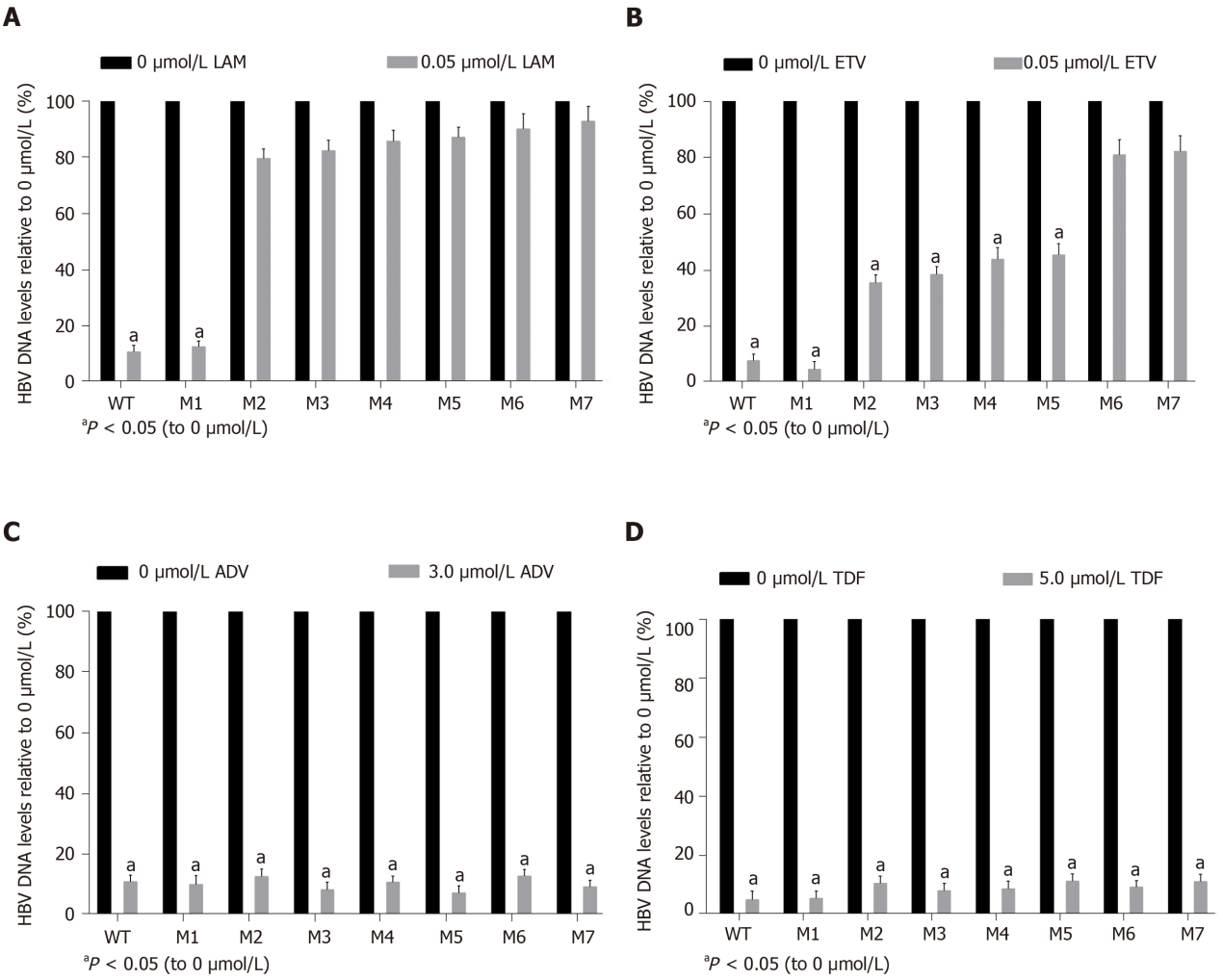

Figure 5 Assessment of drug-induced viral inhibition. Human hepatocellular carcinomas cells were transiently transfected with wild-type or individual viral vectors and cultured with or without one of the following four drugs: (A) 0.05 μmol/L lamivudine, (B) 0.05 μmol/L entecavir, (C) 3.0 μmol/L adefovir, and (D) 5.0 μmol/L tenofovir disoproxil fumarate. Viral inhibition was evaluated as the relative hepatitis B virus deoxyribonucleic acid level of samples with the drug to that without the drug. M1, sA159V; M2, rtM204I; M3, sA159V+rtM204I; M4, rtL180M+rtM204V; M5, sA159V+tL180M+rtM204V; M6, rtL180M+rtT184L+rtM204V; M7, sA159V+rtL180M+rtT184L+rtM204V. $^aP < 0.05$.

mutations. Our analysis of the largest number of resistance mutation-positive patients to date clearly showed that the frequency of immune escape-associated mutations is significantly higher in resistance mutation-positive patients than in resistance mutation-negative patients.

We selected the sA159V mutation for detailed analyses because: (1) Its frequency was significantly higher in resistance mutation-positive patients than in resistance mutation-negative patients; (2) It was frequently detected together with LAM-, ADV-, and ETV-resistance mutations; and (3) Its virological features have not been documented by phenotypic analyses.

In a longitudinal analysis of five patients, the coexistence of sA159V with LAM/ADV/ETV-resistance mutations was frequently detected in the viral pool along with virological breakthrough or an inadequate virological response upon NA therapy. In addition, the sA159V mutation alone was detected before the emergence of the resistance mutation and was recovered after the sA159V-containing resistant mutants were effectively suppressed by rescue therapy. A phylogenetic analysis of Patient A-derived viral strains showed that sA159V+rtM204I (rtL180M) and sA159V+rtM204V (rtL180M) mutants are likely derived from the sA159V mutant as an adaptation to LAM pressure. The sA159V+rtL180M+rtT184L+rtM204V mutant is probably derived from sA159V+rtL180M+rtM204V as an adaptation to ETV pressure.

sA159V mutants had lower HBsAg levels than the WT strain. Viral strains harboring both sA159V and LAM- or ETV-resistance mutations exhibited significantly lower HBsAg levels than their counterpart strains lacking sA159V mutations. In contrast, the HBV DNA levels were partially restored in the LAM- or ETV-resistance viral strains

with sA159V compared to the levels in the WT strain, suggesting that the sA159V mutation has a compensatory effect on replication in resistant viral strains. Notably, the sA159V mutation had no effect on LAM and ETV sensitivity.

In view of these results, it is possible that the sA159V mutation increases the fitness of resistant mutants by alleviating anti-HB immune stress and enhancing viral replication competency rather than by directly increasing drug resistance. This is supported by a previous study demonstrating that two classical immune escape-associated mutations, sG145R and sP120T, significantly reduce HBsAg production and increase the replication capacity of LAM-resistant HBV mutants[31]. Of note, our study was based on patient-derived viral strains rather than artificially generated strains, thus providing convincing evidence.

Nevertheless, *in vitro* experimental data may not always fully reflect *in vivo* processes. In our study, the sA159V mutant had lower HBsAg production than the WT strain. However, sA159V-positive patients had similar serum HBsAg levels to those of sA159V-negative patients. This bias could be explained by the frequent coexistence of the sA159V mutant with the WT virus in these patients. Although a large number of patients were investigated, the study was restricted by the inability to collect serial samples from many patients.

In summary, we provide evidence supporting the influence of HBV immune escape-associated mutations on drug resistance based on a large-scale clinical investigation. We also found that the sA159V mutation might increase the fitness of LAM/ETV-resistant mutants by decreasing the HBsAg levels and increasing the viral replication capacity. These results provide new insights into the association of HBV immune escape with HBV drug resistance.

ARTICLE HIGHLIGHTS

Research background

A large number of patients were surveyed for both immune escape-associated and drug-resistance mutations.

Research motivation

A link between immune escape-associated and resistance mutations was identified.

Research objectives

The association between immune escape-associated mutations and nucleotide analog resistance mutations was evaluated.

Research methods

Upon follow-up, hepatitis B virus (HBV) sA159V was found to have contributed to resistance in several patients.

Research results

HBV sA159V reduced the hepatitis B surface antigen production but increased the replication capacity of lamivudine (LAM)/entecavir (ETV)-resistant mutants.

Research conclusions

sA159V might increase the fitness of LAM/ETV-resistant mutants under environmental pressure in some cases.

Research perspectives

Immune escape-associated and drug-resistance mutations.

ACKNOWLEDGEMENTS

All authors have read and approve the final manuscript, and the authors would like to thank all the individuals who participated in this study. We are grateful to Dai JZ and Yao ZT for their excellent technical assistance.

REFERENCES

1 **Polaris Observatory Collaborators**. Global prevalence, treatment, and prevention of hepatitis B virus infection in 2016: a modelling study. *Lancet Gastroenterol Hepatol* 2018; **3**: 383-403 [PMID: 29599078 DOI: 10.1016/S2468-1253(18)30056-6]

2 **Tang LSY**, Covert E, Wilson E, Kottilil S. Chronic Hepatitis B Infection: A Review. *JAMA* 2018; **319**: 1802-1813 [PMID: 29715359 DOI: 10.1001/jama.2018.3795]

3 **Lok AS**, Zoulim F, Locarnini S, Bartholomeusz A, Ghany MG, Pawlotsky JM, Liaw YF, Mizokami M, Kuiken C; Hepatitis B Virus Drug Resistance Working Group. Antiviral drug-resistant HBV: standardization of nomenclature and assays and recommendations for management. *Hepatology* 2007; **46**: 254-265 [PMID: 17596850 DOI: 10.1002/hep.21698]

4 **Tenney DJ**, Rose RE, Baldick CJ, Pokornowski KA, Eggers BJ, Fang J, Wichroski MJ, Xu D, Yang J, Wilber RB, Colonno RJ. Long-term monitoring shows hepatitis B virus resistance to entecavir in nucleoside-naïve patients is rare through 5 years of therapy. *Hepatology* 2009; **49**: 1503-1514 [PMID: 19280622 DOI: 10.1002/hep.22841]

5 **Zoulim F**, Locarnini S. Optimal management of chronic hepatitis B patients with treatment failure and antiviral drug resistance. *Liver Int* 2013; **33** Suppl 1: 116-124 [PMID: 23286855 DOI: 10.1111/liv.12069]

6 **Zhao Y**, Wu J, Sun L, Liu G, Li B, Zheng Y, Li X, Tao J. Prevalence of mutations in HBV DNA polymerase gene associated with nucleos(t)ide resistance in treatment-naive patients with Chronic Hepatitis B in Central China. *Braz J Infect Dis* 2016; **20**: 173-178 [PMID: 26876337 DOI: 10.1016/j.bjid.2015.12.006]

7 **Park ES**, Lee AR, Kim DH, Lee JH, Yoo JJ, Ahn SH, Sim H, Park S, Kang HS, Won J, Ha YN, Shin GC, Kwon SY, Park YK, Choi BS, Lee YB, Jeong N, An Y, Ju YS, Yu SJ, Chae HB, Yu KS, Kim YJ, Yoon JH, Zoulim F, Kim KH. Identification of a quadruple mutation that confers tenofovir resistance in chronic hepatitis B patients. *J Hepatol* 2019; **70**: 1093-1102 [PMID: 30794889 DOI: 10.1016/j.jhep.2019.02.006]

8 **De Clercq E**. Tenofovir alafenamide (TAF) as the successor of tenofovir disoproxil fumarate (TDF). *Biochem Pharmacol* 2016; **119**: 1-7 [PMID: 27133890 DOI: 10.1016/j.bcp.2016.04.015]

9 **Carrouée-Durantel S**, Durantel D, Werle-Lapostolle B, Pichoud C, Naesens L, Neyts J, Trépo C, Zoulim F. Suboptimal response to adefovir dipivoxil therapy for chronic hepatitis B in nucleoside-naive patients is not due to pre-existing drug-resistant mutants. *Antivir Ther* 2008; **13**: 381-388 [PMID: 18572751]

10 **Rajoriya N**, Combet C, Zoulim F, Janssen HLA. How viral genetic variants and genotypes influence disease and treatment outcome of chronic hepatitis B. Time for an individualised approach? *J Hepatol* 2017; **67**: 1281-1297 [PMID: 28736138 DOI: 10.1016/j.jhep.2017.07.011]

11 **Xue Y**, Wang MJ, Yang ZT, Yu DM, Han Y, Huang D, Zhang DH, Zhang XX. Clinical features and viral quasispecies characteristics associated with infection by the hepatitis B virus G145R immune escape mutant. *Emerg Microbes Infect* 2017; **6**: e15 [PMID: 28325923 DOI: 10.1038/emi.2017.2]

12 **Shirvani-Dastgerdi E**, Winer BY, Celià-Terrassa T, Kang Y, Tabernero D, Yagmur E, Rodríguez-Frías F, Gregori J, Luedde T, Trautwein C, Ploss A, Tacke F. Selection of the highly replicative and partially multidrug resistant rtS78T HBV polymerase mutation during TDF-ETV combination therapy. *J Hepatol* 2017; **67**: 246-254 [PMID: 28392234 DOI: 10.1016/j.jhep.2017.03.027]

13 **Colagrossi L**, Hermans LE, Salpini R, Di Carlo D, Pas SD, Alvarez M, Ben-Ari Z, Boland G, Bruzzone B, Coppola N, Seguin-Devaux C, Dyda T, Garcia F, Kaiser R, Köse S, Krarup H, Lazarevic I, Lunar MM, Maylin S, Micheli V, Mor O, Paraschiv S, Paraskevis D, Poljak M, Puchhammer-Stöckl E, Simon F, Stanojevic M, Stene-Johansen K, Tihic N, Trimoulet P, Verheyen J, Vince A, Lepej SZ, Weis N, Yalcinkaya T, Boucher CAB, Wensing AMJ, Perno CF, Svicher V; HEPVIR working group of the European Society for translational antiviral research (ESAR). Immune-escape mutations and stop-codons in HBsAg develop in a large proportion of patients with chronic HBV infection exposed to anti-HBV drugs in Europe. *BMC Infect Dis* 2018; **18**: 251 [PMID: 29859062 DOI: 10.1186/s12879-018-3161-2]

14 **Zhao L**, Li X, Cheng Y, Chen R, Shao J, Zhou Y, Li Q, Liao H, Zhao Y, Liu L, Su H, Liu Y, Liu Y, Xu D. Hepatitis B virus rtA181T/sW172non-stop mutation may increase resistance fold to adefovir- and entecavir-resistant mutants compared to rtA181T/sW172* mutation. *Antiviral Res* 2018; **154**: 26-34 [PMID: 29630974 DOI: 10.1016/j.antiviral.2018.04.003]

15 **Luo D**, Liu Y, Chen R, Niu M, Liu L, Li X, Li Q, Huang B, Wang J, Xu D, Lin S. Investigation of hepatitis B virus (HBV) rtS78T/sC69* mutation in a large cohort of chronic HBV-infected patients with nucleoside/nucleotide analogue treatment. *Antiviral Res* 2019; **170**: 104579 [PMID: 31398372 DOI: 10.1016/j.antiviral.2019.104579]

16 **Ganji A**, Esmaeilzadeh A, Ghafarzadegan K, Helalat H, Rafatpanah H, Mokhtarifar A. Correlation between HBsAg quantitative assay results and HBV DNA levels in chronic HBV. *Hepat Mon* 2011; **11**: 342-345 [PMID: 22087158]

17 **Chen BF**. Hepatitis B virus pre-S/S variants in liver diseases. *World J Gastroenterol* 2018; **24**: 1507-1520 [PMID: 29662289 DOI: 10.3748/wjg.v24.i14.1507]

18 **Ding H**, Liu B, Zhao C, Yang J, Yan C, Yan L, Zhuang H, Li T. Amino acid similarities and divergences in the small surface proteins of genotype C hepatitis B viruses between nucleos(t)ide analogue-naïve and lamivudine-treated patients with chronic hepatitis B. *Antiviral Res* 2014; **102**: 29-34 [PMID: 24316031 DOI: 10.1016/j.antiviral.2013.11.015]

19 **Shan M**, Shen Z, Sun H, Zheng J, Zhang M. The enrichment of HBV immune-escape mutations during nucleoside/nucleotide analogue therapy. *Antivir Ther* 2017; **22**: 717-720 [PMID: 28300730 DOI: 10.3851/IMP3156]

20 **Chen J**, Liu Y, Zhao J, Xu Z, Chen R, Si L, Lu S, Li X, Wang S, Zhang K, Li J, Han J, Xu D. Characterization of Novel Hepatitis B Virus PreS/S-Gene Mutations in a Patient with Occult Hepatitis B Virus Infection. *PLoS One* 2016; **11**: e0155654 [PMID: 27182775 DOI: 10.1371/journal.pone.0155654]

21 **Zhang K**, Liu Y, Chen R, Li Q, Xu Z, Si L, Cheng Y, Yang Y, Chen J, Xu D, Lin S. Antigenicity reduction contributes mostly to poor detectability of HBsAg by hepatitis B virus (HBV) S-gene mutants isolated from individuals with occult HBV infection. *J Med Virol* 2018; **90**: 263-270 [PMID: 28876463 DOI: 10.1002/jmv.24936]

22 **Chinese Society of Hepatology, Chinese Medical Association**. Chinese Society of Infectious Diseases, Chinese Medical Association. Guideline on prevention and treatment of chronic hepatitis B in China (2005). *Chin Med J (Engl)* 2007; **120**: 2159-2173 [PMID: 18167196]

23 **Xu Z**, Liu Y, Xu T, Chen L, Si L, Wang Y, Ren X, Zhong Y, Zhao J, Xu D. Acute hepatitis B infection associated with drug-resistant hepatitis B virus. *J Clin Virol* 2010; **48**: 270-274 [PMID: 20580309 DOI: 10.1016/j.jcv.2010.05.010]

24 **Liu Y**, Zhou Y, Li X, Niu M, Chen R, Shao J, Si L, Luo D, Lin Y, Li L, Zhang K, Xiao X, Xu Z, Liu M, Lu M, Zoulim F, Xu D. Hepatitis B virus mutation pattern rtL180M+A181C+M204V may contribute to entecavir resistance in clinical practice. *Emerg Microbes Infect* 2019; **8**: 354-365 [PMID: 30866789 DOI: 10.1080/22221751.2019.1584018]

25 **Liu L**, Liu Y, Chen R, Li X, Luo D, Zhao Y, Li Q, Huang B, Wang FS, Liu X, Xu D. Prevalence of the entecavir-resistance-inducing mutation rtA186T in a large cohort of Chinese hepatitis B virus patients. *Antiviral Res* 2019; **164**: 131-138 [PMID: 30796932 DOI: 10.1016/j.antiviral.2019.02.012]

26 **Liu Y**, Wu C, Chen R, Li X, Xu Z, Li Q, Li L, Wang FS, Yang D, Lu M, Xu D. Molecular cloning and phenotypic analysis of drug-resistance mutants with relevant S-region variants of HBV for a patient during 189-month anti-HBV treatment. *Antivir Ther* 2019; **24**: 237-246 [PMID: 30882363 DOI: 10.3851/IMP3305]

27 **Pollicino T**, Cacciola I, Saffioti F, Raimondo G. Hepatitis B virus PreS/S gene variants: pathobiology and clinical implications. *J Hepatol* 2014; **61**: 408-417 [PMID: 24801416 DOI: 10.1016/j.jhep.2014.04.041]

28 **Tang Z**, Li X, Wu S, Liu Y, Qiao Y, Xu D, Li J. Risk of hepatitis B reactivation in HBsAg-negative/HBcAb-positive patients with undetectable serum HBV DNA after treatment with rituximab for lymphoma: a meta-analysis. *Hepatol Int* 2017; **11**: 429-433 [PMID: 28856548 DOI: 10.1007/s12072-017-9817-y]

29 **Hsu HY**, Chang MH, Ni YH, Chiang CL, Wu JF, Chen HL. Universal infant immunization and occult hepatitis B virus infection in children and adolescents: a population-based study. *Hepatology* 2015; **61**: 1183-1191 [PMID: 25501911 DOI: 10.1002/hep.27650]

30 **Wu CC**, Chen YS, Cao L, Chen XW, Lu MJ. Hepatitis B virus infection: Defective surface antigen expression and pathogenesis. *World J Gastroenterol* 2018; **24**: 3488-3499 [PMID: 30131655 DOI: 10.3748/wjg.v24.i31.3488]

31 **Amini-Bavil-Olyaee S**, Vucur M, Luedde T, Trautwein C, Tacke F. Differential impact of immune escape mutations G145R and P120T on the replication of lamivudine-resistant hepatitis B virus e antigen-positive and -negative strains. *J Virol* 2010; **84**: 1026-1033 [PMID: 19889778 DOI: 10.1128/JVI.01796-09]

World Journal of Gastroenterology

Submit a Manuscript: https://www.f6publishing.com

World J Gastroenterol 2020 September 21; 26(35): 5328-5342

DOI: 10.3748/wjg.v26.i35.5328

ISSN 1007-9327 (print) ISSN 2219-2840 (online)

ORIGINAL ARTICLE

Retrospective Study

RBBP4 promotes colon cancer malignant progression *via* regulating Wnt/β-catenin pathway

Yan-Dong Li, Zhen Lv, Wei-Fang Zhu

ORCID number: Yan-Dong Li 0000-0002-7247-6898; Zhen Lv 0000-0002-6487-6023; Wei-Fang Zhu 0000-0003-2587-0160.

Author contributions: Li YD designed, supervised the study and provided consultation during the entire study; Lv Z performed the research; Zhu WF analyzed the data and wrote the manuscript; all authors have read and approved the final manuscript.

Supported by Zhejiang Provincial Natural Science Foundation of China, No. LQ18H160011 and No. LY20H030011.

Institutional review board statement: The study was reviewed and approved by the Research Ethics Committee of the First Affiliated Hospital, School of Medicine, Zhejiang University Institutional Review Board, No. 2019-290.

Conflict-of-interest statement: No benefits in any form have been received or will be received from a commercial party related directly or indirectly to the subject of this article.

Data sharing statement: Technical appendix, statistical code, and dataset available from the corresponding author at

Yan-Dong Li, Division of Colon and Rectal Surgery, The First Affiliated Hospital, Zhejiang University School of Medicine, Hangzhou 310003, Zhejiang Province, China

Zhen Lv, Department of Surgery, Division of Hepatobiliary and Pancreatic Surgery, The First Affiliated Hospital, Zhejiang University School of Medicine, Hangzhou 310003, Zhejiang Province, China

Wei-Fang Zhu, Division of Dermatology, The First Affiliated Hospital, Zhejiang University School of Medicine, Hangzhou 310003, Zhejiang Province, China

Corresponding author: Wei-Fang Zhu, MD, Assistant Professor, Division of Dermatology, The First Affiliated Hospital, Zhejiang University School of Medicine, No. 79 Qingchun Road, Hangzhou 310003, Zhejiang Province, China. wfzhu@163.com

Abstract

BACKGROUND

Our previous study demonstrated that RBBP4 was upregulated in colon cancer and correlated with poor prognosis of colon cancer and hepatic metastasis. However, the potential biological function of RBBP4 in colon cancer is still unknown.

AIM

To investigate the biological role and the potential mechanisms of RBBP4 in colon cancer progression.

METHODS

Real-time polymerase chain reaction and western blot analysis were used to detect the expression of RBBP4 in colon cancer cell lines. The cell proliferation and viability of SW620 and HCT116 cells with RBBP4 knockdown was detected by Cell Counting Kit-8 and 5-ethynyl-2′-deoxyuridine staining. The transwell assay was used to detect the invasion and migration capabilities of colon cancer cells with RBBP4 knockdown. Flow cytometry apoptosis assay was used to detect the apoptosis of colon cancer cells. Western blotting analysis was used to detect the expression of epithelial-mesenchymal transition and apoptosis related markers in colon cancer. The nuclear translocation of β-catenin was examined by Western blotting analysis in colon cancer cells with RBBP4 knockdown. The TOPFlash luciferase assay was used to detect the effect of RBBP4 on Wnt/β-catenin activation. The rescue experiments were performed in colon cancer cells treated

Wfzhu@163.com. Participants gave informed consent for data sharing.

Manuscript source: Unsolicited manuscript

Received: July 6, 2020
Peer-review started: July 6, 2020
First decision: July 28, 2020
Revised: August 7, 2020
Accepted: August 26, 2020
Article in press: August 26, 2020
Published online: September 21, 2020

P-Reviewer: Yu H
S-Editor: Yan JP
L-Editor: Filipodia
P-Editor: Ma YJ

with Wnt/β-catenin activator LiCl and RBBP4 knockdown.

RESULTS

We found that RBBP4 was highly expressed in colon cancer cell lines. The 5-ethynyl-2′-deoxyuridine assay showed that knockdown of RBBP4 significantly inhibited cell proliferation. RBBP4 inhibition reduced cell invasion and migration *via* regulating proteins related to epithelial-mesenchymal transition. Knockdown of RBBP4 significantly inhibited survivin-mediated apoptosis. Mechanistically, the TOPFlash assay showed that RBBP4 knockdown increased activity of the Wnt/β-catenin pathway. Meanwhile, RBBP4 knockdown suppressed nuclear translocation of β-catenin. With Wnt/β-catenin activator, rescue experiments suggested that the role of RBBP4 in colon cancer progression was dependent on Wnt/β-catenin pathway.

CONCLUSION

RBBP4 promotes colon cancer development *via* increasing activity of the Wnt/β-catenin pathway. RBBP4 may serve as a novel therapeutic target in colon cancer.

Key Words: Colon cancer; Wnt/β-catenin; RBBP4; Epithelial-mesenchymal transition; Apoptosis; Invasion

Core Tip: Our previous study demonstrated upregulation of RBBP4 in colon cancer and correlation of poor prognosis with colon cancer and hepatic metastasis. This study explored the potential biological function of RBBP4 in colon cancer. We found that RBBP4 was highly expressed in colon cancer cell lines. Knockdown of RBBP4 significantly inhibited cell proliferation and survivin-mediated apoptosis and suppressed nuclear translocation of β-catenin. RBBP4 inhibition reduced cell invasion and migration *via* regulating proteins related to epithelial–mesenchymal transition. Mechanistically, RBBP4 knockdown increased activity of the Wnt/β-catenin pathway. RBBP4 may serve as a novel therapeutic target in colon cancer.

Citation: Li YD, Lv Z, Zhu WF. RBBP4 promotes colon cancer malignant progression *via* regulating Wnt/β-catenin pathway. *World J Gastroenterol* 2020; 26(35): 5328-5342
URL: https://www.wjgnet.com/1007-9327/full/v26/i35/5328.htm
DOI: https://dx.doi.org/10.3748/wjg.v26.i35.5328

INTRODUCTION

Colon cancer is one of the most common malignancies in developed countries. There are more than one million new cases of colon cancer worldwide and 608000 deaths every year[1]. Although the treatment of colon cancer has made great progress, including surgery or radiotherapy and chemotherapy, the prognosis of patients with colon cancer has shown no marked progress in recent years[2]. The 5-year relative survival rate of patients with stage IV disease is slightly higher than 10%[3,4]. Although considerable efforts have been made in the past few years to clarify the mechanisms underlying the development and progression of colon cancer, it is still far from completely understood. Hence, it is necessary to explore the further mechanisms involved in the pathogenesis of colon cancer and to develop new therapeutic targets.

RBBP4 is a new, 48-kD tumor-specific protein found in HeLa cell lysates[5,6]. RBBP4 belongs to a highly conserved subfamily of nucleoproteins with four WD repeat sequences. RBBP4 binds to retinoblastoma protein *in vivo* and *in vitro*, hence the name[7]. The *RBBP4* gene encodes a protein that is part of several chromatin-modified protein complexes, such as nucleosome remodeling and deacetylation complex[8], polycomb repressor complex 2[9], and SIN3-chromatin modulating complexes[10], which influence gene transcription, and regulates cell cycle and proliferation[11]. In recent decades, accumulated research has demonstrated that RBBP4 plays a key role in the pathogenesis of cancers, such as liver[12], breast[13], and gastric[14,15] cancers. In our previous study, we proved that RBBP4 is upregulated in colon cancer and may serve

as a novel predictor for poor prognosis of colon cancer and liver metastasis[16]. However, its potential role and mechanisms in colon cancer have not been reported.

Therefore, the present study aimed to explore the potential role of RBBP4 in colon cancer aggravation and the underlying molecular mechanisms. We detected expression of RBBP4 in colon cancer cell lines, then investigated the role of RBBP4 in colon cancer cell proliferation, migration, invasion, and apoptosis and finally explored the molecular mechanisms of RBBP4 in colon cancer malignancy characteristics. This study clarifies the role of RBBP4 in colon cancer development through its effect on the Wnt/b-catenin signaling pathway.

MATERIALS AND METHODS

Cell culture

A normal human colon cell line (NCM640) and colon cancer cell lines (SW620, HT29, LoVo, SW480, and HCT-116) were purchased from the Cell Bank of Type Culture Collection of the Chinese Academy of Sciences (Shanghai, China). These cell lines originated from the American Type Culture Collection (ATCC, Manassas, VA, United States). All the cell lines were cultured in the corresponding medium according to the suggestion of ATCC with 10% fetal bovine serum (FBS). All the cells were maintained in a humidified incubator with 5% CO_2 at 37 °C. The Wnt/β-catenin activator LiCl was obtained from Sigma-Aldrich (Munich, Germany).

Plasmids, siRNA, and transfection

The plasmids of the human *RBBP4* gene, siRNA targeting human RBBP4, and their controls were synthesized by Genechem (Shanghai, China). The cells were transfected with siRNAs, plasmids, or their controls using Lipofectamine 3000 (Invitrogen, Carlsbad, CA, United States). In total, 2×10^5–3×10^5 cells were transfected with 100 pmol siRNA or 2 μg plasmid DNA. Western blotting was used to detect the transfection efficiency 24 h and 48 h after transfection, and real-time polymerase chain reaction was used for verification.

Real time polymerase chain reaction detection

Total RNA from colon cancer tissues and cells was extracted using TRIzol reagent (Invitrogen). Total RNA (0.5 μg) was reversed transcribed to cDNA using PrimeScript™ RT reagent Kit with gDNA Eraser (Takara, Dalian, China). SYBR Green Polymerase Chain Reaction Master mix (Takara) was used to determine the mRNA level of *RBBP4* on an ABI 7900Fast Real-time Detection System (Applied Biosystems, Carlsbad, CA, United States) in 20 μL reaction system. All reactions were performed in triplicate. The relative expression of *RBBP4* was normalized to the internal reference *GAPDH*. The 2^{-DDCT} method was used to analyze the data. The primers used in the study were as follows: *GAPDH* forward primer: 5'-ATG GGG AAG GTG AAG GTC G-3', *GAPDH* reverse primer: 5'-GGG GTC ATT GAT GGC AAC AAT A-3'; *RBBP4* forward primer: 5'-GCT ATG GGC TTT CTT GGA-3', and *RBBP4* reverse primer: 5'-CAC AGG CAG ATG GTA TGG-3'.

Cell Counting Kit-8 assay

Cell viability was assessed by Cell Counting Kit-8 (CCK-8) assay (Dojindo Laboratories, Kumamoto, Japan). Cells were seeded in 96-well plates at 3×10^3 cells per well with 200 μL culture medium. With supernatant removed, 10 μL CCK-8 reagent in 100 μL medium was added to each well at 0 h, 24 h, 48 h, 72 h, and 96 h. The plates were incubated in the dark at 37 °C for 2 h, and absorbance at 450 nm was detected with a microplate reader (BioTek, Winooski, VT, United States). The experiments were performed in triplicate.

5-Ethynyl-2'-deoxyuridine cell proliferation assay

5-Ethynyl-2'-deoxyuridine (EdU) assay was performed using Click-iT™ EdU Imaging Kit with Alexa Fluor™ 488 Azides (Invitrogen). Briefly, 1×10^5 cells were plated in six-well plates and incubated at room temperature overnight. The cells were incubated with 10 μM EdU for 1 h at 37 °C and fixed in 3.7% paraformaldehyde. After permeabilization with 0.5% Triton X-100 in phosphate buffered saline for 20 min, the cells were reacted with 1 × Click-iT® reaction cocktail for 20 min. The nuclei were labeled with Hoechst 33342 for 30 min and photographed under a fluorescence microscope. All studies were conducted in triplicate.

Western blotting

Total proteins were extracted using the ice cold radioimmunoprecipitation assay buffer with cocktail protease and phosphatase inhibitors (Cell Signaling Technology, Danvers, MA, United States). NE-PER™ Nuclear and Cytoplasmic Extraction Reagent (Thermo Scientific, Waltham, MA, United States) was used to extract the nuclear and cytoplasmic proteins. Proteins were quantified using a BCA protein assay kit (Thermo Scientific). Then equivalent proteins were separated by 10% SDS-PAGE and transferred to polyvinylidene fluoride membranes (Millipore, Billerica, MA, United States). The membranes were probed with antibodies against RBBP4 (ab92344), survivin (ab134170), GAPDH (ab181620), β-catenin (ab32572), pro-caspase-3 (ab32150) (Abcam, Cambridge, MA, United States), Cleaved caspase-3 (9661), E-cadherin (14472), N-cadherin (13116), vimentin (5741), and histone H3 (14269) (Cell Signaling Technology) overnight at 4 °C and then incubated with horseradish-peroxidase-conjugated secondary antibodies (Cell Signaling Technology) for 1 h at room temperature. The bands were visualized by ECL kit (Millipore).

Migration and invasion assay

The migration and invasion assays were performed by the transwell method. For the invasion assay, the cells were plated on Matrigel-coated upper chambers (24-well inserts; pore size, 8 mm; BD Biosciences, San Jose, CA, United States). For the migration assay, the cells were plated on uncoated upper chambers. In the lower wells, medium was replaced with fresh medium with 5% FBS. The cells were incubated for 24 h in medium containing 1% FBS, trypsinized, and suspended in medium containing 1% FBS at a final concentration of 1×10^6 cells/mL. Then, 200 μL cell suspension was placed in each of the upper wells, and the chamber was incubated at 37 °C for 24 h. Cells were fixed and stained with hematoxylin and eosin. The nonmigrating cells from the upper surface of the filter were wiped with a cotton swab. The cells that migrated to the lower side of the filter were counted and photographed with an optical inverted microscope. Five random fields in each assay were counted and averaged.

Flow cytometry analysis of apoptosis

For the assessment of apoptosis, an Annexin V–FITC/propidium iodide (PI) apoptosis detection kit (BD Biosciences) was used. Colon cancer cells were collected in six-well plates at 1×10^6 cells/mL. After transfection for 48 h, the cells were trypsinized and washed once with phosphate buffered saline. After centrifugation at 1000 r/min for 5 min, the cells were stained with 5 μL Annexin V–FITC and PI in the dark condition for 30 min, and then were analyzed by flow cytometry (BD Biosciences). At least 10000 events were recorded for each sample. The apoptosis data were analyzed by FlowJo V10 software (Tree Star, San Francisco, CA, United States).

Luciferase assays

The TOPFlash assay was performed using the T-cell factor Reporter Plasmid Kit (Millipore). The ratio of luciferase activities from a T-cell factor-responsive reporter (pTOPFlash) *vs* a control luciferase reporter gene construct (pFOPFlash) was determined 48 h after transfection with Lipofectamine 2000 in SW480 and HCT116 cells. Luciferase activities were normalized for transfection efficiency by cotransfection with a β-galactosidase-expressing vector. The cells were transfected with siRBBP4 plasmid or RBBP4 plasmid or control plasmids. The cells were harvested after 24 h and processed for luciferase and β-galactosidase activities, and the data were normalized to β-galactosidase levels.

Statistical analysis

Statistical analyses were performed using GraphPad Prism version 7.0 (GraphPad Software, La Jolla, CA, United States) software and verified by SPSS version 20.0 (SPSS, Chicago, IL, United States). Each experiment was performed at least in triplicate, and the results were expressed as the mean ± standard deviation. Student's *t* test and one-way analysis of variance were conducted to analyze the differences between groups, and a $P < 0.05$ was considered statistically significant.

RESULTS

RBBP4 is upregulated in human colon cancer cell lines

In our previous study, we detected the expression pattern of RBBP4 in colon cancer

tissues and proved that RBBP4 was upregulated. In the present study, we examined the protein and mRNA levels of RBBP4 in five human colon cancer cell lines and a normal human colon cell line. mRNA and protein levels of RBBP4 were significantly higher in colon cancer cell lines compared with the normal human colon cell line. We selected SW480 and HCT116 cells with high RBBP4 levels for subsequent experiments (Figure 1A and 1B).

Knockdown of RBBP4 inhibited cell growth in vitro

To investigate the biological function of RBBP4 in colon cancer cells, we knocked down RBBP4 *via* siRNA-mediated gene silencing. The knockdown efficiency was determined by Western blotting (Figure 1C). We then examined the role of RBBP4 in colon cancer cell viability using the CCK-8 assay. Cell viability was decreased in both HCT116 and SW620 cells after RBBP4 knockdown (Figure 1D and 1E). EdU proliferation assay showed that RBBP4 knockdown significantly reduced proliferation of colon cancer cells (Figure 1F and 1G). These results showed that RBBP4 played an essential role in the growth of colon cancer cells.

RBBP4 knockdown receded migration and invasion of colon cancer cells

We examined the effect of RBBP4 knockdown on colon cancer cell migration and invasion *in vitro* using the transwell assay. The number of migrated and invasive cells in RBBP4 knockdown HCT116 and SW620 colon cancer cells was less than that in the control group (Figure 2A and 2B). The epithelial-mesenchymal transition (EMT) pathway has been proved to play a key role in tumor migration and invasion[17]. To investigate the molecular mechanisms of RBBP4 in regulating colon cancer cell migration and invasion, we performed Western blotting to detect expression of EMT-related proteins including N-cadherin, E-cadherin, and vimentin. RBBP4 knockdown markedly decreased mesenchymal proteins, but upregulated epidermal protein expression (Figure 2C). These results indicated that RBBP4 regulated colon cancer cell migration and invasion *via* the EMT pathway.

RBBP4 knockdown aggravated apoptosis of colon cancer cells

To investigate the mechanism underlying RBBP4-knockdown-induced antiproliferation, we detected the apoptotic rate of colon cancer cells by flow cytometry. Apoptosis rate in HCT116 and SW620 cells with RBBP4 knockdown increased by 42.0% ± 2.2% and 33.3% ± 2.91%, respectively, compared with the control cells (12.95% ± 1.40% and 10.83% ± 0.93%, $P < 0.01$, Figure 3A and 3B). To investigate the molecular mechanisms of RBBP4 in regulating colon cancer cell apoptosis, we detected apoptosis-related proteins, and showed that survivin, an antiapoptotic protein, was downregulated after RBBP4 knockdown, thus leading to the increase of pro-caspase-3 and cleaved caspase-3.

RBBP4 knockdown suppressed activity of the Wnt/β-catenin pathway in colon cancer cells

The Wnt/β-catenin pathway is one of the important signaling pathways inducing EMT, and survivin is a known downstream target of the pathway[17-19]. We hypothesized that the biological role of RBBP4 was executed through the Wnt/β-catenin pathway. To clarify this hypothesis, the TOP/FOP flash luciferase reporter assays were used. Compared with the control cells, overexpression of RBBP4 led to an increase of TOP flash luciferase reporter activity in HCT116 and SW620 cells (Figure 4A and 4B). However, RBBP4 knockdown inhibited the activity of the TOP flash luciferase reporter (Figure 4A and 4B). As reported previously, β-catenin nuclear translocation is an essential event for Wnt/β-catenin pathway activation. To elucidate further the underlying mechanism, we examined the influence of RBBP4 on β-catenin nuclear translocation in colon cancer cells. The level of β-catenin in the nucleus was decreased, while that in cytoplasm was increased by RBBP4 knockdown (Figure 4C). All these data indicated that activity of the Wnt/β-catenin pathway was regulated by RBBP4 *via* regulation of the nuclear translocation of the β-catenin protein in colon cancer cells.

Function of RBBP4 in colon cancer cells was mediated by the Wnt/β-catenin pathway

To examine whether the function of RBBP4 in colon cancer was mediated by the Wnt/β-catenin pathway, we used the Wnt/β-catenin pathway activator LiCl in a rescue experiment. The role of RBBP4 knockdown on the inhibition of β-catenin

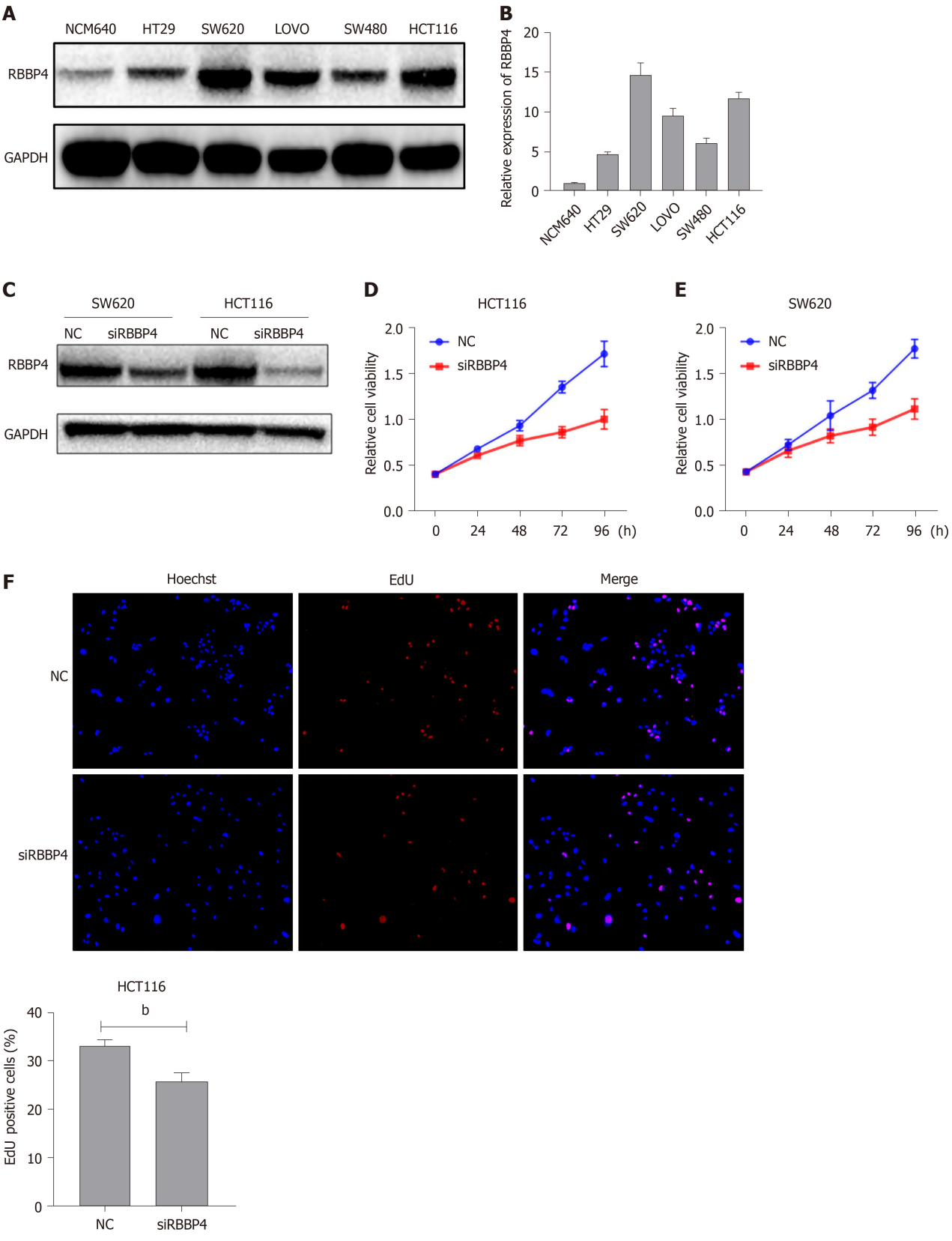
A
NCM640
HT29
SW620
LOVO
SW480
HCT116
RBBP4
GAPDH
B
Relative expression of RBBP4
20
15
10
5
0
NCM640
HT29
SW620
LOVO
SW480
HCT116
C
SW620
HCT116
NC
siRBBP4
NC
siRBBP4
RBBP4
GAPDH
D
HCT116
NC
siRBBP4
Relative cell viability
2.0
1.5
1.0
0.5
0.0
0
24
48
72
96
(h)
E
SW620
NC
siRBBP4
Relative cell viability
2.0
1.5
1.0
0.5
0.0
0
24
48
72
96
(h)
F
Hoechst
EdU
Merge
NC
siRBBP4
HCT116
b
EdU positive cells (%)
40
30
20
10
0
NC
siRBBP4

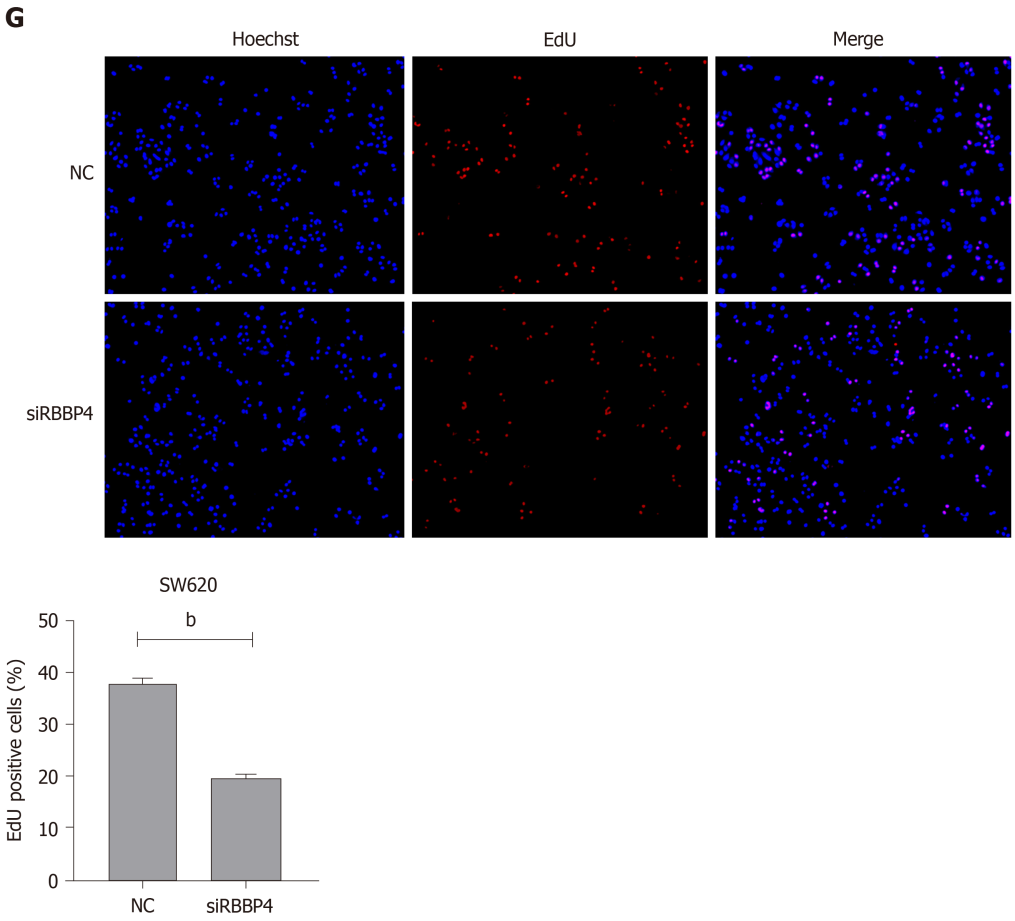

Figure 1 Expression of RBBP4 in colon cancer cell lines and its effect on cell proliferation. A: Protein level of RBBP4 in the colon cancer cell lines quantified by western blotting; B: mRNA level of *RBBP4* in the colon cancer cell lines quantified by polymerase chain reaction; C: RBBP4 siRNA efficiency verified by western blotting in SW620 and HCT116 cells; D: Cell viability was detected by the Cell Counting Kit-8 assay in HCT116 cells; E: Cell viability was detected by the Cell Counting Kit-8 assay in SW620 cells; F and G: Cell proliferation was detected by 5-ethynyl-2'-deoxyuridine assay in HCT116 cells and SW620 cells. $^{b}P < 0.01$ *vs* controls. EdU: 5-Ethynyl-2'-deoxyuridine.

nuclear translocation was partly reversed by LiCl (Figure 5A). CCK-8 assays showed that the viability of HCT116 and SW620 cells treated with RBBP4 siRNA was significantly enhanced when they were cotreated with LiCl compared with untreated cells ($P < 0.05$, Figure 5B and 5C). The transwell assay showed that the inhibition of invasion by RBBP4 knockdown was partly reversed by LiCl ($P < 0.05$, Figure 5C and 5D). The expression of EMT-related proteins was also partly reversed by LiCl compared with the shRBBP4 group (Figure 5E). All these results suggested that the role of RBBP4 in colon cancer progression is mediated by the Wnt/β-catenin pathway.

DISCUSSION

RBBP4, also known as RbAp48, is named for its ability to bind to retinoblastoma proteins *in vivo* and *in vitro*[20]. Previous studies showed that the RBBP4 protein is a component of a variety of complexes involved in chromatin assembly, remodeling, and nucleosome modification, such as SIN3[21], polycomb repressor complex 2[22,23], histone acetyltransferase 1[24], and chromatin assembly factor 1[25] and plays a different role in each complex. It has been demonstrated that RBBP4 expression is upregulated and correlated with the malignant phenotypes in many types of human tumors, such as lung cancer[26], liver cancer[27], thyroid carcinoma[28], and acute lymphoblastic leukemia[29]. However, little is known about RBBP4 in colon cancer.

In our previous study, we demonstrated that RBBP4 was upregulated in colon cancer tissues, and elevated RBBP4 level was correlated with poor prognosis and liver metastasis. Nevertheless, the detailed molecular biological function of RBBP4 and the potential mechanisms in colon cancer are unclear. In the present study, our evidence indicated that RBBP4 knockdown decreased the proliferation, apoptosis, and

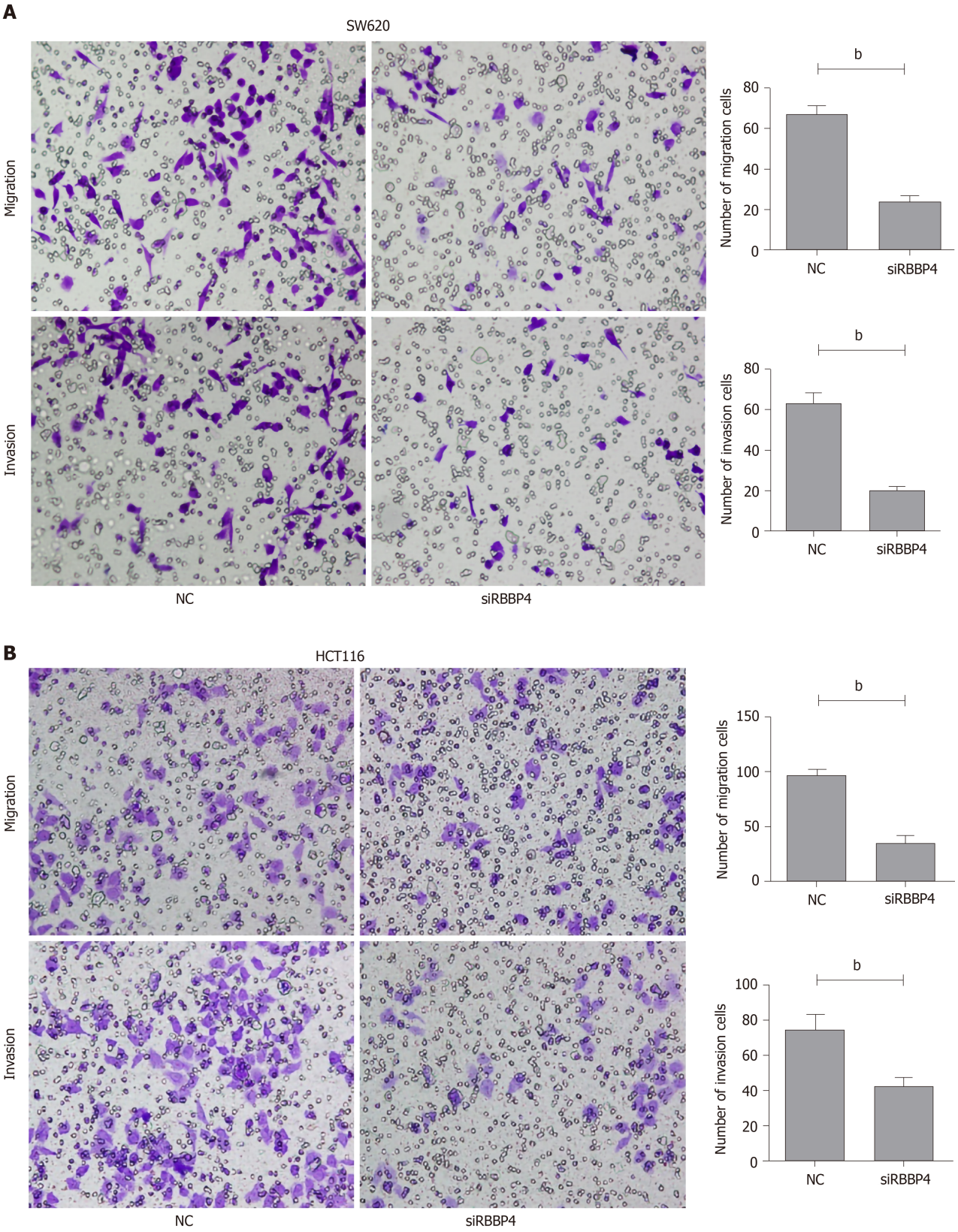
A
SW620
Migration
Invasion
NC
siRBBP4
b
Number of migration cells
Number of invasion cells
0
20
40
60
80
B
HCT116
Migration
Invasion
NC
siRBBP4
b
Number of migration cells
Number of invasion cells
0
50
100
150
0
20
40
60
80
100

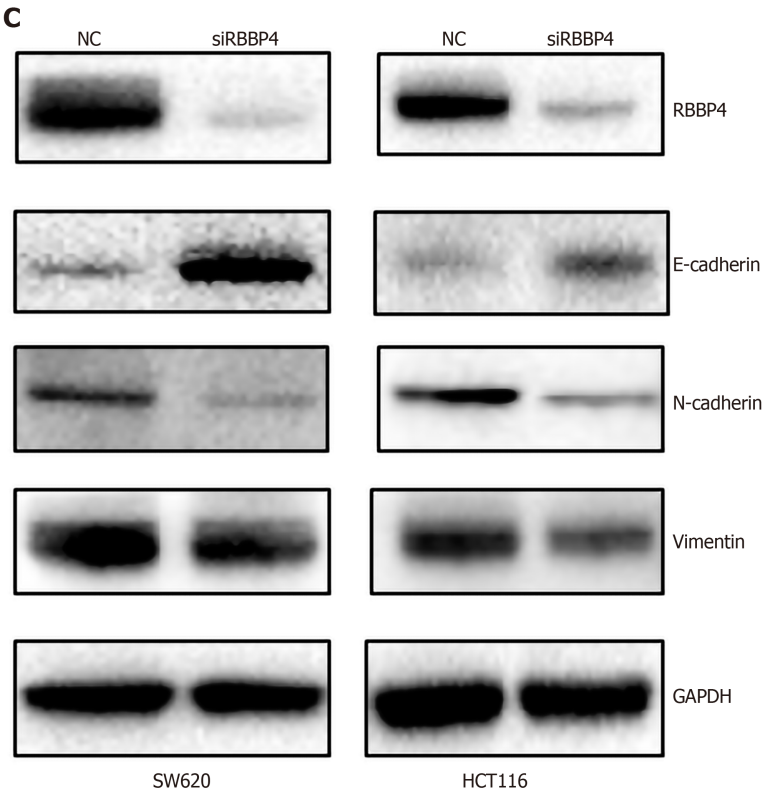

Figure 2 RBBP4 knockdown inhibits migration and invasion of colon cancer cell lines. A: Migration and invasion of RBBP4 knockdown SW620 cells were measured by the transwell assay. Results were quantitated by counting migrating and invasive cells in five randomly chosen high-power fields for each replicate; B: Migration and invasion of RBBP4 knockdown HCT116 cells were measured by the transwell assay; C: Western blotting examination for epithelial-mesenchymal transition related proteins. $^{b}P < 0.01$ *vs* controls.

aggressiveness of colon cancer cells, suggesting its oncogenic functions in colon cancer progression. RBBP4 promoted the nuclear accumulation of β-catenin, thus activating the Wnt/β-catenin signaling pathway. The role of RBBP4 in colon cancer progression was partially dependent on Wnt/β-catenin signaling pathway.

Abnormalities in the Wnt signaling pathway are associated with a variety of tumor types, including colon cancer[30,31]. The Wnt pathway is classified into canonical and noncanonical pathways; the former of which is β-catenin dependent[32]. For the canonical pathway, in the absence of Wnt ligands, free cytoplasmic β-catenin binds to cytoplasmic complexes containing *Adenomatous Polyposis Coli*, axin, casein kinase 1a, and glycogen synthase kinase 3b, which promotes the phosphorylation of β-catenin leading to β-catenin ubiquitination and subsequent proteasomal degradation. The interaction between Wnt and Frizzled leads to the activation of the Disheveled family proteins. The activated Disheveled proteins cause the inhibition of glycogen synthase kinase 3b, resulting in the accumulation of free cytoplasmic β-catenin, which is then transported to the nucleus. In the nucleus, β-catenin binds to various transcription factors, such as T-cell factor and lymphoid enhancer factor 1, to activate Wnt target genes[33-35]. However, the relationship between RBBP4 and the Wnt pathway is poorly understood. In our study, for the first time we proved that RBBP4 could enhance the nuclear translocation of β-catenin and activate the Wnt/β-catenin pathway in colon cancer.

Studies over the past decade have shown that cells that harbor functionally impaired mutations of Wnt signaling cascades, such as *Adenomatous Polyposis Coli*, β-catenin, and axin, are thought to be prevalent in colon cancer[36]. The mutations lead to abnormal transcriptional induction of Wnt/β-catenin downstream genes[37]. Many target genes of Wnt/β-catenin have been identified, such as survivin[38]. Survivin was recently identified as an inhibitor of apoptosis that directly inhibits caspase-3 and caspase-7 activity[39]. The role of survivin in colorectal tumorigenesis has been shown. We found that RBBP4 knockdown inhibited the level of survivin, thus inducing apoptosis of colon cancer cells. This result proved that RBBP4 regulates the Wnt/β-catenin pathway.

Liver metastasis is an important characteristic of colon cancer, and EMT plays a central role[40]. A previous study showed that activation of Wnt/β-catenin signaling

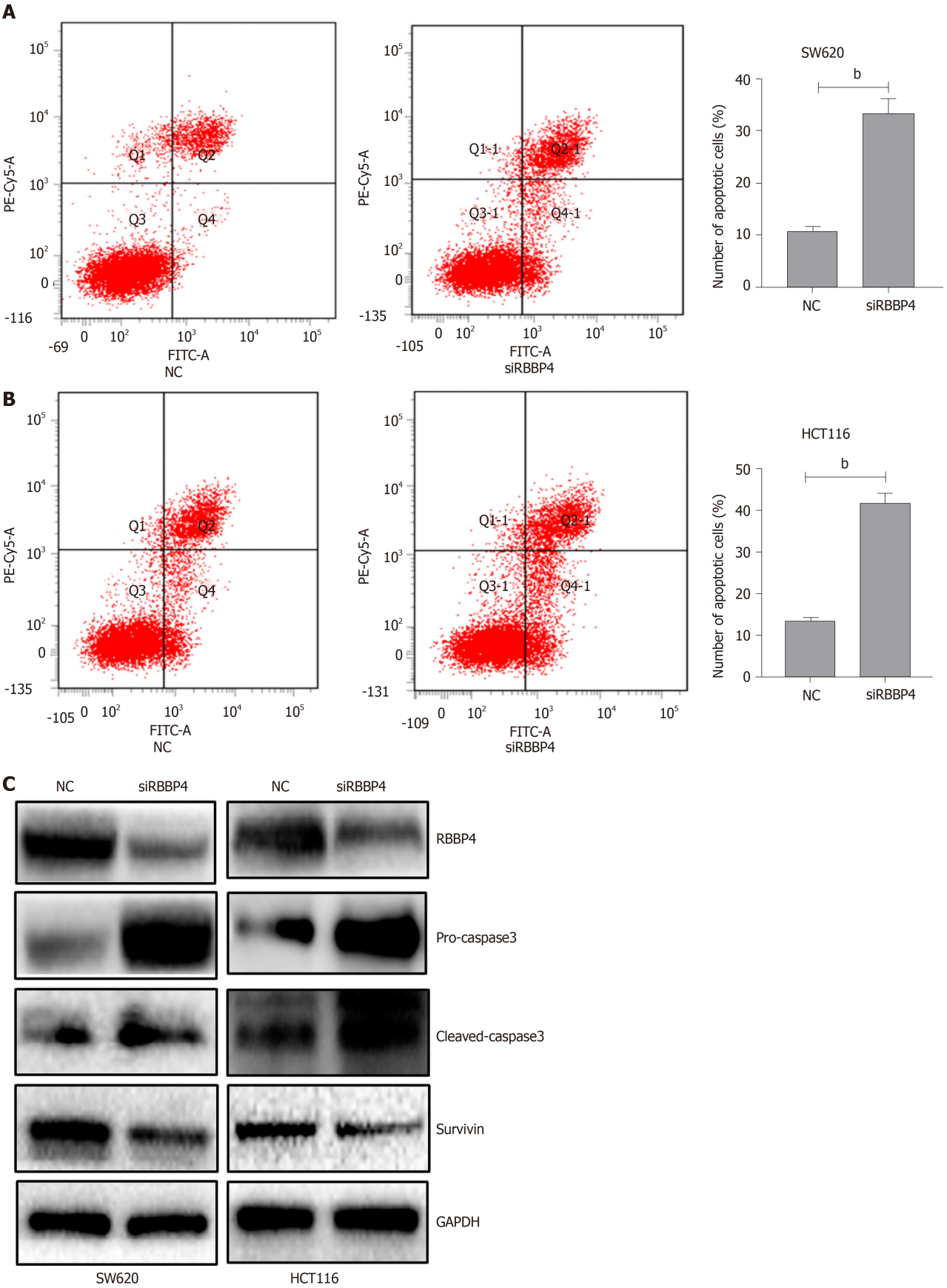

Figure 3 RBBP4 knockdown inhibits apoptosis of colon cancer cell lines. A: Apoptosis of SW620 cells examined by flow cytometry with the Annexin V-FITC/propidium iodide kit. The cells in the Q4 quadrant were defined as the apoptotic cells; B: Apoptosis of HCT116 cells examined by flow cytometry with the Annexin V-FITC/propidium iodide kit; C: Western blotting examination for apoptotic proteins. $^{b}P < 0.01$ *vs* controls.

results in expression of target genes that lead to the dedifferentiated phenotype and

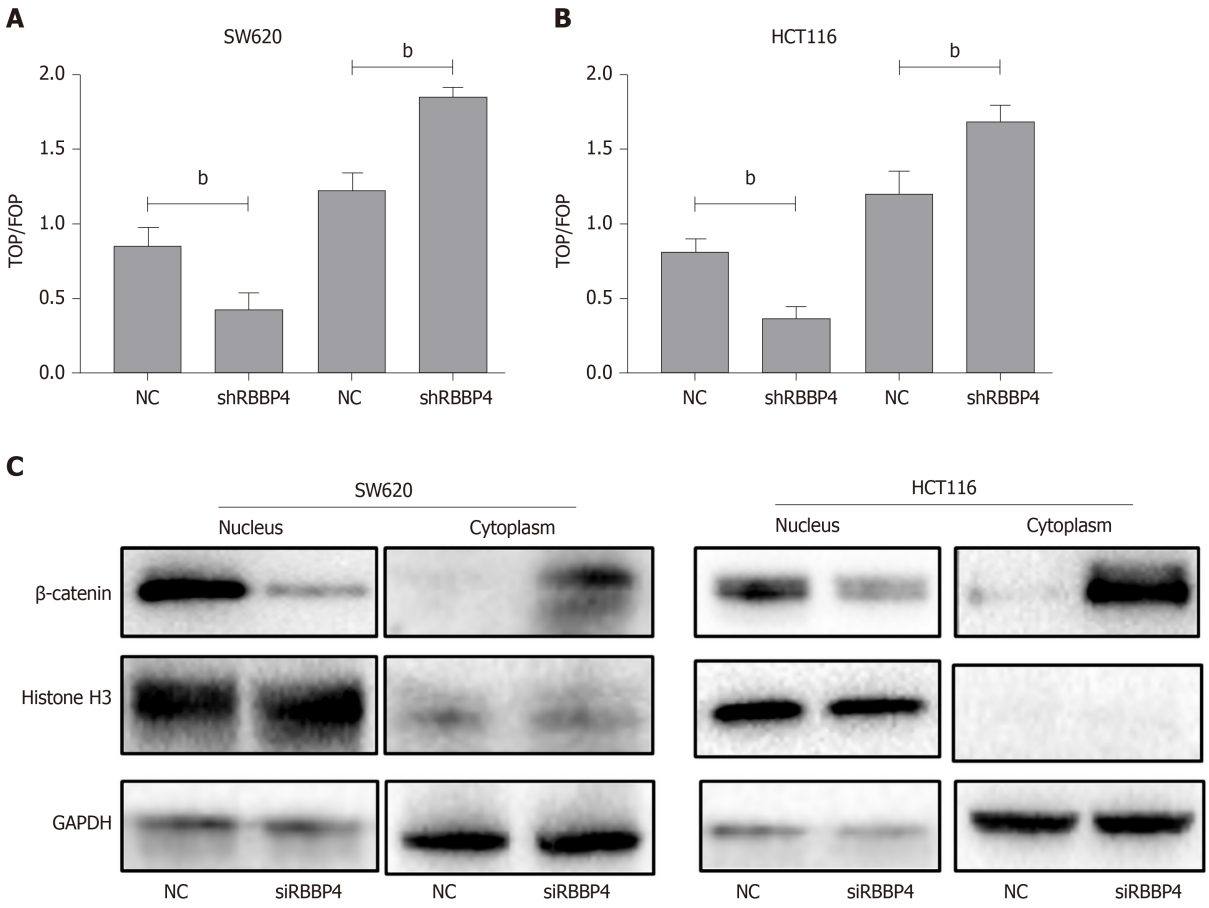

Figure 4 Effect of RBBP4 on activation of Wnt/β-catenin pathway. A: The TOPFlash experiment in SW620 cells with RBBP4 knockdown or RBBP4 overexpression; B: The TOPFlash experiment in HCT116 cells with RBBP4 knockdown or RBBP4 overexpression; C: Western blotting of the level of β-catenin in cell nucleus and cytoplasm. $^{b}P < 0.01$ *vs* controls.

EMT of colon cancer cells[41]. The nuclear translocation of β-catenin was reported to induce Slug and inhibit E-cadherin transcription in colon cancer[42]. However, the relationship between RBBP4 and EMT has not been clarified. In our study, we found that RBBP4 knockdown markedly decreased mesenchymal proteins but upregulated expression of epidermal proteins, indicating inhibition of the EMT pathway. This process may be mediated by the Wnt/β-catenin pathway.

CONCLUSION

In conclusion, the results presented in this study demonstrated that RBBP4 plays an important role in the malignant progression of colon cancer. This is probably induced *via* inhibiting Wnt/β-catenin pathway activity and relocating β-catenin from the nucleus to the plasma membrane. Further investigation of the functional mechanism of *RBBP4* as a tumor oncogene may provide a potential therapeutic strategy for intervention of colon cancer progression.

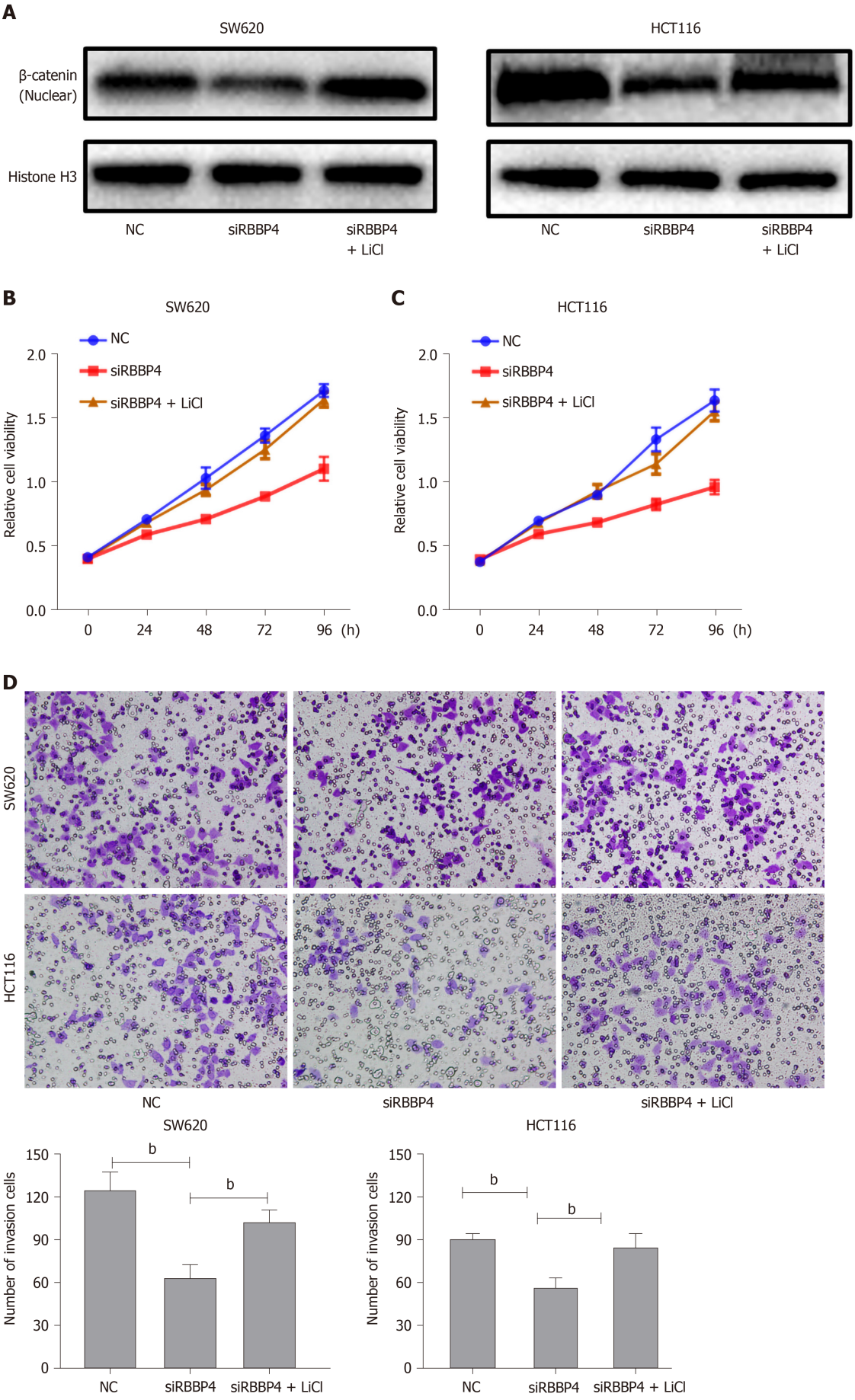
A
SW620
HCT116
β-catenin (Nuclear)
Histone H3
NC
siRBBP4
siRBBP4 + LiCl
B
SW620
C
HCT116
NC
siRBBP4
siRBBP4 + LiCl
Relative cell viability
2.0
1.5
1.0
0.5
0.0
0
24
48
72
96 (h)
D
SW620
HCT116
NC
siRBBP4
siRBBP4 + LiCl
Number of invasion cells
150
120
90
60
30
0
b

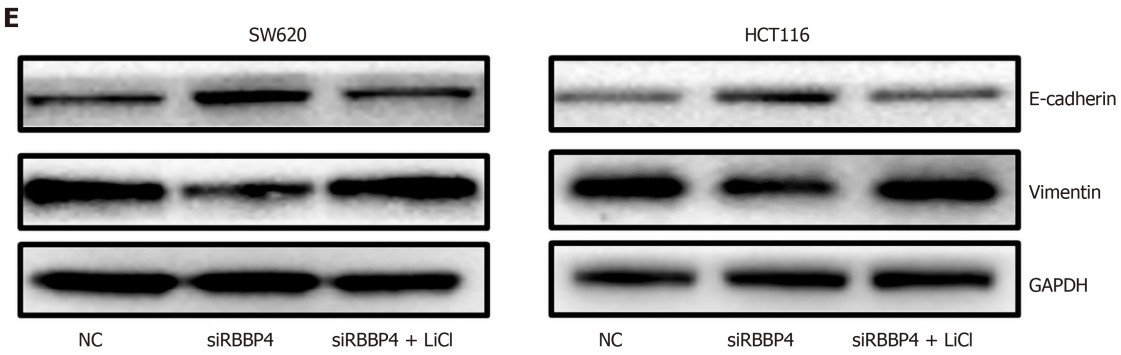

Figure 5 Rescue experiments of RBBP4. A: SW620 and HCT116 cells with RBBP4 siRNA or negative control transfection were incubated with or without 20 mmol/L LiCl, then the level of β-catenin in the nucleus was detected by western blotting; B: The viability of SW620 cells with RBBP4 siRNA or negative control transfection cultured in medium with or without 20 mmol/L LiCl; C: The viability of HCT116 cells with RBBP4 siRNA or negative control transfection cultured in medium with or without 20 mmol/L LiCl; D: Invasion of SW620 and HCT116 cells with RBBP4 siRNA or negative control transfection cultured in medium with or without 20 mmol/L LiCl; E: The protein expression of E-cadherin and vimentin in SW620 and HCT116 cells with RBBP4 siRNA or negative control transfection cultured in medium with or without 20 mmol/L LiCl. $^{b}P < 0.01$ *vs* controls.

ARTICLE HIGHLIGHTS

Research background

Our previous study demonstrated that RBBP4 is upregulated in colon cancer and correlated with poor prognosis of colon cancer and hepatic metastasis. However, the potential biological function of RBBP4 in colon cancer is still unknown.

Research motivation

To explore the potential mechanisms underlying colon cancer development and discover biomarkers for the treatment of colon cancer.

Research objectives

To investigate the underlying mechanisms of RBBP4 in colon cancer malignant development.

Research methods

Real-time polymerase chain reaction and western blot analysis were used to detect the expression of RBBP4 in colon cancer cell lines. The cell proliferation and viability of SW620 and HCT116 cells with RBBP4 knockdown was detected by Cell Counting Kit-8 and 5-ethynyl-2′-deoxyuridine staining. The transwell assay was used to detect the invasion and migration capabilities of colon cancer cells with RBBP4 knockdown. Flow cytometry apoptosis assay was used to detect the apoptosis of colon cancer cells with RBBP4 knockdown. Western blot analysis was used to detect the expression of epithelial-mesenchymal transition and apoptosis related markers in colon cancer with RBBP4 knockdown. The nuclear translocation of β-catenin was examined by western blot analysis in colon cancer cells with RBBP4 knockdown. The TOPFlash luciferase assay was used to detect effect of RBBP4 on Wnt/β-catenin activation. The rescue experiments were performed in colon cancer cells treated with Wnt/β-catenin activator LiCl and RBBP4 knockdown.

Research results

We found that RBBP4 was highly expressed in colon cancer cell lines. The 5-ethynyl-2′-deoxyuridine assay showed that knockdown of RBBP4 significantly inhibited cell proliferation. RBBP4 inhibition reduced cell invasion and migration *via* regulating proteins related to epithelial-mesenchymal transition. Knockdown of RBBP4 significantly inhibited surviving-mediated apoptosis. Mechanistically, the TOPFlash assay showed that RBBP4 knockdown increased activity of the Wnt/β-catenin pathway. RBBP4 knockdown suppressed nuclear translocation of β-catenin. With a Wnt/β-catenin activator, rescue experiments suggested that the role of RBBP4 in colon cancer progression was dependent on the Wnt/β-catenin pathway.

Research conclusions

This study demonstrated that RBBP4 promoted colon cancer development *via*

increasing activity of the Wnt/β-catenin pathway. RBBP4 may serve as a novel therapeutic target in colon cancer.

Research perspectives

In the future, additional research will be carried out to further explore the important role of RBBP4 and whether RBBP4 knockdown can be employed to enhance the sensitivity of chemotherapy of colon cancer and to develop novel anticancer treatments.

ACKNOWLEDGEMENTS

This study was supported by NHC Key Laboratory of Combined Multi-Organ Transplantation. The authors thank the technicians Rong Su and Hui Chen for guiding the experiment.

REFERENCES

1 **Siegel RL**, Miller KD, Jemal A. Cancer statistics, 2018. *CA Cancer J Clin* 2018; **68**: 7-30 [PMID: 29313949 DOI: 10.3322/caac.21442]
2 **Ferlay J**, Colombet M, Soerjomataram I, Dyba T, Randi G, Bettio M, Gavin A, Visser O, Bray F. Cancer incidence and mortality patterns in Europe: Estimates for 40 countries and 25 major cancers in 2018. *Eur J Cancer* 2018; **103**: 356-387 [PMID: 30100160 DOI: 10.1016/j.ejca.2018.07.005]
3 **Miller KD**, Nogueira L, Mariotto AB, Rowland JH, Yabroff KR, Alfano CM, Jemal A, Kramer JL, Siegel RL. Cancer treatment and survivorship statistics, 2019. *CA Cancer J Clin* 2019; **69**: 363-385 [PMID: 31184787 DOI: 10.3322/caac.21565]
4 **Moghimi-Dehkordi B**, Safaee A. An overview of colorectal cancer survival rates and prognosis in Asia. *World J Gastrointest Oncol* 2012; **4**: 71-75 [PMID: 22532879 DOI: 10.4251/wjgo.v4.i4.71]
5 **Tyler JK**, Bulger M, Kamakaka RT, Kobayashi R, Kadonaga JT. The p55 subunit of Drosophila chromatin assembly factor 1 is homologous to a histone deacetylase-associated protein. *Mol Cell Biol* 1996; **16**: 6149-6159 [PMID: 8887645 DOI: 10.1128/mcb.16.11.6149]
6 **Qian YW**, Wang YC, Hollingsworth RE Jr, Jones D, Ling N, Lee EY. A retinoblastoma-binding protein related to a negative regulator of Ras in yeast. *Nature* 1993; **364**: 648-652 [PMID: 8350924 DOI: 10.1038/364648a0]
7 **Qian YW**, Lee EY. Dual retinoblastoma-binding proteins with properties related to a negative regulator of ras in yeast. *J Biol Chem* 1995; **270**: 25507-25513 [PMID: 7503932 DOI: 10.1074/jbc.270.43.25507]
8 **Zhang Y**, Ng HH, Erdjument-Bromage H, Tempst P, Bird A, Reinberg D. Analysis of the NuRD subunits reveals a histone deacetylase core complex and a connection with DNA methylation. *Genes Dev* 1999; **13**: 1924-1935 [PMID: 10444591 DOI: 10.1101/gad.13.15.1924]
9 **Kouznetsova VL**, Tchekanov A, Li X, Yan X, Tsigelny IF. Polycomb repressive 2 complex-Molecular mechanisms of function. *Protein Sci* 2019; **28**: 1387-1399 [PMID: 31095801 DOI: 10.1002/pro.3647]
10 **Vermaak D**, Wade PA, Jones PL, Shi YB, Wolffe AP. Functional analysis of the SIN3-histone deacetylase RPD3-RbAp48-histone H4 connection in the Xenopus oocyte. *Mol Cell Biol* 1999; **19**: 5847-5860 [PMID: 10454532 DOI: 10.1128/mcb.19.9.5847]
11 **Wolffe AP**, Urnov FD, Guschin D. Co-repressor complexes and remodelling chromatin for repression. *Biochem Soc Trans* 2000; **28**: 379-386 [PMID: 10961924]
12 **Li L**, Tang J, Zhang B, Yang W, LiuGao M, Wang R, Tan Y, Fan J, Chang Y, Fu J, Jiang F, Chen C, Yang Y, Gu J, Wu D, Guo L, Cao D, Li H, Cao G, Wu M, Zhang MQ, Chen L, Wang H. Epigenetic modification of MiR-429 promotes liver tumour-initiating cell properties by targeting Rb binding protein 4. *Gut* 2015; **64**: 156-167 [PMID: 24572141 DOI: 10.1136/gutjnl-2013-305715]
13 **Guo Q**, Cheng K, Wang X, Li X, Yu Y, Hua Y, Yang Z. Expression of HDAC1 and RBBP4 correlate with clinicopathologic characteristics and prognosis in breast cancer. *Int J Clin Exp Pathol* 2020; **13**: 563-572 [PMID: 32269697]
14 **Cui F**, Zan X, Li Y, Sun W, Yang Y, Ping L. Grifola frondosa Glycoprotein GFG-3a Arrests S phase, Alters Proteome, and Induces Apoptosis in Human Gastric Cancer Cells. *Nutr Cancer* 2016; **68**: 267-279 [PMID: 27040446 DOI: 10.1080/01635581.2016.1134599]
15 **Ding L**, Zhao Y, Dang S, Wang Y, Li X, Yu X, Li Z, Wei J, Liu M, Li G. Circular RNA circ-DONSON facilitates gastric cancer growth and invasion via NURF complex dependent activation of transcription factor SOX4. *Mol Cancer* 2019; **18**: 45 [PMID: 30922402 DOI: 10.1186/s12943-019-1006-2]
16 **Li YD**, Lv Z, Xie HY, Zheng SS. Retinoblastoma binding protein 4 up-regulation is correlated with hepatic metastasis and poor prognosis in colon cancer patients. *Hepatobiliary Pancreat Dis Int* 2019; **18**: 446-451 [PMID: 31501018 DOI: 10.1016/j.hbpd.2019.08.006]
17 **Findlay VJ**, Wang C, Watson DK, Camp ER. Epithelial-to-mesenchymal transition and the cancer stem cell phenotype: insights from cancer biology with therapeutic implications for colorectal cancer. *Cancer Gene Ther* 2014; **21**: 181-187 [PMID: 24787239 DOI: 10.1038/cgt.2014.15]
18 **Siddharth S**, Das S, Nayak A, Kundu CN. SURVIVIN as a marker for quiescent-breast cancer stem cells-An intermediate, adherent, pre-requisite phase of breast cancer metastasis. *Clin Exp Metastasis* 2016; **33**: 661-675 [PMID: 27411340 DOI: 10.1007/s10585-016-9809-7]
19 **Bastos LG**, de Marcondes PG, de-Freitas-Junior JC, Leve F, Mencalha AL, de Souza WF, de Araujo WM,

Tanaka MN, Abdelhay ES, Morgado-Díaz JA. Progeny from irradiated colorectal cancer cells acquire an EMT-like phenotype and activate Wnt/β-catenin pathway. *J Cell Biochem* 2014; **115**: 2175-2187 [PMID: 25103643 DOI: 10.1002/jcb.24896]

20 **Nicolas E**, Morales V, Magnaghi-Jaulin L, Harel-Bellan A, Richard-Foy H, Trouche D. RbAp48 belongs to the histone deacetylase complex that associates with the retinoblastoma protein. *J Biol Chem* 2000; **275**: 9797-9804 [PMID: 10734134 DOI: 10.1074/jbc.275.13.9797]

21 **Zhang Y**, Iratni R, Erdjument-Bromage H, Tempst P, Reinberg D. Histone deacetylases and SAP18, a novel polypeptide, are components of a human Sin3 complex. *Cell* 1997; **89**: 357-364 [PMID: 9150135 DOI: 10.1016/s0092-8674(00)80216-0]

22 **Qi L**, Sun B, Liu Z, Cheng R, Li Y, Zhao X. Wnt3a expression is associated with epithelial-mesenchymal transition and promotes colon cancer progression. *J Exp Clin Cancer Res* 2014; **33**: 107 [PMID: 25499541 DOI: 10.1186/s13046-014-0107-4]

23 **Schmitges FW**, Prusty AB, Faty M, Stützer A, Lingaraju GM, Aiwazian J, Sack R, Hess D, Li L, Zhou S, Bunker RD, Wirth U, Bouwmeester T, Bauer A, Ly-Hartig N, Zhao K, Chan H, Gu J, Gut H, Fischle W, Müller J, Thomä NH. Histone methylation by PRC2 is inhibited by active chromatin marks. *Mol Cell* 2011; **42**: 330-341 [PMID: 21549310 DOI: 10.1016/j.molcel.2011.03.025]

24 **Shang WH**, Hori T, Westhorpe FG, Godek KM, Toyoda A, Misu S, Monma N, Ikeo K, Carroll CW, Takami Y, Fujiyama A, Kimura H, Straight AF, Fukagawa T. Acetylation of histone H4 lysine 5 and 12 is required for CENP-A deposition into centromeres. *Nat Commun* 2016; **7**: 13465 [PMID: 27811920 DOI: 10.1038/ncomms13465]

25 **Ng C**, Aichinger M, Nguyen T, Au C, Najar T, Wu L, Mesa KR, Liao W, Quivy JP, Hubert B, Almouzni G, Zuber J, Littman DR. The histone chaperone CAF-1 cooperates with the DNA methyltransferases to maintain *Cd4* silencing in cytotoxic T cells. *Genes Dev* 2019; **33**: 669-683 [PMID: 30975723 DOI: 10.1101/gad.322024.118]

26 **Fukuoka J**, Fujii T, Shih JH, Dracheva T, Meerzaman D, Player A, Hong K, Settnek S, Gupta A, Buetow K, Hewitt S, Travis WD, Jen J. Chromatin remodeling factors and BRM/BRG1 expression as prognostic indicators in non-small cell lung cancer. *Clin Cancer Res* 2004; **10**: 4314-4324 [PMID: 15240517 DOI: 10.1158/1078-0432.CCR-03-0489]

27 **Song H**, Xia SL, Liao C, Li YL, Wang YF, Li TP, Zhao MJ. Genes encoding Pir51, Beclin 1, RbAp48 and aldolase b are up or down-regulated in human primary hepatocellular carcinoma. *World J Gastroenterol* 2004; **10**: 509-513 [PMID: 14966907 DOI: 10.3748/wjg.v10.i4.509]

28 **Pacifico F**, Paolillo M, Chiappetta G, Crescenzi E, Arena S, Scaloni A, Monaco M, Vascotto C, Tell G, Formisano S, Leonardi A. RbAp48 is a target of nuclear factor-kappaB activity in thyroid cancer. *J Clin Endocrinol Metab* 2007; **92**: 1458-1466 [PMID: 17244783 DOI: 10.1210/jc.2006-2199]

29 **Casas S**, Ollila J, Aventín A, Vihinen M, Sierra J, Knuutila S. Changes in apoptosis-related pathways in acute myelocytic leukemia. *Cancer Genet Cytogenet* 2003; **146**: 89-101 [PMID: 14553942 DOI: 10.1016/s0165-4608(03)00102-x]

30 **Carreira-Barbosa F**, Nunes SC. Wnt Signaling: Paths for Cancer Progression. *Adv Exp Med Biol* 2020; **1219**: 189-202 [PMID: 32130700 DOI: 10.1007/978-3-030-34025-4_10]

31 **Bienz M**. The subcellular destinations of APC proteins. *Nat Rev Mol Cell Biol* 2002; **3**: 328-338 [PMID: 11988767 DOI: 10.1038/nrm806]

32 **Li H**, Pamukcu R, Thompson WJ. beta-Catenin signaling: therapeutic strategies in oncology. *Cancer Biol Ther* 2002; **1**: 621-625 [PMID: 12642683 DOI: 10.4161/cbt.309]

33 **Bullions LC**, Levine AJ. The role of beta-catenin in cell adhesion, signal transduction, and cancer. *Curr Opin Oncol* 1998; **10**: 81-87 [PMID: 9466489 DOI: 10.1097/00001622-199801000-00013]

34 **Willert K**, Nusse R. Beta-catenin: a key mediator of Wnt signaling. *Curr Opin Genet Dev* 1998; **8**: 95-102 [PMID: 9529612 DOI: 10.1016/s0959-437x(98)80068-3]

35 **Zhong Z**, Virshup DM. Wnt Signaling and Drug Resistance in Cancer. *Mol Pharmacol* 2020; **97**: 72-89 [PMID: 31787618 DOI: 10.1124/mol.119.117978]

36 **Schneikert J**, Behrens J. The canonical Wnt signalling pathway and its APC partner in colon cancer development. *Gut* 2007; **56**: 417-425 [PMID: 16840506 DOI: 10.1136/gut.2006.093310]

37 **Clevers H**. Wnt/beta-catenin signaling in development and disease. *Cell* 2006; **127**: 469-480 [PMID: 17081971 DOI: 10.1016/j.cell.2006.10.018]

38 **Sakoguchi-Okada N**, Takahashi-Yanaga F, Fukada K, Shiraishi F, Taba Y, Miwa Y, Morimoto S, Iida M, Sasaguri T. Celecoxib inhibits the expression of survivin via the suppression of promoter activity in human colon cancer cells. *Biochem Pharmacol* 2007; **73**: 1318-1329 [PMID: 17270149 DOI: 10.1016/j.bcp.2006.12.033]

39 **Ambrosini G**, Adida C, Altieri DC. A novel anti-apoptosis gene, survivin, expressed in cancer and lymphoma. *Nat Med* 1997; **3**: 917-921 [PMID: 9256286 DOI: 10.1038/nm0897-917]

40 **August DA**, Ottow RT, Sugarbaker PH. Clinical perspective of human colorectal cancer metastasis. *Cancer Metastasis Rev* 1984; **3**: 303-324 [PMID: 6394125 DOI: 10.1007/BF00051457]

41 **Cheng R**, Sun B, Liu Z, Zhao X, Qi L, Li Y, Gu Q. Wnt5a suppresses colon cancer by inhibiting cell proliferation and epithelial-mesenchymal transition. *J Cell Physiol* 2014; **229**: 1908-1917 [PMID: 24464650 DOI: 10.1002/jcp.24566]

42 **Zhu QC**, Gao RY, Wu W, Qin HL. Epithelial-mesenchymal transition and its role in the pathogenesis of colorectal cancer. *Asian Pac J Cancer Prev* 2013; **14**: 2689-2698 [PMID: 23803016 DOI: 10.7314/apjcp.2013.14.5.2689]

World Journal of Gastroenterology

Submit a Manuscript: https://www.f6publishing.com

World J Gastroenterol 2020 September 21; 26(35): 5343-5353

DOI: 10.3748/wjg.v26.i35.5343

ISSN 1007-9327 (print) ISSN 2219-2840 (online)

ORIGINAL ARTICLE

Observational Study

Updated bone mineral density status in Saudi patients with inflammatory bowel disease

Mohammed Ewid, Nawaf Al Mutiri, Khalid Al Omar, Amal N Shamsan, Awais A Rathore, Nazmus Saquib, Anas Salaas, Omar Al Sarraj, Yaman Nasri, Ahmed Attal, Abdulrahman Tawfiq, Hossam Sherif

ORCID number: Mohammed Ewid 0000-0001-8118-6975; Nawaf Al Mutiri 0000-0001-7993-1833; Khalid Al Omar 0000-0002-7590-1626; Amal N Shamsan 0000-0001-6264-1186; Awais A Rathore 0000-0002-5047-4656; Nazmus Saquib 0000-0002-2819-2839; Anas Salaas 0000-0003-1203-4024; Omar Al Sarraj 0000-0002-9390-7802; Yaman Nasri 0000-0001-9303-547X; Ahmed Attal 0000-0003-4501-4978; Abdulrahman Tawfiq 0000-0003-1380-2128; Hossam Sherif 0000-0002-7108-6054.

Author contributions: Ewid M, Al Mutiri N, Saquib N, and Sherif H conceived of the idea, developed the theory; Ewid M was the principle investigator; all author contributed towards methodology and towards the writing of the paper, and have read and approved the final manuscript.

Supported by Sulaiman Al Rajhi University, Saudi Arabia, from the Annual Budget of their Research Unit.

Institutional review board statement: The study received ethical approval from the Regional Research Ethics Committee-Qassim province, Ministry of Health, Saudi Arabia (approval number 20180102).

Mohammed Ewid, Internal Medicine Department, College of Medicine, Sulaiman Al Rajhi University, Bukairyah 51941, Al-Qassim, Saudi Arabia

Mohammed Ewid, Internal Medicine Department, Faculty of Medicine, Cairo University, Cairo 11562, Egypt

Nawaf Al Mutiri, Khalid Al Omar, Amal N Shamsan, Awais A Rathore, Gastroenterology Department, King Fahad Specialist Hospital, Buraidah 52366, Al-Qassim, Saudi Arabia

Nazmus Saquib, Epidemiology Department, College of Medicine, Sulaiman Al Rajhi University, Bukairyah 51941, Al-Qassim, Saudi Arabia

Anas Salaas, Omar Al Sarraj, Yaman Nasri, Ahmed Attal, Abdulrahman Tawfiq, Medical students, College of Medicine, Sulaiman Al Rajhi University, Bukairyah 51941, Al-Qassim, Saudi Arabia

Hossam Sherif, Critical Care Medicine Department, College of Medicine, Sulaiman Al Rajhi University, Bukairyah 51941, Al-Qassim, Saudi Arabia

Hossam Sherif, Critical Care Medicine Department, Faculty of Medicine, Cairo University, Cairo 11562, Egypt

Corresponding author: Mohammed Ewid, MD, Assistant Professor, Internal Medicine Department, College of Medicine, Sulaiman Al Rajhi University, PO Box 777, Bukairyah 51941, Al-Qassim, Saudi Arabia. drmohammedowid@yahoo.com

Abstract

BACKGROUND

Little is known about inflammatory bowel disease (IBD) burden and its impact on bone mineral density (BMD) among adult patients in Saudi Arabia. To the best of our knowledge, our study is the only study to give an update about this health problem in adult Saudi patients with IBD. IBD is a great risk factor for reduced BMD due to its associated chronic inflammation, malabsorption, weight loss and medication side effects. Consequently, screening for reduced BMD among patients with IBD is of utmost importance to curb and control anticipated morbidity and mortality among those patients.

Informed consent statement: All study participants provided informed written consent prior to study enrollment.

Conflict-of-interest statement: The authors declare no conflicts of interest.

Data sharing statement: The datasets used and/or analyzed during the current study are available from the corresponding author upon reasonable request.

STROBE statement: The authors have read the STROBE Statement—checklist of items, and the manuscript was prepared and revised according to the STROBE Statement.

Manuscript source: Unsolicited manuscript

Received: May 8, 2020
Peer-review started: May 8, 2020
First decision: June 8, 2020
Revised: June 15, 2020
Accepted: August 22, 2020
Article in press: August 22, 2020
Published online: September 21, 2020

P-Reviewer: Sassaki LY
S-Editor: Ma YJ
L-Editor: A
P-Editor: Ma YJ

AIM

To assess the relationship between IBD and BMD in a sample of adult Saudi patients with IBD.

METHODS

Ninety adult patients with IBD - 62 Crohn's disease (CD) and 28 ulcerative colitis (UC) - were recruited from King Fahad Specialist Hospital gastroenterology clinics in Buraidah, Al-Qassim. All enrolled patients were interviewed for their demographic information and for IBD- and BMD-related clinical data. All patients had the necessary laboratory markers and dual-energy x-ray absorptiometry scans to evaluate their BMD status. Patients were divided into two groups (CD and UC) to explore their clinical characteristics and possible risk factors for reduced BMD.

RESULTS

The CD group was significantly more prone to osteopenia and osteoporosis compared to the UC group; 44% of the CD patients had normal BMD, 19% had osteopenia, and 37% had osteoporosis, while 78% of the UC patients had normal BMD, 7% had osteopenia, and 25% had osteoporosis (P value < 0.05). In the CD group, the lowest t-score showed a statistically significant correlation with body mass index (BMI) (r = 0.45, P < 0.001), lumbar z-score (r = 0.77, P < 0.05) and femur z-score (r = 0.85, P < 0.05). In the UC group, the lowest t-score showed only statistically significant correlation with the lumbar z-score (r = 0.82, P < 0.05) and femur z-score (r = 0.80, P < 0.05). The ROC-curve showed that low BMI could predict the lowest t-score in the CD group with the best cut-off value at ≤ 23.43 (m/kg^2); area under the curve was 0.73 (95%CI: 0.59–0.84), with a sensitivity of 77%, and a specificity of 63%.

CONCLUSION

Saudi patients with IBD still have an increased risk of reduced BMD, more in CD patients. Low BMI is a significant risk factor for reduced BMD in CD patients.

Key Words: Inflammatory bowel disease; Crohn's disease; Ulcerative colitis; Bone mineral density; Osteoporosis; Fracture risk

Core Tip: Saudi patients with inflammatory bowel disease still have a high prevalence of reduced bone mineral density. Osteopenia and osteoporosis burdens were 19% and 37% in Crohn's disease (CD) patients, and 7% and 25% in ulcerative colitis patients, respectively. Low body mass index is a significant risk factor for reduced bone mineral density in CD patients.

Citation: Ewid M, Al Mutiri N, Al Omar K, Shamsan AN, Rathore AA, Saquib N, Salaas A, Al Sarraj O, Nasri Y, Attal A, Tawfiq A, Sherif H. Updated bone mineral density status in Saudi patients with inflammatory bowel disease. *World J Gastroenterol* 2020; 26(35): 5343-5353
URL: https://www.wjgnet.com/1007-9327/full/v26/i35/5343.htm
DOI: https://dx.doi.org/10.3748/wjg.v26.i35.5343

INTRODUCTION

Crohn's disease (CD) and ulcerative colitis (UC) are the main subtypes of inflammatory bowel disease (IBD). Europe and North America have the highest burden of CD and UC, approaching more than 0.3% of the population[1]. However, there has recently been an abrupt rise in the IBD burden in newly industrialized countries worldwide, including Asian countries. This rising trend is a result of multiple factors, including socioeconomic and lifestyle changes[2].

Data about the IBD prevalence in Saudi Arabia are very limited in the literature. However, similar to other Asian countries, Saudi Arabia has experienced lifestyle and industrialization changes over the past decades, with the available data pointing to increasing trends of both CD and UC in the eastern, western and central regions of

Saudi Arabia[3].

IBD is not limited to the gastrointestinal tract (GIT). It also has extraintestinal manifestations that have been recorded in up to half of patients[4]. One of these manifestations is reduced bone mineral density (BMD), namely osteoporosis and osteopenia[5]. The literature shows that the burden of reduced BMD is increased among IBD patients, with a variable prevalence ranging from 5% to 37%[6].

Osteoporosis and osteopenia are well-known predictors of major health problems, including increased fracture risk, and consequently, decreased quality of life. IBD patients' fracture risk is 40% higher than that recorded for non-IBD individuals[7]. Such increased fracture risk has severe implications for the health care system, with additional burden at the individual, social, and public levels[8]. Based on this added risk, screening for reduced BMD in IBD patients should be done on a regular basis to curb the anticipated morbidity and mortality of the disease.

Adding to the general risk factors for osteoporosis and osteopenia, IBD-specific factors include genetic predisposition, disease activity, medications (*i.e.*, steroids), small bowel resection, malabsorption, low body mass index (BMI), and pro-inflammatory cytokines[9].

Little is known about the updated prevalence of reduced BMD and its predisposing factors among adult IBD patients in Saudi Arabia. Additionally, there is a knowledge gap regarding the impact of CD and UC on BMD among Saudi patients in the era of biological therapy. Consequently, our study aimed to investigate these knowledge gaps among IBD patients living in Al-Qassim province, Saudi Arabia.

MATERIALS AND METHODS

Study design and participants

This cross-sectional study took place at King Fahad Specialist Hospital in Buraidah, Al-Qassim, Saudi Arabia between February 2018 and December 2019. The study was approved by the regional ethical committee, and all participants provided informed consent prior to their enrollment in the study.

Ninety adult (> 19 years old) Saudi patients with an IBD diagnosis (62 CD and 28 UC) were recruited from the hospital gastroenterology unit. The IBD diagnosis (either previously established or newly diagnosed) was based on patients' clinical, endoscopic, radiographic, and histopathologic findings according to the European Crohn's and Colitis Organisation (ECCO) diagnostic criteria[10,11].

IBD patients who had any concomitant malignancy, end organ failure, pregnancy, or a GIT pathology other than IBD were excluded from the study.

Procedure

In their interview in the GIT department, patients received the standard of care according to the Saudi Ministry of Health guideline protocols regarding IBD (based on ECCO criteria), including history taking, physical examinations, investigations, and treatment plan. Moreover, all patients were offered the study questionnaire and given appointments to measure their BMD by dual x-ray energy absorptiometry (DXA) scan.

Data extraction

Clinical data: Clinical data were obtained by interviewing the patients and by reviewing their previous records and investigations. Data included age, gender, smoking status, BMI, physical activity, IBD-related extraintestinal manifestations (affecting the eye, skin, joints, liver, gall bladder and/or blood vessels)[12], IBD-related data (disease subtype, childhood onset, duration, extent, clinical presentations, perianal disease, malabsorption, hospital/ICU admissions, endoscopic reports, previous surgeries, and prescription drugs used), and IBD activity scores [Crohn's Disease Activity Index (CDAI) for CD[13] and Mayo Score for UC[14]].

Biochemical measurements: Following the patients' initial interview, venous blood samples were obtained for their full blood count, erythrocyte sedimentation rate (ESR), C-reactive protein, iron panel tests, liver and kidney function tests, calcium, phosphate, alkaline phosphatase (ALP) and 25-hydroxy-vitamin D [25(OH)D]. Stool analysis was done for fecal calprotectin.

BMD measurements: We adopted the World Health Organization's diagnostic criteria[15] for measuring BMD as follows: (1) Normal BMD: *t*-score ≥ -1 standard deviation (SD); (2) Osteopenia: *t*-score between -1.0 and -2.5 SD; and (3) Osteoporosis: *t*

-score ≤ -2.5 SD.

Measurements were conducted on both lumbar spine and left femoral neck. BMD values were expressed as *t*- and *z*-scores[15]. We considered the lowest *t*-score values, obtained either from lumbar spine or femur neck, for BMD measurement. DXA scans were conducted using Discovery W, QDR series (Hologic, Waltham, MA, United States).

Data synthesis and statistical analysis

The statistical package of MedCalc version 19.0.5 was used in our analysis. Quantitative data is presented as mean ± SD, and qualitative data is presented as percentages. Comparisons between groups were made using the Mann-Whitney's *u*-test/unpaired *t* test for ordinal and continuous variables, respectively, and the χ^2-test/Fisher's exact test was used for categorical variables. Correlations between variables were performed using Pearson's/Spearman's rank correlation coefficient when applicable. *P* values less than 0.05 were considered statistically significant.

The statistical methods of this study were reviewed by Nazmus Saquib, PhD, from Sulaiman Al Rajhi University. He attests that the statistical methods in this study are suitable and adequately and appropriately described.

RESULTS

Patient demographics and IBD clinical characteristics

This cross-sectional study included 90 patients (31.5 ± 8.8, 19-60 years; 49 males, 54%). The patients were divided into 2 groups: CD group [62 patients (29.23 ± 7.58, 19-51 years; 32 males, 52%)], and UC group [28 patients (33.22 ± 10.53, 20-60 years; 17 males, 61%)].

Weight loss, malabsorption syndrome, abdominal pain, extraintestinal manifestations, previous related hospital admissions and previous related surgeries were higher, and BMI was lower in the CD group than in the UC group (Table 1).

The disease in the CD group mainly affected the ilio-colicarea in 55% of the patients, 39% in the ileum, 3% in the colon, and the remaining 3% in the upper GIT. On the other hand, 50% of the UC group had left side colitis, 46% had pancolitis, and 4% had proctitis.

The CDAI score was 157.26 ± 98.15 (range: 27-490), and the Mayo score was 3.69 ± 2.27 (range: 1-11) in the CD and UC groups, respectively. There were more patients with severe clinical disease activity and endoscopic activity in the UC group than in the CD group (7 *vs* 3 patients).

Regarding medication history, the percentages of steroid, azathioprine, and anti-tumor necrosis factor (anti-TNF) use were not significantly different between the CD group and the UC group. However, mesalamine use was significantly higher in the UC group.

Patients' laboratory profile

Lab investigations showed that most of the variables were comparable between the two study groups. However, ALP, vitamin B12, and fecal calprotectin showed statistically significant higher values in the UC group than in the CD group (Table 2).

Measurements of BMD in CD and UC patients based on the lowest t-score

Out of all participants (both groups), 46 patients (51%) had normal *t*-scores (-0.27 ± 0.54) and 44 patients (49%) had low *t*-scores (-2.15 ± 0.77, $P < 0.001$). Lower BMD levels, and consequently higher osteopenia/osteoporosis percentages, were detected in the CD group than in the UC group. In the CD group, 44% of the patients had normal BMD, 19% had osteopenia, and 37% had osteoporosis, while in the UC group, 78% of the patients had normal BMD, 7% had osteopenia, and 25% had osteoporosis (*P* value < 0.05) (Table 3, Figure 1).

Risk factors for reduced BMD

In the CD group, the lowest *t*-score showed a statistically significant correlation with BMI ($r = 0.45$, $P < 0.001$) (Figure 2), lumbar *z*-score ($r = 0.77$, $P < 0.05$) and femur *z*-score ($r = 0.85$, $P < 0.05$), but showed inverse correlations with abdominal pain ($r = -0.35$, $P < 0.05$), malabsorption syndrome ($r = -0.44$, $P < 0.001$), extraintestinal manifestations ($r = -0.28$, $P < 0.05$), total number of the symptoms ($r = -0.29$, $P < 0.05$) and with the need for vitamin D therapy ($r = -0.27$, $P < 0.05$).

Table 1 Comparison of demographic characteristics and patients' clinical profile in the Crohn's disease and ulcerative colitis groups

Parameters	CD (62 pts)	UC (28 pts)	*P* value
Age (yr)	29.23 ± 7.58	33.22 ± 10.53	NS
Sex (males), *n* (%)	32 (52)	17 (61)	NS
Smoking (%)	10	29	NS
BMI (kg/m^2)	22.2 ± 3.52	25.646 ± 2.87	< 0.05
Abdominal pain (%)	83	17	NS
Bloody diarrhea (%)	67	96	NS
Bleeding per rectum (%)	3	4	NS
Malabsorption syndrome (%)	19	0	< 0.05
Perianal disease (%)	59	4	NS
Weight loss (%)	11	0	< 0.05
Extraintestinal manifestations (%)	21	7	NS
Comorbidities (%)	8	18	NS
Previous IBD-related admission (*n*)	2.16 ± 1.48	0.7 ± 0.44	< 0.05
Previous related surgeries (%)	33	4	NS
Family history (%)	15	4	NS
Steroid therapy (%)	79	71	NS
Azathioprine (%)	82	37	NS
Mesalamine (%)	10	81	< 0.05
Anti-TNF therapy (%)	65	29	NS

CD: Crohn's disease; UC: Ulcerative colitis; pts: Patients; BMI: Body mass index; IBD: Inflammatory bowel disease; TNF: Tumor necrosis factor; NS: Not significant.

In the UC group, the lowest *t*-score showed only statistically significant correlation with the lumbar *z*-score ($r = 0.82$, $P < 0.05$) and femur *z*-score ($r = 0.80$, $P < 0.05$).

The ROC-curve showed that low BMI could predict low *t*-score much better in the CD rather than the UC group. In the CD group, the cut-off value was ≤ 23.43 (m/kg^2); the area under the curve was 0.73 (95%CI: 0.59–0.84); the sensitivity was 77%, and the specificity was 63% (Figure 3A). In the UC group, the cut-off value was ≤ 23.5 (m/kg^2); the area under the curve was 0.65 (95%CI: 0.43–0.83); the sensitivity was 50%, and the specificity was 81% (Figure 3B).

There was no significant difference in the lowest *t*-score between the CD and UC patients receiving anti-TNF-α therapy and those who did not receive it (Table 4).

DISCUSSION

The main finding in our study is the relatively high percentage of undiagnosed reduced BMD: 56% among CD patients (37% osteopenia and 19% osteoporosis) and 32% among UC (25% osteopenia and 7% osteoporosis). Such high percentages of reduced BMD should alert us to an anticipated increase in fracture risk among Saudi patients with IBD. Hence, there is a need for proper screening programs to better control BMD loss and to ensure better quality of life for those patients.

To the best of our knowledge, our study is the first study to investigate this health problem in Al-Qassim province, Saudi Arabia. Moreover, it is the only study to provide updated data regarding BMD status among adult Saudi patients with IBD.

Based on our results, the burden of reduced BMD among adult Saudi patients with IBD is still high but is showing a decreasing trend compared to the results of a retrospective study conducted between 2001 and 2008 by Ismail *et al*[16] on 95 Saudi patients with IBD; osteopenia burden was 48.6% and 32.6%, and osteoporosis burden was 55.8% and 27.5% among CD and UC patients, respectively.

Table 2 Comparison of laboratory investigations of patients in the Crohn's disease and ulcerative colitis groups

Parameters	CD (62 pts)	UC (28 pts)	*P* value
Hemoglobin (g/dL)	12.41 ± 2.4	12.54 ± 2.58	NS
WBC (× 10^9/L)	6.7 ± 1.1	7.302 ± 3.6	NS
Platelets (× 10^9/L)	333 ± 101	318 ± 121	NS
ALT (U/L)	13.61 ± 10.6	22.55 ± 28.48	NS
AST (U/L)	16.62 ± 8.38	20.69 ± 14.2	NS
ALP (U/L)	72.125 ± 29.02	84.434 ± 38.99	< 0.05
Albumin (g/L)	36.335 ± 6.44	38.13 ± 6.98	NS
Serum creatinine (μmol/L)	60.81 ± 16.15	62.96 ± 16.6	NS
Serum calcium (mmol/L)	2.25 ± 0.17	2.23 ± 0.13	NS
Phosphorus (μmol/L)	1.17 ± 0.34	1.19 ± 0.18	NS
PTT (s)	29.53 ± 0.65	32.09 ± 7.58	NS
PT (s)	12.457 ± 2.65	12.71 ± 1.73	NS
INR	1.32 ± 74.48	1.11 ± 0.23	NS
ESR (mm/h)	22.67 ± 19.33	29.256 ± 31.87	NS
CRP (> 3 mg/L) (%)	21	17	NS
Serum iron (μmol/L)	8.16 ± 6.24	9.423 ± 7.39	NS
TIBC (μg/dL)	46.985 ± 13.52	58.19 ± 20.12	NS
Ferritin (ng/mL)	30.25 ± 12.03	32.34 ± 9.25	NS
Serum vitamin D (ng/mL)	12.09 ± 10.8	12.85 ± 4.21	NS
Serum vitamin B12 (ng/mL)	231.32 ± 182.34	314.67 ± 62.43	< 0.05
Fecal calprotectin (μg/mg)	653 ± 265.13	1688.43 ± 426.79	< 0.05

CD: Crohn's disease; UC: Ulcerative colitis; pts: Patients; WBC: White blood count; ALT: Alanine aminotransferase; AST: Aspartate aminotransferase; ALP: Alkaline phosphatase; PTT: Partial thromboplastin time; PT: Prothrombin time; INR: International normalized ratio; ESR: Erythrocyte sedimentation rate; CRP: C-reactive protein; TIBC: Total iron-binding capacity; NS: Not significant.

Table 3 Comparison of dual x-ray energy absorptiometry-scan parameters in the Crohn's disease and ulcerative colitis groups

Parameters	CD (62 pts)	UC (28 pts)	*P* value
Mean *t*-score femur	-0.94 ± 1.27	-0.51 ± 0.9	NS
Mean *z*-score femur	-0.67 ± 1.06	-0.33 ± 0.82	NS
Mean *t*-score lumbar	-0.97 ± 1.46	-0.49 ± 1.27	< 0.05
Mean *z*-score lumbar	-0.45 ± 1.32	-0.29 ± 1.26	NS
Mean lowest *t*-score	-1.35 ± 0.91	-0.84 ± 0.03	< 0.05
Osteopenia (%)[1]	37	25	< 0.05
Osteoporosis (%)[1]	19	7	< 0.05

[1]Bone mineral density measurement is based on the lowest *t*-score. CD: Crohn's disease; UC: Ulcerative colitis; pts: Patients; NS: Not significant.

The relative improvement in BMD status in our study could be due to the improved standard of care, including increased use of biological therapies in our patients (53%), compared to the previously mentioned study, where the percentage of biological therapy use was 28%.

On the other hand, our results are still generally higher than those found in other Asian counties. In a study conducted by Wada *et al*[17] on 388 Japanese patients with IBD, they reported a prevalence of 40.4% osteopenia and 6.4% osteoporosis among CD

Table 4 The lowest *t*-score in relation to anti-tumor necrosis factor-α therapy in both study groups

Groups	mean ± SD	95%CI	*P* value
CD group			
No anti-TNF-α	-1.10 ± 1.04	-1.56 to -0.63	0.98
Anti-TNF-α	-1.48 ± 1.23	-1.88 to -1.09	
UC group			
No anti-TNF-α	-0.74 ± 1.11	-1.25 to -0.22	0.185
Anti-TNF-α	-1.10 ± 0.87	-1.83 to -0.37	

CD: Crohn's disease; UC: Ulcerative colitis; TNF: Tumor necrosis factor.

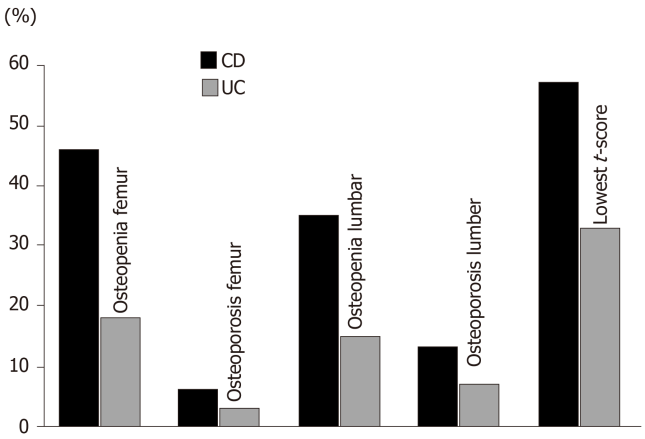

Figure 1 The percentages of patients with reduced bone mineral density in Crohn's disease compared to ulcerative colitis. CD: Crohn's disease; UC: Ulcerative colitis.

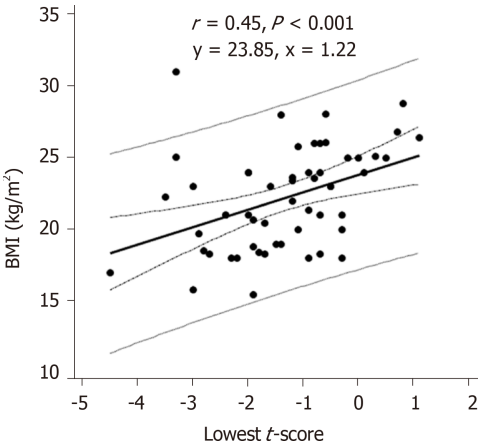

Figure 2 Scatterplot showing the correlation between lowest *t*-score and body mass index. BMI: Body mass index.

patients, and 31.0% osteopenia and 4.3% osteoporosis among UC patients.

In a larger cohort study by Tsai *et al*[18] on the Asian population in Taiwan Province, the incidence of reduced BMD in IBD patients was 40% more than that in non-IBD participants. Moreover, the study showed an osteoporosis incidence rate of 7.3% in CD patients and 6.3% in UC patients, which is comparable to the above-mentioned Japanese study but is much lower than that found in our study. On the other hand, the prevalence among Western populations was initially investigated by Schulte *et al*[19] on German participants and concluded the following ranges: 32% to 36% for osteopenia and 7% to 15% for osteoporosis. Similar findings were later mentioned by Sheth *et al*[20]

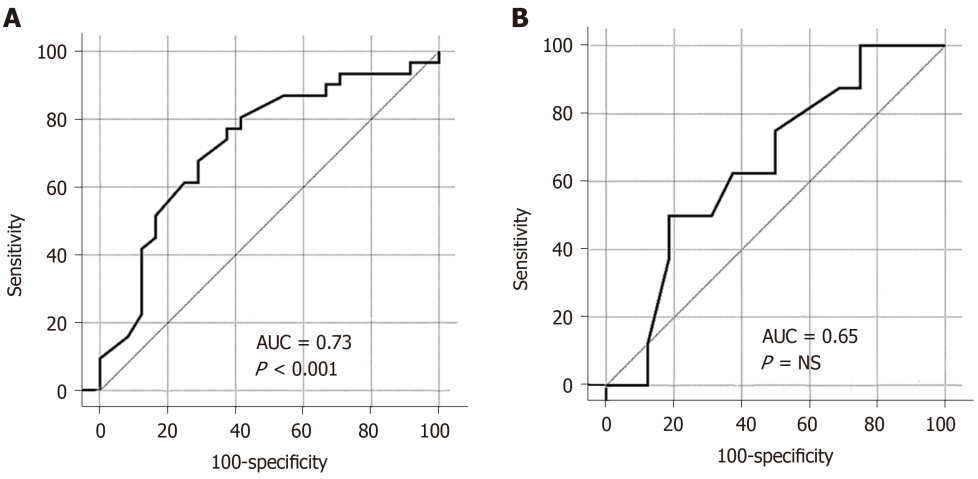

Figure 3 Receiver operating characteristic-curves showing prediction of low body mass index for low *t*-score in Crohn's disease group (A) and in ulcerative colitis group (B). AUC: Area under curve.

Most of the reports that estimated the fracture risk among IBD patients were based on Western populations as highlighted by Szafors *et al*[21] in their systematic review, with an overall 38% higher fracture risk in IBD patients compared to the controls.

The different findings among IBD studies regarding BMD prevalence (including those related to IBD subtypes CD and UC) could be attributed to either variability in research methodology (study design and sample size) or variability in patients' characteristics, including ethnicity, age, gender, IBD severity, nutritional status and quality of health care settings. For example, we conducted our study in the largest central tertiary care hospital in the region, which usually manages advanced cases of complicated disease that need a high level of care. Accordingly, there is a possibility that this setting could partly explain the high prevalence of both osteopenia and osteoporosis in our sample as compared to other studies.

Another important finding in our study is that CD patients were at higher risk of developing both osteoporosis and osteopenia than UC patients, a finding that mirrors previously published data[18,22,23]. This risk could be explained by more chronic inflammation (indicated by higher hospital admissions and biological therapy use and lower BMI) in CD patients than in UC patients. On the other hand, there are other studies that did not show any epidemiological BMD difference between CD and UC patients[24].

The prevalence of CD (69%) was higher than UC (31%) in our sample, a finding that is consistent with previous epidemiological studies in Saudi Arabia[25,26]. Taking into consideration the increasing trend of CD patients in Saudi Arabia, who are at higher risk for reduced BMD than UC patients, health care providers should anticipate more burden of osteoporosis and osteopenia among those patients and take the necessary preventive and screening actions.

It is speculated that the cornerstone pathogenic factor of reduced BMD among IBD patients is chronic inflammation that is induced by pro-inflammatory mediators and cytokines, including interleukin-1 (IL-1), IL-6 and TNF-α. These pro-inflammatory mediators disturb the physiologic bone remodeling process through an imbalance of osteoprotegerin, receptor activator of nuclear factor kappa-B (RANK), and the RANK ligand (RANKL) pathway. When there is a decrease in osteoprotegerin, a decoy receptor that limits RANKL-RANK interaction, it activates osteoclast, which is responsible for bone resorption[27,28].

The third main finding in our study is that low BMI was a risk factor for reduced BMD, which matches data from previous studies[17,29,30]. This finding was more evident in CD patients than in UC patients; BMI could predict the severity of reduced BMD with a sensitivity of 77% and a specificity of 63%, AUC 0.73 (95%CI: 0.59–0.84) in the CD group.

An unexpected finding in our study and in previous studies is the lack of correlation between steroid use and BMD[6,22,31,32]. For our study, this result may be due to the lack of a registry to precisely record our patients' steroid therapy details. Intake of prednisolone > 7.5 mg/d for 3 mo is an established risk for developing osteoporosis[33], as shown in previous studies[17,27,30].

It is known that patients with IBD requiring biological therapy have the most severe

inflammation and a greater anticipated decrease in their BMD than other IBD patients[34]. Our study, in contrast, did not find any significant difference in BMD between the CD and UC patients receiving anti-TNF-α therapy and those not receiving it (P value = 0.980 and 0.185, respectively). This finding could spotlight the beneficial role of biological therapy for BMD in IBD patients, but it needs further clarification in future studies.

Study limitation

The cross-sectional nature of the study precluded us from conducting a follow-up of reduced BMD risk factors in our patients. Moreover, our study is a single-center study, and it may be better to conduct a study in all health care centers in the province in order to enroll a diverse spectrum of IBD patients and increase the sample size.

CONCLUSION

Adult Saudi patients with IBD, although better than before, still have higher reduced BMD than Eastern Asian countries, with a significantly higher risk among CD patients compared to UC patients. Low BMI was a significant risk factor for reduced BMD in the CD group. We recommend further prospective multicenter studies among adult Saudi patients with IBD for a better assessment of reduced BMD risk factors and to investigate the current DXA screening practices among those patients.

ARTICLE HIGHLIGHTS

Research background

Inflammatory bowel disease (IBD) is showing an increasing trend in newly industrialized countries worldwide, including Saudi Arabia. Reduced bone mineral density (BMD) is a major documented extraintestinal complication in patients with IBD. As with other IBD patients, Saudi patients with IBD will have increased fracture risk and lower quality of life if not properly screened for reduced BMD.

Research motivation

Little is known about how much reduced BMD occurs among Saudi patients with IBD or about the predisposing factors in that population. Our study gives an update about reduced BMD among adult Saudi patients with IBD. We hope it will help health care providers curb the anticipated complications through proper preventive and screening measures.

Research objectives

We aimed to assess the current burden of reduced BMD and its possible risk factors among adult Saudi patients with IBD. Moreover, we investigated any possible variations between Crohn's disease (CD) and ulcerative colitis (UC) patients, either in the disease burden or its related risk factors.

Research methods

Ninety adult patients with IBD - 62 CD and 28 UC - were recruited from King Fahad Specialist Hospital gastroenterology clinics in the city of Buraidah, Saudi Arabia. Demographics, clinical workups and dual x-ray energy absorptiometry (DXA) scan data were obtained. Patients were divided into two groups (CD and UC) to explore their clinical characteristics and possible risk factors for reduced BMD. Appropriate statistical tests were used according to the variables. A $P < 0.05$ was considered significant.

Research results

Patients with CD were at higher risk for reduced BMD than those with UC; 19% of CD patients had osteopenia, and 37% had osteoporosis, while among the UC patients, 7% had osteopenia, and 25% had osteoporosis (P value < 0.05). In the CD group, the lowest t-score showed a statistically significant correlation with body mass index (BMI) ($r = 0.45$, $P < 0.001$), best cut-off value at ≤ 23.43 (m/kg^2); area under the curve was 0.73 (95%CI: 0.59–0.84). In the UC group, the lowest t-score showed only statistically significant correlation with the lumbar z-score ($r = 0.82$, $P < 0.05$) and

femur *z*-score ($r = 0.80$, $P < 0.05$).

Research conclusions

There is still an increased risk of reduced BMD for Saudi patients with IBD, more so in CD patients. Low BMI is a significant risk factor for reduced BMD in CD patients.

Research perspectives

We recommend further prospective multicenter studies among adult Saudi patients with IBD for a better assessment of reduced BMD risk factors and to investigate the current DXA screening practices among those patients.

ACKNOWLEDGEMENTS

The authors thank Ms. Erin Strotheide for her editorial contributions to this manuscript.

REFERENCES

1 **Ng SC**, Shi HY, Hamidi N, Underwood FE, Tang W, Benchimol EI, Panaccione R, Ghosh S, Wu JCY, Chan FKL, Sung JJY, Kaplan GG. Worldwide incidence and prevalence of inflammatory bowel disease in the 21st century: a systematic review of population-based studies. *Lancet* 2018; **390**: 2769-2778 [PMID: 29050646 DOI: 10.1016/S0140-6736(17)32448-0]

2 **Kaplan GG**, Ng SC. Understanding and Preventing the Global Increase of Inflammatory Bowel Disease. *Gastroenterology* 2017; **152**: 313-321.e2 [PMID: 27793607 DOI: 10.1053/j.gastro.2016.10.020]

3 **El Mouzan MI**, AlEdreesi MH, Hasosah MY, Al-Hussaini AA, Al Sarkhy AA, Assiri AA. Regional variation of pediatric inflammatory bowel disease in Saudi Arabia: Results from a multicenter study. *World J Gastroenterol* 2020; **26**: 416-423 [PMID: 32063690 DOI: 10.3748/wjg.v26.i4.416]

4 **Bernstein CN**, Blanchard JF, Rawsthorne P, Yu N. The prevalence of extraintestinal diseases in inflammatory bowel disease: a population-based study. *Am J Gastroenterol* 2001; **96**: 1116-1122 [PMID: 11316157 DOI: 10.1111/j.1572-0241.2001.03756.x]

5 **Bjarnason I**, Macpherson A, Mackintosh C, Buxton-Thomas M, Forgacs I, Moniz C. Reduced bone density in patients with inflammatory bowel disease. *Gut* 1997; **40**: 228-233 [PMID: 9071937 DOI: 10.1136/gut.40.2.228]

6 **Lo B**, Holm JP, Vester-Andersen MK, Bendtsen F, Vind I, Burisch J. Incidence, Risk Factors and Evaluation of Osteoporosis in Patients With Inflammatory Bowel Disease: A Danish Population-Based Inception Cohort With 10 Years of Follow-Up. *J Crohns Colitis* 2020; **14**: 904-914 [PMID: 32016388 DOI: 10.1093/ecco-jcc/jjaa019]

7 **Bernstein CN**, Blanchard JF, Leslie W, Wajda A, Yu BN. The incidence of fracture among patients with inflammatory bowel disease. A population-based cohort study. *Ann Intern Med* 2000; **133**: 795-799 [PMID: 11085842 DOI: 10.7326/0003-4819-133-10-200011210-00012]

8 **Viswanathan M**, Reddy S, Berkman N, Cullen K, Middleton JC, Nicholson WK, Kahwati LC. Screening to Prevent Osteoporotic Fractures: Updated Evidence Report and Systematic Review for the US Preventive Services Task Force. *JAMA* 2018; **319**: 2532-2551 [PMID: 29946734 DOI: 10.1001/jama.2018.6537]

9 **Rodríguez-Bores L**, Barahona-Garrido J, Yamamoto-Furusho JK. Basic and clinical aspects of osteoporosis in inflammatory bowel disease. *World J Gastroenterol* 2007; **13**: 6156-6165 [PMID: 18069754 DOI: 10.3748/wjg.v13.i46.6156]

10 **Magro F**, Gionchetti P, Eliakim R, Ardizzone S, Armuzzi A, Barreiro-de Acosta M, Burisch J, Gecse KB, Hart AL, Hindryckx P, Langner C, Limdi JK, Pellino G, Zagó,rowicz E, Raine T, Harbord M, Rieder F, European Crohn',s and Colitis Organisation [ECCO]. Third European Evidence-based Consensus on Diagnosis and Management of Ulcerative Colitis. Part 1: Definitions, Diagnosis, Extra-intestinal Manifestations, Pregnancy, Cancer Surveillance, Surgery, and Ileo-anal Pouch Disorders. *J Crohns Colitis* 2017; **11**: 649-670 [PMID: 28158501 DOI: 10.1093/ecco-jcc/jjx008]

11 **Gionchetti P**, Dignass A, Danese S, Magro Dias FJ, Rogler G, Lakatos PL, Adamina M, Ardizzone S, Buskens CJ, Sebastian S, Laureti S, Sampietro GM, Vucelic B, van der Woude CJ, Barreiro-de Acosta M, Maaser C, Portela F, Vavricka SR, Gomollón F; ECCO. 3rd European Evidence-based Consensus on the Diagnosis and Management of Crohn's Disease 2016: Part 2: Surgical Management and Special Situations. *J Crohns Colitis* 2017; **11**: 135-149 [PMID: 27660342 DOI: 10.1093/ecco-jcc/jjw169]

12 **Hedin CRH**, Vavricka SR, Stagg AJ, Schoepfer A, Raine T, Puig L, Pleyer U, Navarini A, van der Meulen-de Jong AE, Maul J, Katsanos K, Kagramanova A, Greuter T, González-Lama Y, van Gaalen F, Ellul P, Burisch J, Bettenworth D, Becker MD, Bamias G, Rieder F. The Pathogenesis of Extraintestinal Manifestations: Implications for IBD Research, Diagnosis, and Therapy. *J Crohns Colitis* 2019; **13**: 541-554 [PMID: 30445584 DOI: 10.1093/ecco-jcc/jjy191]

13 **Winship DH**, Summers RW, Singleton JW, Best WR, Becktel JM, Lenk LF, Kern F Jr. National Cooperative Crohn's Disease Study: study design and conduct of the study. *Gastroenterology* 1979; **77**: 829-842 [PMID: 38175]

14 **D'Haens G**, Sandborn WJ, Feagan BG, Geboes K, Hanauer SB, Irvine EJ, Lémann M, Marteau P, Rutgeerts P, Schölmerich J, Sutherland LR. A review of activity indices and efficacy end points for clinical trials of medical therapy in adults with ulcerative colitis. *Gastroenterology* 2007; **132**: 763-786 [PMID: 17258735

DOI: 10.1053/j.gastro.2006.12.038]
15 **World Health Organization**. Assessment of fracture risk and its application to screening for postmenopausal osteoporosis: Report of a WHO study group; 1992 June 22-25; Rome, Italy. Available from: https://apps.who.int/iris/handle/10665/39142
16 **Ismail MH**, Al-Elq AH, Al-Jarodi ME, Azzam NA, Aljebreen AM, Al-Momen SA, Bseiso BF, Al-Mulhim FA, Alquorain A. Frequency of low bone mineral density in Saudi patients with inflammatory bowel disease. *Saudi J Gastroenterol* 2012; **18**: 201-207 [PMID: 22626800 DOI: 10.4103/1319-3767.96458]
17 **Wada Y**, Hisamatsu T, Naganuma M, Matsuoka K, Okamoto S, Inoue N, Yajima T, Kouyama K, Iwao Y, Ogata H, Hibi T, Abe T, Kanai T. Risk factors for decreased bone mineral density in inflammatory bowel disease: A cross-sectional study. *Clin Nutr* 2015; **34**: 1202-1209 [PMID: 25618799 DOI: 10.1016/j.clnu.2015.01.003]
18 **Tsai MS**, Lin CL, Tu YK, Lee PH, Kao CH. Risks and predictors of osteoporosis in patients with inflammatory bowel diseases in an Asian population: a nationwide population-based cohort study. *Int J Clin Pract* 2015; **69**: 235-241 [PMID: 25472555 DOI: 10.1111/ijcp.12526]
19 **Schulte C**, Dignass AU, Mann K, Goebell H. Reduced bone mineral density and unbalanced bone metabolism in patients with inflammatory bowel disease. *Inflamm Bowel Dis* 1998; **4**: 268-275 [PMID: 9836078 DOI: 10.1002/ibd.3780040403]
20 **Sheth T**, Pitchumoni CS, Das KM. Musculoskeletal manifestations in inflammatory bowel disease: a revisit in search of immunopathophysiological mechanisms. *J Clin Gastroenterol* 2014; **48**: 308-317 [PMID: 24492406 DOI: 10.1097/MCG.0000000000000067]
21 **Szafors P**, Che H, Barnetche T, Morel J, Gaujoux-Viala C, Combe B, Lukas C. Risk of fracture and low bone mineral density in adults with inflammatory bowel diseases. A systematic literature review with meta-analysis. *Osteoporos Int* 2018; **29**: 2389-2397 [PMID: 29909470 DOI: 10.1007/s00198-018-4586-6]
22 **Jahnsen J**, Falch JA, Aadland E, Mowinckel P. Bone mineral density is reduced in patients with Crohn's disease but not in patients with ulcerative colitis: a population based study. *Gut* 1997; **40**: 313-319 [PMID: 9135518 DOI: 10.1136/gut.40.3.313]
23 **Vestergaard P**, Mosekilde L. Fracture risk in patients with celiac Disease, Crohn's disease, and ulcerative colitis: a nationwide follow-up study of 16,416 patients in Denmark. *Am J Epidemiol* 2002; **156**: 1-10 [PMID: 12076883 DOI: 10.1093/aje/kwf007]
24 **Vázquez MA**, Lopez E, Montoya MJ, Giner M, Pérez-Temprano R, Pérez-Cano R. Vertebral fractures in patients with inflammatory bowel disease compared with a healthy population: a prospective case-control study. *BMC Gastroenterol* 2012; **12**: 47 [PMID: 22584049 DOI: 10.1186/1471-230X-12-47]
25 **Fadda MA**, Peedikayil MC, Kagevi I, Kahtani KA, Ben AA, Al HI, Sohaibani FA, Quaiz MA, Abdulla M, Khan MQ, Helmy A. Inflammatory bowel disease in Saudi Arabia: a hospital-based clinical study of 312 patients. *Ann Saudi Med* 2012; **32**: 276-282 [PMID: 22588439 DOI: 10.5144/0256-4947.2012.276]
26 **Al-Mofarreh MA**, Al-Mofleh IA. Emerging inflammatory bowel disease in saudi outpatients: a report of 693 cases. *Saudi J Gastroenterol* 2013; **19**: 16-22 [PMID: 23319033 DOI: 10.4103/1319-3767.105915]
27 **Agrawal M**, Arora S, Li J, Rahmani R, Sun L, Steinlauf AF, Mechanick JI, Zaidi M. Bone, inflammation, and inflammatory bowel disease. *Curr Osteoporos Rep* 2011; **9**: 251-257 [PMID: 21935582 DOI: 10.1007/s11914-011-0077-9]
28 **Lacey DL**, Boyle WJ, Simonet WS, Kostenuik PJ, Dougall WC, Sullivan JK, San Martin J, Dansey R. Bench to bedside: elucidation of the OPG-RANK-RANKL pathway and the development of denosumab. *Nat Rev Drug Discov* 2012; **11**: 401-419 [PMID: 22543469 DOI: 10.1038/nrd3705]
29 **Jahnsen J**, Falch JA, Mowinckel P, Aadland E. Bone mineral density in patients with inflammatory bowel disease: a population-based prospective two-year follow-up study. *Scand J Gastroenterol* 2004; **39**: 145-153 [PMID: 15000276 DOI: 10.1080/00365520310007873]
30 **Azzopardi N**, Ellul P. Risk factors for osteoporosis in Crohn's disease: infliximab, corticosteroids, body mass index, and age of onset. *Inflamm Bowel Dis* 2013; **19**: 1173-1178 [PMID: 23511037 DOI: 10.1097/MIB.0b013e31828075a7]
31 **Leslie WD**, Miller N, Rogala L, Bernstein CN. Body mass and composition affect bone density in recently diagnosed inflammatory bowel disease: the Manitoba IBD Cohort Study. *Inflamm Bowel Dis* 2009; **15**: 39-46 [PMID: 18623166 DOI: 10.1002/ibd.20541]
32 **Naito T**, Yokoyama N, Kakuta Y, Ueno K, Kawai Y, Onodera M, Moroi R, Kuroha M, Kanazawa Y, Kimura T, Shiga H, Endo K, Nagasaki M, Masamune A, Kinouchi Y, Shimosegawa T. Clinical and genetic risk factors for decreased bone mineral density in Japanese patients with inflammatory bowel disease. *J Gastroenterol Hepatol* 2018; **33**: 1873-1881 [PMID: 29603369 DOI: 10.1111/jgh.14149]
33 **Suzuki Y**, Nawata H, Soen S, Fujiwara S, Nakayama H, Tanaka I, Ozono K, Sagawa A, Takayanagi R, Tanaka H, Miki T, Masunari N, Tanaka Y. Guidelines on the management and treatment of glucocorticoid-induced osteoporosis of the Japanese Society for Bone and Mineral Research: 2014 update. *J Bone Miner Metab* 2014; **32**: 337-350 [PMID: 24818875 DOI: 10.1007/s00774-014-0586-6]
34 **Terdiman JP**, Gruss CB, Heidelbaugh JJ, Sultan S, Falck-Ytter YT; AGA Institute Clinical Practice and Quality Management Committee. American Gastroenterological Association Institute guideline on the use of thiopurines, methotrexate, and anti-TNF-α biologic drugs for the induction and maintenance of remission in inflammatory Crohn's disease. *Gastroenterology* 2013; **145**: 1459-1463 [PMID: 24267474 DOI: 10.1053/j.gastro.2013.10.047]

World Journal of Gastroenterology

Submit a Manuscript: https://www.f6publishing.com

World J Gastroenterol 2020 September 21; 26(35): 5354-5361

DOI: 10.3748/wjg.v26.i35.5354

ISSN 1007-9327 (print) ISSN 2219-2840 (online)

ORIGINAL ARTICLE

Observational Study

Clinical features of cardiac nodularity-like appearance induced by *Helicobacter pylori* infection

Toshihiro Nishizawa, Kosuke Sakitani, Hidekazu Suzuki, Shuntaro Yoshida, Yosuke Kataoka, Yousuke Nakai, Hirotoshi Ebinuma, Takanori Kanai, Osamu Toyoshima, Kazuhiko Koike

ORCID number: Toshihiro Nishizawa 0000-0003-4876-3384; Kosuke Sakitani 0000-0002-4537-6023; Hidekazu Suzuki 0000-0002-3855-3140; Shuntaro Yoshida 0000-0002-9437-9132; Yosuke Kataoka 0000-0002-8374-6558; Yousuke Nakai 0000-0001-7411-1385; Hirotoshi Ebinuma 0000-0001-6604-053X; Takanori Kanai 0000-0002-1466-4532; Osamu Toyoshima 0000-0002-6953-6079; Kazuhiko Koike 0000-0002-9739-9243.

Author contributions: Nishizawa T analyzed data, and wrote the manuscript; Sakitani K and Yoshida S reviewed endoscopic images; Kataoka Y collected the data; Suzuki H, Nakai Y, Ebinuma H, and Kanai T critically revised the manuscript; Koike K supervised the study; Toyoshima O recruited patients, designed the study.

Institutional review board statement: This retrospective study was approved by the Ethical Review Committee of Hattori Clinic on September 6, 2019 (approval no. S1909-U06).

Informed consent statement: Patients were not required to give informed consent to the study because the analysis used anonymous clinical data that were

Toshihiro Nishizawa, Kosuke Sakitani, Shuntaro Yoshida, Yosuke Kataoka, Osamu Toyoshima, Department of Gastroenterology, Toyoshima Endoscopy Clinic, Tokyo 1570066, Japan

Toshihiro Nishizawa, Hirotoshi Ebinuma, Department of Gastroenterology, Narita Hospital, International University of Health and Welfare, Chiba 2868520, Japan

Kosuke Sakitani, Department of Gastroenterology, Sakitani Endoscopy Clinic, Chiba 2740825, Japan

Hidekazu Suzuki, Department of Internal Medicine, Tokai University School of Medicine, Kanagawa 2591193, Japan

Yousuke Nakai, Osamu Toyoshima, Kazuhiko Koike, Department of Gastroenterology, Graduate School of Medicine, The University of Tokyo, Tokyo 1138655, Japan

Takanori Kanai, Department of Internal Medicine, Keio University School of Medicine, Tokyo 1608582, Japan

Corresponding author: Osamu Toyoshima, MD, Doctor, Department of Gastroenterology, Toyoshima Endoscopy Clinic, 6-17-5 Seijo, Setagaya-ku, Tokyo 1570066, Japan. t@ichou.com

Abstract

BACKGROUND

We have previously reported that *Helicobacter pylori* (*H. pylori*)-associated nodular gastritis could occur in both the antrum and the cardia. Cardiac nodularity-like appearance (hereafter, called as cardiac nodularity) had a high predictive accuracy for the diagnosis of *H. pylori* infection. In the previous study, we included only the patients who were evaluated for *H. pylori* infection for the first time, and excluded patients with a history of eradication. Therefore, the prevalence and clinical features of cardiac nodularity remains unknown.

AIM

To perform this cross-sectional study to explore the characteristics of cardiac nodularity.

METHODS

Consecutive patients who underwent esophagogastroduodenoscopy between

May, 2017 and August, 2019 in the Toyoshima Endoscopy Clinic were enrolled in this study. We included *H. pylori*-negative, *H. pylori*-positive, and *H. pylori*-eradicated patients, and excluded patients with unclear *H. pylori* status and eradication failure. *H. pylori* infection was diagnosed according to serum anti-*H. pylori* antibody and the urea breath test or histology. Cardiac nodularity was defined as a miliary nodular appearance or the presence of scattered whitish circular small colorations within 2 cm of the esophagogastric junction. Nodularity was visualized as whitish in the narrow-band imaging mode. We collected data on the patients' baseline characteristics.

RESULTS

A total of 1078 patients were finally included. Among *H. pylori*-negative patients, cardiac nodularity and antral nodularity were recognized in 0.14% each. Among *H. pylori*-positive patients, cardiac nodularity and antral nodularity were recognized in 54.5% and 29.5%, respectively. Among *H. pylori*-eradicated patients, cardiac nodularity and antral nodularity were recognized in 4.5% and 0.6%, respectively. The frequency of cardiac nodularity was significantly higher than that of antral nodularity in *H. pylori*-positive and -eradicated patients. The frequencies of cardiac nodularity and antral nodularity in *H. pylori*-eradicated patients were significantly lower than those in *H. pylori*-positive patients ($P < 0.001$). The patients with cardiac nodularity were significantly younger than those without cardiac nodularity ($P = 0.0013$). Intestinal metaplasia score of the patients with cardiac nodularity were significantly lower than those without cardiac nodularity ($P = 0.0216$). Among *H. pylori*-eradicated patients, the patients with cardiac nodularity underwent eradication significantly more recently compared with those without cardiac nodularity ($P < 0.0001$).

CONCLUSION

This report outlines the prevalence and clinical features of cardiac nodularity, and confirm its close association with active *H. pylori* infection.

Key Words: Cardia; Nodularity; *Helicobacter pylori*; Diagnosis; Gastritis

Core Tip: The prevalence of cardiac and antral nodularity in *Helicobacter pylori* (*H. pylori*) -negative, -positive, and -eradicated patients were 0.14% and 0.14%, 54.5% and 29.5%, and 4.5% and 0.6%, respectively. Cardiac nodularity was more frequent than antral nodularity in *H. pylori*-positive and -eradicated patients. Cardiac nodularity was often found in younger patients and patients with less intestinal metaplasia. Cardiac nodularity decreased after eradication, especially in patients who underwent eradication a long time ago.

Citation: Nishizawa T, Sakitani K, Suzuki H, Yoshida S, Kataoka Y, Nakai Y, Ebinuma H, Kanai T, Toyoshima O, Koike K. Clinical features of cardiac nodularity-like appearance induced by *Helicobacter pylori* infection. *World J Gastroenterol* 2020; 26(35): 5354-5361
URL: https://www.wjgnet.com/1007-9327/full/v26/i35/5354.htm
DOI: https://dx.doi.org/10.3748/wjg.v26.i35.5354

INTRODUCTION

Helicobacter pylori (*H. pylori*) infection leads to the development of gastric atrophy, peptic ulcer, and gastric cancer[1-5]. Eradication of *H. pylori* infection has been reported as an effective strategy for treating atrophic gastritis and peptic ulcer, and preventing gastric cancer[6-9]. Therefore, it is important to evaluate *H. pylori* infection status[10-12].

Nodular gastritis is a form of chronic gastritis that has a unique miliary pattern on endoscopy, with "gooseflesh-like" appearance. Many studies have shown a strong association between nodular gastritis and *H. pylori* infection[13-15]. Children and young women are reported to be predisposed to nodular gastritis. Nodular gastritis improves

obtained after each patient agreed to treatment by written consent.

Conflict-of-interest statement: There are no conflicts of interest to report.

Data sharing statement: No additional data are available.

STROBE statement: The authors have read the STROBE Statement—checklist of items, and the manuscript was prepared and revised according to the STROBE Statement—checklist of items.

Manuscript source: Unsolicited manuscript

Received: May 7, 2020
Peer-review started: May 7, 2020
First decision: May 15, 2020
Revised: May 17, 2020
Accepted: September 2, 2020
Article in press: September 2, 2020
Published online: September 21, 2020

P-Reviewer: Ahmadi Hedayati M, Dinç T
S-Editor: Gong ZM
L-Editor: A
P-Editor: Ma YJ

gradually with age[16]. Several reports have suggested an association between nodular gastritis and diffuse type gastric cancer[13,15,17].

We have previously reported that nodularity could occur in both the antrum and the cardia[18]. Cardiac nodularity-like appearance is found more frequently than antral nodularity. Cardiac nodularity-like appearance (hereafter, called as cardiac nodularity) had a high predictive accuracy for the diagnosis of *H. pylori* infection. Our previous report also showed excellent interobserver agreement on cardiac nodularity. Furthermore, histological examination of cardiac nodularity often revealed lymphoid follicles displaying lymphocyte infiltration in the cardiac gland[18].

However, the prevalence and clinical features of cardiac nodularity remains unknown. Therefore, we performed this cross-sectional study to explore the characteristics of cardiac nodularity.

MATERIALS AND METHODS

Ethics

This study was approved by the ethical review committee of Hattori Clinic on September 6, 2019 (approval no. S1909-U06)[12,19]. All clinical investigations were conducted according to the ethical guidelines of the Declaration of Helsinki.

Patients

Consecutive patients who underwent esophagogastroduodenoscopy (EGD) between May, 2017 and August, 2019 in the Toyoshima Endoscopy Clinic were enrolled in this study. Inclusion criteria included defined *H pylori* status (*H pylori*-negative patients, *H pylori*-positive patients, and *H pylori*-eradicated patients). The patients with unclear *H pylori* status and eradication failure were excluded from the study. EGD was conducted for the examination of symptoms and screening. We collected data on the patients' baseline characteristics, including age and sex, and period since eradication for eradicated patients.

Endoscopic procedures

EGD was performed using the Olympus Evis Lucera Elite system with a GIF-H290Z or GIF-HQ290 endoscope (Olympus Corporation, Tokyo, Japan)[20]. An expert physician (Toyoshima O) performed endoscopic procedures. Furthermore, EGD images were retrospectively reviewed by other expert physicians. Discrepancies in diagnosis between the two sets of physicians were resolved through discussion. Sedation with midazolam and/or pethidine was performed at the patient's discretion[21-23]. Antral nodularity was defined as a miliary nodular appearance consisting of whitish circular micronodules measuring ≤ 1 mm in both height and diameter. Cardiac nodularity was defined as a miliary nodular appearance or the presence of scattered whitish circular small colorations within 2 cm of the esophagogastric junction. Nodularity was visualized as whitish in the narrow-band imaging (NBI) mode. The representative endoscopic images are shown in Figure 1.

We scored atrophy, intestinal metaplasia, diffuse redness, and enlarged folds, according to the Kyoto classification[24].

Endoscopic atrophy was diagnosed based on the Kimura and Takemoto classification[25]. Non-atrophy and C1 were scored as Atrophy score 0, C2, and C3 as Atrophy score 1, and O1 to O3 as Atrophy score 2.

The absence of intestinal metaplasia was scored as Intestinal metaplasia score 0, the presence of intestinal metaplasia within the antrum as Intestinal metaplasia score 1, and intestinal metaplasia extending into the corpus as Intestinal metaplasia score 2. The Intestinal metaplasia score was diagnosed using white light imaging.

The absence of diffuse redness was scored as Diffuse redness score 0, mild diffuse redness or diffuse redness with regular arrangement of collecting venules (RAC) as Diffuse redness score 1, and severe diffuse redness or diffuse redness without RAC as Diffuse redness score 2.

The absence and presence of enlarged folds was scored as Enlarged folds score 0 and 1, respectively.

Diagnosis of H. pylori infection

Serum anti-*H. pylori* antibody was measured on the day of EGD. The antibody titer was measured using an enzyme immunoassay kit with antigens derived from Japanese individuals (E-plate Eiken *H. pylori* antibody II; Eiken Chemical, Tokyo,

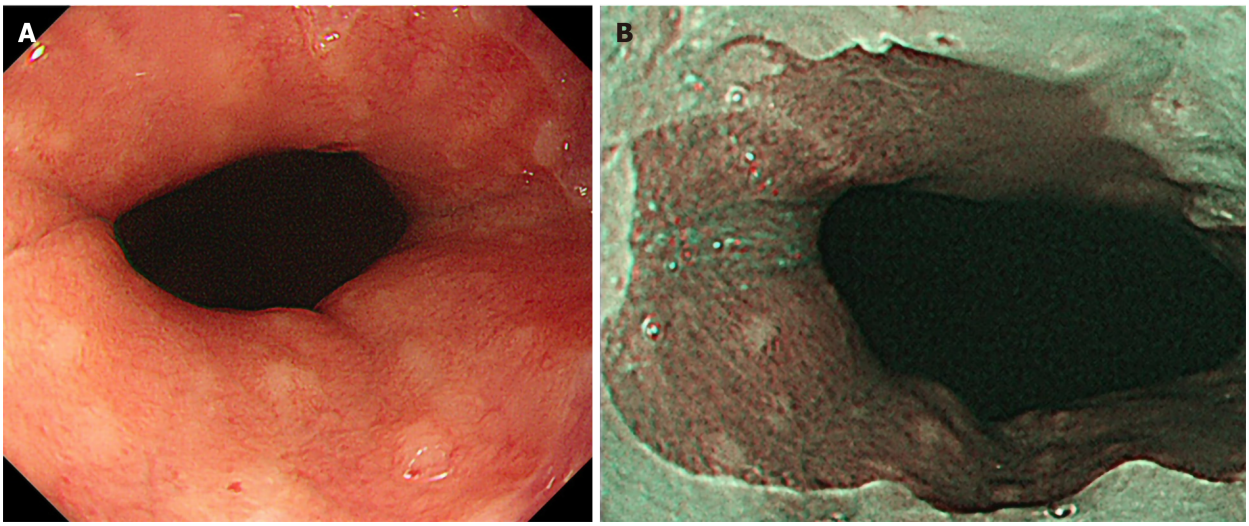

Figure 1 Endoscopic images of cardiac nodularity-like appearance. A: White light observation. A miliary pattern with a "gooseflesh-like" appearance was found in the cardia. Whitish circular micronodules measuring ≤ 1 mm in both diameter and height were observed; B: Narrow-band imaging observation. Whitish coloration denoted nodularity.

Japan). An antibody titer ≥ 10 U/mL (the cut-off value recommended by the manufacturer) was considered positive for *H. pylori*[26]. When the serum anti-*H. pylori* antibody titer was 3.0-9.9 U/mL, the findings of urea breath test or histological assessment was added. If either the urea breath test or histology was positive, patients were considered positive for *H. pylori*[27,28]. An antibody titer < 3.0 U/mL or negative urea breath test was considered to indicate *H. pylori* negativity. Eradication was confirmed by urea breath test.

Statistical analysis

Categorical data were compared using the chi-square test. Continuous data were compared using Student's or Welch's *t*-test, as appropriate. A two-sided *P* value of < 0.05 was considered as statistically significant. Calculations were carried out by the Stat Mate IV software (ATOMS, Tokyo, Japan).

RESULTS

The endoscopist performed 1215 EGDs during the study period. We excluded 137 patients (135 patients with unclear *H. pylori* infection status and two with eradication failure). A total of 1078 patients were finally included.

The characteristics of the participants in the present study are shown in Table 1. Among *H. pylori*-negative patients, cardiac nodularity and antral nodularity were recognized in one patient each (0.14% each). Among *H. pylori*-positive patients, cardiac nodularity and antral nodularity were recognized in 24 (54.5%) and 13 (29.5%) patients, respectively. The frequency of cardiac nodularity was significantly higher than that of antral nodularity ($P < 0.05$). Among *H. pylori*-eradicated patients, cardiac nodularity and antral nodularity were recognized in 15 (4.5%) and 2 (0.6%) patients, respectively. The frequency of cardiac nodularity was significantly higher than that of antral nodularity ($P < 0.01$). The frequencies of cardiac nodularity and antral nodularity in *H. pylori*-eradicated patients were significantly lower than those in *H. pylori*-positive patients ($P < 0.001$).

Clinical characteristics of cardiac nodularity in *H. pylori*-positive patients are shown in Table 2. The patients with cardiac nodularity were significantly younger than those without cardiac nodularity ($P = 0.0013$). Intestinal metaplasia score of the patients with cardiac nodularity were significantly lower than those without cardiac nodularity ($P = 0.0216$).

Among *H. pylori*-eradicated patients, the patients with cardiac nodularity were also significantly younger than those without cardiac nodularity ($P = 0.0003$, Table 3). Furthermore, the patients with cardiac nodularity underwent eradication significantly more recently compared with those without cardiac nodularity ($P < 0.0001$).

Table 1 Characteristics of enrolled subjects

	H. pylori negative	*H. pylori* positive	*H. pylori* eradicated
Patient number	704	44	330
Mean age (standard deviation)	54.2 ± 11.1	51.0 ± 13.4	60.3 ± 12.3
Male:female	358:346	19:25	185:145
Cardiac nodularity	1 (0.14%)	24 (54.5%)[a]	15 (4.5%)[bf]
Antral nodularity	1 (0.14%)	13 (29.5%)	2 (0.6%)[f]

[a]$P < 0.05$,
[b]$P < 0.01$ *vs* antral nodularity;
[f]$P < 0.001$ *vs Helicobacter pylori* positive. *H. pylori*: *Helicobacter pylori*.

Table 2 Clinical characteristics of cardiac nodularity in *Helicobacter pylori* positive patients

	Cardiac nodularity (+)	Cardiac nodularity (-)	*P* value
Patient number	24	20	
Mean age (standard deviation)	44.9 ± 7.8	58.3 ± 15.1	0.0013
Male:female	9:15	10:10	0.598
Atrophy score	1.46 ± 0.59	1.55 ± 0.51	0.588
Intestinal metaplasia score	0.21 ± 0.59	0.80 ± 0.95	0.0216
Enlarged fold score	0.54 ± 0.51	0.60 ± 0.50	0.705
Diffuse redness score	1.75 ± 0.55	1.67 ± 0.64	0.648

Table 3 Clinical characteristics of cardiac nodularity in *Helicobacter pylori* eradicated patients

	Cardiac nodularity (+)	Cardiac nodularity (-)	*P* value
Patient number	15	315	
Mean age (standard deviation)	49.2 ± 12.3	60.8 ± 12.1	0.0003
Male:female	5:10	180:135	0.121
Months after eradication	41.5 ± 30.1	91.6 ± 100.0	< 0.0001

DISCUSSION

The prevalence of cardiac nodularity was 0.14%, 54.5%, and 4.5% in *H. pylori*-negative, -positive, and -eradicated patients, respectively. Cardiac nodularity was more frequent than antral nodularity in *H. pylori*-positive and -eradicated patients. Cardiac nodularity was often found in younger patients and patients with less intestinal metaplasia. Cardiac nodularity decreased after eradication, especially in patients who underwent eradication a long time ago.

Our previous study showed excellent prediction accuracy of cardiac nodularity due to *H. pylori* infection, with 0.928 of accuracy, 0.996 of specificity, 0.571 of sensitivity, 0.960 of positive predictive value, and 0.925 of negative predictive value[18]. In our previous study, we included only the patients who were evaluated for *H pylori* infection for the first time, and excluded patients with a history of eradication. However, the present cross-sectional study included the patients with a history of eradication also. The frequency of cardiac nodularity in *H. pylori*-positive patients was remarkably higher than that in *H. pylori*-negative patients and *H. pylori*-eradicated patients. Cardiac nodularity may serve as one of the predictive markers for active *H. pylori* infection.

Nodular gastritis is more frequent in children than in adults[29]. The prevalence of nodular gastritis has been reported to be 32.9%-85% in *H. pylori*-positive children[30-34]. The prevalence of nodular gastritis gradually decreased with age[13]. Our study also

showed that the patients with cardiac nodularity were significantly younger than those without cardiac nodularity. Age dependence of cardiac nodularity is in line with that of antral nodularity.

Miyamoto *et al*[13] demonstrated that atrophy scores were lower in patients with nodular gastritis than in *H. pylori*-positive controls. Nakashima *et al*[35] also reported that atrophy and intestinal metaplasia were rare in nodular gastritis. Our study also showed that compared with patients without cardiac nodularity, Intestinal metaplasia score of the patients with cardiac nodularity was significantly lower. Cardiac nodularity seemed to disappear with the progression of intestinal metaplasia.

Dwivedi *et al*[36] reported that 87.5% of nodular gastritis patients showed complete normalization of the gastric mucosa after *H. pylori* eradication therapy. Our study also showed significantly low prevalence of cardiac nodularity in *H. pylori*-eradicated patients, especially in patients who underwent eradication a long time ago. Cardiac nodularity seemed to disappear with improvement in gastric inflammation after *H. pylori* eradication.

This study had some limitations. First, this study employed only a single experienced endoscopist. Second, the study was a retrospective review at a single institution. Our results should be validated in diverse settings for generalizability.

CONCLUSION

This report outlined the prevalence and clinical features of cardiac nodularity, and confirmed its close association with active *H. pylori* infection.

ARTICLE HIGHLIGHTS

Research background

Helicobacter pylori (*H. pylori*)-associated nodular gastritis could occur in both the antrum and the cardia. Cardiac nodularity-like appearance is found more frequently than antral nodularity.

Research motivation

Previous study included only the patients who were evaluated for *H. pylori* infection for the first time. There still remains a lack of the prevalence and clinical features of cardiac nodularity-like appearance.

Research objectives

We aimed to evaluate the characteristics of cardiac nodularity-like appearance.

Research methods

We enrolled consecutive patients who underwent esophagogastroduodenoscopy between May, 2017 and August, 2019 in the Toyoshima Endoscopy Clinic. We included *H. pylori*-negative, *H. pylori*-positive, and *H. pylori*-eradicated patients, and excluded patients with unclear *H. pylori* status and eradication failure. Cardiac nodularity was defined as a miliary nodular appearance or the presence of scattered whitish circular small colorations within 2 cm of the esophagogastric junction.

Research results

A total of 1078 patients were finally included. The prevalence of cardiac and antral nodularity in *H. pylori*-negative, -positive, and -eradicated patients were 0.14% and 0.14%, 54.5% and 29.5%, and 4.5% and 0.6%, respectively. Cardiac nodularity-like appearance was more frequent than antral nodularity in *H. pylori*-positive and -eradicated patients. Cardiac nodularity-like appearance was often found in younger patients and patients with less intestinal metaplasia. Cardiac nodularity-like appearance decreased after eradication, especially in patients who underwent eradication a long time ago.

Research conclusions

This report outlines the prevalence and clinical features of cardiac nodularity-like appearance, and confirm its close association with active *H. pylori* infection.

Research perspectives

Our results should be validated in diverse settings for generalizability.

REFERENCES

1 **Suzuki H**, Nishizawa T, Tsugawa H, Mogami S, Hibi T. Roles of oxidative stress in stomach disorders. *J Clin Biochem Nutr* 2012; **50**: 35-39 [PMID: 22247598 DOI: 10.3164/jcbn.11-115SR]

2 **Šterbenc A**, Jarc E, Poljak M, Homan M. *Helicobacter pylori* virulence genes. *World J Gastroenterol* 2019; **25**: 4870-4884 [PMID: 31543679 DOI: 10.3748/wjg.v25.i33.4870]

3 **Kubosawa Y**, Mori H, Kinoshita S, Nakazato Y, Fujimoto A, Kikuchi M, Nishizawa T, Suzuki M, Suzuki H. Changes of gastric ulcer bleeding in the metropolitan area of Japan. *World J Gastroenterol* 2019; **25**: 6342-6353 [PMID: 31754294 DOI: 10.3748/wjg.v25.i42.6342]

4 **Toyoshima O**, Tanikawa C, Yamamoto R, Watanabe H, Yamashita H, Sakitani K, Yoshida S, Kubo M, Matsuo K, Ito H, Koike K, Seto Y, Matsuda K. Decrease in *PSCA* expression caused by *Helicobacter pylori* infection may promote progression to severe gastritis. *Oncotarget* 2018; **9**: 3936-3945 [PMID: 29423095 DOI: 10.18632/oncotarget.23278]

5 **Toyoshima O**, Yamaji Y, Yoshida S, Matsumoto S, Yamashita H, Kanazawa T, Hata K. Endoscopic gastric atrophy is strongly associated with gastric cancer development after Helicobacter pylori eradication. *Surg Endosc* 2017; **31**: 2140-2148 [PMID: 27604367 DOI: 10.1007/s00464-016-5211-4]

6 **Sugimoto M**, Murata M, Yamaoka Y. Chemoprevention of gastric cancer development after *Helicobacter pylori* eradication therapy in an East Asian population: Meta-analysis. *World J Gastroenterol* 2020; **26**: 1820-1840 [PMID: 32351296 DOI: 10.3748/wjg.v26.i15.1820]

7 **Mori H**, Suzuki H. Update on quinolone-containing rescue therapies for *Helicobacter pylori* infection. *World J Gastroenterol* 2020; **26**: 1733-1744 [PMID: 32351290 DOI: 10.3748/wjg.v26.i15.1733]

8 **Nishizawa T**, Suzuki H, Maekawa T, Harada N, Toyokawa T, Kuwai T, Ohara M, Suzuki T, Kawanishi M, Noguchi K, Yoshio T, Katsushima S, Tsuruta H, Masuda E, Tanaka M, Katayama S, Kawamura N, Nishizawa Y, Hibi T, Takahashi M. Dual therapy for third-line Helicobacter pylori eradication and urea breath test prediction. *World J Gastroenterol* 2012; **18**: 2735-2738 [PMID: 22690086 DOI: 10.3748/wjg.v18.i21.2735]

9 **Nishizawa T**, Maekawa T, Watanabe N, Harada N, Hosoda Y, Yoshinaga M, Yoshio T, Ohta H, Inoue S, Toyokawa T, Yamashita H, Saito H, Kuwai T, Katayama S, Masuda E, Miyabayashi H, Kimura T, Nishizawa Y, Takahashi M, Suzuki H. Clarithromycin Versus Metronidazole as First-line Helicobacter pylori Eradication: A Multicenter, Prospective, Randomized Controlled Study in Japan. *J Clin Gastroenterol* 2015; **49**: 468-471 [PMID: 24921211 DOI: 10.1097/MCG.0000000000000165]

10 **de Brito BB**, da Silva FAF, Soares AS, Pereira VA, Santos MLC, Sampaio MM, Neves PHM, de Melo FF. Pathogenesis and clinical management of *Helicobacter pylori* gastric infection. *World J Gastroenterol* 2019; **25**: 5578-5589 [PMID: 31602159 DOI: 10.3748/wjg.v25.i37.5578]

11 **Suzuki H**, Nishizawa T, Tsugawa H, Hibi T. Molecular approaches and modern clinical strategies for the management of Helicobacter pylori infection in Japan. *Keio J Med* 2012; **61**: 109-119 [PMID: 23324305 DOI: 10.2302/kjm.2012-0001-re]

12 **Sakitani K**, Nishizawa T, Arita M, Yoshida S, Kataoka Y, Ohki D, Yamashita H, Isomura Y, Toyoshima A, Watanabe H, Iizuka T, Saito Y, Fujisaki J, Yahagi N, Koike K, Toyoshima O. Early detection of gastric cancer after Helicobacter pylori eradication due to endoscopic surveillance. *Helicobacter* 2018; **23**: e12503 [PMID: 29924436 DOI: 10.1111/hel.12503]

13 **Miyamoto M**, Haruma K, Yoshihara M, Hiyama T, Sumioka M, Nishisaka T, Tanaka S, Chayama K. Nodular gastritis in adults is caused by Helicobacter pylori infection. *Dig Dis Sci* 2003; **48**: 968-975 [PMID: 12772798 DOI: 10.1023/a:1023016000096]

14 **Hayashi S**, Imamura J, Kimura K, Saeki S, Hishima T. Endoscopic features of lymphoid follicles in Helicobacter pylori-associated chronic gastritis. *Dig Endosc* 2015; **27**: 53-60 [PMID: 25092073 DOI: 10.1111/den.12335]

15 **Nishikawa I**, Kato J, Terasoma S, Matsutani H, Tamaki H, Tamaki T, Kuwashima F, Nakata H, Tomeki T, Matsunaka H, Ibata Y, Yamashita Y, Maekita T, Higashi K, Ichinose M. Nodular gastritis in association with gastric cancer development before and after *Helicobacter pylori* eradication. *JGH Open* 2018; **2**: 80-86 [PMID: 30483568 DOI: 10.1002/jgh3.12049]

16 **Zerbib F**, Vialette G, Cayla R, Rudelli A, Sauvet P, Bechade D, Seurat PL, Lamouliatte H. [Follicular gastritis in adults. Relations with Helicobacter pylori, histological and endoscopic aspects]. *Gastroenterol Clin Biol* 1993; **17**: 529-534 [PMID: 8253308]

17 **Kitamura S**, Yasuda M, Muguruma N, Okamoto K, Takeuchi H, Bando Y, Miyamoto H, Okahisa T, Yano M, Torisu R, Takayama T. Prevalence and characteristics of nodular gastritis in Japanese elderly. *J Gastroenterol Hepatol* 2013; **28**: 1154-1160 [PMID: 23432631 DOI: 10.1111/jgh.12180]

18 **Toyoshima O**, Nishizawa T, Sakitani K, Yamakawa T, Watanabe H, Yoshida S, Nakai Y, Hata K, Ebinuma H, Suzuki H, Koike K. Nodularity-like appearance in the cardia: novel endoscopic findings for *Helicobacter pylori* infection. *Endosc Int Open* 2020; **8**: E770-E774 [PMID: 32490162 DOI: 10.1055/a-1136-9890]

19 **Nishizawa T**, Suzuki H, Arano T, Yoshida S, Yamashita H, Hata K, Kanai T, Yahagi N, Toyoshima O. Characteristics of gastric cancer detected within 1 year after successful eradication of *Helicobacter pylori*. *J Clin Biochem Nutr* 2016; **59**: 226-230 [PMID: 27895391 DOI: 10.3164/jcbn.16-43]

20 **Nishizawa T**, Sakitani K, Suzuki H, Yamakawa T, Takahashi Y, Yoshida S, Nakai Y, Hata K, Ebinuma H, Koike K, Toyoshima O. Small-caliber endoscopes are more fragile than conventional endoscopes. *Endosc Int Open* 2019; **7**: E1729-E1732 [PMID: 31828209 DOI: 10.1055/a-1036-6186]

21 **Nishizawa T**, Suzuki H, Arita M, Kataoka Y, Fukagawa K, Ohki D, Hata K, Uraoka T, Kanai T, Yahagi N, Toyoshima O. Pethidine dose and female sex as risk factors for nausea after esophagogastroduodenoscopy. *J Clin Biochem Nutr* 2018; **63**: 230-232 [PMID: 30487674 DOI: 10.3164/jcbn.18-5]

22 **Toyoshima O**, Yoshida S, Nishizawa T, Yamakawa T, Sakitani K, Hata K, Takahashi Y, Fujishiro M, Watanabe H, Koike K. CF290 for pancolonic chromoendoscopy improved sessile serrated polyp detection and procedure time: a propensity score-matching study. *Endosc Int Open* 2019; **7**: E987-E993 [PMID: 31367679 DOI: 10.1055/a-0953-1909]

23 **Nishizawa T**, Sakitani K, Suzuki H, Takeuchi M, Takahashi Y, Takeuchi K, Yamakawa T, Yoshida S, Hata K, Ebinuma H, Koike K, Toyoshima O. Adverse events associated with bidirectional endoscopy with midazolam and pethidine. *J Clin Biochem Nutr* 2020; **66**: 78-81 [PMID: 32001961 DOI: 10.3164/jcbn.19-73]

24 **Toyoshima O**, Nishizawa T, Koike K. Endoscopic Kyoto classification of *Helicobacter pylori* infection and gastric cancer risk diagnosis. *World J Gastroenterol* 2020; **26**: 466-477 [PMID: 32089624 DOI: 10.3748/wjg.v26.i5.466]

25 **Kimura K**, Takemoto T. An endoscopic recognition of the atrophic border and its significance in chronic gastritis. *Endoscopy* 1969; **3**: 87-97 [DOI: 10.1055/s-0028-1098086]

26 **Toyoshima O**, Nishizawa T, Sakitani K, Yamakawa T, Takahashi Y, Yamamichi N, Hata K, Seto Y, Koike K, Watanabe H, Suzuki H. Serum anti-*Helicobacter pylori* antibody titer and its association with gastric nodularity, atrophy, and age: A cross-sectional study. *World J Gastroenterol* 2018; **24**: 4061-4068 [PMID: 30254410 DOI: 10.3748/wjg.v24.i35.4061]

27 **Toyoshima O**, Nishizawa T, Arita M, Kataoka Y, Sakitani K, Yoshida S, Yamashita H, Hata K, Watanabe H, Suzuki H. *Helicobacter pylori* infection in subjects negative for high titer serum antibody. *World J Gastroenterol* 2018; **24**: 1419-1428 [PMID: 29632423 DOI: 10.3748/wjg.v24.i13.1419]

28 **Nishizawa T**, Sakitani K, Suzuki H, Yamakawa T, Takahashi Y, Yamamichi N, Watanabe H, Seto Y, Koike K, Toyoshima O. A combination of serum anti-*Helicobacter pylori* antibody titer and Kyoto classification score could provide a more accurate diagnosis of *H pylori*. *United European Gastroenterol J* 2019; **7**: 343-348 [PMID: 31019702 DOI: 10.1177/2050640619825947]

29 **Al-Enezi SA**, Alsurayei SA, Aly NY, Ismail AE, Ismail WA, Al-Brahim N, El-Dousari A. Endoscopic nodular gastritis in dyspeptic adults: prevalence and association with Helicobacter pylori infection. *Med Princ Pract* 2010; **19**: 40-45 [PMID: 19996618 DOI: 10.1159/000252833]

30 **Bujanover Y**, Konikoff F, Baratz M. Nodular gastritis and Helicobacter pylori. *J Pediatr Gastroenterol Nutr* 1990; **11**: 41-44 [PMID: 2388131 DOI: 10.1097/00005176-199007000-00008]

31 **Mitchell HM**, Bohane TD, Tobias V, Bullpitt P, Daskalopoulos G, Carrick J, Mitchell JD, Lee A. Helicobacter pylori infection in children: potential clues to pathogenesis. *J Pediatr Gastroenterol Nutr* 1993; **16**: 120-125 [PMID: 8450376 DOI: 10.1097/00005176-199302000-00004]

32 **Shiotani A**, Kamada T, Kumamoto M, Nakae Y, Nakamura Y, Kakudo K, Haruma K. Nodular gastritis in Japanese young adults: endoscopic and histological observations. *J Gastroenterol* 2007; **42**: 610-615 [PMID: 17701123 DOI: 10.1007/s00535-007-2073-5]

33 **Prieto G**, Polanco I, Larrauri J, Rota L, Lama R, Carrasco S. Helicobacter pylori infection in children: clinical, endoscopic, and histologic correlations. *J Pediatr Gastroenterol Nutr* 1992; **14**: 420-425 [PMID: 1517945 DOI: 10.1097/00005176-199205000-00008]

34 **Luzza F**, Pensabene L, Imeneo M, Mancuso M, Giancotti L, La Vecchia AM, Costa MC, Strisciuglio P, Pallone F. Antral nodularity and positive CagA serology are distinct and relevant markers of severe gastric inflammation in children with Helicobacter pylori infection. *Helicobacter* 2002; **7**: 46-52 [PMID: 11886473 DOI: 10.1046/j.1523-5378.2002.00055.x]

35 **Nakashima R**, Nagata N, Watanabe K, Kobayakawa M, Sakurai T, Akiyama J, Hoshimoto K, Shimbo T, Uemura N. Histological features of nodular gastritis and its endoscopic classification. *J Dig Dis* 2011; **12**: 436-442 [PMID: 22118692 DOI: 10.1111/j.1751-2980.2011.00532.x]

36 **Dwivedi M**, Misra SP, Misra V. Nodular gastritis in adults: clinical features, endoscopic appearance, histopathological features, and response to therapy. *J Gastroenterol Hepatol* 2008; **23**: 943-947 [PMID: 17614956 DOI: 10.1111/j.1440-1746.2007.05044.x]

World Journal of Gastroenterology

Submit a Manuscript: https://www.f6publishing.com

World J Gastroenterol 2020 September 21; 26(35): 5362-5374

DOI: 10.3748/wjg.v26.i35.5362

ISSN 1007-9327 (print) ISSN 2219-2840 (online)

SYSTEMATIC REVIEWS

Systematic review of the prevalence and development of osteoporosis or low bone mineral density and its risk factors in patients with inflammatory bowel disease

Sofia Kärnsund, Bobby Lo, Flemming Bendtsen, Jakob Holm, Johan Burisch

ORCID number: Sofia Kärnsund 0000-0003-1312-8065; Bobby Lo 0000-0002-0252-9341; Flemming Bendtsen 0000-0002-8419-2104; Jakob Holm 0000-0001-6096-1979; Johan Burisch 0000-0002-3312-5139.

Author contributions: All authors have made significant contributions to the research in this study; all authors approved the submitted version of the manuscript and the authorship list; Kärnsund S and Lo B contributed to acquisition, interpretation and analysis of data; Kärnsund S contributed to writing of manuscript; Lo B contributed to critical revision for important intellectual content; Bendtsen F and Burisch J contributed to conception and design of study, critical revision for important intellectual content; Burisch J contributed to finally approval of submitted manuscript.

Conflict-of-interest statement: Burisch J received consulting fees from Celgene, Janssen-Cilag, AbbVie, Tillots Pharma and Ferring; lecture fees from Abbvie, Pfizer, MSD, Pharmacosmos and Takeda Pharma; unrestricted grant support from Takeda Pharma, MSD, AbbVie and Tillots Pharma. Holm J has participated as a sub

Sofia Kärnsund, Bobby Lo, Flemming Bendtsen, Johan Burisch, Gastrounit, Medical Division, Copenhagen University Hospital Hvidovre, Hvidovre 2650, Denmark

Jakob Holm, Department of Endocrinology, Copenhagen University Hospital Herlev, Herlev 4600, Denmark

Corresponding author: Sofia Kärnsund, BSc, Doctor, Gastrounit, Medical Division, Copenhagen University Hospital Hvidovre, Kettegård Alle 30, Hvidovre 2650, Denmark. sofiakarnsund@hotmail.com

Abstract

BACKGROUND

The inflammatory bowel diseases (IBD), Crohn's disease (CD) and ulcerative colitis (UC) are chronic, immune-mediated disorders of the digestive tract. IBD is considered to be a risk factor for developing osteoporosis; however current literature on this matter is inconsistent.

AIM

To assess prevalence and development of osteoporosis and low bone mineral density (BMD), and its risk factors, in IBD patients.

METHODS

Systematic review of population-based studies. Studies were identified by electronic (January 2018) and manual searches (May 2018). Databases searched included EMBASE and PubMed and abstracts from 2014-2018 presented at the United European Gastroenterology Week, the European Crohn's and Colitis Organisation congress, and Digestive Disease Week were screened. Studies were eligible for inclusion if they investigated either the prevalence of osteoporosis or osteopenia and/or risk factors for osteoporosis or low BMD in IBD patients. Studies on children under the age of 18 were excluded. Only population-based studies were included. All risk factors for osteoporosis and low BMD investigated in any included article were considered. Study quality and the possibility of bias were analysed using the Newcastle-Ottawa scale.

RESULTS

Twelve studies including 3661 IBD patients and 12789 healthy controls were included. Prevalence of osteoporosis varied between 4%-9% in studies including

investigator in studies by Amgen and MSD and received payment for lectures sponsored by Amgen and LEO Pharma. Kärnsund S, Lo B and Bendtsen F have nothing to declare.

PRISMA 2009 Checklist statement: The authors have read the PRISMA 2009 Checklist, and the manuscript was prepared and revised according to the PRISMA 2009 Checklist.

Manuscript source: Unsolicited manuscript

Received: March 28, 2020
Peer-review started: March 28, 2020
First decision: April 25, 2020
Revised: May 4, 2020
Accepted: August 22, 2020
Article in press: August 22, 2020
Published online: September 21, 2020

P-Reviewer: Faye AS, Lee JI, Musumeci G
S-Editor: Ma YJ
L-Editor: A
P-Editor: Ma YJ

both CD and UC patients; 2%-9% in studies including UC patients, and 7%-15% in studies including CD patients. Among healthy controls, prevalence of osteoporosis was 3% and 10% in two studies. CD diagnosis, lower body mass index (BMI), and lower body weight were risk factors associated with osteoporosis or low BMD. Findings regarding gender showed inconsistent results. CD patients had an increased risk for osteoporosis or low BMD over time, while UC patients did not. Increased age was associated with decreased BMD, and there was a positive association between weight and BMI and BMD over time. Great heterogeneity was found in the included studies in terms of study methodologies, definitions and the assessment of osteoporosis, and only a small number of population-based studies was available.

CONCLUSION
This systematic review found a possible increase of prevalence of osteoporosis in CD cohorts when compared to UC and cohorts including both disease types. Lower weight and lower BMI were predictors of osteoporosis or low BMD in IBD patients. The results varied considerably between studies.

Key Words: Inflammatory bowel disease; Osteoporosis; Systematic review; Epidemiology; Bone mineral density

Core Tip: Being diagnosed with inflammatory bowel disease (IBD) is considered a risk factor for development of osteoporosis, which leads to an increased risk of pathological fractures. This makes osteoporosis associated with great economic and psychological burden. Research made on the relationship between IBD and osteoporosis differs in study design and study populations, and results are inconsistent. The aims with this research are to assess the prevalence of osteoporosis among IBD patients compared to healthy individuals, assess the disease course of osteoporosis or low bone mineral density (BMD) in IBD patients and assess risk factors associated with osteoporosis and low BMD in IBD patients.

Citation: Kärnsund S, Lo B, Bendtsen F, Holm J, Burisch J. Systematic review of the prevalence and development of osteoporosis or low bone mineral density and its risk factors in patients with inflammatory bowel disease. *World J Gastroenterol* 2020; 26(35): 5362-5374
URL: https://www.wjgnet.com/1007-9327/full/v26/i35/5362.htm
DOI: https://dx.doi.org/10.3748/wjg.v26.i35.5362

INTRODUCTION

The inflammatory bowel diseases (IBD), encompassing Crohn's disease (CD) and ulcerative colitis (UC) are chronic, immune-mediated disorders of the digestive tract of unknown aetiology. Being diagnosed with IBD is considered a risk factor for the development of osteoporosis, which leads to an increased risk of pathological fractures[1]. It is hypothesized that the severity and extent of gut inflammation and intestinal malabsorption leading to calcium and vitamin D deficiency in IBD patients might have a detrimental effect on bone[2-4]. Other known risk factors for osteoporosis, that also apply to the population without IBD are female gender, older age, low BMI and smoking[2-5]. As bone-protecting factors, physical activity has been found to have beneficial effects on both bone and cartilage in patients with osteoporosis, whether it's glucocorticoid-induced or not[6-8].

While osteoporosis is asymptomatic before fractures occur, the development of osteoporotic fractures as a consequence makes osteoporosis associated with great economic and psychological burden[9,10]. Several studies have investigated the relationship between inflammatory bowel diseases and osteoporosis but differences in study design and study populations, as well as inconsistent results and diverging interpretations of them, make it difficult to draw firm conclusions.

With this systematic review, we aimed to assess the prevalence of osteoporosis among IBD patients compared to healthy individuals, as well as the disease course of

osteoporosis or low BMD in IBD patients. We also aimed to assess risk factors associated with osteoporosis and low BMD in IBD patients with the intention to find more substantial evidence as to the cause of osteoporosis or low BMD in this patient group.

MATERIALS AND METHODS

Protocol and registration

This systematic review was conducted in accordance with the MOOSE (Meta-analyses Of Observational Studies in Epidemiology) guidelines. Prior to data extraction and analysis, a protocol was registered with PROSPERO (ID CRD42018084259) that has been updated regularly.

Sources

Studies were identified through electronic searches and by manually reviewing the reference lists of these studies, as well as relevant review articles. Electronic searches were conducted on January 30, 2018. Databases searched included EMBASE and PubMed. Searches were adjusted where needed for each database. Terms related to "inflammatory bowel disease", "osteoporosis", "osteopenia" and "study design" were used. The detailed search strategy is presented in Supplementary Table 1. Prior to title and abstract screening, duplicates and articles written in a language other than English were excluded. Titles and abstracts were screened independently by two of the review's authors (SK/BL). Disagreement was resolved by consensus. Potentially eligible studies were read in full by the same two authors (SK/BL). Disagreements that could not be resolved by consensus were discussed with a third author (JB) until an agreement was reached. Screening and study selection were made using the review management tool Covidence (www.covidence.org).

The search for unpublished articles occurred between May 14-16, 2018, where abstracts from 2014-2018 presented at the United European Gastroenterology Week, the European Crohn's and Colitis Organisation congress, and Digestive Disease Week were screened. Only the European Crohn's and Colitis Organisation congress had published abstracts from 2018. The screening was made by searching for the terms "osteoporosis", "osteopenia", "bone mineral density" and "inflammatory bowel disease".

Study selection, eligibility criteria and quality assessment

Studies were eligible for inclusion if they investigated either the prevalence of osteoporosis or osteopenia and/or risk factors for osteoporosis or low BMD in IBD patients. Studies on children under the age of 18 were excluded. Only population-based studies were included. All risk factors for osteoporosis and low BMD investigated in any included article were considered.

Quality assessment and risk of bias assessment were performed using the Newcastle-Ottawa scale (NOS), a scale developed for assessment of nonrandomized studies including cohort studies[11]. Stars were given to each article based on criteria in the categories of "selection", "comparability" and "outcome". A maximum of nine stars could be allocated to any one study.

Data extraction

From each included study the following information was extracted: (1) Author, year of publication, study period, number of patients included, country of study; (2) Prevalence of osteoporosis in patient groups and, if included in the study, healthy control groups; (3) T, Z and BMD (g/cm^2) scores in patient groups and, if included in the study, healthy control groups; (4) Prevalence of osteoporosis and T, Z and BMD (g/cm^2) scores in subgroups including gender, type of IBD, age (>/< 50 years), treatment (steroid/non-steroid), previous surgery, and Montreal disease classification; (5) Information regarding changes in rates of osteoporosis over a period of time; and (6) All clinical and socio-demographic risk factors that are investigated to be associated with osteoporosis or lowering of BMD in IBD patients.

Dual-energy X-ray absorptiometry (DXA) is performed on several bone areas and studies were therefore expected to present both overall measurements and/or information on each specific area. Examining risk factors for osteoporosis or low BMD in IBD patients, we considered it an association if at least one measured bone area showed significant association to an investigated risk factor, or if at least one measured

bone area showed significantly lower BMD than that same area in a comparison group. If a study only presented the proportion of patients with osteoporosis in each individual bone area, the overall prevalence was defined as that in the bone area in which most patients had osteoporosis. Prevalence of osteopenia was not considered.

If several studies analyzed the same cohort, prevalence estimates and risk factors were only registered once for each cohort. Authors were contacted for possible unpublished data. Studies analyzing CD and UC patients combined are referred to as "IBD studies", while studies analyzing CD or UC exclusively are described as "CD studies" or "UC studies", respectively.

RESULTS

Study characteristics

The search identified 449 records. After removing duplicates, non-English language studies and screening abstracts, 84 full-text articles were assessed for eligibility. A total of 12 papers were included in our study, one[12] of which was found *via* screening of references. An overview of the number of titles, abstracts and full-text articles that were excluded, with justification for their exclusion, can be found in the PRISMA flow diagram, Figure 1. No conference abstracts matched our criteria for inclusion. Authors either declined to provide data or did not respond to our queries in eight cases.

A detailed overview of the characteristics of each study is presented in Table 1. The 12 studies were based on a total of seven cohorts. All twelve studies contributed with unique information despite the fact that some included the same cohort. Information was only registered once for each cohort. Six studies investigated only CD patients[12-17], while the remainder investigated both CD and UC patients. No studies investigated only CD patients. Four studies included a healthy control group[12,15,17,18]. Five were follow up studies[3,12,18-20]. Two studies investigated only premenopausal women[21,22]. Two studies presented only the number of patients that had osteoporosis in each measured bone area but no overall number[13,17]. The total population across all studies was 3661 IBD patients, of which 1833 (50%) were women and 1828 (50%) men. A total of 1546 (42%) patients had UC and 2115 (58%) had CD. The control groups consisted of 12789 healthy individuals.

Quality assessment

Table 2 provides detailed quality assessments of the studies according to the NOS. All included studies were allocated stars for the representativeness of the exposed cohort – the average IBD patient – since they are all population based. Osteoporosis was either diagnosed by DXA scan or from ICD-10 codes and hence all studies received at least two stars with regards to selection. With regards to comparability, gender and age were identified to be the most relevant confounding variables. With reference to outcome, 2 years were set as long enough follow-up time for outcomes (osteoporosis or change in BMD) to occur. A maximum of 25% of patients could be lost to follow up in order to receive a star for adequacy of follow up of cohorts.

Prevalence of osteoporosis (diagnosis based on T- and Z-scores or ICD-10 codes)

The prevalence of osteoporosis in IBD patients ranged from 2%[18] to 15%[16]. In patients with UC, this range was 2%-9%[18,19], while it was 7%-15%[16,18,19] in CD patients. Two studies provided age- and sex matched controls and in these the prevalence of osteoporosis was 3%[18] and 10%[17], respectively.

Risk factors for low bone mineral density

Nine studies based on six study cohorts investigated risk factors for osteoporosis or low BMD of which four, based on two study cohorts, investigated both UC and CD patients[19-22] and of which five, based on four study cohorts, investigated only CD patients[12-15,17]. An overview of the most relevant risk factors associated with osteoporosis or low BMD can be found in Table 3, while a detailed list can be found in Supplementary Table 2. Overall, a CD diagnosis, lower body mass index (BMI) and lower body weight were associated with osteoporosis or low BMD. Female gender was found to be associated with lower BMD in a study of both CD and UC patients[20]. In CD cohorts, one study found males to have lower BMD than women[12], one study found no significance[13] and one study found female gender to be predictive for decreased BMD[17]. Use of corticosteroids in any form and with any duration was found to be associated with osteoporosis or low BMD only in studies investigating CD

Table 1 Study characteristics

Ref.	Publication year	Country of study	Type of study	DXA scan[1]	No. of patients	Average age of patients	Cohort	Control group	Follow-up	Comments
Andreassen *et al*[1]	1998	Denmark	Cross-sectional study inviting all IBD patients from a well-defined area	Yes	115	37 (16-75); median (range)	CD only	No	No	
Andreassen *et al*[2]	1999	Denmark	Cross-sectional case-control study inviting all IBD patients from a well-defined area	Yes	113	37 (16-75); median (range)	CD only	Yes; *n* = 113	No	Same cohort used as in Andreassen *et al*[14] (1998)
Bernstein *et al*[3]	2003[2]	United States	Cross-sectional data extracted from population-based Manitoba IBD research registry	Yes	70; UC: *n* = 12; CD: *n* = 58	33.0 (7.4); mean (SD)	UC and CD	No	No	Includes only premenopausal women
Bernstein *et al*[4]	2003[3]	United States	Cross-sectional data extracted from population-based Manitoba IBD research registry	Yes	66 (DXA results: *n* = 70); UC: *n* = 11; CD: *n* = 55	33.3 (18-44); mean (range)	UC and CD	No	No	Includes only premenopausal women. Same cohort used as in Bernstein (2002)
Haugeberg *et al*[5]	2001	Norway	Cross-sectional data from a population-based study. Case control study	Yes	55	38.5 (12.7); mean (SD)	CD only	Yes; *n* = 52	No	
Jahnsen *et al*[6]	1997	Norway	Cross-sectional case control study	Yes	60	36 (21-75); median (range)	CD only	Yes; *n* = 60	No	Includes a cohort of UC patients that is not population-based which was therefore not included
Jahnsen *et al*[7]	2004	Norway	Follow-up study	Yes	60	36 (21-75); median (range)	CD only	No	Yes	Includes a cohort of UC patients that is not population-based which was therefore not included
									2 yr	Same cohort used as in Jahnsen (1997)
Leslie *et al*[8]	2008	Canada	Follow-up study with cohort extracted from population-based Manitoba IBD research registry	Yes	101; UC: *n* = 45; CD: *n* = 56	46.9 (15.5); mean (SD)	UC and CD	No	Yes; 2.3 ± 0.3 yr	
Leslie *et al*[9]	2009	Canada	Follow-up study with cohort extracted from population-based Manitoba IBD research registry	Yes	101 UC: *n* = 45 CD: *n* = 56	47 (15); mean (SD)	UC and CD	No	Yes; 2.3 ± 0.3 yr	Same cohort used as in Leslie *et al*[19] (2008)
Schoon *et al*[10]	2000	The Netherlands	Cross-sectional cohort	Yes	119	42 (14); mean (SD)	CD only	No	No	
Targownik *et al*[11]	2012	Canada	Follow-up study with data extracted from population-based Manitoba IBD research registry	Yes	86; UC: *n* = 32; CD: *n* = 50; Unclass: *n* = 4	46.7 (14.9); mean (SD); 46 (35-57) median (IQR)	UC and CD	No	Yes; 4.3 ± 0.3 yr	Same cohort used as in Leslie *et al*[19] (2008)
Tsai *et al*[12]	2015	Taiwan	Follow-up case control study with data extracted from population-based registry	No	3141; UC: *n* = 1489; CD: *n* = 1652	46.7 (35.6-61.0); median (IQR)	UC and CD	Yes; *n* = 12564	Yes; 6.49 ± 3.09 yr	Diagnosis of osteoporosis based on ICD-10 codes

[1]BMD scores derived from DXA scan.
[2]published in May.

[3]published in November. CD: Crohn's disease; UC: Ulcerative colitis; IQR: interquartile range; Unclass.: unclassified; IBD: inflammatory bowel diseases.

Table 2 Quality assessment according to the Newcastle–Ottawa Scale

	Schoon *et al*[13] (2000)	Jahnsen *et al*[12] (1997)	Jahnsen *et al*[16] (2004)	Tsai *et al*[18] (2015)	Targownik *et al*[3] (2012)	Leslie *et al*[20] (2009)	Leslie *et al*[19] (2008)	Andreassen *et al*[14] (1998)	Andreassen *et al*[15] (1999)	Bernstein *et al*[21] (2003, May)	Bernstein *et al*[22] (2003, November)	Haugeberg *et al*[17] (2001)
Selection	**	***	**	****	**	**	**	**	***	**	**	***
Comparability		**		**					**			**
Outcome	*	*	**	**	***	**	**	*	*	*	*	*
Total number of stars allocated	3	6	4	7	5	4	4	3	6	3	3	6

exclusively. Age was associated with osteoporosis or low BMD in studies including only CD patients, where one study found increased age to be a risk factor[15], and one study found patients with reduced BMD to be significantly younger than the patient group without reduced BMD[17].

Risk factors for change in bone mineral density over time

Five studies based on three cohorts analysed risk factors for a change in BMD over a period of time[3,16,18-20]. Follow-up for the studies varied between 2 years[16] and 6.49 ± 3.09 years[18]. One study included only CD patients[16]. An overview of the most relevant risk factors for change in BMD can be found in Table 4, while a detailed list of all risk factors can be found in Supplementary Table 3. CD patients appeared to have an increased risk of developing lower BMD or osteoporosis over time, while UC patients had no such increased risk. Gender analyses showed contradicting results. An increase in age was found to be associated with a decrease in BMD, whereas an increase (or decrease) in weight and BMI was associated with an increase (or decrease) in BMD.

DISCUSSION

This systematic review summarises the prevalence and development of, and risk factors for, osteoporosis or low BMD among patients with IBD. Though not statistically proven to be significant, it seems that CD cohorts have a higher prevalence of osteoporosis as compared to the UC cohorts. We found an association between

Table 3 Overview of most relevant risk factors for low bone mineral density or osteoporosis

Risk factors for reduced BMD	CD	CD + UC	Comments
General risk factors			
Gender[5,6,9,10]	+/-	+	Female gender was found to be significantly correlated by Leslie *et al*[20] (2009) investigating both CD and UC patients. In CD studies, Haugeberg *et al*[5] found female gender to be a predictive factor for osteoporosis. Jahnsen *et al*[6] found men to have lower Z-scores than women, whereas Schoon *et al*[10] found no significant association.
Age[2,3,5,9]	+	+/-	Age was significantly associated in the CD studies. However, Haugeberg *et al*[5] found patients with reduced BMD to be significantly younger than those without reduced BMD.
Weight[2,3,5,9]	+, -[1]	+	Low weight was found to be a risk factor for low BMD in both CD + UC cohorts. In CD cohorts, Andreassen *et al*[15] (1999) found a significant positive correlation only in males. Haugeberg *et al*[17] found a positive correlation between weight and BMD for both genders.
BMI[2,5,6,9]	+/-	+	Leslie *et al*[20] (2009), the only study investigating BMI in CD + UC, found a positive correlation between BMI and BMD. Haugeberg *et al*[17] found a significant association for CD patients in a bivariate analysis, but not in a multiple linear regression analysis.
Steroid treatment[2,3,5,6,9]	+/-[2]	-	Multiple risk factors related to steroid usage were investigated. No correlation was found in CD + UC. However, most CD studies did find a correlation.
Height[3,5,9]	+/-	+/-	
Smoking[3,5,6]	-	-	
Vitamin D supplement[3-5]	-	-	
Calcium supplement[3-5]	-	-	
Serum 25(OH)D[1,5,8]	+/-	+/-	
Serum calcium[1,5,8]	-	-	
Serum parathyroid hormone[1,5,8]	+/-	+	
Disease-specific risk factors			
UC diagnosis[3,9]	Not relevant	-	
CD diagnosis[3,6,9]	Not relevant	+/-	
Disease location[1,3,5]	-	-	
Disease duration[2,3,5,6]	+[3],-	-	
Surgery[2,3,5,6]	+/-	-	

[1]Only in females.
[2]Only in males.
[3]Postmenopausal females. A plus sign means that a significant association was found and a minus sign means that no association was found. If studies found different results, both signs are present. CD: Crohn's disease; UC: Ulcerative colitis; BMI: Body mass index; BMD: Bone mineral density; +: Positive association; -: No association; +/-: Significant association and no association were found, depending on the study and/or statistical analysis carried out.

osteoporosis or low BMD and lower weight and lower BMI in both CD cohorts and cohorts including both CD and UC patients. Two out of four studies investigating gender found female gender to be associated with lower BMD. Age and steroid usage were found to be associated only among CD cohorts. In cohorts that analysed change in BMD over time, increased age was associated with a decrease in BMD and increased weight and BMI were associated with increased BMD. Furthermore, and unlike UC patients, CD patients had an increased risk of osteoporosis or low BMD over time.

Prevalence of osteoporosis

The prevalence of osteoporosis among IBD patients ranged from 2%[18] to 15%[16], with a range of 2%[18] to 9%[19] in UC patients and 7%[18,19] to 15%[16] in CD patients. The prevalence among healthy controls was investigated in two studies and was found to be 3%[18] and 10% respectively[17]. Since the data for osteoporosis prevalence in some studies were extracted from measurements of only one bone area, these numbers

Table 4 Overview of the most relevant risk factors for change in bone mineral density over time

Risk factors for change in BMD	CD	CD + UC	Comments
General risk factors			
Gender[8,9,11,12]	No data	+/-	No difference was found between genders in one study cohort[8,9,12], whilst another cohort[11] found a greater incidence of osteoporosis in women than in men.
Age[8,9,11,12]	No data	+/-	
Weight[9,11]	No data	+	
BMI[7,9,11]	+	+	
Steroid treatment[7-9,11]	-	+/-	
Smoking[7]	-	No data	
Serum 25-OH D[7,8,11]	+	+/-	
Disease-specific risk factors			
Diagnosis[9,11,12]	Not relevant	+[1], -	One[13] out of three studies found CD to be associated with an increased risk of osteoporosis. The others found no associations.
Disease location[7]	-	No data	
Disease activity[11]	No data	-	

[1]Only in Crohn's disease. CD: Crohn's disease; UC: Ulcerative colitis; +: Positive association; -: No association; +/-: Significant association and no association were found, depending on the study and/or statistical analysis carried out. A plus sign means that a significant association was found and a minus sign means that no association was found. If studies found different results, both signs are present. Follow-up time for the respective studies was as follows: Jahnsen *et al*[16]: 2 yr; Leslie *et al*[19]: 2.3 ± 0.3 yr; Leslie *et al*[20]: 2.3 ± 0.3 yr; Targownik *et al*[3]: 4.3 ± 0.3 yr; Tsai *et al*[18]: 6.49 ± 3.09 yr.

could be underestimations. The available data did not allow for a meaningful comparison of IBD patients and healthy controls.

When looking at osteoporosis prevalence worldwide in people without IBD, the numbers vary. Approximately 172400 people (around 3%) had osteoporosis in Denmark in 2017 according to the Danish Health Authority[23] and The International Osteoporosis Foundation relies on the estimate that over 200 million people worldwide (around 3%) suffer from it[9]. However, it has been estimated that the actual number of people aged 50 years or older with osteoporosis in Denmark, including undiagnosed inhabitants, is between 146481 and 518272, depending of the calculation method[23]. A nationwide register based Danish study showed that the estimated prevalence of osteoporosis was 40.8% in women and 17.7 % in men, all ≥ 50 years[24]. Due to the wide range of estimates for the prevalence of osteoporosis and the small number of papers included in our study, it is not possible for us to conclude whether its overall prevalence is higher among IBD patients.

General risk factors for osteoporosis and low BMD

The included studies investigated many different risk factors using a variety of methodologies, making it difficult to draw firm, generalized conclusions. We found lower BMI and lower body weight to be associated with lower BMD. Female gender was found to be associated in two out of four studies investigating this risk factor. These are well-documented risk factors for osteoporosis in the background population as well[5].

Surprisingly, use of prednisolone in any dose and duration was found to be associated with decreased BMD in cross-sectional analyses only in CD patients. Steroids are well-recognized bone-resorbing agents[25,26]. Our finding might be explained by the fact that we have considered all forms of prednisolone use with any duration and hence the bones of some patients included in the analyses might have not been exposed enough to prednisolone to be affected[27].

Older age is a well-known risk factor for osteoporosis[5]. Remarkably, age showed significant association with BMD in studies including CD patients only, and one study found the patient group with reduced BMD to be younger than the patients with normal BMD. These studies were small and one of them only included premenopausal women. Hence the analysed population might not be fully representative.

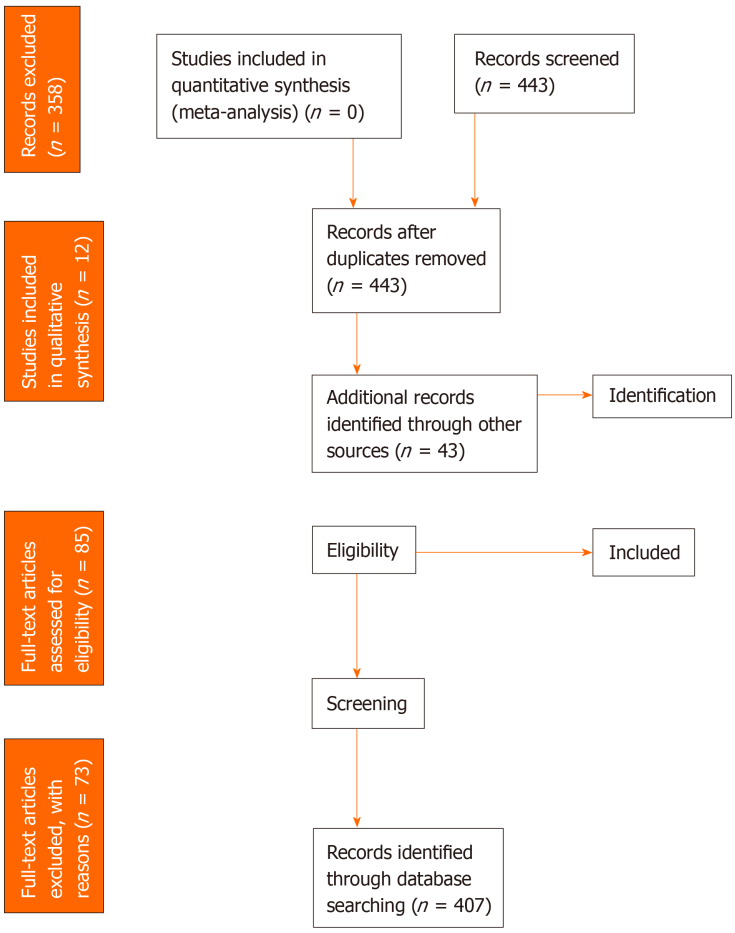

Figure 1 PRISMA flow diagram for the systematic review of the literature.

General risk factors for development of osteoporosis or low BMD over time

We found that increased age was associated with a decrease in BMD and that increased weight and BMI were associated with an increase in BMD over time. The results of analyses of gender and use of steroids showed no uniformity. These discrepant results are additionally surprising since females are known to be at higher risk of developing osteoporosis[5]. This might again be explained by the lack of large-scale studies and that one study only includes premenopausal women. The only register-based study included in our review concluded that female gender was a risk factor for osteoporosis[18].

Disease-specific risk factors

The CD cohorts presented the highest range in the prevalence of osteoporosis, though the numbers overlapped. CD, and not UC, appeared to be associated with osteoporosis or low BMD. Only CD patients seemed to have an increased risk for osteoporosis or low BMD over time. Suggested risk factors for developing osteoporosis are small-bowel disease or resection, smoking and corticosteroid treatment[28]. Small-bowel disease and resection are specific to CD and as such could partly explain why the risk of osteoporosis appears to be greater among CD patients. Moreover, CD patients have been shown to have a higher prevalence of smoking than UC patients[29]. Two population-based studies of CD and UC patients, respectively, have shown that on average around 2% of UC patients take corticosteroids at any given time, whereas almost 10% of CD patients do[30,31]. Future analyses ought to be made of UC and CD separately.

Gut inflammation is a disease-specific risk factor that few of the studies included here chose to analyse. According to a synopsis on research evaluating bone disease in patients with IBD from 2014, increased systemic inflammation increases bone resorption[1]. Inflammation serum markers and their role in IBD is an interesting subject that should be researched further.

Screening and treatment of osteoporosis

Current guidelines recommend that high risk IBD patients should be screened for osteoporosis[32,33]. A Danish study found in a cohort of 513 unselected IBD patients with ten years of follow-up that the incidence of osteoporosis was twice as high for IBD patients compared to a control population[34]. This indicates that adequate screening of osteoporosis could benefit IBD patients.

Strengths and limitations

There are several limitations to this systematic review. A systematic review is evidently dependent on the quality of the studies under review. The number of available studies was small, as was the number of patients in most cohorts. Furthermore, the quality of the studies reviewed varied considerably, as did the statistical analyses and use of covariates. This has precluded the possibility of performing a meta-analysis. Also, as all but one study originated in Europe, United States or Canada, their data might not be representative of other parts of the world. Half of the studies investigated only CD patients, while studies analysing both UC and CD patients did not provide stratified information on IBD subtype. Therefore, no data on UC patients exclusively were available. The risk factors discussed above were considered to be associated with osteoporosis if only one measurement (*e.g.*, total hip, femoral neck, *etc.*) was significant. Therefore, the association between BMD and some risk factors may vary in strength. The follow up time for the included studies varied between two and 6,5 years and hence may have been too short in some studies to identify any change in BMD. One study[18] excluded patients diagnosed with osteoporosis before their IBD diagnosis; to compare this study with other studies that did not exclude this patient group might have affected our results. Finally, analyses conducted during each study were based on different measurements, *i.e.*, T, Z, and BMD scores, and this may also have distorted our analyses.

CONCLUSION

In conclusion, there seems to be an increased prevalence of osteoporosis among CD, as compared to UC, patients. We found an association between osteoporosis or low BMD and lower weight and lower BMI for CD and UC patients while findings regarding gender were inconsistent across studies. Steroid usage was found to be associated with an increased risk of osteoporosis or low BMD only in patients with CD. Increase in age, decrease in weight and BMI, and diagnosis of CD seem to be associated with a decrease in BMD over time. Firm conclusions are difficult to draw due to considerable heterogeneity in terms of study methodologies, definitions and the assessment of osteoporosis, and the small number of population-based studies. Osteoporosis is a common disease that is associated with great economic and psychological burden worldwide due to the consequences of the disease in terms of osteoporotic fractures, and physicians treating patients with IBD should be aware of the risk for osteoporosis in this patient group. Given the importance of adequate screening and treatment of osteoporosis, there is a need for more prospective population-based research on the relationship between osteoporosis and IBD-patients and subgroups in this population. Any such future studies should assess CD and UC separately, should include healthy subjects as controls, and should assess disease specific risk factors such as gut inflammation markers.

ARTICLE HIGHLIGHTS

Research background

The inflammatory bowel diseases (IBD), encompassing Crohn's disease (CD) and ulcerative colitis (UC) are chronic, immune-mediated disorders of the digestive tract. Being diagnosed with IBD is considered a risk factor for the development of osteoporosis. The consequence of development of osteoporosis is the increased risk of pathological fractures that in turn are associated with great economic and psychological burden. Several studies have investigated the relationship between inflammatory bowel diseases and osteoporosis but differences in study design and study populations, as well as inconsistent results and diverging interpretations of them, make it difficult to draw firm conclusions.

Research motivation

Considering the severe consequences of osteoporosis, research on risk factors and prevalence of the disease in IBD patients is of great importance in order to conclude how prevailing the disease is in this patient group and its subgroups. It may give clues on how guidelines for screening and treatment of osteoporosis in IBD-patients should be developed, as well pinpointing what areas need more research.

Research objectives

The objectives with this research was to assess the prevalence of osteoporosis among IBD patients compared to healthy individuals, as well as the disease course of osteoporosis or low BMD in IBD patients. We also aimed to assess risk factors associated with osteoporosis and low BMD in IBD patients with the intention to find more substantial evidence as to the cause of osteoporosis or low BMD in this patient group.

Research methods

For this systematic review, we searched databases including EMBASE and PubMed as well as abstracts from 2014-2018 presented at the United European Gastroenterology Week, the European Crohn's and Colitis Organisation congress, and Digestive Disease Week were screened. Studies were eligible for inclusion if they investigated either the prevalence of osteoporosis or osteopenia and/or risk factors for osteoporosis or low bone mineral density (BMD in IBD patients. Studies on children under the age of 18 were excluded. Only population-based studies were included. All risk factors for osteoporosis and low BMD investigated in any included article were considered. Study quality and the possibility of bias were analysed using the Newcastle-Ottawa scale.

Research results

Twelve studies including 3661 IBD patients and 12789 healthy controls were included. Prevalence of osteoporosis varied between 4%-9% in studies including both CD and UC patients; 2%-9% in studies including UC patients, and 7%-15% in studies including CD patients. Among healthy controls, prevalence of osteoporosis was 3% and 10% in two studies. CD diagnosis, low body mass index (BMI) and low body weight were risk factors associated with osteoporosis or low BMD. Two out of four studies investigating gender found an association between female gender and lower BMD. CD patients had an increased risk for osteoporosis or low BMD over time, while UC patients did not. Increased age was associated with decreased BMD, and there was a positive association between weight and BMI and BMD over time. Great heterogeneity was found in the included studies in terms of study methodologies, definitions and the assessment of osteoporosis, and only a small number of population-based studies was available.

Research conclusions

This systematic review found a possible increase of prevalence of osteoporosis in CD cohorts when compared to UC and cohorts including both disease types. Lower weight and lower BMI were predictors of osteoporosis or low BMD in IBD patients. The results varied considerably between studies. Firm conclusions are difficult to draw due to considerable heterogeneity in terms of study methodologies, definitions and the assessment of osteoporosis, and the small number of population-based studies.

Research perspectives

Osteoporosis is a common disease that is associated with great economic and psychological burden worldwide due to the consequences of the disease in terms of osteoporotic fractures. Given the importance of adequate screening and treatment of osteoporosis, there is a need for more prospective population-based research on the relationship between osteoporosis and IBD-patients and subgroups in this population. Any such future studies should assess CD and UC separately, should include healthy subjects as controls, and should assess disease specific risk factors such as gut inflammation markers.

REFERENCES

1 **Targownik LE**, Bernstein CN, Leslie WD. Risk factors and management of osteoporosis in inflammatory

bowel disease. *Curr Opin Gastroenterol* 2014; **30**: 168-174 [PMID: 24419292 DOI: 10.1097/MOG.0000000000000037]
2 **Siffledeen JS**, Fedorak RN, Siminoski K, Jen H, Vaudan E, Abraham N, Seinhart H, Greenberg G. Bones and Crohn's: risk factors associated with low bone mineral density in patients with Crohn's disease. *Inflamm Bowel Dis* 2004; **10**: 220-228 [PMID: 15290915 DOI: 10.1097/00054725-200405000-00007]
3 **Targownik LE**, Leslie WD, Carr R, Clara I, Miller N, Rogala L, Graff LA, Walker JR, Bernstein CN. Longitudinal change in bone mineral density in a population-based cohort of patients with inflammatory bowel disease. *Calcif Tissue Int* 2012; **91**: 356-363 [PMID: 22983212 DOI: 10.1007/s00223-012-9650-1]
4 **Schüle S**, Rossel JB, Frey D, Biedermann L, Scharl M, Zeitz J, Freitas-Queiroz N, Pittet V, Vavricka SR, Rogler G, Misselwitz B; Swiss IBD cohort study. Prediction of low bone mineral density in patients with inflammatory bowel diseases. *United European Gastroenterol J* 2016; **4**: 669-676 [PMID: 27733909 DOI: 10.1177/2050640616658224]
5 **International Osteoporosis Foundation**. Who's at risk. [cited 19 February 2019]. Available from: https://www.iofbonehealth.org/whos-risk
6 **Castrogiovanni P**, Trovato FM, Szychlinska MA, Nsir H, Imbesi R, Musumeci G. The importance of physical activity in osteoporosis. From the molecular pathways to the clinical evidence. *Histol Histopathol* 2016; **31**: 1183-1194 [PMID: 27311988 DOI: 10.14670/HH-11-793]
7 **Pichler K**, Loreto C, Leonardi R, Reuber T, Weinberg AM, Musumeci G. RANKL is downregulated in bone cells by physical activity (treadmill and vibration stimulation training) in rat with glucocorticoid-induced osteoporosis. *Histol Histopathol* 2013; **28**: 1185-1196 [PMID: 23553492 DOI: 10.14670/HH-28.1185]
8 **Musumeci G**, Loreto C, Leonardi R, Castorina S, Giunta S, Carnazza ML, Trovato FM, Pichler K, Weinberg AM. The effects of physical activity on apoptosis and lubricin expression in articular cartilage in rats with glucocorticoid-induced osteoporosis. *J Bone Miner Metab* 2013; **31**: 274-284 [PMID: 23263781 DOI: 10.1007/s00774-012-0414-9]
9 **International Osteoporosis Foundation**. Epidemiology. [cited 19 February 2019]. Available from: https://www.iofbonehealth.org/epidemiology
10 **Targownik LE**, Bernstein CN, Leslie WD. Inflammatory bowel disease and the risk of osteoporosis and fracture. *Maturitas* 2013; **76**: 315-319 [PMID: 24139749 DOI: 10.1016/j.maturitas.2013.09.009]
11 **Wells GA**, Shea B, O'Connell D, Peterson J, Welch V, Losos M, Tugwell P. The Ottawa Hospital Research Institute. [cited 19 February 2019]. Available from: http://www.ohri.ca/programs/clinical_epidemiology/oxford.asp
12 **Jahnsen J**, Falch JA, Aadland E, Mowinckel P. Bone mineral density is reduced in patients with Crohn's disease but not in patients with ulcerative colitis: a population based study. *Gut* 1997; **40**: 313-319 [PMID: 9135518 DOI: 10.1136/gut.40.3.313]
13 **Schoon EJ**, van Nunen AB, Wouters RS, Stockbrügger RW, Russel MG. Osteopenia and osteoporosis in Crohn's disease: prevalence in a Dutch population-based cohort. *Scand J Gastroenterol Suppl* 2000; 43-47 [PMID: 11232491]
14 **Andreassen H**, Rix M, Brot C, Eskildsen P. Regulators of calcium homeostasis and bone mineral density in patients with Crohn's disease. *Scand J Gastroenterol* 1998; **33**: 1087-1093 [PMID: 9829365 DOI: 10.1080/003655298750026804]
15 **Andreassen H**, Hylander E, Rix M. Gender, age, and body weight are the major predictive factors for bone mineral density in Crohn's disease: a case-control cross-sectional study of 113 patients. *Am J Gastroenterol* 1999; **94**: 824-828 [PMID: 10086673 DOI: 10.1111/j.1572-0241.1999.00866.x]
16 **Jahnsen J**, Falch JA, Mowinckel P, Aadland E. Bone mineral density in patients with inflammatory bowel disease: a population-based prospective two-year follow-up study. *Scand J Gastroenterol* 2004; **39**: 145-153 [PMID: 15000276 DOI: 10.1080/00365520310007873]
17 **Haugeberg G**, Vetvik K, Stallemo A, Bitter H, Mikkelsen B, Stokkeland M. Bone density reduction in patients with Crohn disease and associations with demographic and disease variables: cross-sectional data from a population-based study. *Scand J Gastroenterol* 2001; **36**: 759-765 [PMID: 11444476 DOI: 10.1080/003655201300192030]
18 **Tsai MS**, Lin CL, Tu YK, Lee PH, Kao CH. Risks and predictors of osteoporosis in patients with inflammatory bowel diseases in an Asian population: a nationwide population-based cohort study. *Int J Clin Pract* 2015; **69**: 235-241 [PMID: 25472555 DOI: 10.1111/ijcp.12526]
19 **Leslie WD**, Miller N, Rogala L, Bernstein CN. Vitamin D status and bone density in recently diagnosed inflammatory bowel disease: the Manitoba IBD Cohort Study. *Am J Gastroenterol* 2008; **103**: 1451-1459 [PMID: 18422819 DOI: 10.1111/j.1572-0241.2007.01753.x]
20 **Leslie WD**, Miller N, Rogala L, Bernstein CN. Body mass and composition affect bone density in recently diagnosed inflammatory bowel disease: the Manitoba IBD Cohort Study. *Inflamm Bowel Dis* 2009; **15**: 39-46 [PMID: 18623166 DOI: 10.1002/ibd.20541]
21 **Bernstein CN**, Leslie WD, Taback SP. Bone density in a population-based cohort of premenopausal adult women with early onset inflammatory bowel disease. *Am J Gastroenterol* 2003; **98**: 1094-1100 [PMID: 12809833 DOI: 10.1111/j.1572-0241.2003.07415.x]
22 **Bernstein CN**, Bector S, Leslie WD. Lack of relationship of calcium and vitamin D intake to bone mineral density in premenopausal women with inflammatory bowel disease. *Am J Gastroenterol* 2003; **98**: 2468-2473 [PMID: 14638350 DOI: 10.1111/j.1572-0241.2003.07676.x]
23 Osteoporosis – A disclosure of the collective effort against osteoporosis. [Osteoporose - En afdækning af den samlede indsats mod osteoporose.] [cited 15 April 2019] København: Sundhedsstyrelsen; 2018. Available from: http://www.sst.dk
24 **Vestergaard P**, Rejnmark L, Mosekilde L. Osteoporosis is markedly underdiagnosed: a nationwide study from Denmark. *Osteoporos Int* 2005; **16**: 134-141 [PMID: 15197546 DOI: 10.1007/s00198-004-1680-8]
25 **Buehring B**, Viswanathan R, Binkley N, Busse W. Glucocorticoid-induced osteoporosis: an update on effects and management. *J Allergy Clin Immunol* 2013; **132**: 1019-1030 [PMID: 24176682 DOI: 10.1016/j.jaci.2013.08.040]
26 **Rizzoli R**, Biver E. Glucocorticoid-induced osteoporosis: who to treat with what agent? *Nat Rev Rheumatol* 2015; **11**: 98-109 [PMID: 25385412 DOI: 10.1038/nrrheum.2014.188]

27 **Harslof T**, Langdahl B, Vestergaard P, Eiken P, Hermann P, Stilgren L, Grove D, Folkestad L, Jensen T, Brask-Lindemann DD. Glucocorticoid-induced Osteoporosis. [Glukokortikoid-induceret Osteoporose.] [cited 07 December 2019] Dansk Endokrinol Selsk. 2018. Available from: http://www.endocrinology.dk/index.php/3-calcium-og-knoglemetaboliske-sygdomme/4-glukokortikoid-induceret-osteoporose

28 **Harbord M**, Annese V, Vavricka SR, Allez M, Barreiro-de Acosta M, Boberg KM, Burisch J, De Vos M, De Vries AM, Dick AD, Juillerat P, Karlsen TH, Koutroubakis I, Lakatos PL, Orchard T, Papay P, Raine T, Reinshagen M, Thaci D, Tilg H, Carbonnel F; European Crohn's and Colitis Organisation. The First European Evidence-based Consensus on Extra-intestinal Manifestations in Inflammatory Bowel Disease. *J Crohns Colitis* 2016; **10**: 239-254 [PMID: 26614685 DOI: 10.1093/ecco-jcc/jjv213]

29 **Lunney PC**, Kariyawasam VC, Wang RR, Middleton KL, Huang T, Selinger CP, Andrews JM, Katelaris PH, Leong RW. Smoking prevalence and its influence on disease course and surgery in Crohn's disease and ulcerative colitis. *Aliment Pharmacol Ther* 2015; **42**: 61-70 [PMID: 25968332 DOI: 10.1111/apt.13239]

30 **Burisch J**, Kiudelis G, Kupcinskas L, Kievit HAL, Andersen KW, Andersen V, Salupere R, Pedersen N, Kjeldsen J, D'Incà R, Valpiani D, Schwartz D, Odes S, Olsen J, Nielsen KR, Vegh Z, Lakatos PL, Toca A, Turcan S, Katsanos KH, Christodoulou DK, Fumery M, Gower-Rousseau C, Zammit SC, Ellul P, Eriksson C, Halfvarson J, Magro FJ, Duricova D, Bortlik M, Fernandez A, Hernández V, Myers S, Sebastian S, Oksanen P, Collin P, Goldis A, Misra R, Arebi N, Kaimakliotis IP, Nikuina I, Belousova E, Brinar M, Cukovic-Cavka S, Langholz E, Munkholm P; Epi-IBD group. Natural disease course of Crohn's disease during the first 5 years after diagnosis in a European population-based inception cohort: an Epi-IBD study. *Gut* 2019; **68**: 423-433 [PMID: 29363534 DOI: 10.1136/gutjnl-2017-315568]

31 **Burisch J**, Katsanos KH, Christodoulou DK, Barros L, Magro F, Pedersen N, Kjeldsen J, Vegh Z, Lakatos PL, Eriksson C, Halfvarson J, Fumery M, Gower-Rousseau C, Brinar M, Cukovic-Cavka S, Nikulina I, Belousova E, Myers S, Sebastian S, Kiudelis G, Kupcinskas L, Schwartz D, Odes S, Kaimakliotis IP, Valpiani D, D'Incà R, Salupere R, Chetcuti Zammit S, Ellul P, Duricova D, Bortlik M, Goldis A, Kievit HAL, Toca A, Turcan S, Midjord J, Nielsen KR, Andersen KW, Andersen V, Misra R, Arebi N, Oksanen P, Collin P, de Castro L, Hernandez V, Langholz E, Munkholm P; Epi-IBD Group. Natural Disease Course of Ulcerative Colitis During the First Five Years of Follow-up in a European Population-based Inception Cohort-An Epi-IBD Study. *J Crohns Colitis* 2019; **13**: 198-208 [PMID: 30289522 DOI: 10.1093/ecco-jcc/jjy154]

32 **Kornbluth A**, Hayes M, Feldman S, Hunt M, Fried-Boxt E, Lichtiger S, Legnani P, George J, Young J. Do guidelines matter? Implementation of the ACG and AGA osteoporosis screening guidelines in inflammatory bowel disease (IBD) patients who meet the guidelines' criteria. *Am J Gastroenterol* 2006; **101**: 1546-1550 [PMID: 16863559 DOI: 10.1111/j.1572-0241.2006.00571.x]

33 **Farraye FA**, Melmed GY, Lichtenstein GR, Kane SV. ACG Clinical Guideline: Preventive Care in Inflammatory Bowel Disease. *Am J Gastroenterol* 2017; **112**: 241-258 [PMID: 28071656 DOI: 10.1038/ajg.2016.537]

34 **Lo B**, Holm JP, Vester-Andersen MK, Bendtsen F, Vind I, Burisch J. Incidence, Risk Factors and Evaluation of Osteoporosis in Patients With Inflammatory Bowel Disease: A Danish Population-Based Inception Cohort With 10 Years of Follow-Up. *J Crohns Colitis* 2020; **14**: 904-914 [PMID: 32016388 DOI: 10.1093/ecco-jcc/jjaa019]

World Journal of Gastroenterology

Submit a Manuscript: https://www.f6publishing.com

World J Gastroenterol 2020 September 21; 26(35): 5375-5386

DOI: 10.3748/wjg.v26.i35.5375

ISSN 1007-9327 (print) ISSN 2219-2840 (online)

CASE REPORT

Gastrointestinal tract injuries after thermal ablative therapies for hepatocellular carcinoma: A case report and review of the literature

Teresa Marzia Rogger, Andrea Michielan, Sandro Sferrazza, Cecilia Pravadelli, Luisa Moser, Flora Agugiaro, Giovanni Vettori, Sonia Seligmann, Elettra Merola, Marcello Maida, Francesco Antonio Ciarleglio, Alberto Brolese, Giovanni de Pretis

ORCID number: Teresa Marzia Rogger 0000-0002-0395-4219; Andrea Michielan 0000-0003-1353-0935; Sandro Sferrazza 0000-0002-7595-0129; Cecilia Pravadelli 0000-0003-1392-466X; Luisa Moser 0000-0003-4929-4030; Flora Agugiaro 0000-0003-4119-6014; Giovanni Vettori 0000-0002-6507-9317; Sonia Seligmann 0000-0002-5045-0013; Elettra Merola 0000-0001-9553-7684; Marcello Maida 0000-0002-4992-9289; Francesco Antonio Ciarleglio 0000-0001-9505-8181; Alberto Brolese 0000-0002-6362-9055; Giovanni de Pretis 0000-0001-7636-0422.

Author contributions: Pravadelli C, Michielan A and Sferrazza S contributed to study concept and design; Rogger TM, Michielan A, Sferrazza S, Pravadelli C, Maida M and Ciarleglio FA contributed to drafting of the manuscript; Moser L, Seligmann S, Vettori G, Agugiaro F and Merola E contributed to critical revision of the manuscript for important intellectual content; Brolese A and de Pretis G contributed to study supervision and final approval.

Informed consent statement: Informed consent was obtained from the patient for publication of this report and any accompanying images.

Teresa Marzia Rogger, Andrea Michielan, Sandro Sferrazza, Cecilia Pravadelli, Luisa Moser, Flora Agugiaro, Giovanni Vettori, Sonia Seligmann, Elettra Merola, Giovanni de Pretis, Department of Surgery, Gastroenterology and Digestive Endoscopy Unit, Santa Chiara Hospital, Trento 38122, Italy

Marcello Maida, Gastroenterology and Endoscopy Unit, S.Elia-Raimondi Hospital, Caltanissetta, Caltanissetta 93100, Italy

Francesco Antonio Ciarleglio, Alberto Brolese, Department of Surgery, Hepato-biliary Surgery Unit, Santa Chiara Hospital, Trento 38122, Italy

Corresponding author: Andrea Michielan, MD, Doctor, Department of Surgery, Gastroenterology and Digestive Endoscopy Unit, Santa Chiara Hospital, Largo Medaglie D'Oro 9, Trento 38122, Italy. andrea.michielan@apss.tn.it

Abstract

BACKGROUND

Radiofrequency ablation (RFA) and microwave ablation (MWA) represent the standard of care for patients with early hepatocellular carcinoma (HCC) who are unfit for surgery. The incidence of reported adverse events is low, ranging from 2.4% to 13.1% for RFA and from 2.6% to 7.5% for MWA. Gastrointestinal tract (GIT) injury is even more infrequent (0.11%), but usually requires surgery with an unfavourable prognosis. Due to its low incidence and the retrospective nature of the studies, the literature reporting this feared complication is heterogeneous and in many cases lacks information on tumour characteristics, comorbidities and treatment approaches.

CASE SUMMARY

A 77-year-old man who had undergone extended right hepatectomy for HCC was diagnosed with early disease recurrence with a small nodule compatible with HCC in the Sg4b segment of the liver with a subcapsular location. He was treated with percutaneous RFA and a few week later he was urgently admitted to the Surgery ward for abdominal pain and fever. A subcutaneous abscess was diagnosed and treated by percutaneous drainage. A fistulous tract was then documented by the passage of contrast material from the gastric antrum to the abdominal wall. The oesophagogastroduodenoscopy confirmed a circular wall

Conflict-of-interest statement: All authors declare no conflict of interest related to this publication.

CARE Checklist (2016) statement: The authors have read the CARE Checklist (2016), and the manuscript was prepared and revised according to the CARE Checklist (2016).

Manuscript source: Invited manuscript

Received: June 28, 2020
Peer-review started: June 28, 2020
First decision: July 28, 2020
Revised: August 11, 2020
Accepted: September 1, 2020
Article in press: September 1, 2020
Published online: September 21, 2020

P-Reviewer: Sun JH, Tolga E
S-Editor: Yan JP
L-Editor: A
P-Editor: Ma YJ

defect at the lesser curvature of gastric antrum, leading directly to the purulent abdominal collection. An over-the-scope clip (OTSC) was used to successfully close the defect

CONCLUSION
This is the first reported case of RFA-related GIT injury to have been successfully treated with an OTSC, which highlights the role of this endoscopic treatment for the management of this complication.

Key Words: Gastrointestinal tract; Radiofrequency ablation; Hepatocellular carcinoma; Complications; Endoscopy; Over-the-scope clip; Case report

Core Tip: Thermal ablative therapies have a key role in the treatment algorithm for hepatocellular carcinoma, and besides their efficacy and tolerability, several studies have proven their overall safety. Nevertheless, albeit rarely, a number of complications have been reported and awareness is crucial to proposing the best treatment for each patient. We report the unusual case of a gastric perforation that was treated in our division and how it was managed with an endoscopic over-the-scope clip for the first time. The literature review aims to discuss the most relevant published data on gastrointestinal tract injuries after thermal ablation therapies.

Citation: Rogger TM, Michielan A, Sferrazza S, Pravadelli C, Moser L, Agugiaro F, Vettori G, Seligmann S, Merola E, Maida M, Ciarleglio FA, Brolese A, de Pretis G. Gastrointestinal tract injuries after thermal ablative therapies for hepatocellular carcinoma: A case report and review of the literature. *World J Gastroenterol* 2020; 26(35): 5375-5386
URL: https://www.wjgnet.com/1007-9327/full/v26/i35/5375.htm
DOI: https://dx.doi.org/10.3748/wjg.v26.i35.5375

INTRODUCTION

Hepatocellular carcinoma (HCC) represents about 90% of primary liver cancers and, with an ever-greater incidence, is the seventh most common malignant tumour and the fourth major cause of cancer death worldwide[1]. Approximately 70%-90% of HCC cases occur in cirrhotic liver and the choice of the most appropriate treatment must take into account not only cancer staging, but also liver function assessment, evaluation of extrahepatic disease, patient comorbidities and performance status[2-4]. All the available therapeutic options have drawbacks that can affect both safety and health-related quality of life. Clinicians have to choose those interventional procedures whose benefits outweigh the risks for each individual patient[5,6].

Although liver transplantation and surgical resection remain the gold standard for HCC, only a small proportion of patients are eligible, making locoregional therapies valuable options with a good survival benefit and safety profile[7,8]. Of these, according to the most widely accepted staging and treatment algorithm for HCC, the Barcelona Clinic Liver Cancer algorithm[9,10], ablative modalities have earned a pivotal role, representing the first-line option with curative intent for unresectable Stage 0 (very early) or Stage A (early) HCC. In addition, they can represent an alternative to resection in single tumours with favourable locations or for those tumours < 3 cm in size[11]. They can also be included in a multimodal approach for intermediate and advanced cases, or play a role as a bridging therapy prior to transplantation[12,13]. Radiofrequency ablation (RFA) and microwave ablation (MWA) are the most extensively clinically-validated thermal ablative therapies[14,15]. Using one or more electrodes that generate electrical current and electromagnetic energy respectively, they induce heat in the tumour tissue above a lethal threshold, leading to coagulative necrosis[15,16]. Although they are less invasive than surgical resection, the complication rate ranges from 2.4% to 13.1% for RFA and from 2.6% to 7.5% for MWA[8], with no significant difference between the two techniques[14]. Direct mechanical injury caused by the passage of the electrode through the vessels or biliary tree may lead to bleeding or bile leakage[17,18]. Heat damage represents the other mechanism that can complicate

these procedures causing gastrointestinal tract (GIT), diaphragm or gallbladder injury, pleural effusion, bile duct strictures, biloma, vascular injury with consequent liver infarction and grounding pad burns. Other possible adverse events include tumour seeding along the tract, septic complications with hepatic abscess or cholangitis, and vasovagal reflex[12,19,20]. GIT haemorrhagic complications after thermal ablative therapies have also been reported and appear to be mostly associated with a worsening of pre-existing portal hypertension or portal vein thrombosis[19,21,22].

Thermal damage with GIT injury is an uncommon yet severe complication. At the current time, there are a few reviews analysing the complications of thermal ablation treatments, none specifically investigating GIT injuries[23-25].

We report the case of an RFA-related gastric perforation that was successfully managed using an over-the-scope clip (OTSC). To the best of our knowledge, this is the first reported endoscopic treatment for an RFA-related GIT complication. We also briefly review and discuss the most relevant published data on GIT injuries after thermal ablation therapies, with regard to their prevalence, risk factors and proposed treatment.

CASE PRESENTATION

Chief complaints

In March 2020, a 77-year-old man was urgently admitted to the Surgery ward for abdominal pain and fever.

History of present illness

In June 2019, he was diagnosed with a bulky hepatic mass with a maximum diameter of 28 cm involving the whole right lobe, with no evidence of pre-existing liver disease. The condition was diagnosed at another hospital and the patient was subsequently treated with combined extended right hepatectomy, hepatic pedicle lymphadenectomy and cholecystectomy. The histopathological study showed a moderately differentiated hepatocellular carcinoma and confirmed a healthy liver parenchyma. No lymph nodes were involved and the tumour resection margins were clear (staging pT3N0G2 – R0). The 6-mo follow-up total-body computed tomography scan showed early disease recurrence and progression with a small 27 mm nodule compatible with HCC in the Sg4b segment of the liver with a subcapsular location, on the edge of the previous partial resection site, and a 5 cm adrenal metastasis. A subsequent contrast-enhanced ultrasound (US) scan of the liver confirmed the diagnosis (Figure 1). In January 2020, the patient had a multidisciplinary consultation at our hospital and was deemed fit for locoregional treatments. In February 2020, he was admitted in our Surgery ward and, once written informed consent had been obtained, he was treated with chemioembolisation of the adrenal metastasis and percutaneous RFA of the small HCC in Sg4b. The ablation was performed with anaesthesiological support, and under real-time US guidance. The device used to apply the radiofrequency current was a 20 cm long, 17-Gauge electrode with an uninsolated 3 cm tip (RF-AMICA probe, HS Hospital Service, Aprilia, Italy). No immediate complications were reported after the procedure.

History of past illness

The patient's medical history included arterial hypertension, surgical resection of a parathyroid adenoma and radioactive iodine therapy for Plummer's disease.

Physical examination

The clinical abdominal examination revealed epigastric tenderness. The patient's temperature was 38.5 °C, blood pressure was 140/90 mmHg, heart rate was 100 bpm, respiratory rate was 15 breaths per min, and oxygen saturation in room air was 99%.

Laboratory examinations

The patient's biochemistry tests showed no clear evidence of systemic inflammation. White blood cells and serum C-reactive protein were at the upper limit of the normal range. Serum transaminases, liver function tests and routine blood biochemistry were normal.

Imaging examinations

A subcutaneous abscess was diagnosed by abdominal ultrasound and treated with

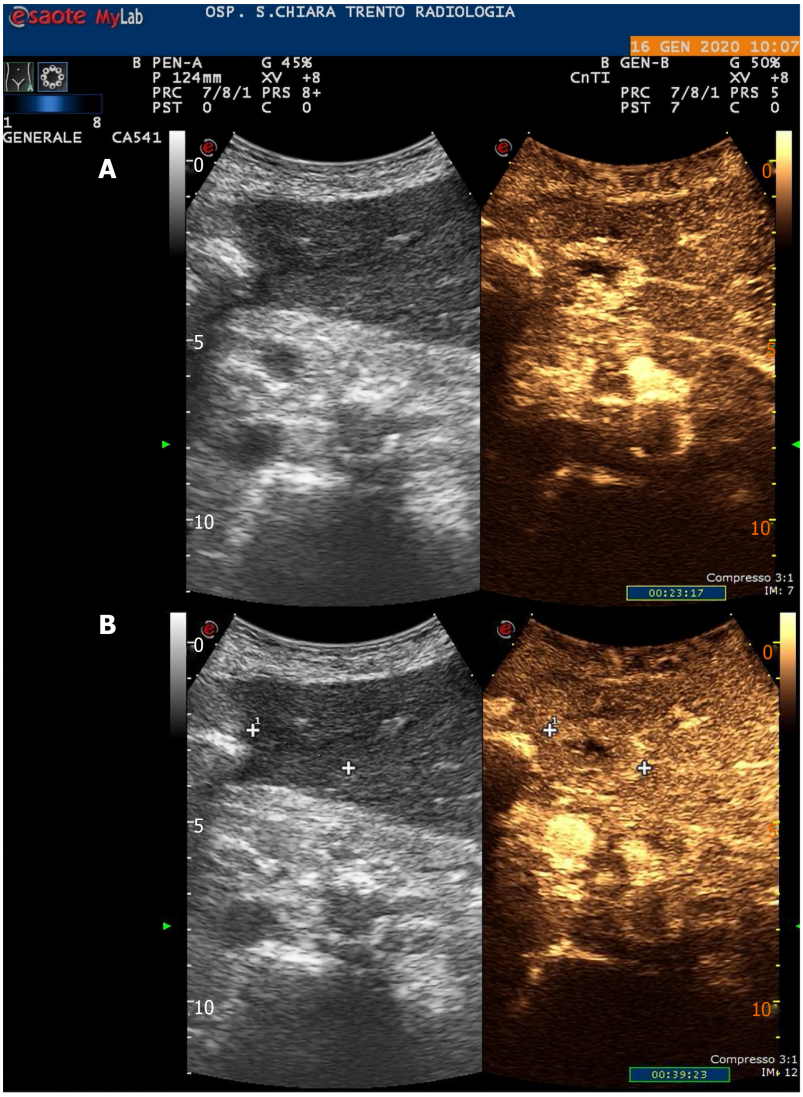

Figure 1 Contrast-enhanced ultrasonography showing the subcapsular 20 mm hepatocellular carcinoma at the 4th liver segment. A: During wash-in phase; B: During wash-out phase.

percutaneous drainage, observing necrotic and purulent secretion, together with air leak. Since no decrease in drain output was observed over the following d, an abdominal film with oral water-soluble contrast agent was performed. A fistulous tract was documented by the passage of contrast material from the gastric antrum to the abdominal wall (Figure 2).

FINAL DIAGNOSIS

The final diagnosis of the presented case was RFA-related gastric perforation.

TREATMENT

The patient was treated conservatively with fasting and broad-spectrum antibiotics; a prompt endoscopic assessment was planned. The oesophagogastroduodenoscopy confirmed a circular wall defect, approximately 15 mm in size, at the lesser curvature of gastric antrum, leading directly to the purulent abdominal collection (Figure 3). An OTSC was used to successfully close the defect (Figure 4) and there were no immediate complications. Technical success was confirmed after one week by an abdominal film with oral water-soluble contrast agent (Figure 5). The patient gradually resumed oral feeding and was finally discharged in good conditions.

Figure 2 Abdominal film with oral water-soluble contrast agent showing a gastric perforation with a gastro-cutaneous fistulous tract (surgical drain in place).

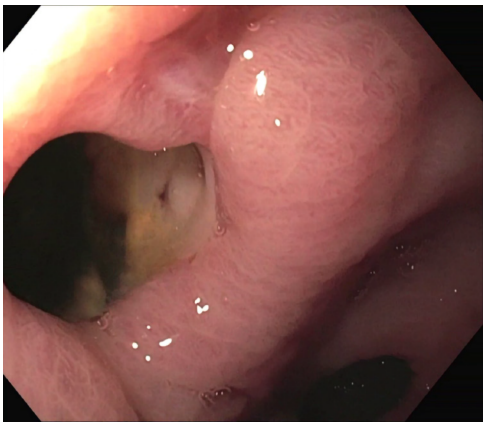

Figure 3 Endoscopic finding of the gastric perforation in communication with a purulent collection. Pylorus can be seen in the lower part of the picture.

OUTCOME AND FOLLOW-UP

A short time after the complete closure of the external fistula, recurrence of a mild cutaneous leakage (less than 40 mL/d) was observed for 40 d, followed by spontaneous closure. In June 2020, no signs of perforation recurrence were detected and the HCC was in remission in the remaining liver, according to mRECIST criteria[26]. The case report timeline is showed in Supplementary Figure 1.

DISCUSSION

We performed a review of the literature reporting the largest series of GIT complications published to date, highlighting the features that may help clinicians in the detection and management of these feared events (Table 1). Published studies are mainly retrospective and extremely heterogeneous as regards information on tumour size and location, comorbidities and treatment approach, which are often missing, or otherwise include lesions other than HCC.

Epidemiology and outcome

The reported prevalence of GIT injuries ranges from 0.04% to 2.5%, particularly when

Table 1 Studies reporting gastrointestinal tract injuries after thermal ablation therapies for hepatocellular carcinoma

Ref.	Study design	Number of patients	Overall complication rate(%)	GIT injury rate (%)	Type of GIT injury	Thermoablative treatment	Timing of GIT injury	Management of GIT injury	Outcome	Associated conditions
Livraghi *et al*[29], 2003	Multicentre, retrospective, questionnaire-based[1]	2320	7.1 (2.4[2])	0.7[2]	5 colonic perforations; 1 jejunal perforation; 1 gastric perforation	Percutaneous RFA	2 d-4 d	Surgery (7/7)	2 deaths after colonic perforation	Gut wall distance < 1 cm (7/7); adherence due to previous abdominal surgery or inflammatory chronic cholecystitis (6/7); large superficial HCC in left lobe + aggressive treatment (1/7)
De Baere *et al*[31], 2003	Multicentre, prospective[1]	312	12 (5.7[2])	0.3[2]	1 colonic perforation	RFA[3]	4 d	Surgery	Death	NA
Curley *et al*[57], 2004	Multicentre, prospective[1]	608	9.5	0.16[2]	1 stomach wall necrosis	Open RFA	Immediate	Surgery	Recovery	Left lobe
Jansen *et al*[58], 2005	Multicentre, prospective[1]	122	9.8 (6.3[2])	2.5 (0[2])	2 transient paralitic ileus	RFA[3]	NA	Spontaneous resolution (2/2)	Recovery	NA
Casaril *et al*[32], 2007	Single-centre, retrospective[1]	83	25 (7.2[2])	0.7[2]	1 colonic perforation	Percutaneous RFA	36 d	NA	Death	Superficial HCC in Sg4; Child-Pugh B
Kasugai *et al*[22], 2007	Multicentre, retrospective, questionnaire-based	2614	7.9[2]	0.2[2]	1 duodenum injury; 1 stomach injury; 1 colonic perforation	RFA[3]	NA	External drainage (1/3)	Recovery	NA
Chen *et al*[34], 2008	Single-centre, retrospective[1]	104	5.2[2]	0.6[2]	1 colonic peroration with fistula and abscess	Percutaneous RFA	3 wk	External drainage	Recovery	Superficial HCC in Sg4; previous surgery for Denver shunt
Liang *et al*[30], 2009	Single-centre, retrospective[1]	1136	2.6[2]	0.2[2]	2 colonic perforations	Percutaneous MWA	3 d-5 d	Surgery (2/2)	Recovery	HCC located < 1 cm from colonic wall + prior right partial hepatectomy (2/2)
Livraghi *et al*[33], 2012	Multicentre, retrospective, questionnaire-based[1]	736	10.2 (2.9[2])	0.2[2]	1 ileal perforation; 1 colonic perforation	Percutaneous MWA	NA	Surgery (2/2)	Recovery	Superficial HCC in Sg4 + abdominal adhesions (2/2)
Koda *et al*[53], 2012	Multicentre, retrospective, questionnaire-based	13283	3.5[2]	0.05 (0.04[2])	1 colonic perforation; 3 stomach injuries; 2 duodenum injuries	RFA[3]	NA	Surgery (3/6)	1 Death after colonic perforation	NA
Ding *et al*[19], 2013	Single-centre, retrospective[1]	879	8.8-9.4 (3.1-3.5[2])	0.3[2]	1 bowel perforation	Percutaneous RFA	Immediate	External drainage	Recovery	Previous Whipple procedure

Park *et al*[54], 2017	Single-centre, retrospective	1211	6.8 (2[2])	0.2[2]	1 colonic perforation	Percutaneous RFA	NA	NA	Recovery	NA
Jeong *et al*[28], 2017	Single-centre, retrospective[1]	3933	NA	1.32 (0.05[2])	28 stomach injuries; 16 colonic injuries; 6 small bowel injuries; 1 small bowel perforation; 1 colonic perforation	Percutaneous RFA	2 d-13 d (perforations)	Surgery (2/2 perforations)	Recovery	Subcapsular HCC (47/52); previous percutaneous treatments (7/52) or abdominal surgery (19/52)
Maeda *et al*[59], 2020	Multicentre, retrospective, questionnaire based	9411	3.5[2]	0.04[2]	2 colonic perforations	NA	NA	NA	1 Death	NA

[1]HCC and other liver tumors included;
[2]Major complications;
[3]Route approach not specified. GIT: Gastrointestinal tract; HCC: Hepatocellular carcinoma; RFA: Radiofrequency ablation; MWA: Microwave ablation; NA: Not available.

thermal ablative therapies were administered percutaneously.

The great variability in the GIT injury rate depends on whether minor injuries were included in the studies. Most literature concerns only major complications, strictly defined as those that increase the level of care, leading to significant morbidity and disability[27]. This probably plays down the effect that thermal ablation may have on GIT. Two previous reviews on the complications of thermoablative treatments found an extremely low prevalence of GIT injuries (0.11%-0.5%)[23,24]. However, a subsequent study on radiological predictors of major GIT injury reported a rate of 1.32%[28] and in a review that included also minor injuries, this rate rose to 3.2%[25].

Outcome is often unfavourable, as confirmed by previous studies. After sepsis and liver failure, GIT injuries were more frequently associated with death than other more commonly-observed complications[24,29,30]. GIT complications accounted for two in six fatal adverse events in one Italian multicentre study[29], one in five in the series from De Baère *et al*[31], and the only lethal event observed by Casaril *et al*[32].

Predisposing conditions

Associated conditions that may represent precipitating factors for GIT injury are HCC nodules or gut wall close to liver capsule (< 1 cm), previous abdominal surgery or percutaneous treatments.

It is well known that structures located within 0.5 cm-1 cm from the tumour margin are at-risk of heat-induced damage, since ablative treatment usually includes an area of healthy peritumoral tissue, in order to eradicate any microscopic satellites and prevent local recurrence[12]. However, this is not the only factor involved, as stressed by Liang *et al*[30] in their retrospective analysis, which did not identify any significant difference in tumour location between patients with *vs* without major complications[30]. The association of an unfavourable location and a predisposing history is clearly shown by the data reported in the literature. In two studies analysing

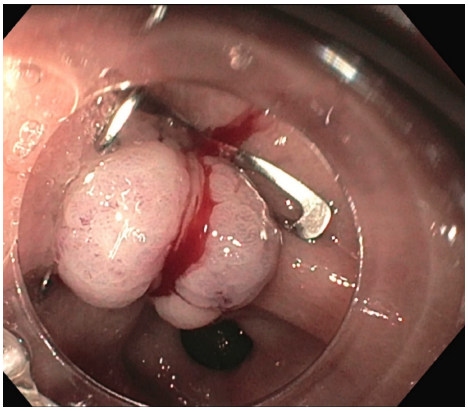

Figure 4 Endoscopic closure of the perforation using an over-the-scope clip.

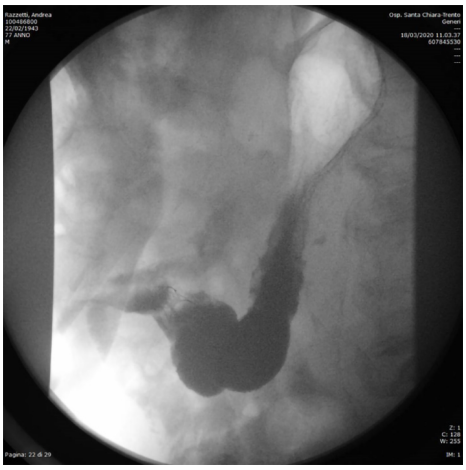

Figure 5 Abdominal film with oral water-soluble contrast agent showing no active leakage from the stomach. The over-the-scope clip can be seen in gastric antrum.

complications after both RFA and MWA, Livraghi *et al*[29,33] reported nine major GIT complications. All occurred after the treatment of superficial lesions, mostly in patients who had had previous abdominal surgery or had inflammatory abdominal processes (89%, 8/9 patients). Other studies confirmed that GIT injuries exclusively followed the treatment of subcapsular tumours in a specific subset of patients, whose history included Whipple resection, right partial hepatectomy or peritoneovenous shunt[19,30,34]. In line with these data, a more recent Korean study found that of 52 patients who experienced GIT complications 47 (90.4%) had a tumour located in a subcapsular portion of the liver and in half of these patients previous abdominal surgery or repeated percutaneous treatments were reported[28].

Clinical presentation

In the majority of the studies examined, the colon appears the most commonly involved organ, with a delay in presentation of several days. Its vulnerability is associated with its thin wall and relatively stable position compared to the stomach's thick wall and to the small intestine's active peristalsis[20,35]. In case of aggressive treatments with repeated or prolonged sessions, particularly in high-risk settings as previously discussed, caution is warranted as other organs than the colon may be involved[36-38].

GIT injuries can be difficult to recognise because their clinical presentation is subtler than classic digestive perforation and they may be misdiagnosed as post-ablation syndrome. Unresolved or delayed-onset fever, pain or increase in white blood cell count several days after the procedure, should raise suspicions and careful patient assessment is warranted. The presence of an abscess, although more commonly related with other aetiologies, could be the result of a contaminating digestive tract perforation, and consequently close monitoring of GIT is also recommended in these

cases[39].

Imaging

Some authors advocate using of imaging techniques soon after RFA. Gastrointestinal wall thickening, fat stranding and free fluid can be found around the injured area as a result of minimal insult[39,40]. Similarly, the presence of free air does not always indicate a major perforation, as it is found in more than half of all patients with minor complications and usually subsides within one month[41]. On the other hand, immediate post-treatment computed tomography, may show concentric bowel wall thickening with mucosal disruption, which significantly correlates with the risk of major GIT injury requiring surgery[28]. However, immediate imaging is not routinely performed in all centres, as it is not always possible to make a distinction between transient hyperaemia and the residual unablated tumour, which hampers the evaluation of treatment efficacy[41]. Nevertheless, in selected cases, when dealing with tumours with a high-risk location in high-risk patients, close imaging parallel to clinical follow-up could be advised.

Management

Few studies focused on the detailed course of these complications and their management, although the impact on patient morbidity and quality of life is non-negligible. Whenever possible, patients were treated minimally-invasively with fasting and percutaneous drain placement, but most required surgical intervention to repair the injured GIT[39]. To the best of our knowledge, the case reported here is the first case of gastric perforation after thermal ablation therapies to be managed endoscopically with an OTSC.

OTSCs differ from traditional through-the-scope clips in several characteristics, namely higher compression force, larger diameter and grasping accessories that allow the closure of wall defects of up to 30 mm, including the muscle layer[42-44]. They have been successfully used and validated in literature in different settings, *i.e.*, haemostasis in acute GI bleeding, closure of GI perforations, leaks and fistulas or as anchor to prevent stent migration[45]. While clinical success is nearly 100% for haemostasis, it decreases to 40%-75% for GI defect closure, with best outcomes in acute perforations, which have fresh edges with less fibrosis[44,46,47]. Nevertheless, their use has been increasingly reported in postoperative leakages or fistulas as well, owing to the attractive possibility of avoiding complex surgery[48-50]. Clinicians must take into account that a multidisciplinary approach should always be taken, since surgical or radiological placement of a drain is often advisable to prevent abscess formation after defect closure.

Preventive measures

An interesting issue is whether preventive measures may reduce the incidence of GIT injuries caused by thermal ablation therapies. These lesions are mainly associated with the percutaneous route and surgical management showed the presence of fibrotic adhesions that affixed the GI wall to the liver. Thus, a laparoscopic or intraoperative thermal ablation approach may allow the mechanical separation of the GIT from the surface of the liver and protect it from subsequent thermal damage[32,51]. Nevertheless, the rate of other complications of these invasive routes is higher than for the percutaneous route[21].

One well-established, easy and safe procedure is the use of artificial ascites. This technique allows the displacement of the liver, with its considered high-risk ablation area, from the adjacent organs[52]. Authors who routinely perform this procedure reported a lower incidence of GIT complications despite dealing with high-risk tumours[53,54]. Nevertheless, the presence of perihepatic adhesions due to previous abdominal surgery, other locoregional treatments such as transarterial chemoembolization or intra-abdominal inflammation, represent a limit for technical success. Moreover, this technique may be of limited efficacy in tumours located in left liver, since the nearby stomach is not easy to displace[55]. Two other tips to help minimise adjacent organ injury are the interposition of thermocouples that ensure controlled temperature increase[30] and the use of straight needle electrodes, which are more appropriate for monitoring the distance from GIT than expandable devices[56].

CONCLUSION

This is the first reported case of RFA-related GIT injury endoscopically treated with OTSC. OTSCs have become part of the endoscopist's armamentarium and are now widely used to treat GI defects. This application may help reduce the need for complex surgery for this rare yet severe complication.

Our review raises awareness on an overlooked but severe complication of thermal ablative treatments. Nowadays, following the expansion of ablation criteria for HCC, these therapeutic modalities are gaining wider application. Therefore, clinicians must consider possible complications and accurately weigh up the risks and benefits, choosing the best treatment option not only according to fixed algorithms for HCC, but also tailored to the specific patient.

Since GIT injuries are rare but have an unfavourable prognosis and outcome, careful patient evaluation may help detect the tumour-related (location < 1 cm from the GI tract) or patient-related (previous surgery or locoregional treatments) risk factors that may trigger this event. These features do not represent an absolute contraindication to thermal ablation therapies, since these treatments remain safe and have an acceptable complication rate. However, according to local expertise, a non-percutaneous (laparoscopic or intraoperative) route should be chosen or preventive measures such as artificial ascites should be used. Otherwise, other ablative methods for HCC should be preferred.

In the case of GIT injury occurrence, the initial subtle clinical presentation warrants a low threshold for GI imaging. Finally, prompt identification of the injury is mandatory to avoid diagnostic delay and provide timely management.

REFERENCES

1 **Bray F**, Ferlay J, Soerjomataram I, Siegel RL, Torre LA, Jemal A. Global cancer statistics 2018: GLOBOCAN estimates of incidence and mortality worldwide for 36 cancers in 185 countries. *CA Cancer J Clin* 2018; **68**: 394-424 [PMID: 30207593 DOI: 10.3322/caac.21492]

2 **Forner A**, Llovet JM, Bruix J. Hepatocellular carcinoma. *Lancet* 2012; **379**: 1245-1255 [PMID: 22353262 DOI: 10.1016/S0140-6736(11)61347-0]

3 **Gadsden MM**, Kaplan DE. Multidisciplinary Approach to HCC Management: How Can This Be Done? *Dig Dis Sci* 2019; **64**: 968-975 [PMID: 30887152 DOI: 10.1007/s10620-019-05593-8]

4 **Couri T**, Pillai A. Goals and targets for personalized therapy for HCC. *Hepatol Int* 2019; **13**: 125-137 [PMID: 30600478 DOI: 10.1007/s12072-018-9919-1]

5 **Fan SY**, Eiser C, Ho MC. Health-related quality of life in patients with hepatocellular carcinoma: a systematic review. *Clin Gastroenterol Hepatol* 2010; **8**: 559-64.e1-10 [PMID: 20304101 DOI: 10.1016/j.cgh.2010.03.008]

6 **Das A**, Gabr A, O'Brian DP, Riaz A, Desai K, Thornburg B, Kallini JR, Mouli S, Lewandowski RJ, Salem R. Contemporary Systematic Review of Health-Related Quality of Life Outcomes in Locoregional Therapies for Hepatocellular Carcinoma. *J Vasc Interv Radiol* 2019; **30**: 1924-1933.e2 [PMID: 31685362 DOI: 10.1016/j.jvir.2019.07.020]

7 **Dimitroulis D**, Damaskos C, Valsami S, Davakis S, Garmpis N, Spartalis E, Athanasiou A, Moris D, Sakellariou S, Kykalos S, Tsourouflis G, Garmpi A, Delladetsima I, Kontzoglou K, Kouraklis G. From diagnosis to treatment of hepatocellular carcinoma: An epidemic problem for both developed and developing world. *World J Gastroenterol* 2017; **23**: 5282-5294 [PMID: 28839428 DOI: 10.3748/wjg.v23.i29.5282]

8 **Habib A**, Desai K, Hickey R, Thornburg B, Lewandowski R, Salem R. Locoregional therapy of hepatocellular carcinoma. *Clin Liver Dis* 2015; **19**: 401-420 [PMID: 25921670 DOI: 10.1016/j.cld.2015.01.008]

9 **Maida M**, Orlando E, Cammà C, Cabibbo G. Staging systems of hepatocellular carcinoma: a review of literature. *World J Gastroenterol* 2014; **20**: 4141-4150 [PMID: 24764652 DOI: 10.3748/wjg.v20.i15.4141]

10 **Faria SC**, Szklaruk J, Kaseb AO, Hassabo HM, Elsayes KM. TNM/Okuda/Barcelona/UNOS/CLIP International Multidisciplinary Classification of Hepatocellular Carcinoma: concepts, perspectives, and radiologic implications. *Abdom Imaging* 2014; **39**: 1070-1087 [PMID: 24695938 DOI: 10.1007/s00261-014-0130-0]

11 **European Association for the Study of the Liver**. EASL Clinical Practice Guidelines: Management of hepatocellular carcinoma. *J Hepatol* 2018; **69**: 182-236 [PMID: 29628281 DOI: 10.1016/j.jhep.2018.03.019]

12 **Kim YS**, Lim HK, Rhim H, Lee MW. Ablation of hepatocellular carcinoma. *Best Pract Res Clin Gastroenterol* 2014; **28**: 897-908 [PMID: 25260316 DOI: 10.1016/j.bpg.2014.08.011]

13 **Nault JC**, Sutter O, Nahon P, Ganne-Carrié N, Séror O. Percutaneous treatment of hepatocellular carcinoma: State of the art and innovations. *J Hepatol* 2018; **68**: 783-797 [PMID: 29031662 DOI: 10.1016/j.jhep.2017.10.004]

14 **Izzo F**, Granata V, Grassi R, Fusco R, Palaia R, Delrio P, Carrafiello G, Azoulay D, Petrillo A, Curley SA. Radiofrequency Ablation and Microwave Ablation in Liver Tumors: An Update. *Oncologist* 2019; **24**: e990-e1005 [PMID: 31217342 DOI: 10.1634/theoncologist.2018-0337]

15 **Facciorusso A**, Serviddio G, Muscatiello N. Local ablative treatments for hepatocellular carcinoma: An updated review. *World J Gastrointest Pharmacol Ther* 2016; **7**: 477-489 [PMID: 27867681 DOI: 10.4292/wjgpt.v7.i4.477]

16 **Poulou LS**, Botsa E, Thanou I, Ziakas PD, Thanos L. Percutaneous microwave ablation *vs* radiofrequency ablation in the treatment of hepatocellular carcinoma. *World J Hepatol* 2015; **7**: 1054-1063 [PMID: 26052394 DOI: 10.4254/wjh.v7.i8.1054]

17 **Llovet JM**, Vilana R, Brú C, Bianchi L, Salmeron JM, Boix L, Ganau S, Sala M, Pagès M, Ayuso C, Solé M, Rodés J, Bruix J; Barcelona Clínic Liver Cancer (BCLC) Group. Increased risk of tumor seeding after percutaneous radiofrequency ablation for single hepatocellular carcinoma. *Hepatology* 2001; **33**: 1124-1129 [PMID: 11343240 DOI: 10.1053/jhep.2001.24233]

18 **Livraghi T**, Lazzaroni S, Meloni F, Solbiati L. Risk of tumour seeding after percutaneous radiofrequency ablation for hepatocellular carcinoma. *Br J Surg* 2005; **92**: 856-858 [PMID: 15892154 DOI: 10.1002/bjs.4986]

19 **Ding J**, Jing X, Liu J, Wang Y, Wang F, Wang Y, Du Z. Complications of thermal ablation of hepatic tumours: comparison of radiofrequency and microwave ablative techniques. *Clin Radiol* 2013; **68**: 608-615 [PMID: 23399463 DOI: 10.1016/j.crad.2012.12.008]

20 **Poggi G**, Tosoratti N, Montagna B, Picchi C. Microwave ablation of hepatocellular carcinoma. *World J Hepatol* 2015; **7**: 2578-2589 [PMID: 26557950 DOI: 10.4254/wjh.v7.i25.2578]

21 **Kong WT**, Zhang WW, Qiu YD, Zhou T, Qiu JL, Zhang W, Ding YT. Major complications after radiofrequency ablation for liver tumors: analysis of 255 patients. *World J Gastroenterol* 2009; **15**: 2651-2656 [PMID: 19496197 DOI: 10.3748/wjg.15.2651]

22 **Kasugai H**, Osaki Y, Oka H, Kudo M, Seki T; Osaka Liver Cancer Study Group. Severe complications of radiofrequency ablation therapy for hepatocellular carcinoma: an analysis of 3,891 ablations in 2,614 patients. *Oncology* 2007; **72** Suppl 1: 72-75 [PMID: 18087185 DOI: 10.1159/000111710]

23 **Mulier S**, Mulier P, Ni Y, Miao Y, Dupas B, Marchal G, De Wever I, Michel L. Complications of radiofrequency coagulation of liver tumours. *Br J Surg* 2002; **89**: 1206-1222 [PMID: 12296886 DOI: 10.1046/j.1365-2168.2002.02168.x]

24 **Bertot LC**, Sato M, Tateishi R, Yoshida H, Koike K. Mortality and complication rates of percutaneous ablative techniques for the treatment of liver tumors: a systematic review. *Eur Radiol* 2011; **21**: 2584-2596 [PMID: 21858539 DOI: 10.1007/s00330-011-2222-3]

25 **Baker EH**, Thompson K, McKillop IH, Cochran A, Kirks R, Vrochides D, Martinie JB, Swan RZ, Iannitti DA. Operative microwave ablation for hepatocellular carcinoma: a single center retrospective review of 219 patients. *J Gastrointest Oncol* 2017; **8**: 337-346 [PMID: 28480072 DOI: 10.21037/jgo.2016.09.06]

26 **Maida M**, Cabibbo G, Brancatelli G, Genco C, Alessi N, Genova C, Romano P, Raineri M, Giarratano A, Midiri M, Cammà C. Assessment of treatment response in hepatocellular carcinoma: a review of the literature. *Future Oncol* 2013; **9**: 845-854 [PMID: 23718305 DOI: 10.2217/fon.13.33]

27 **Goldberg SN**, Grassi CJ, Cardella JF, Charboneau JW, Dodd GD 3rd, Dupuy DE, Gervais DA, Gillams AR, Kane RA, Lee FT Jr, Livraghi T, McGahan J, Phillips DA, Rhim H, Silverman SG, Solbiati L, Vogl TJ, Wood BJ, Vedantham S, Sacks D; Society of Interventional Radiology Technology Assessment Committee and the International Working Group on Image-guided Tumor Ablation. Image-guided tumor ablation: standardization of terminology and reporting criteria. *J Vasc Interv Radiol* 2009; **20**: S377-S390 [PMID: 19560026 DOI: 10.1016/j.jvir.2009.04.011]

28 **Jeong YS**, Kim SH, Lee JM, Lee JY, Kim JH, Lee DH, Kang HJ, Yoon CJ, Han JK. Gastrointestinal tract complications after hepatic radiofrequency ablation: CT prediction for major complications. *Abdom Radiol (NY)* 2018; **43**: 583-592 [PMID: 28676999 DOI: 10.1007/s00261-017-1239-8]

29 **Livraghi T**, Solbiati L, Meloni MF, Gazelle GS, Halpern EF, Goldberg SN. Treatment of focal liver tumors with percutaneous radio-frequency ablation: complications encountered in a multicenter study. *Radiology* 2003; **226**: 441-451 [PMID: 12563138 DOI: 10.1148/radiol.2262012198]

30 **Liang P**, Wang Y, Yu X, Dong B. Malignant liver tumors: treatment with percutaneous microwave ablation--complications among cohort of 1136 patients. *Radiology* 2009; **251**: 933-940 [PMID: 19304921 DOI: 10.1148/radiol.2513081740]

31 **de Baère T**, Risse O, Kuoch V, Dromain C, Sengel C, Smayra T, Gamal El Din M, Letoublon C, Elias D. Adverse events during radiofrequency treatment of 582 hepatic tumors. *AJR Am J Roentgenol* 2003; **181**: 695-700 [PMID: 12933462 DOI: 10.2214/ajr.181.3.1810695]

32 **Casaril A**, Abu Hilal M, Harb A, Campagnaro T, Mansueto G, Nicoli N. The safety of radiofrequency thermal ablation in the treatment of liver malignancies. *Eur J Surg Oncol* 2008; **34**: 668-672 [PMID: 17681717 DOI: 10.1016/j.ejso.2007.05.003]

33 **Livraghi T**, Meloni F, Solbiati L, Zanus G; Collaborative Italian Group using AMICA system. Complications of microwave ablation for liver tumors: results of a multicenter study. *Cardiovasc Intervent Radiol* 2012; **35**: 868-874 [PMID: 21833809 DOI: 10.1007/s00270-011-0241-8]

34 **Chen TM**, Huang PT, Lin LF, Tung JN. Major complications of ultrasound-guided percutaneous radiofrequency ablations for liver malignancies: single center experience. *J Gastroenterol Hepatol* 2008; **23**: e445-e450 [PMID: 17683478 DOI: 10.1111/j.1440-1746.2007.05078.x]

35 **Meloni MF**, Goldberg SN, Moser V, Piazza G, Livraghi T. Colonic perforation and abscess following radiofrequency ablation treatment of hepatoma. *Eur J Ultrasound* 2002; **15**: 73-76 [PMID: 12044857 DOI: 10.1016/s0929-8266(01)00171-9]

36 **Falco A**, Orlando D, Sciarra R, Sergiacomo L. A case of biliary gastric fistula following percutaneous radiofrequency thermal ablation of hepatocellular carcinoma. *World J Gastroenterol* 2007; **13**: 804-805 [PMID: 17278208 DOI: 10.3748/wjg.v13.i5.804]

37 **Frich L**, Edwin B, Brabrand K, Rosseland AR, Mala T, Mathisen O, Gladhaug I. Gastric perforation after percutaneous radiofrequency ablation of a colorectal liver metastasis in a patient with adhesions in the peritoneal cavity. *AJR Am J Roentgenol* 2005; **184**: S120-S122 [PMID: 15728002 DOI: 10.2214/ajr.184.3_supplement.0184s120]

38 **Yamane T**, Imai K, Umezaki N, Yamao T, Kaida T, Nakagawa S, Yamashita YI, Chikamoto A, Ishiko T, Baba H. Perforation of the esophagus due to thermal injury after laparoscopic radiofrequency ablation for hepatocellular carcinoma: a case for caution. *Surg Case Rep* 2018; **4**: 127 [PMID: 30315431 DOI: 10.1186/s40792-018-0534-0]

39 **Kwon HJ**, Kim PN, Byun JH, Kim KW, Won HJ, Shin YM, Lee MG. Various complications of

percutaneous radiofrequency ablation for hepatic tumors: radiologic findings and technical tips. *Acta Radiol* 2014; **55**: 1082-1092 [PMID: 24277883 DOI: 10.1177/0284185113513893]

40 **Akahane M**, Koga H, Kato N, Yamada H, Uozumi K, Tateishi R, Teratani T, Shiina S, Ohtomo K. Complications of percutaneous radiofrequency ablation for hepato-cellular carcinoma: imaging spectrum and management. *Radiographics* 2005; **25** Suppl 1: S57-S68 [PMID: 16227497 DOI: 10.1148/rg.25si055505]

41 **Kim YS**, Rhim H, Lim HK. Imaging after radiofrequency ablation of hepatic tumors. *Semin Ultrasound CT MR* 2009; **30**: 49-66 [PMID: 19358437 DOI: 10.1053/j.sult.2008.12.004]

42 **Baron TH**, Song LM, Ross A, Tokar JL, Irani S, Kozarek RA. Use of an over-the-scope clipping device: multicenter retrospective results of the first U.S. experience (with videos). *Gastrointest Endosc* 2012; **76**: 202-208 [PMID: 22726484 DOI: 10.1016/j.gie.2012.03.250]

43 **Manta R**, Galloro G, Mangiavillano B, Conigliaro R, Pasquale L, Arezzo A, Masci E, Bassotti G, Frazzoni M. Over-the-scope clip (OTSC) represents an effective endoscopic treatment for acute GI bleeding after failure of conventional techniques. *Surg Endosc* 2013; **27**: 3162-3164 [PMID: 23436101 DOI: 10.1007/s00464-013-2871-1]

44 **Lee HL**, Cho JY, Cho JH, Park JJ, Kim CG, Kim SH, Han JH. Efficacy of the Over-the-Scope Clip System for Treatment of Gastrointestinal Fistulas, Leaks, and Perforations: A Korean Multi-Center Study. *Clin Endosc* 2018; **51**: 61-65 [PMID: 28847073 DOI: 10.5946/ce.2017.027]

45 **Donatelli G**, Cereatti F, Dhumane P, Vergeau BM, Tuszynski T, Marie C, Dumont JL, Meduri B. Closure of gastrointestinal defects with Ovesco clip: long-term results and clinical implications. *Therap Adv Gastroenterol* 2016; **9**: 713-721 [PMID: 27582884 DOI: 10.1177/1756283X16652325]

46 **Goenka MK**, Rai VK, Goenka U, Tiwary IK. Endoscopic Management of Gastrointestinal Leaks and Bleeding with the Over-the-Scope Clip: A Prospective Study. *Clin Endosc* 2017; **50**: 58-63 [PMID: 27802375 DOI: 10.5946/ce.2016.028]

47 **Verlaan T**, Voermans RP, van Berge Henegouwen MI, Bemelman WA, Fockens P. Endoscopic closure of acute perforations of the GI tract: a systematic review of the literature. *Gastrointest Endosc* 2015; **82**: 618-28.e5 [PMID: 26005015 DOI: 10.1016/j.gie.2015.03.1977]

48 **Kim JS**, Kim BW, Kim JI, Kim JH, Kim SW, Ji JS, Lee BI, Choi H. Endoscopic clip closure versus surgery for the treatment of iatrogenic colon perforations developed during diagnostic colonoscopy: a review of 115,285 patients. *Surg Endosc* 2013; **27**: 501-504 [PMID: 22773239 DOI: 10.1007/s00464-012-2465-3]

49 **Haito-Chavez Y**, Law JK, Kratt T, Arezzo A, Verra M, Morino M, Sharaiha RZ, Poley JW, Kahaleh M, Thompson CC, Ryan MB, Choksi N, Elmunzer BJ, Gosain S, Goldberg EM, Modayil RJ, Stavropoulos SN, Schembre DB, DiMaio CJ, Chandrasekhara V, Hasan MK, Varadarajulu S, Hawes R, Gomez V, Woodward TA, Rubel-Cohen S, Fluxa F, Vleggaar FP, Akshintala VS, Raju GS, Khashab MA. International multicenter experience with an over-the-scope clipping device for endoscopic management of GI defects (with video). *Gastrointest Endosc* 2014; **80**: 610-622 [PMID: 24908191 DOI: 10.1016/j.gie.2014.03.049]

50 **Morrell DJ**, Winder JS, Johri A, Docimo S, Juza RM, Witte SR, Alli VV, Pauli EM. Over-the-scope clip management of non-acute, full-thickness gastrointestinal defects. *Surg Endosc* 2020; **34**: 2690-2702 [PMID: 31350610 DOI: 10.1007/s00464-019-07030-3]

51 **Swan RZ**, Sindram D, Martinie JB, Iannitti DA. Operative microwave ablation for hepatocellular carcinoma: complications, recurrence, and long-term outcomes. *J Gastrointest Surg* 2013; **17**: 719-729 [PMID: 23404173 DOI: 10.1007/s11605-013-2164-y]

52 **Song I**, Rhim H, Lim HK, Kim YS, Choi D. Percutaneous radiofrequency ablation of hepatocellular carcinoma abutting the diaphragm and gastrointestinal tracts with the use of artificial ascites: safety and technical efficacy in 143 patients. *Eur Radiol* 2009; **19**: 2630-2640 [PMID: 19557416 DOI: 10.1007/s00330-009-1463-x]

53 **Koda M**, Murawaki Y, Hirooka Y, Kitamoto M, Ono M, Sakaeda H, Joko K, Sato S, Tamaki K, Yamasaki T, Shibata H, Shimoe T, Matsuda T, Toshikuni N, Fujioka S, Ohmoto K, Nakamura S, Kariyama K, Aikata H, Kobayashi Y, Tsutsui A. Complications of radiofrequency ablation for hepatocellular carcinoma in a multicenter study: An analysis of 16 346 treated nodules in 13 283 patients. *Hepatol Res* 2012; **42**: 1058-1064 [PMID: 22583706 DOI: 10.1111/j.1872-034X.2012.01025.x]

54 **Park JG**, Park SY, Tak WY, Kweon YO, Jang SY, Lee YR, Hur K, Lee HJ, Lee HW. Early complications after percutaneous radiofrequency ablation for hepatocellular carcinoma: an analysis of 1,843 ablations in 1,211 patients in a single centre: experience over 10 years. *Clin Radiol* 2017; **72**: 692.e9-692.e15 [PMID: 28364952 DOI: 10.1016/j.crad.2017.03.001]

55 **Kondo Y**, Yoshida H, Shiina S, Tateishi R, Teratani T, Omata M. Artificial ascites technique for percutaneous radiofrequency ablation of liver cancer adjacent to the gastrointestinal tract. *Br J Surg* 2006; **93**: 1277-1282 [PMID: 16783759 DOI: 10.1002/bjs.5374]

56 **Rhim H**, Yoon KH, Lee JM, Cho Y, Cho JS, Kim SH, Lee WJ, Lim HK, Nam GJ, Han SS, Kim YH, Park CM, Kim PN, Byun JY. Major complications after radio-frequency thermal ablation of hepatic tumors: spectrum of imaging findings. *Radiographics* 2003; **23**: 123-34; discussion 134-6 [PMID: 12533647 DOI: 10.1148/rg.231025054]

57 **Curley SA**, Marra P, Beaty K, Ellis LM, Vauthey JN, Abdalla EK, Scaife C, Raut C, Wolff R, Choi H, Loyer E, Vallone P, Fiore F, Scordino F, De Rosa V, Orlando R, Pignata S, Daniele B, Izzo F. Early and late complications after radiofrequency ablation of malignant liver tumors in 608 patients. *Ann Surg* 2004; **239**: 450-458 [PMID: 15024305 DOI: 10.1097/01.sla.0000118373.31781.f2]

58 **Jansen MC**, van Duijnhoven FH, van Hillegersberg R, Rijken A, van Coevorden F, van der Sijp J, Prevoo W, van Gulik TM. Adverse effects of radiofrequency ablation of liver tumours in the Netherlands. *Br J Surg* 2005; **92**: 1248-1254 [PMID: 15997440 DOI: 10.1002/bjs.5059]

59 **Maeda M**, Saeki I, Sakaida I, Aikata H, Araki Y, Ogawa C, Kariyama K, Nouso K, Kitamoto M, Kobashi H, Sato S, Shibata H, Joko K, Takaki S, Takabatake H, Tsutsui A, Takaguchi K, Tomonari T, Nakamura S, Nagahara T, Hiraoka A, Matono T, Koda M, Mandai M, Mannami T, Mitsuda A, Moriya T, Yabushita K, Tani J, Yagi T, Yamasaki T. Complications after Radiofrequency Ablation for Hepatocellular Carcinoma: A Multicenter Study Involving 9,411 Japanese Patients. *Liver Cancer* 2020; **9**: 50-62 [PMID: 32071909 DOI: 10.1159/000502744]

Published by **Baishideng Publishing Group Inc**
7041 Koll Center Parkway, Suite 160, Pleasanton, CA 94566, USA
Telephone: +1-925-3991568
E-mail: bpgoffice@wjgnet.com
Help Desk: https://www.f6publishing.com/helpdesk
https://www.wjgnet.com